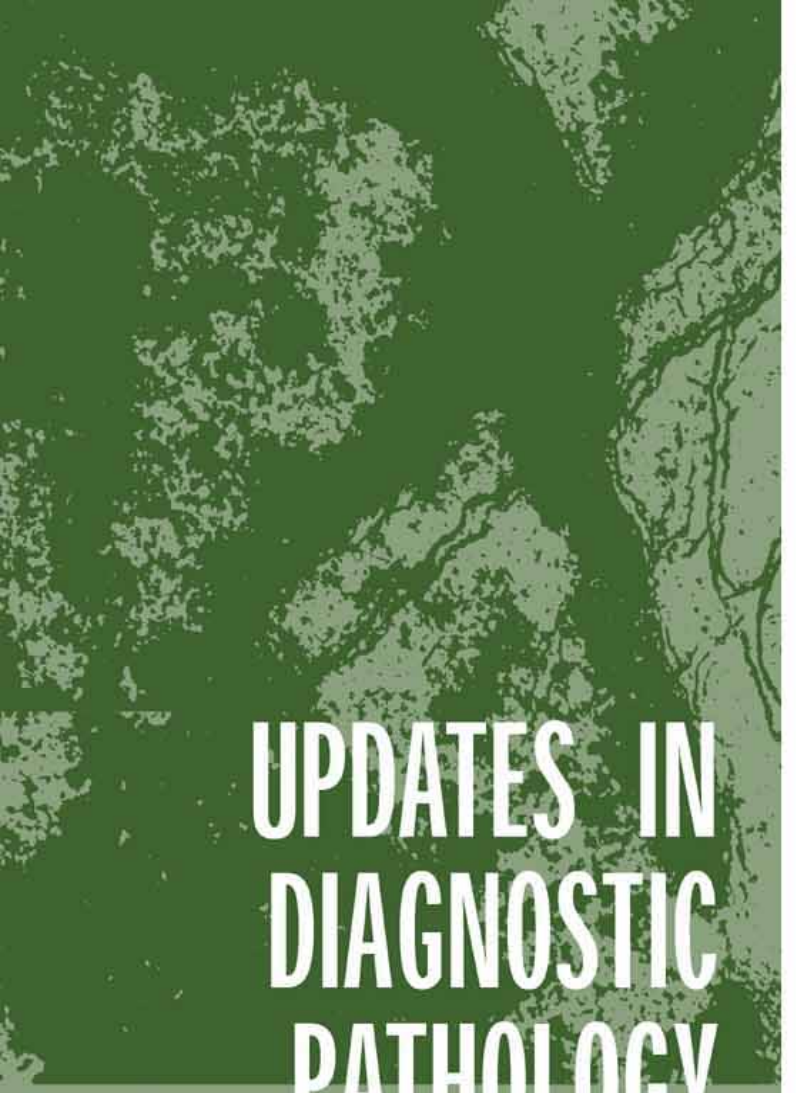

ADVANCES IN EXPERIMENTAL MEDICINE AND BIOLOGY

Volume 563

UPDATES IN DIAGNOSTIC PATHOLOGY

Edited by David C. Chhieng and Gene P. Siegal

UPDATES IN DIAGNOSTIC PATHOLOGY

ADVANCES IN EXPERIMENTAL MEDICINE AND BIOLOGY

Recent Volumes in this Series

Volume 557
BRAIN REPAIR
Edited by M. Bähr

Volume 558
DEFECTS OF SECRETION IN CYSTIC FIBROSIS
Edited by Carsten Schultz

Volume 559
CELL VOLUME AND SIGNALING
Edited by Peter K. Lauf and Norma C. Adragna

Volume 560
MECHANISMS OF LYMPHOCYTE ACTIVATION AND IMMUNE REGULATION X: Innate Immunity
Edited by Sudhir Gupta, William Paul, and Ralph Steinman

Volume 561
CHEMISTRY AND SAFETY OF ACRYLAMIDE IN FOOD
Edited by Mendel Friedman and Don Mottram

Volume 562
CHOLINERGIC MECHANISMS
Edited by José Gonzalez-Ros

Volume 563
UPDATES IN DIAGNOSTIC PATHOLOGY
Edited by David C. Chhieng and Gene P. Siegal

Volume 564
GLYCOBIOLOGY AND MEDICINE
Edited by John S. Axford

Volume 565
SLIDING FILAMENT MECHANISM IN MUSCLE CONTRACTION: Fifty Years of Research
Edited by Haruo Sugi

UPDATES IN DIAGNOSTIC PATHOLOGY

Edited by

David C. Chhieng
University of Alabama at Birmingham
Birmingham, Alabama

and

Gene P. Siegal
University of Alabama at Birmingham
Birmingham, Alabama

Springer

David C. Chhieng, M.D., M.B.A.
Associate Professor
Director, Immunohistochemistry Laboratory
Department of Pathology
University of Alabama at Birmingham
Birmingham, Alabama
dchhieng@path.uab.edu

Gene P. Siegal, M.D., Ph.D.
Professor of Pathology, Cell Biology, and Surgery
Director, Division of Anatomic Pathology
Senior Scientist, UAB Comprehensive Cancer Center
and the Gene Therapy Center
University of Alabama at Birmingham
Birmingham, Alabama
gsiegal@path.uab.edu

Library of Congress Control Number: 2005923324

ISSN: 0065 2598
ISBN-10: 0-387-25357-2
ISBN-13: 9780387253572
Printed on acid-free paper

Printed in the United States of America

9 8 7 6 5 4 3 2 1

springeronline.com

FOREWORD —ANOTHER BRIEF HISTORY IN TIME

By November 1997, we had built the corpus of a Division of Anatomic Pathology (AP) Department at the University of Alabama at Birmingham which had begun some 7 years earlier. It had become evident, however, that the breadth, depth and quality of our faculty remained mostly unknown outside the medical center. To remedy that problem and to give our younger faculty experience lecturing to broad audiences of knowledgeable pathologists, I secured the agreement of the chair, Dr. Jay McDonald, to offer a course outside the institutional walls stressing recent advances in anatomic pathology. To heighten the drawing power of the conference, I called upon the great kindness of Dr. Virginia Livolsi, of the University of Pennsylvania, to be the keynote speaker. At the time she was the president of the Arthur Purdy Stout Society of Surgical Pathologists, then and now the preeminent academic surgical pathology organization. Her worldwide reputation, especially in the field of thyroid pathology, assured us a chance at success, but really that was guaranteed by Mr. Donald Bowen, the Departmental Administrator for Clinical Affairs who spent countless hours on the business side of the operation identifying and securing the meeting sites, directing the catering and social events, obtaining industry underwriting support including microscopes and organizing our thick binder of "hand-outs" and accompanying slides.

Since that time, about half of the original faculty have left our institution for others. Some like William Rogers have gone on to be division directors in their own right, while still others like Guilermo Herrera have become distinguished chairs, leading their own pathology department. The mountains of North Carolina, however, proved to be a powerful academic aphrodisiac and now some 8 years later we're still at it. Our AP faculty has grown to nearly 30 individuals and the department stands at 75. Over the years our curriculum has been broadened to include selected topics from laboratory medicine, the basic sciences as applied to practice and teaching and laboratory management as well as to the complementary but more esoteric portions of anatomic pathology, that is, forensic pathology, perinatal pathology, oral pathology and neuropathology. We have varied the meeting sites across the southeast, having gone to resorts in Georgia, North and South Carolina, Florida, and this year Mississippi. We have also maintained the general format of a visiting expert sandwiched between the institutional faculty. Such notables as Stacey [Chuck] Mills, Mark Wick, John [Jack] Brooks, Danny Santa Cruz, Robert Petras, David Page, and this year Christopher Fletcher have all shared their considerable gifts with us. Photographic slides have been replaced

by CDs, but we continue to utilize the same general format of morning didactics and afternoon glass slide review and small group interactions.

One of our biggest successes was in the ever-expanding set of didactic lecture notes and radiologic, gross, microscopic, ultrastructural, and other images that course participants received, so it wasn't much of a surprise when we were approached by the publisher to consider creating an updated compilation of some of the best talks and packaging them in a monograph available to a broader population of physicians and scientists. With the extraordinary attention to detail that he is known for, my co-editor David Chhieng has been both the brains and the brawn of this project, resulting in the bringing together of such a collection while trying to be sensitive and representative of the various branches of pathology reflected in the actual course. From surgical pathology, chapters cover select topics in endocrine, gynecologic, GU, and GI pathology with contributions from Walter Bell, Michael Conner, Katrin Klemm, and Audrey Lazenby, respectively. Tom Winokur has begun to prepare us for the near future with a treatise on molecular markers in breast cancer. The interactive nature of cytopathology and surgical pathology are brought together by Claudia Castro [now at the U.T. Medical Branch at Galveston] and David Chhieng in three chapters covering mediastinal, pleural, and pulmonary pathology. Fine needle aspiration (FNA) of the pancreas is covered by Dharshana and Nirag Jhala, while the head of our surgical pathology service, Michael Klein-covers the critical topic of using imaging data in orthopedic pathology. From hematopathology, Vishnu Reddy presents selected case studies amply demonstrating why he is a master teacher. A second hematopathology selection on aggressive B-cell lymphoma is contributed by Cathy Listinsky who has moved to Case Western Reserve University. Cheryl Palmer representing neuropathology demystifies gliomas for us, while Nasser Said-A-Naief does the same for odontogenic tumors. Ken Waites covers microbiology with an outstanding treatise on antimicrobial susceptibility testing, and Peter Anderson and his associates cover the use of digital images in pathology for both clinical practice and teaching.

For my colleagues and I, this book is an experiment. Its ultimate success or failure is dependent upon the usefulness of the topics you, the reader, derive. We trust the reading of this monograph will be time well spent and I look forward to either hearing from you about what you liked or disliked or seeing you at a future course offering.

Gene P. Siegal, M.D., Ph.D.
Birmingham, AL

CONTENTS

CHAPTER 1
SURGICAL PATHOLOGY OF THE PARATHYROID GLANDS

Walter C. Bell, M.D.*

1. INTRODUCTION

Figure 1. Distribution of parathyroid glands. Distribution of the superior (A) and inferior (B) parathyroid glands. Numbers indicate sites in order of decreasing frequency. Modified from Gilmour (1938).

* Assistant Professor, Department of Pathology, University of Alabama, Birmingham, AL.

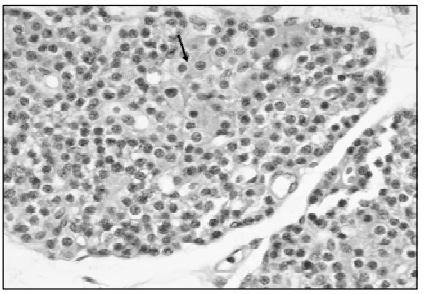

Figure 2. Cellular components of parathyroid gland. The normal parathyroid gland is composed of chief cells with small uniform nuclei and a moderate amount of pale cytoplasm. Clusters of oxyphil cells (indicated by arrow) are present exhibiting larger, more irregular nuclei and abundant granular cytoplasm. (H&E)

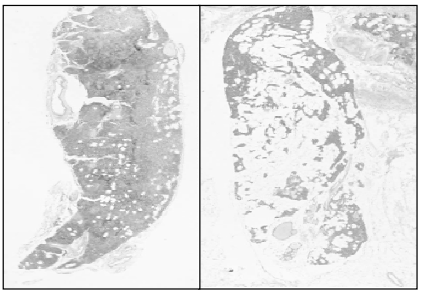

Figure 3. Stromal fat variability. Illustrated are two suppressed parathyroids from a single patient with an adenoma. Differences in fat content and distribution are readily appreciated. (H&E)

The parathyroid glands arise as paired structures from the third and fourth branchial pouches. The superior glands arise from pouch IV and assume their usual (approximately 80%) location at the cricothyroid junction or at the junction of the recurrent laryngeal nerve and inferior thyroid artery (see Figure 1a). The lower glands arising from pouch III have a more variable distribution. Usually the inferior glands are found at the lower pole of the thyroid lobe, but may be found at the level of the hyoid, within the mediastinum, and even within the pericardium (see Figure 1b). Most individuals (>90%) have the expected four parathyroid glands, but supernumery glands may be present with up to 12 glands reported in rare cases. These supernumery glands likely arise from embryologic rests of the developing glands, and most are found within the thymus, which arises from pouch III along with the inferior glands.

Normal parathyroid glands are small with a flattened appearance. They measure 3 to 6 mm in length, 2 to 4 mm in width, and 0.5 to 2.0 mm in thickness. The mean gland weight is approximately 30 mg. Glands are invested within a thin fibrous capsule, although nests of parenchymal cells may lie outside of this capsule. The parenchyma is composed of chief cells and oxyphilic cells (see Figure 2). Chief cells predominate with oxyphilic cells becoming more frequent with increasing age. Stromal fat is extremely variable in normal glands with studies reporting means ranging from 11% to 50% (see Figure 3). In adults, 70-80% of chief cells contain prominent

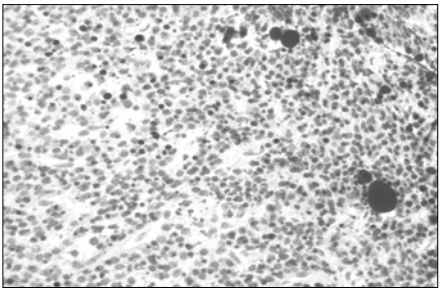

Figure 4. Intracytoplasmic fat. The normal or suppressed parathyroid gland contains abundant intracytoplasmic fat as demonstrated by oil red-O stain. Small intracytoplasmic fat droplets are present within the chief cells. Larger staining areas represent adipocytes distributed within the parathyroid parenchyma (oil red-O stain).

intracytoplasmic lipid droplets which can be visualized by lipid stains on fresh tissue (see Figure 4).

The parathyroid glands function in the regulation of serum calcium and phosphate levels through the production of parathyroid hormone (PTH). Intact PTH is an 84-amino-acid peptide with a weight of 9500 daltons and is produced by the chief cells. The parathyroid glands are extremely sensitive to minute changes in serum calcium levels, and reduced calcium stimulates production of PTH. PTH raises serum calcium by increasing absorption from bone (rapid and late phases) and decreasing calcium excretion by the kidneys. As serum calcium levels rise and return to normal, feedback inhibition results in decreased secretion of PTH (see Figure 5). The hormone is metabolized within 2 to 5 minutes in the liver, kidney, and bones into N-terminal and C-terminal fragments (see Figure 6). The N-terminal fragment is biologically active but also has a half-life of only minutes.

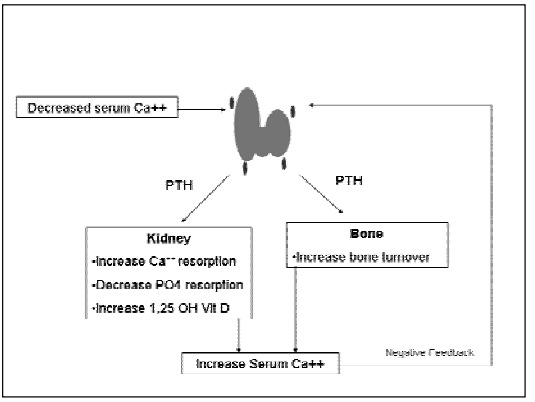

Figure 5. Parathyroid hormone function. The parathyroid hormone exerts its action on the kidney and within bone to increase levels of serum calcium. As calcium levels rise, a negative feedback loop inhibits hormone production.

2. HYPERPARATHYROIDISM

Hyperparathyroidism is characterized by increased production of PTH. Primary hyperparathyroidism is the leading cause of hypercalcemia in the United States with approximately 100,000 cases diagnosed each year. The majority of cases are discovered in asymptomatic patients by a routine chemistry profile. Symptoms of hypercalcemia may include weakness, constipation, abdominal pain, and decreased function of the central and peripheral nervous systems. Other causes of hypercalcemia include malignant neoplasms metastatic to bone, various drugs, granulomatous disease, and renal disease. The diagnosis of primary hyperparathyroidism can be confirmed by laboratory testing

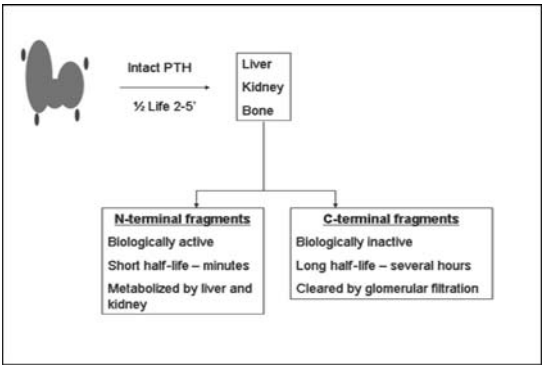

Figure 6. Parathyroid hormone metabolism. Intact parathyroid hormone has a short half-life of between 2 and 5 minutes. It is metabolized in the liver, kidney, and bones into N-terminal and C-terminal fragments. The N-terminal fragments are active but also have a very short half-life.

including confirmation of elevated serum calcium (with correction for serum albumin) and increased PTH concentration. Parathyroid adenoma is the leading cause of primary hyperparathyroidism, accounting for approximately 85% of cases. Primary hyperplasia accounts for approximately 13% of cases, and parathyroid carcinoma is responsible for the remaining 2%. The treatment of primary hyperparathyroidism is surgical. Preoperative imaging studies may be utilized to assist in the identification of abnormal glands.

Secondary parathyroid hyperplasia occurs in conditions that lead to hypocalcemia, such as renal disease or malabsorption. Hypocalcemia stimulates the parathyroid glands causing gland enlargement due to chief cell hyperplasia. Secondary hyperplasia usually responds to medical therapy and is uncommonly encountered as a surgical specimen. Histologically, these glands have a similar appearance to the nodular variant of primary hyperplasia.

3. PARATHYROID ADENOMA

Parathyroid adenoma is the most common cause of primary hyperparathyroidism. These are neoplasms composed of chief cells, oxyphil cells, or a mixture of cell types. Adenomas are more common in women than men and most commonly are identified during the fourth decade of life.

Adenomas are more common in the lower parathyroid glands resulting in glandular enlargement, usually measuring greater than 1.5 cm in length and weighing greater than 1 g. Adenomas are generally oval and lobulated and easily separate from the surrounding tissues. The shape may be altered by the surrounding structures, and previous surgery with scarring may make the glands more difficult to identify and dissect.

Histologically, adenomas are hypercellular with minimal or no stromal fat. They are composed most commonly of chief cells, but oxyphil cells may be admixed, and occasional adenomas are composed entirely of oxyphil cells. The cells are arranged in a variety of histologic patterns including sheet-like proliferations, trabecular arrangements, and tubular patterns. Tubules may contain eosinophilic colloid-like material. A rim of compressed normal or suppressed gland may be identified in approximately half of adenomas. This rim is most commonly located at the hilum of the gland and contains cells which are smaller than the cells of the adenoma (see Figure 7).

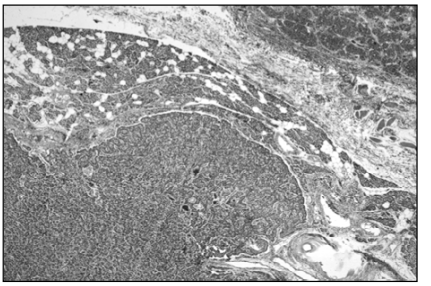

Figure 7. Parathyroid adenoma. A parathyroid adenoma is shown, demonstrating a hypercellular proliferation of chief cells with compression of normal parathyroid tissue (with greater fat content) at the periphery. (H&E)

The cytologic features of adenomas are usually uniform and bland, but occasionally prominent nuclear pleomorphism may be observed, particularly in adenomas undergoing degenerative changes. Cysts may also occur as a degenerative change within parathyroid adenomas. These cysts may have thick fibrous capsules with calcification.

Fat stains typically show minimal intracytoplamic parenchymal fat within the neoplastic cells.

4. PRIMARY CHIEF CELL HYPERPLASIA

Primary chief hyperplasia is a condition in which there is an increase in the parathyroid cell mass due to cellular proliferation involving multiple glands without a known stimulus for PTH hypersecretion. Primary hyperplasia accounts for approximately 13% of cases of hyperparathyroidism.

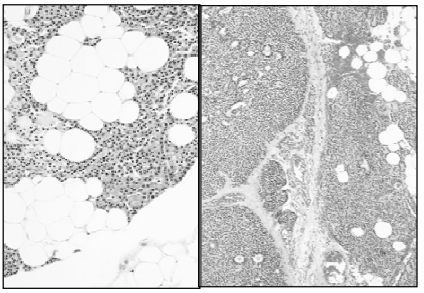

Figure 8. Primary chief cell hyperplasia. It is characterized by glandular enlargement and increased cellularity. Fat content is variable with entrapment of groups of adipocytes by chief cells. (H&E)

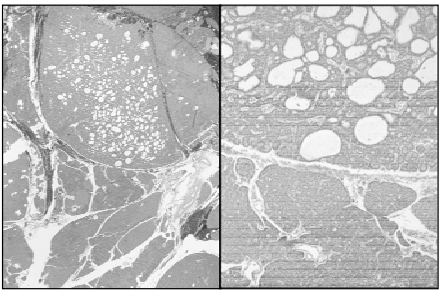

Figure 9. Nodular hyperplasia. In nodular hyperplasia, nodules may compress the adjacent tissue. Depending on fat content, this may simulate compression of normal parathyroid tissue by an adenoma. (H&E)

Classical primary hyperplasia presents with enlargement of all four glands, but in half of patients, enlargement may be asymmetric. Total gland weight in primary hyperplasia ranges from 150 mg to 10 g with the majority of cases having total gland weights of less than 1 g. Histologically, the chief cell proliferation may be diffuse or nodular with nodules containing few stromal fat cells and perinodular regions containing more numerous stromal fat cells (see Figure 8). This may simulate the compressed rim of normal tissue seen in an adenoma (see Figure 9). Large oxyphil cell nodules may also simulate adenoma.

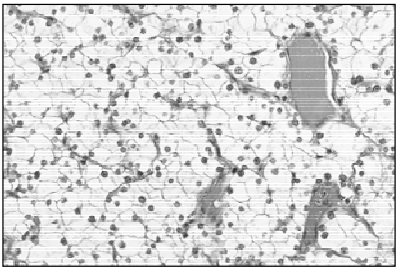

Figure 10. Clear cell hyperplasia. Water clear cell hyperplasia is an increasingly uncommon form of primary parathyroid hyperplasia characterized by cells with abundant clear cytoplasm. (H&E)

Increasingly uncommon is the finding of clear cell hyperplasia (see Figure 10). In clear cell hyperplasia all four glands are enlarged, with the upper glands more severely affected. Glands are usually larger than in chief cell hyperplasia with total gland weights in the majority of cases exceeding 5 g.

5. PARATHYROID CARCINOMA

Parathyroid carcinoma is a rare cause of primary hyperparathyroidism accounting for approximately 2% of cases. The mean age at presentation is 44 years with an equal distribution between men and women. Parathyroid carcinoma usually presents with severe symptomatic hypercalcemia (serum calcium usually greater than 14 mg/dL. A neck mass may be palpable.

The surgeon typically encounters a gland that is densely adherent to the surrounding tissues, but occasional cases are encapsulated and not grossly distinguishable from adenoma. Carcinomas range in size from 1.5 to 6.5 cm and range in weight from 1.5 to 27 g with a mean weight of 6.7 g.

Histologic features useful in diagnosis of parathyroid carcinoma are invasion of the surrounding tissues, vascular invasion, thick fibrous capsule and broad fibrous bands within the gland, capsular invasion, tumor necrosis, and increased mitotic activity (see Figure 11). Invasion of the surrounding tissues is diagnostic of carcinoma (see Figure 12). Many of the other features may also be seen in adenomas undergoing degenerative changes.

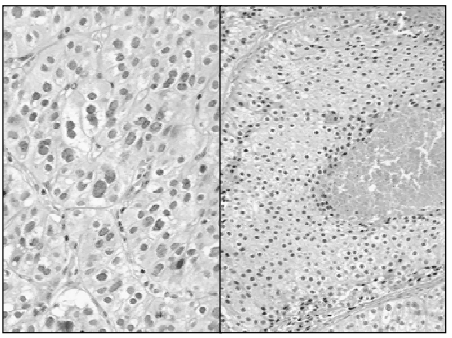

Figure 11. Parathyroid carcinoma. Parathyroid carcinoma showing nuclear enlargement and atypia (left) with fibrous bands and areas of necrosis (right). (H&E)

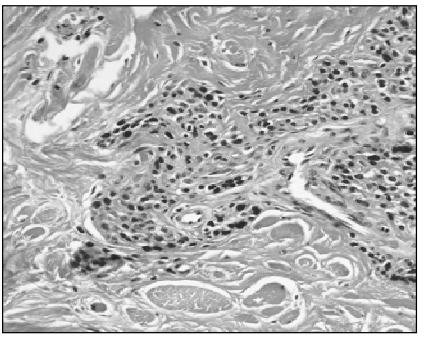

Figure 12. Parathyroid carcinoma with invasion. The section shows invasion by parathyroid carcinoma exhibiting nuclear hyperchromasia and atypia. There is a dense fibrotic response to the invading carcinoma. (H&E)

6. INTRAOPERATIVE CONSULTATION IN PARATHYROID PATHOLOGY

The role of the pathologist in frozen section during parathyroid surgery is twofold. The first objective is to identify the tissue submitted. Often nodules of thyroid tissue, skeletal muscle, lymph node, or thymic tissue are sampled by the surgeon as possible parathyroid tissue. For the most part this tissue identification is straightforward, but occasionally there may be difficulty in histologic distinction between thyroid and parathyroid tissue. This is particularly true when parathyroid cells are arranged in a follicular pattern with central colloid-like material (see Figure 13). Usually careful examination of multiple levels will reveal areas with histology more distinctive for

parathyroid tissue. On permanent section, identification can be confirmed by immunoperoxidase stains for thyroglobulin and PTH.

The second major objective at frozen section is to determine the etiology of the hyperparathyroidism. The initial evaluation of a parathyroid gland should be to determine whether the gland appears normal or abnormal. This determination requires information from the clinician regarding gland size, location, ease of removal, and whether the specimen represents a complete gland or a gland biopsy. Changes that are consistent with gland abnormality, either adenoma or hyperplasia, include enlarged gland with size >6 mm, enlarged gland weighing >60 mg (this is a trimmed weight with attached fat removed), absent or rare fat cells within the gland, and decreased intracellular lipid on fat stains. It is not possible by examination of a single gland to make a specific anatomic differentiation between hyperplasia and adenoma; although a diagnosis of adenoma may be favored if a rim of compressed normal appearing tissue is identified at the periphery. Diagnosis requires examination of additional glands by the surgeon to determine size, and preferably, in the case of a presumed adenoma, biopsy of a normal appearing gland for histologic examination. The grossly normal suppressed glands associated with an adenoma should exhibit more stromal fat than the abnormal gland and intracellular lipid should be abundant. In the case of hyperplasia, additional enlarged glands should be identified with histologic confirmation of hyperplasia.

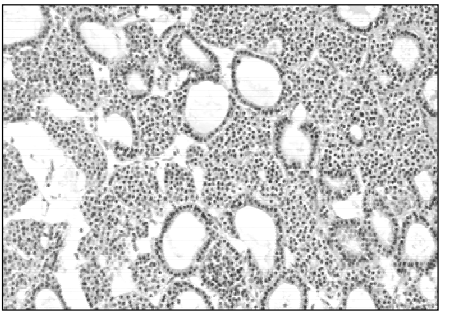

Figure 13. Parathyroid adenoma with a follicular pattern. This parathyroid adenoma exhibits a follicular pattern with spaces containing pale eosinophilic material. When this pattern is prominent, it may be difficult to distinguish parathyroid from thyroid tissue at frozen section. Additional levels may reveal more typical parathyroid architecture. (H&E)

7. MINIMALLY INVASIVE PARATHYROID SURGERY

The classic surgical approach to hyperparathyroidism has been bilateral neck exploration with identification of all four parathyroid glands. With identification of a single enlarged gland, this gland would be presumed to be an adenoma. With multiple enlarged glands the presumed diagnosis would be hyperplasia. Current practice is increasingly turning to a minimally invasive approach to parathyroid surgery. Patients are injected with radioactive technetium-99m sestamibi prior to surgery. This substance accumulates in the thyroid and parathyroid glands initially, but after 2 hours will pass out of the thyroid. A gamma-ray detector quantitates radioactivity so that enlarged parathyroid glands may be identified. If the parathyroid scan localizes to a single gland, this is a presumed adenoma. With preoperative localization, the surgeon is able to make a small localized incision to remove only the preoperatively identified enlarged gland. To assure that the removed gland does indeed represent an adenoma, intraoperative PTH levels are determined. The surgeon waits 15 minutes following removal of the gland, allowing time for metabolism of circulating PTH, and sends a blood sample for intact PTH determination. A 50% drop is considered indicative of adenoma and no further

exploration is undertaken. If the PTH fails to drop the classic operation is performed to evaluate the other glands. There are several obvious advantages to this minimal approach including a shorter hospital stay, reduction of scar tissue if reoperation is required, and reduced time under anesthesia.

8. REFERENCES

8.1 Historical Perspectives

1. Gilmour JR, Martin WJ, The weight of the parathyroid glands. *Journal of Pathology and Bacteriology*, 44 (431-62 (1937).
2. Gilmour JR, The embryology of the parathyroid glands, the thymus and certain associated rudiments. *Journal of Pathology and Bacteriology*, 1937 (45), 507-22 (1937).
3. Gilmour JR, The gross anatomy of the parathyroid glands. *Journal of Pathology and Bacteriology*, 1938 (133-49 (1938).
4. Gilmour JR, The normal histology of parathyroud glands. *Journal of Pathology and Bacteriology*, 48 (187-222 (1939).
5. Welsh MA, Concerning the parathyroid glands: a critical anatiomical and experimental study. *Journal of Anatomy and Physiology*, 32 (292-403 (1898).
6. Welsh MA, On the parathyroid glands of the cat: a preliminary study. *Journal of Pathology and Bacteriology*, 5 (202-21 (1898).

8.2 Normal Anatomy and Physiology

1. Abu-Jawdeh GM, Roth SI. Parathyroid glands. In: Sternbery SS, ed. *Histology for Pathology*. New York, NY: Raven Press, 1992; 311-20.
2. Akerstrom G, Grimelius L, Johansson H, Pertoft H, Lundqvist H, Estimation of the parathyroid parenchymal cell mass by density gradients. *American Journal of Pathology*, 99 (3), 685-94 (1980).
3. Dekker A, Dunsford HA, Geyer SJ, The normal parathyroid gland at autopsy: the significance of stromal fat in adult patients. *Journal of Pathology*, 128 (3), 127-32 (1979).
4. Dufour DR, Wilkerson SY, The normal parathyroid revisited: percentage of stromal fat. *Human Pathology*, 13 (8), 717-21 (1982).
5. Dufour DR, Wilkerson SY, Factors related to parathyroid weight in normal persons. *Archives of Pathology and Laboratory Medicine*, 107 (4), 167-72 (1983).
6. Saffos RO, Rhatigan RM, Urgulu S, The normal parathyroid and the borderline with early hyperplasia: a light microscopic study. *Histopathology*, 8 (3), 407-22 (1984).
7. Vail AD, Coller FC, The number and location of the parathyroid glands. *Journal of the Missouri State Medical Association*, 63 (347-50 (1966).
8. Wang C, The anatomic basis of parathyroid surgery. *Annals of Surgery*, 183 (3), 271-5 (1976).

8.3 Hyperparathyrodisms

1. Bondeson AG, Bondeson L, Ljungberg O, Tibblin S, Surgical strategy in nonfamilial primary parathyroid hyperplasia: long-term follow-up of thirty-nine cases. *Surgery*, 97 (5), 569-73 (1985).
2. Dekker A, Watson CG, Barnes EL, Jr., The pathologic assessment of primary hyperparathyroidism and its impact on therapy: a prospective evaluation of 50 cases with oil red-O stain. *Annals of Surgery*, 190 (5), 671-5 (1979).
3. Geelhoed GW, Silverberg SG, Intraoperative imprints for the identification of parathyroid tissue. *Surgery*, 96 (6), 1124-31 (1984).
4. Ghandur-Mnaymneh L, Cassady J, Hajianpour MA, Paz J, Reiss E, The parathyroid gland in health and disease. *American Journal of Pathology*, 125 (2), 292-9 (1986).
5. Kasdon EJ, Rosen S, Cohen RB, Silen W, Surgical pathology of hyperparathyroidism: usefulness of fat stain and problems in interpretation. *American Journal of Surgical Pathology*, 5 (4), 381-4 (1981).
6. King DT, Hirose FM, Chief cell intracytoplasmic fat used to evaluate parathyroid disease by frozen section. *Archives of Pathology and Laboratory Medicine*, 103 (12), 609-12 (1979).
7. LiVolsi VA, Hamilton R, Intraoperative assessment of parathyroid gland pathology. A common view from the surgeon and the pathologist. *American Journal of Clinical Pathology*, 102 (3), 365-73 (1994).

8. Ljungberg O, Tibblin S, Preoperative fat staining of frozen sections in primary hyperparathyroidism. *American Journal of Pathology*, 95 (3), 633-41 (1979).
9. Roth SI, Recent advances in parathyroid gland pathology. *American Journal of Medicine*, 50 (5), 612-22 (1971).
10. Roth SI, Gallagher MJ, The rapid identification of "normal" parathyroid glands by the presence of intracellular fat. *American Journal of Pathology*, 84 (3), 521-8 (1976).
11. Udelsman R, Six-hundred fifty-six consecutive explorations for primary hyperparathyroidism. *Annals of Surgery*, 235 (5), 665-70; discussion 70-2 (2002).

8.4 Minimally Invasive Parathyroid Surgery

1. Goldstein RE, Blevins L, Delbeke D, Martin WH, Effect of minimally invasive radioguided parathyroidectomy on efficacy, length of stay, and costs in the management of primary hyperparathyroidism. *Annals of Surgery*, 231 (5), 732-42 (2000).
2. Jaskowiak NT, Sugg SL, Helke J, Koka MR, Kaplan EL, Pitfalls of intraoperative quick parathyroid hormone monitoring and gamma probe localization in surgery for primary hyperparathyroidism. *Archives of Surgery*, 137 (6), 659-68; discussion 68-9 (2002).
3. Moore FD, Jr., Mannting F, Tanasijevic M, Intrinsic limitations to unilateral parathyroid exploration. *Annals of Surgery*, 230 (3), 382-8; discussion 8-91 (1999).
4. Sofferman RA, Standage J, Tang ME, Minimal-access parathyroid surgery using intraoperative parathyroid hormone assay. *Laryngoscope*, 108 (10), 1497-503 (1998).
5. Song AU, Phillips TE, Edmond CV, Moore DW, Clark SK, Success of preoperative imaging and unilateral neck exploration for primary hyperparathyroidism. *Otolaryngology: Head and Neck Surgery*, 121 (4), 393-7 (1999).
6. Udelsman R, Donovan PI, Sokoll LJ, One-hundred consecutive minimally invasive parathyroid explorations. *Annals of Surgery*, 232 (3), 331-9 (2000).

CHAPTER 2
UNCOMMON AND RELATIVELY UNCOMMON LESIONS OF THE FEMALE REPRODUCTIVE SYSTEM

Michael G. Conner, M.D.*

1. INTRODUCTION

This chapter will be devoted to infrequently encountered lesions of the female reproductive tract. Some of these will be lesions that are rarely seen, while others will be lesions that you may anticipate seeing from time to time, although certainly not every day.

2. UTERINE SARCOMAS

Malignant mesenchymal tumors of the uterus as a group comprise less than 5% of all malignant uterine neoplasms. Three groups of sarcoma account for the vast majority of the malignant mesenchymal tumors of the uterus (see Table 1). These are leiomyosarcomas, endometrial stromal sarcomas, and malignant mixed Müllerian tumors (MMMT). Leiomyosarcomas are considerably more common than the others.

Table 1. Classification of uterine mesenchymal lesions

	Smooth muscle lesions	Endometrial stromal lesions	Biphasic müllerian lesions
Benign	Leiomyoma	Stromal nodule	Adenofibroma
Uncertain malignant potential	Smooth muscle tumor of uncertain malignant potential	None recognized	Biphasic Müllerian tumor of uncertain malignant potential
Malignant	Leiomyosarcoma	Endometrial stromal sarcoma	MMMT[a] Adenosarcoma

[a] Malignant mixed Müllerian tumors.

* Associate Professor, Department of Pathology, University of Alabama, Birmingham, AL.

These three groups of uterine sarcomas are probably best considered as individual subsets of three distinct groups of uterine mesenchymal tumors, each of which demonstrates a spectrum of histopathologic changes ranging from obviously benign at the lower end to obviously malignant at the upper end. Some of these exhibit lesions of uncertain malignant potential between the two extremes.

Other extremely rare uterine sarcomas have been described including Ewing's sarcoma, rhabdomyosarcoma, malignant fibrous histiocytoma, osteosarcoma, angiosarcoma, liposarcoma, granulocytic sarcoma, and alveolar soft-part sarcoma. Some of these may represent pure monophasic MMMTs with sarcomatous overgrowth. Exceedingly rare are "mixed" sarcomas containing two or more sarcomatous components but no epithelial component.

3. UTERINE ADENOSARCOMA

Adenosarcoma is by definition a biphasic Müllerian neoplasm which consists of a benign epithelial component and a malignant sarcomatous component. The epithelial component may be somewhat atypical but never malignant. The sarcomatous component is usually low-grade. These lesions may be thought of as being part of a spectrum of lesions that range from benign adenofibromas on the lower end to malignant mixed Müllerian tumors (carcinosarcoma) on the higher end.

These lesions generally occur in post-menopausal women (70%) but have been described in virtually all age groups (14 to 89 years with a median age of 58 years in one study). They usually present with abnormal vaginal bleeding and may be associated with pelvic pain and an enlarged uterus. In approximately one-half of the cases the lesion protrudes through the external cervical os where it may be confused with endocervical polyps clinically.

The typical gross appearance of the lesion is similar to a malignant mixed Müllerian tumor. It usually is present within the endometrial cavity or endocervical canal as a large polypoid mass. Ninety percent are endometrial in origin while ten percent are endocervical. In rare instances there may be two separate primary lesions involving both the endometrium and the endocervix. Adenosarcomas are almost always stage I lesions at presentation.

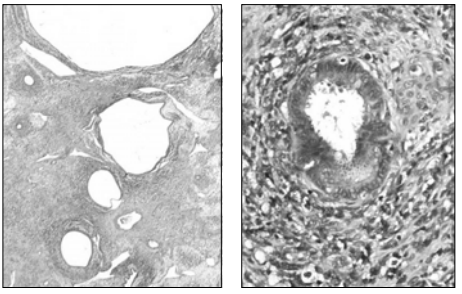

Figure 1. Adenosarcoma. The lesion exhibits a benign glandular component and a malignant sarcomatous component. (Left: H&E x100) High magnification showing concentric concentration of spindle cells surrounding a benign gland in a 'cambium' layer. (Right: H&E x 400)

Histologically, the lesion exhibits a benign glandular component and a malignant sarcomatous component (see Figure 1A). The glandular component may exhibit dilated glands and occasionally shows architectural and cytologic atypia. The glands are usually lined by proliferative-type endometrium but may also show endocervical epithelium, tubal metaplasia, squamous metaplasia, or hobnail metaplasia. The sarcomatous component is predominant and usually low-grade, consisting of round to

spindled cells. The spindled cells are present in whorls while the round cells are somewhat loosely dispersed. The appearance is usually that of an endometrial stromal sarcoma, fibrosarcoma, or a combination of the two. Smooth muscle differentiation is uncommon. A characteristic finding is a concentric concentration of spindled cells surrounding benign glands in a type of "cambium" layer (see Figure 1B). Mitotic activity is highest in these areas where 4 or more mitotic figures per ten HPFs are found in 80% of the cases. Heterologous elements such as small foci of fat, cartilage, or rhabdomyoblasts may be found in 20% of the cases. Myometrial invasion is present in only about 15% of these lesions.

Approximately 10% of the cases are associated with sarcomatous overgrowth which by definition means that 25% of the lesion consists of a pure sarcoma. The sarcoma in the area of the overgrowth is usually higher grade and exhibits more mitotic activity than that in the adenosarcomatous portion of the lesion.

Adenosarcomas of the uterus are in general much less aggressive than their carcinosarcomatous cousins. Approximately 25% of women with this tumor eventually die of their disease, often after prolonged intervals of 5 years or more. Factors that adversely affect the prognosis are sarcomatous overgrowth and myometrial invasion.

4. MALIGNANT MIXED MÜLLERIAN TUMOR ("CARCINOSARCOMA")

Malignant mixed Müllerian tumors (MMMTs) are defined as malignant neoplasms which contain both a carcinomatous and a sarcomatous component and account for roughly 2% to 5% of all uterine corpus malignancies. They are further subdivided into types depending on the nature of the sarcomatous component. The homologous type is characterized by a sarcomatous component composed of tissue types native to the uterus, that is, endometrial stroma (endometrial stromal sarcoma), fibrous tissue (fibrosarcoma), and smooth muscle (leiomyosarcoma) (see Figure 2). The heterologous type contains a sarcomatous component composed of tissue types not native to the uterus, that is, cartilage (chrondrosarcoma), skeletal muscle (rhabdomyosarcoma), and less commonly bone (osteosarcoma) (see Figure 3). The carcinomatous and sarcomatous components usually demonstrate an intimate admixture, but it is not unusual to find focal areas of pure carcinoma or pure sarcoma. Less commonly, one component may predominate to the

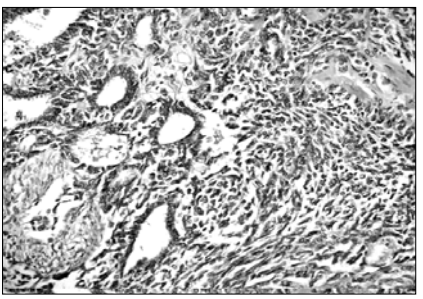

Figure 2. Malignant mixed Müllerian tumors with homologous type. The sarcomatous component resembles that of endometrial stromal sarcoma. (H&E, x 200)

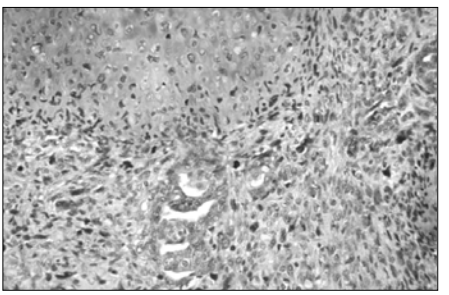

Figure 3. Malignant mixed Müllerian tumors with heterologous type. The sarcomatous component demonstrates cartilagenous differentiation which is foreign to the uterus. (H&E, x 200)

extent that it is difficult to find the other component. Grossly, the lesion typically presents as a broad-based polypoid mass which fills and distends the endometrial cavity and may extend distally into the endocervical canal. Some extend through the external cervical os and may present as a "polyp." Occasionally the uterus is greatly enlarged. Myometrial invasion deeper than the inner third is very frequent (80%) and extension into the outer half occurs in approximately 40% of cases.

MMMTs occur predominantly in postmenopausal women with a median age of about 66 years. Unusual cases have been found in younger women and rarely in children. Some of the risk factors for developing an MMMT are similar (but weaker) to those of routine endometrial adenocarcinoma and include obesity, exogenous estrogenic stimulation, and nulliparity. Some studies have linked tamoxifen therapy to an increased risk for developing an MMMT. There is also a positive relationship with previous pelvic irradiation and the subsequent development of MMMTs. Various studies have shown that between 7% and 37% of women who develop MMMTs have a history of previous pelvic irradiation. Pelvic irradiation was used for benign conditions in the past such as abnormal uterine bleeding. Today the most common situation is a history of pelvic irradiation for carcinoma of the cervix. Postradiation MMMTs develop between 10 and 20 years after the irradiation therapy. Some studies have reported that postradiation MMMTs develop at a younger age than in those women without a history of pelvic irradiation and that the lesion is more widespread at the time of diagnosis in those women. It has also been reported that women with a history of radiation exposure who develop MMMTs are more likely to exhibit heterologous elements in the sarcomatous component.

There is some debate with respect to the nomenclature of this lesion. "Malignant mixed Müllerian tumor" is an older term but one that exerts a strong "hold" on gynecologic oncologists. At one time the term "carcinosarcoma" was reserved for those lesions in which the sarcomatous component was homologous. The terms "malignant mixed Müllerian tumor" or "mixed mesodermal tumor" were reserved for those lesions in which the sarcomatous component was heterologous. At one time it was felt that the heterologous lesions had a worse prognosis, but this is no longer felt to be true. It is now recommended that all these lesions be called "carcinosarcoma" and subdivided into homologous and heterologous types. The term "malignant mixed Müllerian tumor" is deeply ingrained in the clinical gynecologic literature and therefore will not soon disappear.

The histogenesis of this lesion is interesting and in some ways reflects the nomenclature controversy. In an attempt to explain the histogenesis of this lesion three theories have been proposed, that is, the "collision" theory, the "composition" theory, and the "combination" theory (see Table 2).

Table 2. Theoretical developmental schemes for malignant mixed Müllerian tumors

Theory	Mechanism of action
Collision	Epithelial and mesenchymal neoplastic components arise independently and collide giving the appearance of a single mixed tumor.
Composition	The tumor is an adenocarcinoma which provokes the stroma to a degree that results in the development of reactive stromal atypia.
Combination	The tumor develops from a single pluripotential stem cell which retains the ability to differentiate along both epithelial and mesenchymal lines.

"Collision" tumors do occur but they are usually easily recognized. Such tumors are not true MMMTs and should result in little if any diagnostic difficulty.

The "combination" theory is probably the most widely accepted theory at present. Several studies have shown that most (but not all) MMMTs are monoclonal, that is, derived from a single cell line. During embryological development the uterine fundus is formed by fusion of a portion of the Müllerian ducts. The Müllerian epithelium (derived from coelomic epithelium) then differentiates into endometium and stroma. It is thought that MMMTs develop in a similar fashion, that is, from a primitive pluripotential stem cell that gives rise to a monoclonal population which differentiates into both epithelial and stromal components. The development of primary peritoneal carcinomas ("ovarian carcinoma of extraovarian origin") is theoretically related to this same process.

There is evidence that the "combination" theory may not apply in all cases of MMMTs. The "composition" theory explains some of the observations in MMMTs better than does the "combination" theory. Not all MMMTs are monoclonal. The epithelial portion of MMMTs is generally the most aggressive component. Lymphovascular invasion almost always involves the epithelial component. Distant metastasis is almost always of the epithelial component. The sarcomatous component seems to have little metastatic ability. The biological behavior of MMMTs does not seem to be related to the grade, mitotic index, or type of sarcomatous elements present but is much more reflective of the type and grade of epithelial elements present. These findings offer support to the "composition" theory in which the "sarcomatous" component may be only an atypical bystander. However, when MMMTs and pure carcinomas of the endometrium are compared, matching the epithelial components by type and grade and the patients by stage, MMMTs have a poorer prognosis.

Women with stage I disease have about a 50% five-year survival. In general, the overall five-year survival rate with MMMTs is less than 20%.

5. UTERINE LEIOMYOSARCOMA

Leiomyosarcoma is the most common "pure" sarcoma that occurs in the uterus. They account for approximately 45% of uterine sarcomas. If malignant mixed Müllerian tumors are excluded from the category of uterine sarcomas (as some believe they should be) then leiomyosarcomas account for approximately 80% of all uterine sarcomas. The proportion of smooth muscle tumors of the uterus that are malignant reportedly ranges from 0.13% to 6%. That is a 50-fold variation which reflects the various diagnostic criteria used by different pathologists in making that diagnosis.

Leiomyosarcomas occur during the third to ninth decade of life. Most women are over the age of 40 years when diagnosed. This is about 10 years older than the typical patient with benign leiomyomata. Leiomyosarcomas may be more common in black women (similar to leiomyomata) and there has been some indication of increased frequency in women taking tamoxifen for breast cancer (a similar observation has been made in uterine adenosarcomas as well). These lesions usually present with abnormal vaginal bleeding, pelvic pain, and an enlarged uterus.

Grossly, these lesions typically present as a solitary mass that may or may not be accompanied by one or more benign leiomyoma. If several smooth muscle lesions are present the leiomyosarcoma is usually the largest of the group. Two-thirds of the leiomyosarcomas are intramural in location while the remaining are submucosal or subserosal. Gross examination may be helpful in making a diagnosis. Leiomyosarcomas

often exhibit an infiltrative border grossly, which is markedly different in appearance from the sharply circumscribed border of a leiomyoma (see Figure 4). The cut surface of a leiomyosarcoma often lacks the "bulging" appearance of a leiomyoma and the typical whorled appearance of the leiomyoma is absent. The consistency of leiomyosarcomas differs from that of leiomyomata. The typical leiomyoma has a firm, rubbery consistency, whereas a leiomyosarcoma typically has a softer "fleshy" consistency.

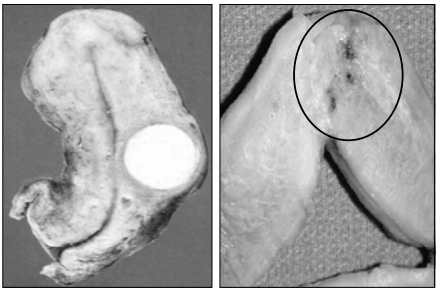

Figure 4. Right: Leiomyoma exhibits a sharply circumscribed border. Left: Leimyosarcoma exhibits an infiltrative border (circled area).

The variation in the percentage of malignant smooth muscle tumors noted above reflects the variation in diagnostic histopathologic criteria used in making a diagnosis of leiomyosarcoma. There is a wide range of histologic appearances that fall within the scope of leiomyosarcomas of the uterus, depending on the grade of the lesion and whether or not any of the less typical varieties are present. The typical features of a leiomyosarcoma include hypercellularity, diffuse cytologic (nuclear) atypia, and increased mitotic activity (usually ten or more mitotic figures per 10 HPFs) (see Figure 5). Other factors of importance include the presence of coagulative tumor cell necrosis, atypical mitotic figures, and an infiltrative tumor border.

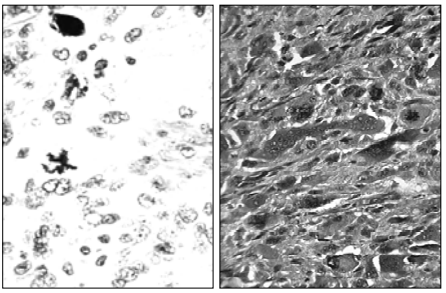

Figure 5. Leiomyosarcoma. The tumor is hypercellular and individual cells show marked nuclear atypia and increased mitotic activity. (H&E, x400)

Survival rates obviously depend upon the grade and extent of the lesion at the time of diagnosis. Survival rates have been variously quoted ranging from 15% to 30% with a mean survival ranging from 13 to 43 months. Most tumor-related deaths are due to distant metastasis often associated with local recurrence. Tumor size of less than 5 cm has been noted to be a relatively good prognostic indicator while a tumor size larger than 8 cm, vascular invasion, and infiltrative margins have been cited as adverse prognostic indicators.

6. PAGET'S DISEASE OF THE VULVA

Extramammary Paget's disease remains a mystery with respect to the cell of origin and its pathogenesis. Origin from intraepithelial stem cells or cells from sweat ducts has been postulated but never proven. Unlike Paget's disease of the breast there is almost never an underlying malignancy in extramammary Paget's disease. However, it has been stated that about 30% of the patients with extramammary Paget's disease will have a

synchronous internal carcinoma, usually involving the breast, uterine cervix, or urinary bladder unrelated to the Paget's disease.

Extramammary Paget's disease accounts for 1% to 5% of all vulvar malignancies. The patients are older, usually in the seventh decade of life although the disease may occur in late reproductive life. The disease may be present for years prior to diagnosis as a result of either the patient neglecting the disease or its being treated as some type of inflammatory reaction which it may resemble. The disease presents as a moist, weeping, erythematous, raised plaque associated with intense pruritis and burning. The erythematous weeping patches may be interspersed with areas of "leukoplakia" (hyperkeratosis) or ulceration. The lesion may initially be confined to the labia but later may extend to involve the clitoris, mons pubis, urethra, perianal area, and medial areas of the thighs.

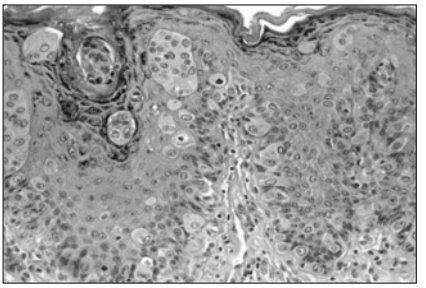

Figure 6. Paget disease of the vulva. The lesion is characterized by the presence of large, pale-staining epithelioid cells in the epidermis. (H& E, x200)

Histologically, the lesion is characterized by the presence of large, pale-staining epithelioid cells which are larger than the surrounding keratinocytes (see Figure 6). These cells are present within the epidermis as single cell, in small clusters, and occasionally in glandular formation. A characteristic finding is clustering of tumor cells in the basal areas of the epithelium but epidermotrophic infiltration of the upper areas of the epidermis is usually present. The cells may infiltrate into the pilosebaceous units and sweat ducts. Rarely, the tumor cells will exhibit superficial invasion into the underlying dermis. Regional metastasis to local lymph nodes is a rare occurrence. The individual tumor cells are large, contain a vesicular nucleus, prominent nucleolus, and abundant pale amphophic cytoplasm.

The differential diagnosis includes superficial spreading malignant melanoma and pagetoid vulvar intraepithelial neoplasia. Diagnosis may be facilitated by histochemical stains for mucin and immunohistochemical stains for S-100, HMB-45, CEA, and CK7 (see Table 3).

Table 3. Differential immunophenotype

Entities	Mucin	S-100	HMB-45	CEA	CK7
Paget's disease	Positive	Negative	Negative	Positive	Positive
Pagetoid VIN[†]	Negative	Negative	Negative	Negative	Negative
Melanoma	Negative	Positive	Positive	Negative	Negative

Recurrence is extremely common following excision of the lesion. In fact, the margins of excision on resected lesions are more often positive for tumor cells than not. This, plus the fact that the tumor cells spread down into pilosebaceous units and sweat ducts, account for a very high rate of recurrence. Multiple recurrences are common over a

[†] VIN: vulval intraepithelial neoplasia.

period of many years. Progression to invasive disease rarely occurs. Invasion to a depth of greater than 1.0 mm, when it does occur, is associated with a worse prognosis with increased risk of regional lymph node metastasis, distant metastasis, and potential death from the disease.

7. ADENOID BASAL CARCINOMA OF THE CERVIX

Adenoid basal carcinoma is a rare and frequently asymptomatic tumor of the cervix which occurs in older postmenopausal females, especially Afro-American females. The median age of these patients is 60 years. The lesion is often associated with high-grade CIN and frequently is diagnosed incidentally during evaluation of hysterectomy or cervical cold knife cone specimens for HGSIL following an abnormal Pap smear. An association with HPV (typically HPV-16) has been observed as the neoplastic cells exhibit immunoreactivity with HPV-16 antibodies. Occasionally, the lesion is a completely incidental finding in hysterectomy specimens done for other unrelated conditions such as endometrial hyperplasia in patients with a normal cytology history. Grossly, the cervix is usually unremarkable or at most may demonstrate a slight degree of nodularity.

Microscopically, the tumor resembles basosquamous cell carcinoma of the skin with nests of relatively bland small tumor cells which exhibit peripheral palisading. The individual tumor cells are oval and hyperchromatic with an increased N/C ratio and occur in small nests and cords which may exhibit branching. These nests may be widely spaced. A stromal response may or may not be present. The edges of the neoplastic nests and cords are smooth rather than irregular and jagged (as seen in typical invasive squamous cell carcinoma). The centers of the nests may demonstrate focal areas of glandular differentiation with small acini lined by a single layer of cuboidal to columnar epithelium sometimes producing mucin. Squamous differentiation is also encountered. Nests containing areas of squamous differentiation usually retain peripheral palisading of small oval cells. The lesion is frequently associated with areas of high-grade squamous dysplasia and rarely may be found merging with areas which demonstrate microinvasive or invasive squamous cell carcinoma. The lesion is thought to arise from pluripotential reserve cells of the endocervix. It is usually found deep to the endocervical glands and for that reason may not be seen in routine cervical biopsy or superficial LEEP cone specimens. This lesion must be distinguished from the more aggressive adenoid cystic carcinoma of the cervix which is similar in appearance to an adenoid cystic carcinoma of the salivary glands.

No pure case of adenoid basal carcinoma of the cervix has ever been reported to have metastasized or to have caused the death of the patient. For that reason some have argued that this is not a malignant lesion and have proposed the term “adenoid basal epithelioma” for it. Others argue that the lesion should retain its malignant classification based on the fact that it can be deeply infiltrative, occasionally extends to the lower uterine segment, and has occasionally presented as a grossly ulcerated symptomatic mass.

8. SMALL-CELL NEUROENDOCRINE CARCINOMA OF THE CERVIX

This highly aggressive tumor is basically an “oat” cell carcinoma similar to those seen in the lung and other organs. Small-cell neuroendocrine carcinomas, carcinoid

tumors, atypical carcinoid tumors, and large-cell neuroendocrine carcinomas of the cervix are generally placed into a heterogeneous group referred to as “endocrine tumors” by some investigators. Small-cell neuroendocrine carcinomas are the most frequently encountered lesion among those within this group, accounting for about 2% of all cervical carcinomas. They are thought to arise from agyrophilic cells found within endocervical and ectocervical epithelium in normal females. Molecular studies have demonstrated that these tumors share features with both small-cell carcinomas of the lung and typical squamous cell carcinoma of the cervix. These tumors are found within a wide range of age from the third to the ninth decades of life. The median and mean is in the fifth decade. These lesions usually present with vaginal bleeding. Rarely, there is evidence of hormonal production (ACTH, insulin, serotonin, or vasopressin), either biochemical or clinical. A history of abnormal Pap smear may or may not be present in these women. Pelvic examination generally reveals a cervical mass that is often ulcerated and deeply infiltrative.

Histologically, these tumors are very similar to their counterparts in the lung. They consist of sheets, nests, and cords of small hyperchromatic cells associated with areas of necrosis. Pseudo-rosette or acinar structures may be present. The nuclear features are those classically found in neuroendocrine differentiation, that is, a finely dispersed granular “salt-and-pepper” pattern and may exhibit smudging and “molding.” Nucleoli generally are not prominent. Mitotic activity may be brisk. The tumor may exhibit crush artifact. Occasionally, a tumor will exhibit so-called “intermediate type cells” which have larger round to oval more uniform nuclei with coarser chromatin and prominent nucleoli. These cells are often admixed with the more classical “small-cells.” Small-cell neuroendocrine carcinoma of the cervix may be present in a “pure” form but frequently it is admixed with a typical squamous cell carcinoma or endocervical adenocarcinoma. I have seen one case in which an endometrial small-cell neuroendocrine carcinoma was present in association with an endometrial adenocarcinoma.

The histopathological features on routinely stained sections of small-cell neuroendocrine carcinoma usually suggest the possibility of that diagnosis. However, the differential diagnosis includes poorly differentiated nonkeratinizing squamous cell carcinoma of the small-cell type, malignant lymphoma, and less commonly other lesions such as endometrial stromal sarcoma. The diagnosis is confirmed immunohistochemically with neuroendocrine markers (NSE, synaptophysin, and chromogranin). A negative leukocyte common antigen (CD45) effectively excludes malignant lymphoma.

About 75% of these women present as clinical stage I or II, but over 50% of them are found to be surgical stage III or IV, attesting to the aggressive nature of this lesion and its propensity for early and widespread metastasis. Frequent sites of metastasis are distant lymph nodes, lung, bone, brain, and liver. The overall five-year survival is less than 25% and most patients die within the first two years. The prognosis is better in surgical stage I or II patients who as a group exhibit a five-year survival of about 70%.

9. SCLEROSING STROMAL TUMOR OF THE OVARY

Sclerosing stromal tumors are benign unilateral ovarian tumors 80% of which usually present within the first three decades of life (mean age is 27 years). All reported cases have been clinically benign. They usually present as a pelvic mass but rare cases

have been associated with estrogen or androgen production. Grossly, the tumor is present as a discrete mass that is well circumscribed. The cut surface is usually white but may show yellowish areas, edema, and cystic changes. Rarely, the tumor presents as a cystic mass.

The typical low-power microscopic feature of this lesion is the presence of a distinctive pseudolobular pattern with cellular neoplastic islands separated by a paucicellular fibrous, collagenous, or edematous connective tissue stroma. Another distinctive low-power feature of this lesion is the presence of a prominent vascular pattern. The blood vessels are thin-walled and may be dilated, resembling a hemangiopericytoma.

Higher-powered microscopic examination reveals the cellular islands to be predominantly composed of relatively large rounded neoplastic cells with vacuolated cytoplasm and an eccentric nucleus with a "shrunkened" appearance and may occasionally exhibit a "signet ring" appearance (however, they cells contain lipid rather than mucin). These cells are mixed with variable numbers of fibroblasts and areas of collagenous deposition ("sclerosis") are frequently found. Mitotic figures are infrequent. In the rare case of a functioning sclerosing stromal tumor one may encounter luteinized cells similar to those seen in luteinized thecomas. Occasionally, nonfunctioning sclerosising stromal tumors may contain prominent typically luteinized cells.

The differential diagnosis includes ovarian fibromas and thecomas. Sclerosing stromal tumors exbibit a more heterogeneous appearance than either of these tumors which lack a pseudolobular appearance, prominent vascularity, and intimate admixture of vacuoalted tumor cells and fibroblasts. Krukenberg tumors may be confused with sclerosing stromal tumors but the signet ring cells contain mucin rather than the lipid found in sclerosing stromal tumors. The prominent vascular pattern may suggest a hemangiopericytoma, but these tumors do not exhibit any of the other characteristic features of sclerosing stromal tumors.

10. SERTOLI CELL TUMOR

These relatively uncommon ovarian tumors account for about 4% of all ovarian stromal tumors, generally following a benign clinical course. They occur in all age ranges with a mean of 30 years. They usually present as a pelvic mass but may produce various hormone- related symptoms in the rare case of a functioning tumor. Hormonal production may include estrogens, androgens, and rarely progesterones and renin (leading to hypertension).

These tumors are usually unilateral and present as a solid, lobular cut surface which is usually yellow or brown.The average diameter is about 9.0 cm. Microscopically, the most characteristic finding is the production of tubules which are always present and, depending upon the degree of differentiation, may be abundant. The tubules may be hollow or solid and are thought to represent the recapitulaion of seminiferous tubules. They are occasionally present in lobules that are separated by fibrous stroma which may show areas of hyalinization. The individual tubules are lined by cuboidal cells which may be either eosinophilic or pale and vacuolated. These cells are typically reactive for cytokeratin and occasionally for vimentin. About 50% of the tumors are reactive for inhibin. Nuclear atypia and mitotic activity are usually minimal but may be present to a greater degree in poorly differentiated lesions.

The differential diagnosis includes well-differentiated Sertoli–Leydig cell tumors. Pure Sertoli cell tumors lack the Leydig cells found in the Sertoli–Leydig cell tumors. Occasionally, a Sertoli cell tumor is confused with a granulosa cell tumor which may exhibit a pronounced trabecular pattern simulating the appearance of the tubules found in a Sertoli cell tumor. However, the other distinctive features of a granulosa cell tumor are not present. Granulosa cell tumors usually produce a variety of patterns which aids in making that diagnosis.

11. REFERENCES

1. Kurman RJ, Norris HJ, Wilkinson E, *Tumors of the Cervix, Vagina, and Vulva* (Armed Forces Institute of Pathology, Washington, DC, 1992).
2. Silverberg SG, Kurman RJ, *Tumors of the Uterine Corpus and Gestational Trophoblastic Disease* (Armed Forces Institute of Pathology, Washington, DC, 1992).
3. Gompel C, Silverberg S, *Pathology in Gynecology and Obstetrics* (J.B. Lippincott, Philadephia, PA, 1994).
4. Kurman R, *Blaustein's Pathology of the Female Genital Tract,* (Springer-Verlag, New York, NY, 1994).
5. Scully RE, Young RH, P.B. C, *Tumors of the Ovary, Maldeveloped Gonads, Fallopian Tube, and Broad Ligament* (Armed Forces Institute of Pathology, Washington, DC, 1998).
6. Clement PB, Young RH, *Atlas of Gynecologic Surgical Pathology* (W.B. Saunders, Philadephia PA, 2000).
7. Robboy SJ, Anderson MC, Russell P, *Pathology of the Female Reproductive Tract* (Churchill Livingstone, London, UK, 2001).

CHAPTER 3
WHO IS WHO AMONG UROTHELIAL NEOPLASMS?

Katrin M. Klemm, M.D.*

1. INTRODUCTION

The objectives of this review are: (1) review WHO/ISUP Consensus Classification with comments on particular lesions to follow; (2) review of flat lesions of the urinary bladder; (3) review of invasive neoplasms with an emphasis on the potential diagnostic pitfalls and problems.

Table 1 summarizes the most WHO/ISUP Consensus Classification for urothelial neoplasms.[1]

Table 1. WHO/ISUP consensus classification for urothelial neoplasms (modified from Ref. 1)

Category	Lesions
Normal	Normal urothelium
Hyperplasia	Flat hyperplasia
	Papillary hyperplasia
Flat lesions with atypia	Reactive epithelial atypia (inflammatory)
	Atypia of unknown significance
	Dysplasia (low-grade intraurothelial neoplasms, previously known as mild dysplasia)
	Carcinoma in situ (high-grade intraurothelial neoplasm, including severe dysplasia)
Papillary neoplasms	Papilloma
	Inverted papilloma
	Papillary neoplasms of low malignant potential
	Papillary carcinoma, low-grade
	Papillary carcinoma, high-grade
Invasive neoplasms	Lamina propria invasion
	Muscularis propria invasion

* Assistant Professor, Department of Pathology, University of Alabama, Birmingham, AL.

2. NORMAL UROTHELIUM

These lesions are characterized by orderly to minimally disordered architecture, normal cytology, with three to five layers of cells. Caution must be exercised when evaluating these cases, as variation in staining and fixation may make benign nuclei appear hyperchromatic, resulting in overcalled cases of mild dysplasia.

3. UROTHELIAL HYPERPLASIA

3.1 Flat Urothelial Hyperplasia

It is characterized by markedly thickened (>7 cell layers) mucosa that *lacks cytologic atypia.*(see Figure 1).[2] When this is present as the sole lesion, flat urothelial hyperplasia has no premalignant potential.

3.2 Papillary Urothelial Hyperplasia

This lesion is characterized by variably thickened urothelium without *cytologic atypia*. These lesions exhibit a corrugated or papillary growth pattern and are mostly

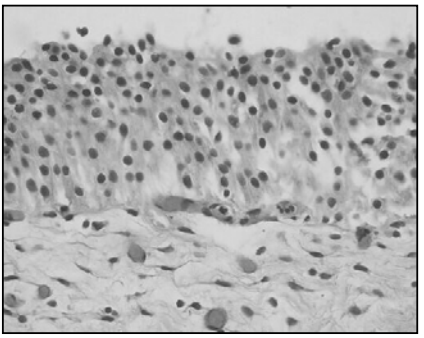

Figure 1. Flat urothelial hyperplasia. Note thickened epithelium devoid of cytologic atypia. (H&E)

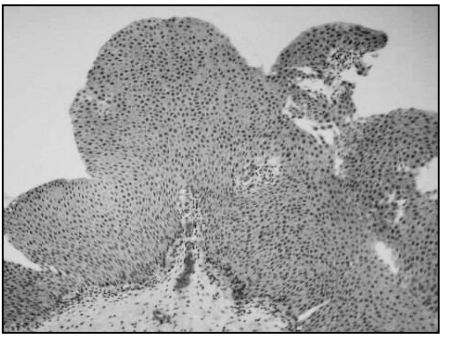

Figure 2. Papillary urothelial hyperplasia. Note the thickened epithelium without cytologic atypia covering a rudimentary papillary structure. Also note the dilated capillaries at the base of the lesion. (H&E)

found on follow-up for papillary urothelial neoplasms (see Figure 2). These lesions lack the well-developed fibrovascular cores and papillary architecture of papillary neoplasms. Often, these lesions show a small proliferation of ectatic capillaries at the base of the papillae.

The diagnosis of papillary urothelial hyperplasia is clinically significant, and follow-up of a diagnosis of papillary urothelial hyperplasia is warranted.[3] This clinical significance was based on the findings that approximately 70% of patients have prior or synchronous papillary cancer; concurrent moderate urothelial atypia is seen in approximately 5-10% of cases; the longest disease-free survival in a patient without a

history of urothelial neoplasia in a study by Taylor et al. was 5 years; and a diagnosis of PUH in a patient with a prior papillary neoplasm may be associated with an increased risk of recurrence.

Papillary urothelial hyperplasia differs from papillary urothelial neoplasms by a lack of cellular atypia, arborization, and detached papillary fronds.[3] This lesion must also be distinguished from papillary and polypoid cystitis, which represent inflammatory rather than preneoplastic lesions characterized by a polypoid or papillary growth pattern, reactive cellular atypia, and an inflammatory background (see Figure 3). These lesions are often seen in the setting of indwelling catheters or a history of instrumentation.

4. FLAT LESIONS WITH ATYPIA

4.1 Reactive (Inflammatory) Atypia

This entity encompasses the nuclear atypia seen in chronically inflamed urothelium. Mildly disordered cellular arrangement is often present in these lesions. The acceptable nuclear changes that may be seen in this lesion include vesicular chromatin, uniform nuclear enlargement, and prominent central nucleoli (see Figure 4). Mitotic figures are customarily present and can often be numerous. However, atypical mitotic figures may not be seen. A history of instrumentation, catheterization, stones, or prior therapy is often found upon investigation of the clinical setting.

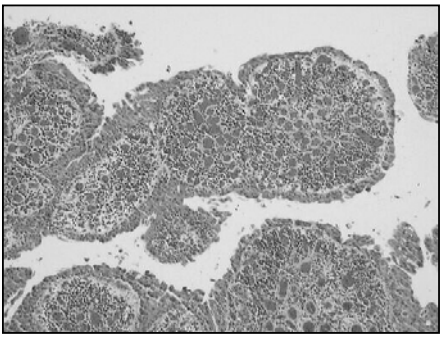

Figure 3. Polypoid cystitis. Note the markedly inflamed stroma, reactive cellular atypia, and broad fibrovascular core with abundant dilated capillaries. The cellular atypia is not supportive of a diagnosis of papillary urothelial carcinoma. (H&E)

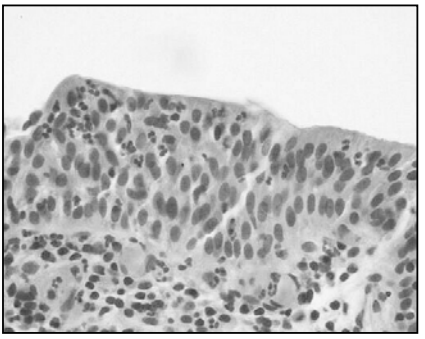

Figure 4. Reactive atypia. This lesion shows a mixture of acute and chronic inflammation and cellular atypia that falls short of dysplasia. Often there are ectatic capillaries at the base of the lesion. (H&E)

4.2 Atypia of Unknown Significance

This category is of utility when a lesion exhibits pleomorphism and hyperchromasia that appears out of proportion to the amount of inflammation present. In these lesions, it may be difficult to exclude with certainty the presence of dysplasia. Rendering this diagnosis is of utility when the pathologist is uncertain, as it will effect closer patient follow-up with further evaluation after resolution of the inflammatory process.

4.3 Dysplasia (Low-Grade Intraurothelial Neoplasia)

This lesion is characterized by preneoplastic cytologic and architectural changes that do not meet the diagnostic criteria of urothelial carcinoma in situ. Poor interobserver reproducibility is seen with these lesions. These lesions are common in urinary bladders with concurrent neoplasia and are uncommon in bladders without neoplasms.[4] A diagnosis of dysplasia in a patient with a known bladder neoplasm represents an increased risk for recurrence and/or progression. Thus, a diagnosis of dysplasia in a patient with a prior diagnosis of neoplasm is likely to result in therapy, given the increased likelihood for recurrence/ progression (see Figure 5).

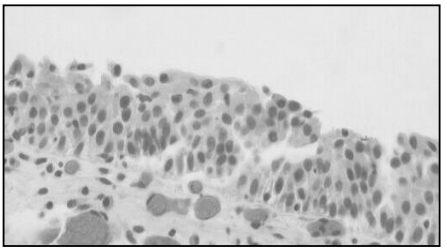

Figure 5. Low-grade intraurothelial neoplasia. Urothelial atypia is present but falls short of CIS. The cells exhibit variation in nuclear size and shape as well as hyperchromasia. The urothelium is slightly thickened. (H&E)

4.4 Urothelial Carcinoma in Situ (High-Grade Intraurothelial Neoplasia)

By definition, the flat lesions of urothelial carcinoma in situ represent high-grade lesions, *thus subclassification by grade is not necessary.* They represent flat urothelial lesions that exhibit atypia in the form of large, irregular and hyperchromatic nuclei that occupy part or all of the thickness of the urothelium. (see Figure 6) Mitoses may be seen at any level of the urothelium, and atypical mitoses can be present. Contrary to prior beliefs, there may still be an umbrella cell layer; the atypia must not necessarily be full thickness; and a high nuclear:cytoplasmic ratio is not always seen. The patterns of carcinoma in situ that may be seen include full thickness involvement by atypical cells, scattered CIS cells, pagetoid spread of CIS, and clinging CIS (also known as denuded cystitis pattern) (see Figure 7).

5. PAPILLARY UROTHELIAL NEOPLASMS

General considerations in evaluating papillary lesions require attention given to the architectural pattern, the organization of the cells within the papillae and the cytology of the constituent cells. (see Table 2) Of note is that the lesions are graded according to the highest grade of abnormality seen, not the most prevalent grade seen.

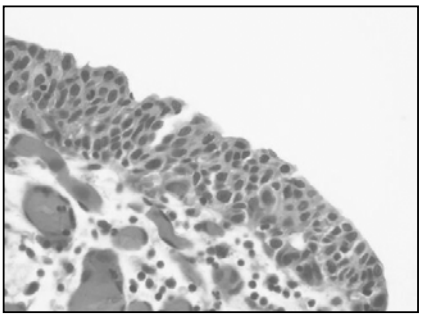

Figure 6. Carcinoma in situ. This lesion exhibits full thickness atypia with enlarged, hyperchromatic nuclei throughout. (H&E)

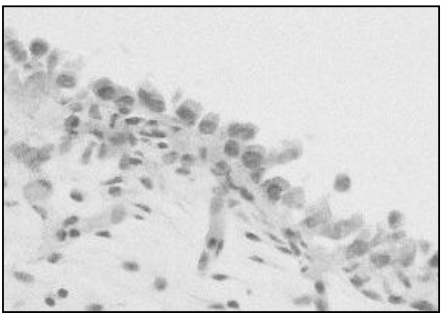

Figure 7. Denuding cystitis pattern of carcinoma in situ: Care must be taken not to miss the few remaining attached cells in this lesion. These cells exhibit marked nuclear atypia, hyperchromasia, and a reduced N/C ratio. Despite the fact that only one cell layer remains in many places, the cytologic features are diagnostic of carcinoma in situ. (H&E)

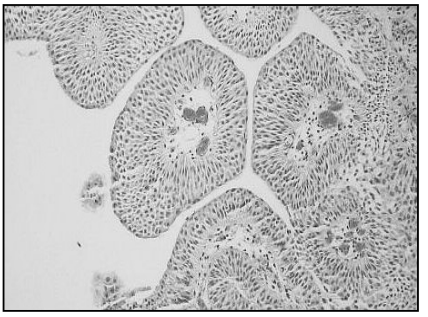

Figure 8. Papillary urothelial neoplasm of low malignant potential. The cells covering the papillae in this lesion are only minimally enlarged and hyperchromatic. Mild epithelial thickening is noted. Mitotic figures are not a prominent feature. (H&E)

5.1 Urothelial Papilloma

These lesions represent an exophytic papillary growth that has a central fibrovascular core lined by urothelium of normal thickness and that is devoid of cytologic atypia.[5] The papillomas represent rare, solitary lesions in predominantly young patients.

5.2 Papillary Urothelial Neoplasm of Low Malignant Potential

These lesions are considered of low malignant potential because there is a finite risk of developing new bladder tumors that are usually of a similar histologic grade, with rare lesions exhibiting more aggressive histologic features and clinical progression. Thus, follow up of these lesions is warranted. No significant association with stromal invasion or metastatic disease has been documented.

Histologically, these lesions retain an orderly cellular arrangement, with minimal architectural aberrations and nuclear pleomorphism. The major distinction from papilloma is that these lesions exhibit thicker urothelium and enlarged nuclei. (see Figure 8) Rare, basally located mitotic figures may be seen.

5.3 Papillary Urothelial Carcinoma, Low-Grade

Low-power overview of these lesions usually reveals distinctly recognizable variation in both cytologic and architectural features. The cytologic features of the lesional cells include mild variation in nuclear size, shape, and chromatin pattern (see Figure 9). Mitoses may be present but are usually confined to the lower layers of the epithelium, though occasional mitoses may be present in the upper layers.

Table 2. Comparison of old and new classification schemes and pathologic features of various entities (modifiedfrom Ref. 1)

WHO/ISP 1998	Papilloma	Papillary urothelial neoplasm of low malignant potential	Low-grade papillary urothelial carcinoma	High-grade papillary urothelial carcinoma
WHO 1973	Papilloma	Papillary TCC, grade I	Papillary TCC, grade II	Papillary TCC, grade III
Papillae	Delicate architecture	Delicate-Occasional fused branches	Any architecture from Fused-Branching-Delicate	Any architecture from Fused-Branching-Delicate
Organization of cells	Normal	Polarity normal, any thickness, cells remain cohesive.	Predominantly ordered arrangement, minimal cellular crowding and loss of polarity. Cohesive.	Predominantly disordered with loss of polarity. Any thickness. Discohesive.
Nuclear size	Normal	May have uniform enlargement	Enlarged with variation in size	Enlarged with variation in size
Nuclear shape	Normal	Elongated, round-oval, uniform	Round-oval with slight variation in shape/contour	Moderate-marked pleomorphism
Nuclear chromatin	Fine	Fine	Mild variation within and between cells	Moderate-marked variation within and between cells and hyperchromasia; chunky chromatin may be seen
Nucleoli	Absent	Absent to inconspicuous	Usually inconspicuous	Multiple prominent nucleoli may be present.
Mitoses	Absent	Rare, when present usually located basally	Occasional, may be seen at any level	Frequent at any level, atypical mitoses often seen
Umbrella cells	Uniformly present	Present	Usually present	May be absent

Caution must be exercised in interpreting tangential sections through the base of the urothelium, as these may yield an appearance of full thickness atypia, resulting in overgrading of the lesion.

5.4 Papillary Urothelial Carcinoma, High-Grade

Low-power overview reveals full thickness atypia with moderate to severe cytologic and architectural abnormalities (see Figure 10). Nuclei exhibit clumped chromatin and marked nuclear irregularities with occasional prominent nucleoli. Mitoses are frequent, found at all levels of the epithelium, and may be atypical. All of the patterns of growth that are seen in flat carcinoma in situ may be seen in these papillary lesions, as both represent high-grade lesions.

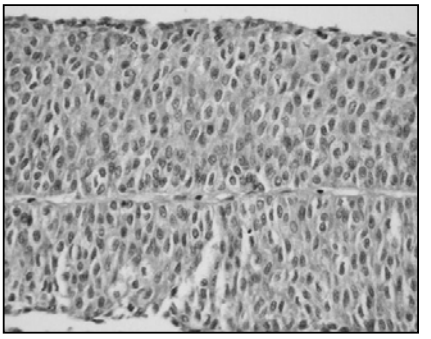

Figure 9. Papillary urothelial carcinoma, low grade. Note the thicker epithelium with increased cellular atypia and slight loss of polarity. The cells exhibit nuclear irregularities and hyperchromasia. (H&E)

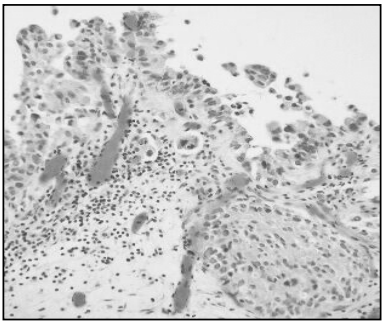

Figure 10. High-grade papillary urothelial neoplasia. Note the denuding cystitis pattern of growth in this high-grade papillary lesion. The cells show loss of cohesion, marked anaplasia, and hyperchromasia. (H&E)

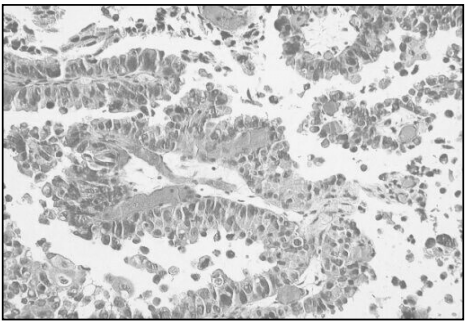

Figure 11. Papillary urothelial neoplasm with superficial invasion and retraction. Superficial stromal invasion with stromal retraction from the invading nests of cells mimicking vascular invasion. (H&E)

Clinically, a diagnosis of high-grade papillary urothelial carcinoma implies a high risk of progression (15-40%) as well as a high risk of a concurrent invasive lesion. Close clinical follow-up with re-biopsy is advised in this setting.

6. INVASIVE UROTHELIAL NEOPLASMS

The layers of the bladder wall include the urothelium, lamina propria/submucosa (+/- muscularis mucosae),[6] and muscularis propria (detrusor muscle). A diagnosis of invasion

should include a statement of the depth of invasion and if the muscularis propria is present.

Potential reporting pitfalls are present when terminology such as “superficial muscle invasion” versus “deep muscle invasion” is used, when the muscle invasion is not further specified (muscle invasion, NOS), and when nonspecific terms such as “superficial bladder cancer,” a term that encompasses CIS, noninvasive papillary neoplasms, and carcinoma with lamina propria invasion, are used (see Figure 11).

Potential diagnostic pitfalls in evaluating invasive neoplasms include problems with the differentiation of invasive disease from inverted growth patterns of noninvasive disease. Careful examination of the basement membrane is of assistance in resolving this dilemma. Another problem that often results in the overdiagnosis of vascular invasion is seen in cases with superficial lamina propria invasion that exhibit retraction (see Figure 12). In cases of uncertainty about lymphovascular invasion, it is best to confirm the presence of CD31, CD34, or Factor VIII–related antigen immunoreactive vascular lining cells. This is especially true in cases of superficial invasion, in which vascular invasion is relatively rare.

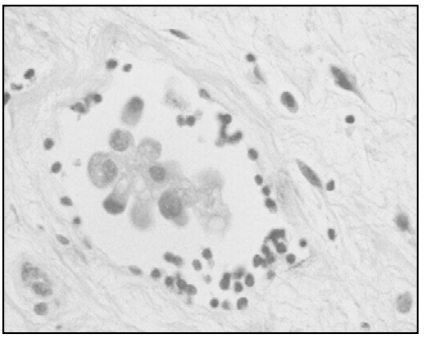

Figure 12. True lymphovascular (LV) invasion. True LV invasion present in the stalk of a papillary urothelial carcinoma. Most cases of LV invasion are subtle, and the use of immunohistochemical study is advocated for a definitive diagnosis of LV invasion. (H&E)

Lastly, the distinction between muscularis mucosa and muscularis propria invasion is sometimes difficult to establish. While it is encouraged that a distinction be made, sometimes it is not possible to do so with certainty on biopsy specimens. In these cases it is best to confirm the presence of smooth muscle invasion, with a comment explaining the uncertainty about which of the muscle coats is involved. In these cases, a follow-up biopsy will be required to establish the depth of invasion with certainty.

6.1 Lamina Propria Invasion

Lamina propria invasion is characterized by clusters of neoplastic urothelial cells or single cells within the lamina propria. The invading neoplasm may be in the form of irregular clusters of cells, single cells, nests of cells with increased architectural complexity, or it may merely exhibit disruption, irregularity or absence of the basement membrane. Morphologic alterations may arise when these tumors invade, in that the lesional cells may appear to have more cytoplasm, often with increased eosinophilia, or merely exhibit an enhanced degree of cellular atypia (see Figure 13).

A high level of suspicion for lamina propria invasion should exist in cases with a high histologic grade in the in situ component. Jordan et al. showed that 96.5% of all invasive neoplasms were associated with high-grade papillary urothelial neoplasms.[7]

The stromal response to an invasive neoplasm is often varied. Awareness of the many variations of stromal response may assist in identification of early stromal invasion. The different stromal reaction patterns range from an absent response, to desmoplasia,

retraction, inflamed stroma, myxoid stroma, and pseudosarcomatous stroma. The retraction pattern of invasion is common in early invasive lesions, especially when the micropapillary growth pattern is prominent. A heavily inflamed stroma can obscure invasive foci. Care must be exercised to recognize the pseudosarcomatous stroma, as this may be misinterpreted as sarcomatoid carcinoma.

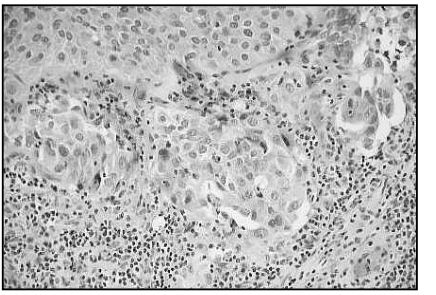

Figure 13. Superficial invasion, cytologic features. Cytoplasm with increased eosinophilia in superficial stromal invasion. (H&E)

6.2 Muscularis Propria Invasion

The presence of muscularis propria invasion must be accurately documented, as its presence represents the level of invasion at which aggressive therapy is often invoked.

The muscularis propria is characterized by thick, not wispy, bundles of smooth muscle below the large vessels of the submucosa. Uncertainty about which muscle layer is invaded must be conveyed to the clinician so that appropriate follow-up studies may be obtained.

7. REFERENCES

1. Epstein JI, Amin MB, Reuter VR, Mostofi FK, The World Health Organization/International Society of Urological Pathology consensus classification of urothelial (transitional cell) neoplasms of the urinary bladder. Bladder Consensus Conference Committee.[see comment]. *American Journal of Surgical Pathology*, **22**(12), 1435-48 (1998).
2. Mostofi FK, Sesterhenn IA, Davis CJJ. Dysplasia versus atypia versus carcinoma in situ of bladder. In: McCullough DL, ed. *Difficult Diagnoses in Urology*. New York, NY: Churchill Livingston, 1988.
3. Taylor DC, Bhagavan BS, Larsen MP, Cox JA, Epstein JI, Papillary urothelial hyperplasia: A precursor to papillary neoplasms. *American Journal of Surgical Pathology,* **20**(12), 1481-8 (1996).
4. Koss LG, Mapping of the urinary bladder: its impact on the concepts of bladder cancer. *Human Pathology,* **10**(5), 533-48 (1979).
5. Cheng L, Darson M, Cheville JC, et al., Urothelial papilloma of the bladder. Clinical and biologic implications.[see comment]. *Cancer,* **86**(10), 2098-101 (1999).
6. Ro JY, Ayala AG, el-Naggar A, Muscularis mucosa of urinary bladder: importance for staging and treatment. *American Journal of Surgical Pathology,* **11**(9), 668-73 (1987).
7. Jordan AM, Weingarten J, Murphy WM, Transitional cell neoplasms of the urinary bladder: can biologic potential be predicted from histologic grading?[erratum appears in *Cancer* 1988 Apr 1;61(7):1385]. *Cancer,* **60**(11), 2766-74 (1987).

CHAPTER 4
DIVERTICULAR COLITIS

Audrey J. Lazenby, M.D.*

1. DIVERTICULAR DISEASE

Diverticular disease is very common in Western countries, with the prevalence increasing with age to involve over 50% of the population by age 85. The pathogenesis is thought to be due to a lack of fiber in the Western diet with resultant low stool volumes. In fiber-rich diets, stools are bulky, which serves to keep the colon distended during muscular activity. On the other hand, with fiber-poor small-volume stools, muscular contraction closes off small areas or segments of the colon, and these segments develop high intraluminal pressure with further muscular contraction. In response to this pressure, portions of mucosa then herniate out along perforating arteries.

While diverticular disease is common, the vast majority of patients (70%) remain asymptomatic. Diverticular bleeding, which can be massive, supervenes in 5-10% of patients, and diverticulitis develops in another 10-25%. Most cases of diverticulits can be treated conservatively with bulk in the diet or with antibiotics, but with complicated diverticulitis (abcess, perforation), surgery is necessary.

The mucosa in the usual case of diverticulitis may show focal ulceration and/or be obliterated by an abcess, but the majority of the mucosa, particularly outside of the diverticula shows little inflammation. However, there are uncommon cases of diverticular disease where there is extensive mucosal inflammation which may be accompanied by crypt distortion and even granulomas. This can cause diagnostic confusion with chronic IBD such as ulcerative colitis or Crohn's disease.

2. CROHN'S DISEASE AND DIVERTICULITIS

For several decades, there have been occasional reports of Crohn's disease complicating diverticular disease. These reports have primarily been small retrospective series in which granulomas were noticed in the histology of resected cases for clinical

* Associate Professor, Department of Pathology, University of Alabama, Birmingham, AL.

diverticulitis. Discussion in these series noted how fistulizing diverticulits was morphologically very similar to Crohn's disease, with both entities showing thickened muscular walls, transmural chronic inflammation, and occasional granulomas. Figures 1 and 2 show a case of diverticular colitis that resmebls the transmural changes of Crohn's disease. Suggested ways to separate the two disorders primarily involved radiologic criteria such as long intramural fistulous tracts. What these case series lacked was good long-term follow-up data on the patients diagnosed as having both Crohn's disease and diverticulitis.

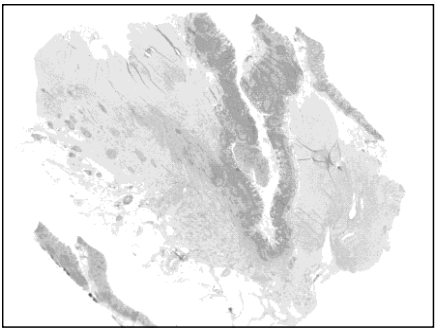

Figure 1. This low-power photomicrograph shows a diverticulum with thickened, surrounding bowel wall and transmural lymphoid aggregates. (H&E)

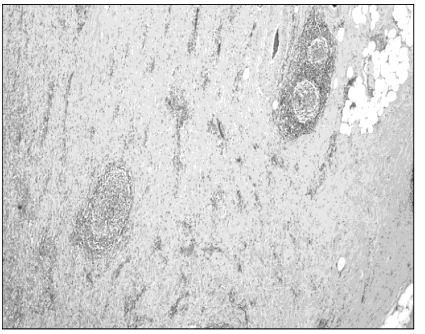

Figure 2. In this higher magnification, the transmural deep lymphoid aggregates are highlighted, which resembles the transmural lymphoid aggregates in Crohn's disease. (H&E)

More recent series (three since 1998) have focused on this same population but have added long-term follow-up. In a study from Wales, eight patients had sigmoid colectomies showing diverticulitis as well as well-formed granulomas and transmural lymphoid aggregates. On mean follow-up of 51 months, none of these patients developed more conventional IBD. From Leeds, England, Gledhill and and Dixon evaluated eleven patients with colonic resections initially diagnosed as both Crohn's disease and diverticulitis. Two patients had a prior diagnosis of chronic bowel disease of some type. One of these was found to have Crohn's disease extending to the hepatic flexure on resection, had been on long-term steroids, and died from complications of wound dehiscence shortly after surgery. The second patient had Crohn's disease of the terminal ileum as well as the sigmoid colon (adherent mass), but remained well since the surgery. The remaining nine patients remained well with no other signs of IBD on follow-up of over ten years. Finally, in work by Neil Goldstein, 29 patients were studied who had sigmoid colon resections that had features of both diverticulits and Crohn's disease. Four out of 29 had a preoperative diagnosis of Crohn's disease and on follow up continued to manifest clinical evidence of Crohn's disease. Of the 25 with no pre-existent IBD, 23 remained free of disease with a median follow-up of 6 years. Two out of the 25, however, developed Crohn's disease in other parts of the bowel.

To mesh older and current work, it appears that with resected specimens showing diverticulitis plus Crohn's-like reactions, the majority do not have Crohn's disease but rather have a marked inflammatory response to the diverticular disease which

histologically mimics Crohn's. A smaller group of patients have a prior diagnosis of Crohn's elsewhere in the GI tract, and do have co-existent Crohn's disease and diverticulitis. And there is a small group of patients whose diverticulitis is the first manifestation of Crohn's disease and go on to develop Crohn's disease elsewhere in the gut. The bottom line is to be wary of the diagnosis of Crohn's disease based solely on the pattern of inflammation accompanying diverticulitis in resected specimens.

3. ULCERATIVE COLITIS AND DIVERTICULAR DISEASE

Also in the literature are reports of a chronic mucosal inflammatory disease accompanying diverticulitis, which had histologic features similar to ulcerative colitis. These cases have been reported under a variety of names including segmental colitis, diverticular disease associated chronic colitis, sigmoiditis, and endoscopic crescentic fold disease. These cases, for the most part, are based on endoscopic and biopsy findings—not resections. Most of the these patients presented as hematochezia and abdominal pain, and on endoscopy were found to have diverticular disease as well as endoscopic features of IBD (granularity and friability) limited to the segment with diverticula. The abnormal mucosa had a variable distribution, ranging from just around the mouths of "tics" to patchy areas extending away from the tics to diffuse disease. Most of these series deal primarily with endoscopic findings and gloss over the histology. One series by Makapugay and Dean did, however, focus on the pathologic findings in these cases. In this series, biopsies of the affected mucosa had features of active chronic IBD, with crypt distortion, basal plasmacytosis, cryptitis, and crypt abcesses. Also noted were prominent lymphoid aggregates at the base of the mucosa and granulomatous inflammation (26%). Rectal biopsies were normal. Despite the presence of granulomas and rectal sparing, Makapugay et al. felt that the histology most closely resembled UC. Figure 3 shows a case of diverticular colitis that resembles ulcerative colitis. Other authors, describing the same type of cases (usually with no pathologist included in the author list), have described the inflammation on biopsy only in passing as "focal active chronic colitis" or "nonspecific."

The outcomes on these patients are variable, in part reflecting a variety of treatments. From an Italian series, by Imperiali et al. 20 patients with hematochezia, pain, and/or diarrhea, met the endoscopic criteria for segmental colitis. In six of these patients, a subsequent second diagnosis was made to explain the endoscopic findings (three Crohn's, two amyloid, one pseudomembranous). Thirteen of the remaining 14 patients had complete resolution of clinical symptoms and endoscopic abnormalities on no specific therapy and one had a clinical and endoscopic relapse that resolved spontaneously after 2 weeks. Peppercorn

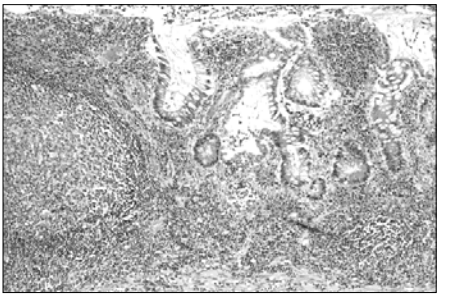

Figure 3. This mucosal biopsy is from a patient with inflammatory changes limited to the region of the diverticula. The rectum (with no diverticula) was normal. Crypt distortion, markedly increased chronic inflammation, and scattered crypt abcesses were present diffusely on the biopsies—a finding that resembles ulcerative colitis. (H&E)

described eight patients who presented with rectal bleeding and mucous and complaints of constipation alternating with loose stools and abdominal pain. All were found to have endoscopic features of chronic IBD limited to the areas of diverticular disease. Peppercorn treated his patients with IBD-type drugs. Five patients went into remission after oral sulfasalazine and three patients had a relapsing and remitting course on therapeutic enemas (hydrocortisone of mesalamine). From Makapugay's series of 23 patients, 14 were treated with high-fiber diets or antibiotics or both and improved clinically as did nine patients who received sulfasalazine or 5ASA. Five patients had to have resection of the diseased area of the sigmoid for stricture or chronic blood loss. While none of the Imperiati or Peppercorm series developed IBD on follow-up, Makapugay's three of 23 patients developed ulcerative colitis at a later date.

4. DIVERTICULAR COLITIS

It is unclear whether the cases of diverticular disease associated with a Crohn's-like reaction and those described as a UC-like reaction are descriptions of the same or different diseases. Because the Crohn's-like reaction can only be fully appreaciated with a resection demonstrating transmural lymphoid aggregates, and because the UC-like cases have been described mainly on biopsies and have been described as having prominent lymphoid aggregates and occasionally granulomatous inflammation, one suspects that these are the same type of disease process, just examined by different methods. It is much like the blind men examining the elephant; the one touching the tusk felt he was examining a spear, the one feeling the trunk decided he was examining a snake, the one touching the tail thought he was holding a rope, and so on. In these patients, with either Crohn's- or UC-like inflammatory reactions, the majority do not appear to progress to classical IBD and can be thought of as an unusual inflammatory reaction associated with diverticular disease. A few patients in each group will progress to classical IBD and some may even have pre-existent IBD. Because both Crohn's and UC like inflammation in diverticular disease have more similarities than differences, I prefer to lump them together and use the designation by Neil Shepherd (Gloucester, England) of "diverticular colitis."

Diverticular colitis is uncommon but not vanishingly rare. In one prospective endoscopic study, it was diagnosed in .25% of all colonoscopies and has been seen in 1–2% of resected diverticulitis cases. While some patients require resection because of complicated diverticulitis, others may be managed by either diverticulitis treatment (high-fiber diet, antibiotics) or with IBD medications (oral or topical). The main take-home message is to be cautious in the diagnosis of Crohn's disease or UC in the face of diverticultar disease. Knowledge of whether there is classic IBD elsewhere in the colon or small bowel is particularly helpful in establishing a dual diagnosis.

5. REFERENCES

1. Berman IR, Corman ML, Coller JA, Veidenheimer MC, Late onset Crohn's disease in patients with colonic diverticulitis. *Diseases of the Colon and Rectum*, **22**(8), 524-9 (1979).
2. Burroughs SH, Bowrey DJ, Morris-Stiff GJ, Williams GT, Granulomatous inflammation in sigmoid diverticulitis: two diseases or one? *Histopathology*, **33**(4), 349-53 (1998).
3. Gledhill A, Dixon MF, Crohn's-like reaction in diverticular disease. *Gut*, **42**(3), 392-5 (1998).

4. Goldstein NS, Leon-Armin C, Mani A, Crohn's colitis-like changes in sigmoid diverticulitis specimens is usually an idiosyncratic inflammatory response to the diverticulosis rather than Crohn's colitis. *American Journal of Surgical Pathology*, **24**(5), 668-75 (2000).
5. Imperiali G, Meucci G, Alvisi C, et al., Segmental colitis associated with diverticula: a prospective study. Gruppo di Studio per le Malattie Infiammatorie Intestinali (GSMII). *American Journal of Gastroenterology*, **95**(4), 1014-6 (2000).
6. Kelly JK, Polypoid prolapsing mucosal folds in diverticular disease. *American Journal of Surgical Pathology*, **15**(9), 871-8 (1991).
7. Makapugay LM, Dean PJ, Diverticular disease-associated chronic colitis. *American Journal of Surgical Pathology*, **20**(1), 94-102 (1996).
8. Marshak RH, Janowitz HD, Present DH, Granulomatous colitis in association with diverticula. *New England Journal of Medicine*, **283**(20), 1080-4 (1970).
9. McCue J, Coppen MJ, Rasbridge SA, Lock MR, Coexistent Crohn's disease and sigmoid diverticulosis. *Postgraduate Medical Journal*, **65**(767), 636-9 (1989).
10. Peppercorn MA, Drug-responsive chronic segmental colitis associated with diverticula: a clinical syndrome in the elderly. *American Journal of Gastroenterology*, **87**(5), 609-12 (1992).
11. Schmidt GT, Lennard-Jones JE, Morson BC, Young AC, Crohn's disease of the colon and its distinction from diverticulitis. *Gut*, **9**(1), 7-16 (1968).
12. Shepherd NA, Pathological mimics of chronic inflammatory bowel disease.[see comment]. *Journal of Clinical Pathology*, **44**(9), 726-33 (1991).
13. Shepherd NA, Diverticular disease and chronic idiopathic inflammatory bowel disease: associations and masquerades. *Gut*, **38**(6), 801-2 (1996).
14. Sladen GE, Filipe MI, Is segmental colitis a complication of diverticular disease? *Diseases of the Colon and Rectum*, **27**(8), 513-4 (1984).

CHAPTER 5
MOLECULAR MARKERS IN BREAST CANCER
Current Practice and Future Possibilities

Thomas Winokur, M.D.*

1. INTRODUCTION

What are we actually speaking of when we use the term "marker"? Practicing pathologists and oncologists have applied the concept for many years without necessarily giving deep thought to what they were doing. Markers are features (of tumors, in the context we are using) that predict future behavior. In fact, the whole exercise of histopathology could arguably be thought of as interpretation of "markers." Traditionally, the features that proved most useful were tumor stage and grade. As useful as these have been there was always an element of stock market disclaimer to them: "Past performance does not necessarily predict future results." The effort to identify important features of tumors has moved inexorably to attempts to identify molecular features of tumors or biomarkers. Ideally, biomarkers would impact oncology in five main areas: cancer screening, diagnosis, tumor classification, prognosis, and predicting therapeutic response.

In breast cancer, stage and grade are statistically successful at predicting the outcome of a population of cancer sufferers, but they lack the ability to aid the therapeutic decision-making process for individuals. For example, a critical question that defies the application of stage and grade is whether a stage I breast cancer will recur and the patient should therefore receive additional therapy at the time of diagnosis. The 1980 National Cancer Institute consensus report recommended therapy for late-stage breast cancer but could find no convincing evidence that women with early-stage tumors benefited from adjuvant therapy.[1] The only useful marker identified beside stage and grade was hormone receptor status. The 2000 consensus report recommended that most women with early-stage tumors should receive adjuvant therapy, but as before the only markers added to stage and grade were hormone receptors. cerbB2, p53, tumor angiogenesis and vascular

* Associate Professor, Department of Pathology, University of Alabama, Birmingham, AL.

invasion were mentioned as possible important markers but were not yet considered sufficiently validated to direct patient management.[2]

Despite this relatively disappointing history of biomarkers, there has been renewed interest in them for two major reasons. First, high-throughput methods in biology allow the simultaneous evaluation of thousands of parameters. This raises the possibility that large panels of markers will be sufficiently sensitive and specific to allow prediction of prognosis in individual patients. Second, pharmacology and pharmaceutical chemistry are identifying molecular targets for therapy. These therapies will only succeed if the target is present, thus driving the industry to develop methods to evaluate tumors for the presence or absence of specific molecular features, that is, amplified cerbB2 in breast cancers or mutated, over expressed c-Kit in gastrointestinal stromal tumors.

2. POTENTIAL USES OF BIOMARKERS

2.1 Screening

The ultimate goal of cancer screening is to inexpensively identify tumors early enough in their histogenesis that they can be extirpated without affecting the host. To date only the PAP smear has served as a proven screening test. Serum PSA and mammography have their advocates but controversy surrounds them. Of these few tests only PSA fits into the biomarker universe. More recently, the use of mass spectrometry of serum has successfully identified ovarian cancer sufferers; however, this there are problems of reproducibility and cost that are likely to restrict this as a screening modality. Ultimately, the species identified by mass spectrometry may be assayed in a more cost-effective manner, allowing cost-effective screening

2.2 Diagnosis

Essentially, diagnostic markers are nonexistent. B-cell clonality comes close as a diagnostic marker of lymphoma, but clonal populations are identified in benign processes. Again, mass spectrometry of serum proteins is touted as a potential diagnostic technique, but it is far from a routine clinical application.

2.3 Classification

This is the one area where molecular signatures commonly impact pathologic diagnosis and ultimately treatment. Virtually all of the currently available immunohistochemical stains play a role in the classification of tumors. Crude classifications are derived from stains such as broad-spectrum keratin, S-100, and leukocyte common antigen, whereas finer subdivisions are made with antibodies to antigens such as prostate-specific antigen and keratin subtypes.

2.4 Prognosis/Therapy

Prognostic markers are of relatively little use unless they can be utilized as determinants of therapeutic action. In breast cancer the two markers currently utilized are the estrogen receptor and the cerbB2 receptor. The expression of these two molecules has specific therapeutic consequences in early- and late-stage breast cancers. Other markers

have been shown to possess some prognostic power, but in the absence of therapeutic consequences they do not fill a critical role and have not gained a foothold in clinical practice.

3. METHODS OF IDENTIFYING MOLECULAR MARKERS

As noted, the availability of new methods to identify biomarkers and groups of biomarkers has driven renewed interest in the field. Several old techniques and many new ones are used in this effort and can be generally grouped by their target. Detailed descriptions of the technologies listed are beyond the scope of this review but are readily available both in the medical literature and on the Web.

3.1 Genome Screening

Screening for abnormalities in genomic DNA has identified tumor markers and has a long history that mostly focuses on relative large structural changes. Gene rearrangements, deletions and amplifications are the focus of these techniques.

The original method for broad screening of the genome for alteration is cyogenetics. Although it requires special expertise, not available in every institution, classical cytogenetics views the entire genome and has the ability to identify changes in a non-directed fashion. Many of the genomic aberrations identified in lymphomas and sarcomas were initially identified this way. In general, carcinomas demonstrate such complex cytogenetic alterations that it has not been possible to reproducibly identify critical structural defects. Breast cancer falls into this category.

A more recent technique for broad genomic screening is comparative genomic hybridization. In this technique DNA from normal and tumor tissue is labeled with different color fluorescent compounds, mixed and used to hybridize to chromosome spreads. The color ratio at any given location on the chromosomes can be used to identify regions of DNA amplification or loss. A recent variation of this is to place the target DNA onto microarrays making this readily available in institutions with microarray readers.

3.2 Expression Screening

Examining RNA expression was a difficult exercise requiring isolation RNA followed by hybridization to one or a few RNA species. Several techniques now allow evaluation of hundreds to thousands of genes simultaneously. This has revolutionized thinking about biomarkers, solidifying the concept of panels. Theoretically, an assay could quantitatively evaluate a large number of RNA messages that would allow molecular grading or staging. Realistically, these assays have so far been utilized more to identify potential biomarkers or biomarker panels. No panels have yet become standard in oncology but some are on the horizon.

3.2.1 Microarrays

Small amounts of specific cDNA or oligonucleotides are spotted onto a solid support in a grid arrangement. Test RNA from normal or tumor (or mixed in some variations) is

hybridized to the grid and the amount of RNA in the test sample can be quantitated. Thousands of RNAs can be simultaneously evaluated. Complex computational algorithms are used to identify genes whose expression is altered in the tumor. Subsequently, custom arrays can be use to evaluate a subset of RNAs that have been identified using large arrays. These smaller arrays can yield prognostic or classification information. This technology has identified a new subset of large-cell lymphoma and has been used to subclassify breast tumors (vide infra).

3.2.2 Serial Analysis of Gene Expression (SAGE)

Quantifying RNA is inherently difficult using microarrays. SAGE is an inherently quantitiative method of examining RNA expression, but the technical complexity of the method has limited its use to a few sophisticated research laboratories.

3.2.3 Reverse Transcriptase-Polymerase Chain Reaction (RT-PCR)

Reverse transcription followed by a polymerase chain reaction is the final method used to evaluate RNA expression. Originally developed to evaluate single messages, RT-PCR can identify and measure several species through multiplexing technologies. At least one clinical assay is about to be commercialized using this technology.[3]

3.3 Proteomics/Protein Screening

As with expression screening, most traditional methods evaluate a single protein. The most prominent example of this in pathology is immunohistochemistry but ELISAs and radioimmunoassays are other examples. Recent advances in separation technologies and mass spectrometry allow measurement of multiple species. Specifically, selective ion desorption ionization (SELDI) and matrix-assisted laser desorption/ionization (MALDI) mass spectrometry can identify hundreds of peptide species from tissue samples. Comparison of tumor and normal tissues can be achieved, or sera from patients with and without cancer can be evaluated. At least one group has claimed to be able to identify ovarian cancer patients by using SELDI evaluation of serum. The reproducibility of the assay has been questioned, but this assay will soon be available commercially. As yet, no similar claims have been made about breast cancer.

3.4 Educated Guessing

This is, in fact, the most successful method of identifying biomarkers. The estrogen receptor, cerbB2 and p53 were all characterized by investigators who understood the basic biology and applied it to breast cancer. This tradition continues as the first large panel that will be offered for breast cancer prognosis was assembled by educated guessing and tested against a group of patients enrolled in the NBSAP breast cancer trials.

4. WHAT IS THE STATE OF THE ART?

A search of Pubmed (Medline) for the search terms “breast cancer” and “molecular markers” identifies 9556 citations, but the NCI consensus report identifies less than a handful of important markers. Which is the real state of affairs?

In 1999, the College of American Pathologists classified available markers into three categories:[4] Category I markers are proven to have prognostic value and are used for therapeutic decisions. The markers in this group were tumor size, nodal status, nodal micrometastasis, sentinel node status, histologic grade, histologic type, mitotic count and hormone receptor status. It is readily apparent that only hormone receptor status qualifies as a molecular marker and it is not new.

Category II markers are have been extensively evaluated but are not completely validated. In 1999, they included cerbB2 status, p53 mutation, lympho-vascular invasion, proliferation markers, and S-phase fraction. Of these, only cerbB2 has acquired status as a proven marker and only p53 is a novel biomarker that provides information that doesnot overlap with traditional morphologic evaluation. (Both mitotic count and proliferation markers measure the growth rate of the tumor.)

Category III markers are those that have been identified but not extensively evaluated. Interestingly, this is a group composed primarily of molecular markers. It includes DNA ploidy analysis, tumor angiogenesis, epidermal growth factor receptor transforming growth factor alpha, Bcl-2, pS2, and cathepsin D. None of these markers has risen to the category II status, although Bcl-2 appears to be of interest in some studies. It seems reasonable to conclude that new molecular markers have failed to achieve the promise that has been predicted, but several new developments have, once again, raised hopes that real progress is in the offing.

5. ON THE HORIZON

Several groups of investigators have started the arduous task of evaluating huge numbers of potential biomarkers for the classification of breast cancer. By far the most advanced and mature approach is the use of cDNA microarrays. At least three groups have evaluated significant sets of breast cancer for the expression of thousands of genes. The results are simultaneously expected and surprising. As one might predict, based on previous knowledge, the estrogen receptor remains the most powerful discriminator. Both molecular classification and prognosis are highly associated with estrogen receptor status. More surprisingly, breast cancers can be classified by a relatively small number of markers. The largest studies to date resulting from a collaboration of researches from Stanford University and a Norwegian cancer hospital divide breast cancer into five subgroups.[5,6] Two “luminal” types of carcinoma are ER positive and keratin 8/18 positive. There are three ER negative groups. One subgroup overexpresses cerbB2. One subgroup is distinguished by basal-type keratins (keratin 5/6) and one group expresses genes that are typical of normal breast tissue including some genes typical of nonepithelial tissue types. These classifications are further refined by much larger sets of genes. As one would hope, these classifications also correlate with prognosis, with the ER positive groups displaying better prognosis and the basal and cerbB2 positive tumors behaving more aggressively.

A second group based in the Netherlands focused more directly on prognosis (rather than classification) and was able to identify a core group of 70 genes that can strongly predict outcome.[7] Examination of the identified genes demonstrates association with tumor parameters such as proliferation, proteolysis, angiogenesis, and intracellular signal transduction. One of the most surprising aspects of this study was the failure to identify the estrogen receptor or cerbB2 as important prognostic biomarkers. This is especially puzzling because the gene profile successfully distinguishes between ER positive and

negative tumors. A follow-up study of a larger group of tumors duplicated these results and demonstrated a powerful ability to identify both poor prognosis among a group clinically identified as good prognosis and good prognosis among a group clinically identified as poor prognosis.[8] This gene profile has been commercialized and is available from Agendia (in the Netherlands) under the trade name Mammaprint.

A third group based at Duke University also concentrated on the prediction and prognosis. The questions addressed were somewhat different. The presence of ER status and lymph node metastases could be predicted by the expression profiles.[9,10] Of particular interest was the association of interferon-related genes in the profile associated with lymph node metastasis. This, ultimately, will allow testing for susceptibility for metastasis.

Finally, a start-up biotechnology company, Genomic Health, has combined the microarray approach with educated guessing to arrive at a 21-gene profile.[11] The selected markers were grouped into proliferation-associated markers, estrogen receptor and estrogen-regulated markers, cerbB2-related markers, invasion-associated proteases and miscellaneous markers previously shown to have prognostic power. When tested against an archival group of tumors from a National Breast Surgical Adjuvant Project study this group of markers was a powerful prognostic tool. This test result is expressed as a score that is said to correlate with prognosis; however, the method of arriving at the score is not well described. The caveat when evaluating this study is that the women in the study had all been treated with tamoxifen raising the possibility that this test is only valid in a select subset of breast cancers. This test, Oncotype DX, is also commercially available from the company Genomic Health and oncologists have expressed keen interest in using it.

Pathologists are now confronted with at least four groups of data suggesting that multiparameter panels of biomarkers have significant prognostic power, but many questions remain unanswered about the role these tests will play in clinical and pathology practice. First, it is clear that the groups have not arrived at a set of consensus genes. The Stanford/Norway group has used the data from the Dutch and Duke studies and finds their classification is only partially reproduced. The Duke studies identify different genes depending on the exact question posed by the investigators. Should an oncologist use the Mammaprint or Oncotype test? How will the choice drive treatment decisions? These tests cost thousands of dollars. If there is not a clear treatment imperative provided by the results, the test will add cost with limited benefit. Second-generation profiles are already being evaluated to answer some therapeutic questions. Finally, it should be noted that none of these tests has been validated in a large clinical trial. They are offered commercially as lab services, in part, to avoid the stringent validation requirements of the FDA. Until large, diverse groups of patients are studied, a healthy dose of skepticism should be applied.

It is becoming clear that a new era of biomarkers is dawning and that it will center on panels of markers. Of the potential uses of biomarkers only classification and prognosis have been clearly addressed, but investigators have screening, diagnosis, and treatment response on their agendas. The practical implications for pathologists are not yet clear, but while we continue to evaluate traditional histopathologic features as well as ER, PR, and cerbB2 we should remain aware that changes in our practice patterns are near and we need to remain involved in setting the testing agenda for breast cancer specimens.

6. REFERENCES

1. Anonymous, Adjuvant therapy of breast cancer. *NIH Consensus Statement*, 3(3), 1-4 (1980).
2. Anonymous, Adjuvant therapy for breast cancer. *NIH Consensus Statement*, 17(4), 1-35 (2000).
3. Porter DA, Krop IE, Nasser S, et al., A SAGE (serial analysis of gene expression) view of breast tumor progression. *Cancer Res*, 61(15), 5697-702 (2001).
4. Fitzgibbons PL, Page DL, Weaver D, et al., Prognostic factors in breast cancer. College of American Pathologists Consensus Statement 1999. *Arch Pathol Lab Med*, 124(7), 966-78 (2000).
5. Sorlie T, Tibshirani R, Parker J, et al., Repeated observation of breast tumor subtypes in independent gene expression data sets. *Proc Natl Acad Sci U S A*, 100(14), 8418-23 (2003).
6. Sorlie T, Perou CM, Tibshirani R, et al., Gene expression patterns of breast carcinomas distinguish tumor subclasses with clinical implications. *Proc Natl Acad Sci U S A*, 98(19), 10869-74 (2001).
7. van 't Veer LJ, Dai H, van de Vijver MJ, et al., Gene expression profiling predicts clinical outcome of breast cancer. *Nature*, 415(6871), 530-6 (2002).
8. van de Vijver MJ, He YD, van't Veer LJ, et al., A gene-expression signature as a predictor of survival in breast cancer. *N Engl J Med*, 347(25), 1999-2009 (2002).
9. West M, Blanchette C, Dressman H, et al., Predicting the clinical status of human breast cancer by using gene expression profiles. *Proc Natl Acad Sci U S A*, 98(20), 11462-7 (2001).
10. Huang E, West M, Nevins JR, Gene expression profiling for prediction of clinical characteristics of breast cancer. *Recent Prog Horm Res*, 58(55-73 (2003).
11. Garber K, Genomic medicine. Gene expression tests foretell breast cancer's future. *Science*, 303(5665), 1754-5 (2004).

CHAPTER 6
CYTOLOGY AND SURGICAL PATHOLOGY OF THE MEDIASTINUM

Claudia Y. Castro, M.D.,[*] and David C. Chhieng, M.D., M.B.A.[†]

1. INTRODUCTION

Mediastinum refers to the space in the thoracic cavity that is bound by the pleura, sternum, vertebral column, thoracic inlet, and diaphragm. It contains major anatomic structures and can be involved by diverse pathologic processes. It is customarily to divide the mediastinum into several compartments: superior, anterior, middle, and posterior because the lists of differential diagnoses vary according to the location. (see Table 1) In addition, the patient's age may also be helpful. For example, thymoma and carcinoid are less common in children.

Table 1. Differential diagnosis of mediastinal lesions according to its location

Superior and anterior	Middle	Posterior
Thymus	Cysts	Neurogenic neoplasm
Lymph nodes	Lymph node	Lymph node
Germ cell tumors		Cysts
Carcinoid		
Cysts		
Thyroid		
Parathyoid		

Mediastinal lesions are often asymptomatic and detected incidentally in chest x-rays. Occasional patients may present with specific syndromes such as myasthenia gravis in patients with thymoma. Because diagnostic imaging cannot accurately determine the nature of the lesions, fine needle aspiration biopsy (FNA) is often performed to establish a diagnosis preoperatively. The sensitivity and specificity of FNA in diagnosing mediastinal malignant neoplasms range from 87% to 90% and 88% to 100%,

[*] Assistant Professor and Director of Immunohistochemistry Laboratory, Department of Pathology, University of Texas, Galveston, TX.

[†] Associate Professor and Director of Immunohistochemistry Laboratory, Department of Pathology, University of Alabama, Birmingham, AL.

respectively. False positive cases are rare. False negative cases are often encountered in lesions with extensive fibrosis, necrosis, or cystic degeneration. The nondiagnostic rate averages 10%. Major complications, such as pneumothorax and massive hemorrhage, are rare.

This chapter will discuss the two most commonly encountered primary neoplasms of the mediastinum—thymoma and germ cell tumor.

2. THYMOMA

2.1 Classification of Thymoma

The classification of thymic epithelial neoplasm is controversial due to their wide variety of histologic appearances and biologic behavior. The first classification was the one proposed by Dr. Bernatz from the Mayo Clinic in 1961. Since then, other classifications have appeared, some taking into account only histologic features and others combining histologic features and stage.

The current opinions of the thymoma classification are divided between those who believe that histologic classification of thymomas is enough to determine the biologic behavior of these tumors (Bernatz et al. Muller-Hermelink) and those who claim that staging of this tumor (status of the capsule) is the best and only parameter for the evaluation of thymomas (Levine and Rosai, Suster and Moran). Given this controversy, the WHO commissioned Dr. Juan Rosai to establish a panel for the classification of thymomas. After long discussions, a new terminology (not a new classification) was proposed that combined letters and numbers to the various histologic types of thymomas in order to facilitate comparison among the various terms from the existing classifications (see Table 1).

Table 1. Comparison of various classification for thymoma

WHO schema	Barnatz et al.	Muller-Hermelink et al.
Type A	Spindle cell	Medullary thymoma
Type AB	—	Mixed thymoma
Type B1	Lymphocyte rich	Predominant cortical
Type B2	Mixed	Cortical thymoma
Type B3	Epithelial rich	Well-diff thymic carcinoma
Type C	Thymic carcinoma	—

It seems that thymic epithelial neoplasms are a continuum in a spectrum of differentiation, with the mature, encapsulated thymoma representing one end of this spectrum and thymic carcinoma representing the opposite end. We believe (in agreement with Suster and Moran) that the best classification is the one that combines the histologic grading and clinical staging of the lesion as follows:

1. Thymoma (well differentiated): preservation of organotypical features, lack of cytologic atypia.
2. Atypical thymoma (moderately differentiated): preservation of organotypical features, mild to moderate cytologic atypia.
3. Thymic carcinoma (poorly differentiated): loss of organotypical features of thymic differentiation, presence of overt cytologic atypia.

Table 2 summarizes the various staging schemes for thymoma. An interesting observation is that the fifth and sixth editions of the cancer staging by the AJCC do not propose any staging for the classification of thymomas and thymic carcinomas.

Table 2. Comparison of various staging schemes for thymoma

Masaoka et al. (1981)	WHO (1999)	Suster and Moran (1999)
Stage I : encapsulated	Encapsulated	Encapsulated
Stage II: invasion of capsule and or perithymic fat	Minimally invasive	Locally invasive
Stage III gross invasion of adjacent organ	Widely invasive	Widely invasive
Stage IV A: implants	With implants	Metastatic
Stage IV B: metastasis	With distant metastasis	

2.2 Thymoma

Thymomas usually arise in the anterior mediastinum. Other locations include neck, pulmonary hilum and parenchyma, and pleura. Half are found incidentally on chest x-ray in asymptomatic individuals. When symptoms are present, they include cough, chest pain, dysphagia, respiratory infections, cardiac tamponade, and superior vena cava syndrome. Thymomas (30–50%) are associated with red cell aplasia (spindle cell thymoma), hypogammaglobulinemia, combined variable immunodeficiency, pancytopenia, peripheral T-cell lymphocytosis, rheumatoid arthritis, systemic lupus erythematosus, and mysthemia gravis. Thymomas occur in 10–15% of patients with myastemia gravis, and 40% of the patients with thymoma have myasthemia gravis.

Grossly, 80–90% of the thymomas is encapsulated and is easily excised. The cut surface is tan and soft. Fibrous septa extend from the capsule and separate the neoplasm into angulated lobules. Cystic degeneration is common in larger tumors.

Thymomas represent one of the tumors that exhibit the widest varieties of morphological appearances. Classic features include a well-developed lobular architecture under scanning magnification i.e. large, angulated lobules separated by broad bands of fibroconnective tissue. (see Figures 1 and 2) The tumors often demonstrate dual cell population—an admixture of neoplastic thymic epithelial cells and thymic

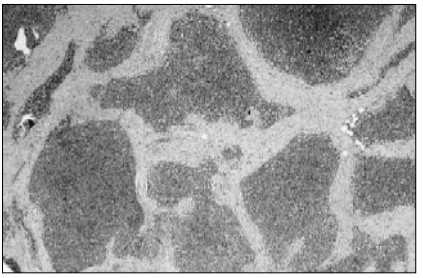

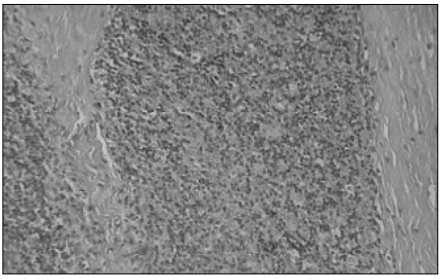

Figures 1 and 2. Thymoma: Low- (left) and medium-power (right) view of encapsulated thymoma with a well developed lobular architecture composed of large, angulated lobules separated by broad bands of fibroconnective tissue. (H&E)

lymphocytes. (see Figure 3) Based on the ratio of the lymphocyte to epithelial cells, thymomas can be classified into the following:

1. "lymphocyte-rich thymoma": massive immature lymphocytes intermixed with few epithelial cells.
2. "epithelial-rich thymoma or predominant cortical thymoma" composed of predominantly epithelial cell with scanty immature lymphocytes.
3. "spindle cell thymoma or medullary thymoma" proliferation of spindled thymic epithelial cells.

Other characteristic features include bland appearance of the epithelial cells, the presence of distended perivascular spaces, and areas of medullary differentiation. The latter consists of solid nodules composed of plump epithelial cells without cytologic evidence of atypia.

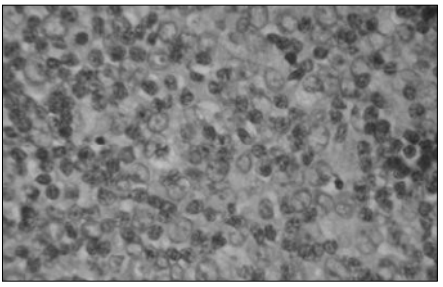

Figure 3. High-power view of thymoma with dual-cell population composed of an admixture of bland thymic epithelial cells and lymphocytes. (H&E)

Morphologic feature that may lead to confusion is the presence of fibrous adhesions to surrounding mediastinal structures accompanied by areas of infarction within cystic spaces which may be mistaken for areas of tumor necrosis, when in reality they represent inflammation/cystic changes.

Unusual variants of thymomas include prominent rhabdoid cell component, heavy plasma-cellular component, pseudosarcomatous spindle cell stromal component, prominent cystic change, and epithelial rosette-like structures.

About 5% of the patients with thymoma will develop mestastasis, most commonly to the chest wall, pleura, lung, bone, spleen, and lymph nodes. Pulmonary metastases from "benign" thymoma in the absence of cytological atypical or evidence of invasion have been well documented. Although it happen with any histologic type of thymoma, is common in the thymoma composed by round or polygonal epithelial cells, but rarely occur in cases of spindle cell thymoma.

Staging is independent of the histologic type: thymomas can be encapsulated or invasive tumors (see Table 2).

The optimal treatment for thymoma is complete excision. The 10-year survival for thymoma by stage is 78% for stage I, 74% for stage II, and 20% for stage III. Stage II patients should receive postoperative radiotherapy. Stages III and IVA should have radiotherapy and chemotherapy. Follow-op after surgery, even for stage I, should be a minimum of 10 years.

2.3 Atypical Thymoma

Similar to thymomas, atypical thymomas retain organotypical characteristics including lobular architecture, dual epithelial/lymphoid cell populations with lesser numbers of immature T-lymphocytes, and an abundance of perivascular spaces.

In contrast to thymomas, atypical thymomas are characterized by a proliferation of large, round to polygonal epithelial cells with abundant cytoplasm, larger vesicular nuclei, prominent nucleoli, and occasional mitotic figures. Foci displaying squamoid features or frank areas of squamous differentiation are frequently present. Palisading of epithelial cells around perivascular spaces simulating glandular lumens is usually seen.

Atypical thymomas can be well circumscribed and completely encapsulated or can be invasive. They tend to be more often invasive than conventional thymomas and infiltrate surrounding structures such as great vessels, pericardium trachea, pleura, and lungs. These lesions correspond to the "well-differentiated thymic carcinomas" by Kirschner and Muller-Hermelink.

2.4 Thymic Carcinoma

The currently reported number is approximately 130 cases. It is defined as a primary thymic epithelial neoplasm with obvious cytological features of malignancy which has lost the organotypical features of thymoma (lobular architectures, dual-cell population composed of epithelial cells and lymphocytes, perivascular spaces, areas of medullary differentiation). A definitive classification of thymic carcinoma has not yet been universally agreed upon. Suster and Rosai in 1991 classified the thymic carcinomas into low-grade and high-grade tumors (Table 3)

The low-grade tumors have a favorable prognosis in contrast to the high-grade ones, which show an aggressive clinical behavior with an average survival of only 15 months.

Table 3. Histology of low- and high-grade thymic carcinoma

Low-grade histology	High-grade histology
Well-differentiated squamous cell carcinoma	Lymphoepithelioma-like carcinoma
Well-differentiated mucoepidermoid carcinoma	Poorly differentiated mucoepidermoid carcinoma
Basaloid carcinoma	Small-cell/neuroendocrine carcinoma
	Clear cell carcinoma
	Sarcomatoid carcinoma
	Anaplastic/undifferentiated carcinoma.

The age ranges from 10 to 75 years with a male/female ratio of 1.5:1. The majority of the patients are symptomatic. Symptoms result from the compression of adjacent structures by the tumor and include dyspnea and superior vena cava syndrome. CXR shows widening of the mediastinum with infiltration of the surrounding structures in high-grade lesions. In low-grade lesions there is a well-circumscribed mediastinal mass.

There is a wide variety of histologic variants, similar to tumors arising at other organs. There is nothing distinctive or pathognomonic about the histology of thymic carcinoma, making it very difficult to establish the primary nature of the lesion in the thymus. Clinical and radiologic correlation is mandatory before making a diagnosis of primary thymic carcinoma. In these carcinomas, the stroma may show infiltration by plasma cells and lymphocytes (the majority are B-cells and mature T-lymphocytes). The clear cell carcinoma represents a well or moderately differentiated squamous cell carcinoma with clear cell change due to the presence of glycogen. The sarcomatoid carcinoma has a biphasic morphology. The stromal component is usually formed by a fibroblastic spindle cell proliferation with marked nuclear atypia. The epithelial component is usually a poorly differentiated carcinoma with high-grade cytology. The

anaplastic variant is a carcinoma with marked cellular pleomorphism, bizarre nuclear features, and atypical mitoses. Lymphoepithelial-like carcinoma, basaloid carcinoma, and small-cell carcinoma show similar morphologic features than the ones arising in the lung.

In one study recurrences were observed in 35% of the cases and metastasis in 50% of cases. Sites of metastases were regional lymph nodes, bone, lung, and liver. The 5- and 10-year survivals of the low-grade tumors were 83% and 67%, respectively, compared to 18% and 15%, respectively, for high-grade tumors. Treatment of the high-grade tumors includes a platinum-based combination of chemotherapy.

2.5 Cytology of Thymoma

Aspirates of thymomas are usually cellular. The key diagnostic feature is the presence of a dual population of epithelial cells and lymphocytes in variable proportion (see Figure 4). The epithelial cells are readily recognizable by their cohesiveness. Rosettes or gland formation and whorls may be present. Individual cells appear round to oval or spindle shaped with variable amount of cytoplasm and nuclear pleomorphism. The lymphoid population is comprised predominantly of small, mature lymphocytes of T phenotypes admixed with scattered larger, transformed lymphocytes. Tissue fragments of variable size and shape are a frequent finding (see Figure 5). They are composed of both lymphocytes and epithelial cells. Fibrovascular stroma is observed in some of the tissue fragments. The presence of tissue fragments may be helpful in the differential diagnosis because they are not usually present in seminomas, lymphomas, or thymic carcinoids. The presence of nuclear atypia in the epithelial cells and/or necrosis correlates with the aggressive behavior. Tumors that are well encapsulated and have a benign clinical course tend to demonstrate benign-appearing epithelial nuclei. However, the converse may not be true. In one study, about two-thirds of thymomas that display aggressive behavior demonstrate no atypia. Other cytologic parameters, such as the ratio of lymphocyte to epithelial cells and the presence of nucleoli, bear no relation to tumor aggressiveness.

Table 4 summarizes the differential diagnosis of thymoma based on the relative proportion of lymphoid and epithelial cells. Distinguishing an enlarged thymus from thymoma can be challenging. The finding of well-formed Hassall corpuscles favors an enlarged thymus gland, but they may not be present in every case. Thymic hyperplasia usually occurs in children whereas thymoma often occurs in adults.

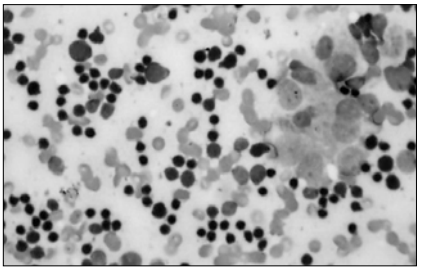

Figure 4. Thymoma. A cohesive group of epithelial cells with lymphocytes in the background. (Diff Quik stain)

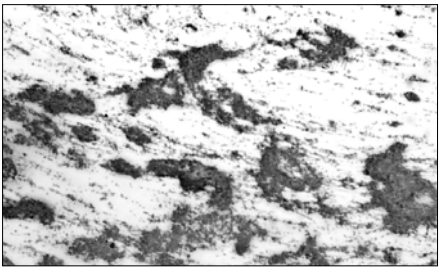

Figure 5. Thymoma. Cellular smear showing numerous tissue fragments of variable size and shape. (Diff Quik Stain)

Table 4. Differential diagnosis of thymoma according to the L:E ratio and cell types

Cytologic features	Differential diagnosis
Dual lymphoid and epithelial populations	Enlarged thymus gland
	Seminoma
Predominantly lymphoid population	Lymphoma
	Hodgkin's disease
	Large-cell lymphoma
	Lymphoblasticlymphoma
	Follicular hyperplasia
Predominantly epithelial population	Carcinoma, primary and metastatic
	Germ cell tumor
	Carcinoid
Spindle-shaped cells	Granulomatous inflammation
	Spindle cell carcinoid
	Peripheral nerve sheath tumor
	Malignant spindle cell neoplasms
	Sarcomatoid carcinoma
	Melanoma
	Sarcoma

Most primary lymphomas of the mediastinum are Hodgkin's disease, large-cell lymphoma, and lymphoblastic lymphoma. They usually affect children and young adults. One exception is large-cell lymphoma, which can occur in older men. Cytologically, the lack of lymphoglandular bodies and the presence of cohesive aggregates of epithelial cells and tissue fragments are not features of malignant lymphomas. In addition, large-cell lymphomas are usually of B-phenotype. Hodgkin's disease is recognizable by the finding of Reed-Sternberg cells and variants as well as background reactive inflammatory infiltrate. The differential diagnosis should also include follicular hyperplasia of adjacent lymph nodes. The mixed lymphoid population is mostly of B-phenotype and there is a conspicuous presence of plasma cells. The presence of cytokeratin positive cells favors a thymoma. However, entrapped thymic tissue in lymphoma, resulting in the presence of cytokeratin-positive epithelial cells, may be misinterpreted as thymoma.

3. MEDIASTINAL GERM CELL TUMORS

Primary mediastinal seminomas (MS) are pure and/or combined neoplasms histologically similar to their gonadal counterparts. After teratoma, seminoma is the second most common example of pure germ cell tumors of the mediastinum, accounting for 37% of all mediastinal germ cell tumors. MS arise from primordial germ cells that have become displaced and embedded outside the gonads along midline structures during embryogenesis.

The majority of cases occur in men, with occasional reports in women. The ages range from 14 to 79, with a mean of 49 years. Most patients are asymptomatic and the mass is found incidentally on routine chest x-ray. When symptoms are present, they include pain, cough, dyspnea, dysphagia, and superior vena cava syndrome (5–10%). Other conditions associated with MS include ventricular septal defect and congenital

absence of seventh thoracic left hemivertebrae, pulmonary stenosis, and gynecomastia. Chest x-rays show a bulky, well-circumscribed lobulated noncalcified anterior mediastinal mass that may extend into the inferior and posterior compartments.

The tumor size varies from 5 to 10 cm. The parenchyma is homogenous gray-tan, solid, multinodular, and soft. Focal areas of necrosis and hemorrhage are common. Some tumors may appear encapsulated, while others have infiltrative borders.

The histology of primary mediastinal seminoma resembles its counterpart of the testes and ovaries. However, cases of anaplastic seminoma occurring in the mediastinum are very rare. On low power, the tumor is divided in nests or lobules by thin delicate fibrovascular septa. The neoplastic cells show round to polygonal distinct cell borders, clear or light pink cytoplasm, and round nuclei with prominent nucleoli (see Figures 6 and 7). Variable mitotic figures are seen, ranging from 3 to 7 per 10 high power fields. Cellular atypia is uncommon. The tumor is usually associated with a prominent lymphoid infiltrate and noncaseating granulomas are seen in 45–80% of the cases. The number of mitosis, presence or absence of lymphocytes, necrosis, or atypia do not have any prognostic significance.

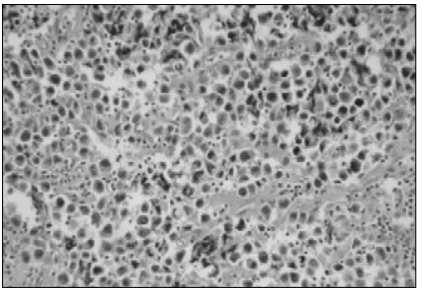

Figure 6. Seminoma. Low-power view showing nest of cells divided by thin fibrovascular septa into lobules. The tumor is associated with a mild lymphoid infiltrate. (H&E)

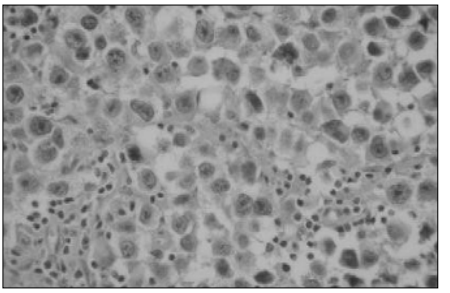

Figure 7. Seminoma. High-power view showing round to polygonal cells with indistinct cell borders, clear to light pink cytoplasm, and round nuclei with prominent nucleoli. (H&E)

Occasionally, seminomas may resemble grossly and histologically benign thymic multilocular cysts. Histologically, the cysts are lined by squamous or low cuboidal epithelium with cholesterol cleft granulomas, chronic inflammation, and scattered foci of thymic epithelium embedded in the cyst's wall. The distinguishing feature is the presence of neoplastic seminoma cells admixed with the cystic structures that often requires extensive sampling and careful evaluation for identification.

Similar to their testicular counterpart, mediastinal seminomas are positive for PLAP (see Figure 8) and for CAM 5.2 (dotlike paranuclear

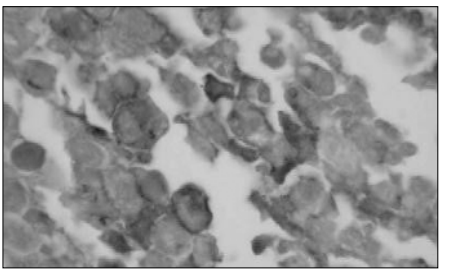

Figure 8 Seminoma. Positive staining for PLAP.

positivity). The tumor cells are weakly positive for broad-spectrum keratin and negative for EMA, CD45, AFP, and CEA. If the seminoma is associated with syncytiotrophoblastic giant cells, these cells will be positive for B-HCG and keratin.

The differential diagnosis includes a metastasis from a primary gonadal tumor. Careful clinical history and physical examination is crucial in these cases. Some use a negative testicular ultrasound as the defining criteria for a primary germ cell tumor of the mediastinum. It is imperative to exclude the coexistence of nonseminomatous elements because the treatment and the prognosis will vary. Serum AFP may be helpful in this regard, as elevated AFP level suggests a nonseminomatous component. The presence of multiple granulomas in a prominent inflammatory background will suggest the possibility of Hodgkin's lymphoma and a thorough search for Reed-Sternberg cells with appropriated immunohistochemical evaluation are indicated. Extensive sampling is important in cystic lesion, particularly in those occurring in young males, as the possibility of a cystic seminoma must be ruled out. Other differential diagnoses include melanoma, lymphoma, thymoma, and metastatic carcinoma. Careful examination and immunohistochemical stains for S-100, Mart-1, B- and T-cell markers, and keratins will be helpful in this context.

Patients with mediastinal senimona have a 5-year survival rate of 75–80%. Although most MS will have a better prognosis than nonseminomatous lesions, they will have a worse prognosis than their testicular counterparts. Bad prognostic factors include age greater than 35 years, presentation with superior vena cava syndrome, presence of supraclavicular or cervical adenopathy or radiologic evidence of hilar disease. The treatment of choice is surgical resection or biopsy followed by irradiation therapy including the supraclavicular, infraclavicular, and low cervical lymph node regions. For disseminated disease, the use of cisplatin-bleomycin sulfate based regiments are recommended.

3.1 Cytology of Mediastinal Germ Cell Tumor

The cytology of mediastinal germ cell tumors (GCTs) are similar to those originating from the gonad. Typical seminomas consist of uniform, large, round neoplastic cells with prominent nucleoli admixed with small lymphocytes in a tigroid background (see Figure 9). The latter is characterized by interwoven, lacy, PAS +ve materials, best appreciated on air-dried preparation. The tigroid background is characteristic of seminoma but may not be present in every case. In addition, the tigroid background has rarely been reported in other malignancies such as renal cell carcinoma.

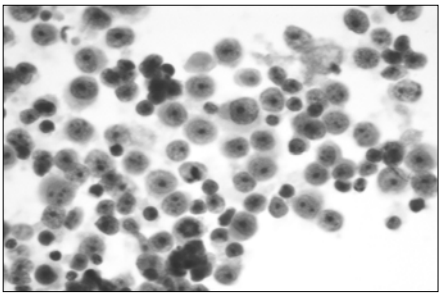

Figure 9. FNA of seminoma. Uniform, large, round neoplastic cells with prominent nucleoli admixed with small lymphocytes. (Papanicolaou stain)

Nonseminomatous GCTs include embryonal carcinoma, yolk sac tumor, and choriocarcinoma. The aspirates of these tumors often demonstrate cohesive groups of pleomorphic epithelioid cells with prominent nucleoli (see Figure 10).

The cytoplasm is usually scant with indistinct cell borders, resulting in a syncytial growth pattern. In addition, the neoplastic cells can also demonstrate a papillary and/or glandular arrangement. Necrosis is frequently noted. Schiller-Duval bodies or glomeruloid structures formed by invagination of neoplastic cells and capillaries into a small space are characteristic of yolk sac tumors in histology but are only occasionally noted in cytologic preparations. Another feature of yolk sac tumors is the presence of cytoplasmic and extracellular, PAS-positive and diastase resistant as well as AFP positive, hyaline globules. However, they are by no means pathognomonic or diagnostic of yolk sac tumors because they can be found in many different neoplasms. The finding of multinucleated tumor giant cells (syncytiotrophoblasts) suggests choriocarcinoma. Mixed GCTs are relatively frequent in the mediastinum and consist of two or more of the aforementioned histologic subtypes of GCTs. Recognition of all the components of mixed GCTs based on FNAB material may not be possible because of sampling limitations.

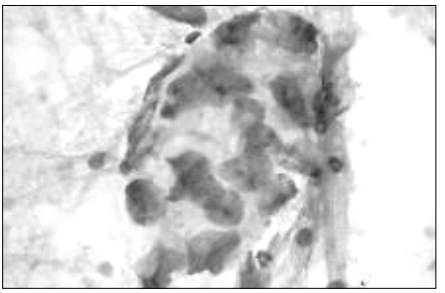

Figure 10. FNA of embroynal carcinoma. Large, pleomorphic neoplastic cells with prominent nucleoli and indistinct cell borders. (Papanicolaou stain)

Because of the diverse morphology of GCT, the differential diagnosis includes a wide variety of entities. Ancillary studies, particularly immunocytochemistry, are helpful in the differential diagnosis. Table 5 summarizes the differential diagnosis of GCTs based on immunocytochemical findings. It is important to note that all GCTs, both seminomatous and nonseminomatous, can demonstrate variable degree of staining with certain anticytokeratin antibodies including CK7, CAM 5.2, and AE1/AE3.

4. REFERENCES

4.1 General

1. Rosai J. Histological typing of tumors of the thymus. World Health Organization International Histological Classification of Tumors, ed. Second. Berlin, Germany: Springer Verlag, 1999.
2. Shimosato B, Mukai K, *Tumors of the Mediastinum*, AFIP, Washington DC (1997).
3. Baker JJ, Solanki PH, Schenk DA, Van Pelt C, Ramzy I, Transbronchial fine needle aspiration of the mediastinum. Importance of lymphocytes as an indicator of specimen adequacy. *Acta Cytologica*, 34(4), 517-23 (1990).
4. Geisinger KR, Differential diagnostic considerations and potential pitfalls in fine-needle aspiration biopsies of the mediastinum. *Diagnostic Cytopathology*, 13(5), 436-42 (1995).
5. Morrissey B, Adams H, Gibbs AR, Crane MD, Percutaneous needle biopsy of the mediastinum: review of 94 procedures. *Thorax*, 48(6), 632-7 (1993).
6. Powers CN, Silverman JF, Geisinger KR, Frable WJ, Fine-needle aspiration biopsy of the mediastinum. A multi-institutional analysis. *American Journal of Clinical Pathology*, 105(2), 168-73 (1996).
7. Singh HK, Silverman JF, Powers CN, Geisinger KR, Frable WJ, Diagnostic pitfalls in fine-needle aspiration biopsy of the mediastinum. *Diagnostic Cytopathology*, 17(2), 121-6 (1997).
8. Slagel DD, Powers CN, Melaragno MJ, Geisinger KR, Frable WJ, Silverman JF, Spindle-cell lesions of the mediastinum: diagnosis by fine-needle aspiration biopsy. *Diagnostic Cytopathology*, 17(3), 167-76 (1997).

Table 5. Immunophenotypes of germ cell tumors and their differential diagnosis

Markers	Seminoma	Yolk sac tumor	Embryonal carcinoma	Chorio-carcinoma	Carcinoma	Carcinoid	Lymphoma	Melanoma
Cytokeratin	±	+	+	+	+	+	−	−
Placental-like alkaline phosphatase	+	+	+	±	−	−	−	−
Alpha fetoprotein	−	+	±	−	−	−	−	−
Beta-human chorionic gonadotrophin	−*	−	−	+	−	−	−	−
S-100 protein	−	−	−	−	−	±	−	+
Neuroendocrine markers (NSE, chromogranin, synaptophysin)	−	−	−	−	−	+	−	−
Leukocyte common antigen	−	−	−	−	−	−	+	−
CD 30	−†	−	+	−	±	−	±	−

* Except multinucleated giant cells
† Rare positive cells

9. Sterrett G, Whitaker D, Shilkin KB, Walters MN, The fine needle aspiration cytology of mediastinal lesions. *Cancer*, 51(1), 127-35 (1983).
10. Shabb NS, Fahl M, Shabb B, Haswani P, Zaatari G, Fine-needle aspiration of the mediastinum: a clinical, radiologic, cytologic, and histologic study of 42 cases. *Diagnostic Cytopathology*, 19(6), 428-36 (1998).

4.2 Thymoma and Related Lesions

1. Bernatz PE, Khonsari S, Harrison EG, Jr., Taylor WF, Thymoma: factors influencing prognosis. *Surgical Clinics of North America*, 53(4), 885-92 (1973).
2. Ho FC, Fu KH, Lam SY, Chiu SW, Chan AC, Muller-Hermelink HK, Evaluation of a histogenetic classification for thymic epithelial tumours. *Histopathology*, 25(1), 21-9 (1994).
3. Kirchner T, Muller-Hermelink HK, New approaches to the diagnosis of thymic epithelial tumors. *Progress in Surgical Pathology*, 10(167-89 (1989).
4. Levine GD, Rosai J, Thymic hyperplasia and neoplasia: a review of current concepts. *Human Pathology*, 9(5), 495-515 (1978).
5. Marino M, Muller-Hermelink HK, Thymoma and thymic carcinoma. Relation of thymoma epithelial cells to the cortical and medullary differentiation of thymus. *Virchows Archiv - A, Pathological Anatomy & Histopathology*, 407(2), 119-49 (1985).
6. Masaoka A, Monden Y, Nakahara K, Tanioka T, Follow-up study of thymomas with special reference to their clinical stages. *Cancer*, 48(11), 2485-92 (1981).
7. Quintanilla-Martinez L, Wilkins EW, Jr., Choi N, Efird J, Hug E, Harris NL, Thymoma. Histologic subclassification is an independent prognostic factor. *Cancer*, 74(2), 606-17 (1994).
8. Suster S, Moran CA, Primary thymic epithelial neoplasms: current concepts and controversies. *Anatomic Pathology*, 2(1-19 (1997).
9. Suster S, Moran CA, Primary thymic epithelial neoplasms showing combined features of thymoma and thymic carcinoma. A clinicopathologic study of 22 cases. *American Journal of Surgical Pathology*, 20(12), 1469-80 (1996).
10. Suster S, Moran CA, Thymic carcinoma: spectrum of differentiation and histologic types. *Pathology*, 30(2), 111-22 (1998).
11. Suster S, Moran CA, Thymoma, atypical thymoma, and thymic carcinoma. A novel conceptual approach to the classification of thymic epithelial neoplasms. *American Journal of Clinical Pathology*, 111(6), 826-33 (1999).
12. Suster S, Moran CA, Primary thymic epithelial neoplasms: spectrum of differentiation and histological features. *Seminars in Diagnostic Pathology*, 16(1), 2-17 (1999).
13. Wick MR, Assessing the prognosis of thymomas. *Annals of Thoracic Surgery*, 50(4), 521-2 (1990).
14. Tao LC, Pearson FG, Cooper JD, Sanders DE, Weisbrod G, Donat EE, Cytopathology of thymoma. *Acta Cytologica*, 28(2), 165-70 (1984).
15. Wang DY, Kuo SH, Chang DB, et al., Fine needle aspiration cytology of thymic carcinoid tumor. *Acta Cytologica*, 39(3), 423-7 (1995).
16. Nichols GL, Jr., Hopkins MB, 3rd, Geisinger KR, Thymic carcinoid. Report of a case with diagnosis by fine needle aspiration biopsy. *Acta Cytologica*, 41(6), 1839-44 (1997).
17. Chhieng DC, Rose D, Ludwig ME, Zakowski MF, Cytology of thymomas: emphasis on morphology and correlation with histologic subtypes. *Cancer*, 90(1), 24-32 (2000).
18. Ali SZ, Erozan YS, Thymoma. Cytopathologic features and differential diagnosis on fine needle aspiration. *Acta Cytologica*, 42(4), 845-54 (1998).

4.3 Primary Mediastinal Germ Cell Tumors

1. Dehner LP, Germ cell tumors of the mediastinum. *Seminars in Diagnostic Pathology*, 7(4), 266-84 (1990).
2. Dulmet EM, Macchiarini P, Suc B, Verley JM, Germ cell tumors of the mediastinum. A 30-year experience. *Cancer*, 72(6), 1894-901 (1993).
3. Economou JS, Trump DL, Holmes EC, Eggleston JE, Management of primary germ cell tumors of the mediastinum. *Journal of Thoracic & Cardiovascular Surgery*, 83(5), 643-9 (1982).
4. Goss PE, Schwertfeger L, Blackstein ME, et al., Extragonadal germ cell tumors. A 14-year Toronto experience. *Cancer*, 73(7), 1971-9 (1994).
5. Hurt RD, Bruckman JE, Farrow GM, Bernatz PE, Hahn RG, Earle JD, Primary anterior mediastinal seminoma. *Cancer*, 49(8), 1658-63 (1982).
6. Luna MA, Valenzuela-Tamariz J, Germ-cell tumors of the mediastinum, postmortem findings. *American Journal of Clinical Pathology*, 65(4), 450-4 (1976).

7. Moran CA, Suster S, Koss MN, Primary germ cell tumors of the mediastinum: III. Yolk sac tumor, embryonal carcinoma, choriocarcinoma, and combined nonteratomatous germ cell tumors of the mediastinum--a clinicopathologic and immunohistochemical study of 64 cases. *Cancer*, 80(4), 699-707 (1997).
8. Moran CA, Suster S, Przygodzki RM, Koss MN, Primary germ cell tumors of the mediastinum: II. Mediastinal seminomas--a clinicopathologic and immunohistochemical study of 120 cases. *Cancer*, 80(4), 691-8 (1997).
9. Moran CA, Suster S, Primary germ cell tumors of the mediastinum: I. Analysis of 322 cases with special emphasis on teratomatous lesions and a proposal for histopathologic classification and clinical staging. *Cancer*, 80(4), 681-90 (1997).
10. Moran CA, Suster S, Germ-cell tumors of the mediastinum. *Advances in Anatomic Pathology*, 5(1), 1-15 (1998).
11. Moran CA, Germ cell tumors of the mediastinum. *Pathology*, *Research & Practice*, 195(8), 583-7 (1999).
12. Suster S, Moran CA, Dominguez-Malagon H, Quevedo-Blanco P, Germ cell tumors of the mediastinum and testis: a comparative immunohistochemical study of 120 cases. *Human Pathology*, 29(7), 737-42 (1998).
13. Raghavan D, Barrett A, Mediastinal seminomas. *Cancer*, 46(5), 1187-91 (1980).
14. Stanley MW, Powers CN, Pitman MB, Korourian S, Bardales RH, Khurana K, Cytology of germ cell tumors: extragonadal, extracranial masses and intraoperative problems. *Cancer*, 81(4), 220-7 (1997).
15. Motoyama T, Yamamoto O, Iwamoto H, Watanabe H, Fine needle aspiration cytology of primary mediastinal germ cell tumors. *Acta Cytologica*, 39(4), 725-32 (1995).
16. Chhieng DC, Lin O, Moran CA, et al., Fine-needle aspiration biopsy of nonteratomatous germ cell tumors of the mediastinum. *American Journal of Clinical Pathology*, 118(3), 418-24 (2002).

CHAPTER 7
CYTOLOGY AND SURGICAL PATHOLOGY OF PLEURAL CAVITIES

Claudia Y. Castro, M.D.,* and David C. Chhieng, M.D., M.B.A.†

1. INTRODUCTION

Accumulation of an excess amount of fluid, or effusion, in the pleural or pericardial cavities is always pathological. About 20% of effusions are caused by malignancy. Metastatic diseases are more common than primary malignancy. Among the former, the majority are adenocarcinomas. The primary indication of cytologic examination of exfoliated cells in fluid is to rule out a malignancy.

This chapter will discuss the morphology and differential diagnosis of mesothelioma and metastatic adenocarcinoma involving the pleura.

2. NORMAL CELLULAR CONSTITUENTS

Normal mesothelial cells don't exfoliate. Therefore, any exfoliated mesothelial cells present are the result of the process causing the effusion. These reactive mesothelial cells can appear singly or in groups of variable sizes. The latter can be 3-dimensional clusters, papillae, cell-in-cell, and even single filing. The cellular clusters often demonstrate lobulated, knobby borders. A characteristic feature of mesothelial cells is the presence of a clear space, or window, between adjacent cells due to the presence of long microvilli on the surface of the cells (see Figure 1). Another characteristic feature is that cytoplasm is dense in the central area (due to perinuclear accumulation of filaments) and pale in the periphery, resulting in two-tone staining. Blunt cytoplasmic processes or projections as well as cytoplasmic vacuoles may be noted. The nuclei are usually central or

* Assistant Professor and Director of Immunohistochemistry Laboratory, Department of Pathology, University of Texas, Galveston, TX.

† Associate Professor and Director of Immunohistochemistry Laboratory, Department of Pathology, University of Alabama, Birmingham, AL.

paracentrally located. Nucleoli range from inconspicuous to prominent. Bi- and multinucleation are common. Mitotic figures may be present but are not indicative of malignancy.

Another cellular component is histiocytes which tend to have indistinct cytoplasmic borders and phagocytic vacuoles. They do not form papillae and 3-dimensional cohesive groups. Histiocytes may be difficult to distinguish from reactive mesothelial cells. Cells from lung, liver, muscle, cartilage, skin and appendages, and fat can be seen from time to time in fluid as they are "picked up" by the needle during the tapping of the effusion.

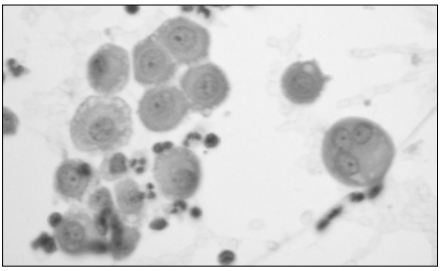

Figure 1. Reactive mesothelial cells. A small group of mesothelial cells showing intercellular window and two-tone cytoplasmic staining. Multinucleated giant cell is also noted. (Papanicolaou stain)

3. MALIGNANT MESOTHELIOMA

Malignant mesothelioma (MM) is a primary malignant neoplasm of serosal surfaces of pleura, peritoneum, pericardium, and tunica vaginalis. The most common location is pleura followed by peritoneum. The highest incidence rate is observed in Australia (the rate in 1997 was 29.8 cases per million inhabitants per year) while the lowest rates were observed in the United States and Norway with 15 and 14 cases per million inhabitants/year, respectively.

The close relationship between asbestos exposure and mesothelioma was first brought to light in 1960 by Wagner et al.; 97% of male patients have a history of asbestos exposure. However, only 7.3% of female patients have such a history. Overall, 10–20% of patients with MM have no evidence of asbestos exposure. The risk of mesothelioma associated with asbestos depends on the size and shape of the fiber, duration of exposure, and time after exposure. Crocidolite is the most common fiber used commercially and is about ten times more carcinogenic than the serpentine fibers (chrysotile). Crocidolite is the fiber associated with the highest risk of mesothelioma.

Asbestos workers are at much higher risk for cancer than for pulmonary fibrosis. The expected incidence of lung carcinoma in the general population is 7%; in asbestos workers the risk for lung cancer is 25%. The risk seen in asbestos workers is thought to be due to the synergistic effect of cigarette smoking and exposure to asbestos dust.

Other etiologic factors for MM include radiation, chronic pleural irritation, SV40, and genetic predisposition.

3.1 Distribution of Malignant Mesothelioma

Ninety-four percent of MM affects the pleura, 6.5% the peritoneum, and 0.5% the pericardium or tunica vaginalis or the testes. In men, 94.5% involve the pleura and 5.5% the peritoneum, whereas in women, 86% affect the pleura and 13.5% the peritoneum.

3.2 Clinical Findings

Patients are usually old (median age 60 years old) with a history of professional, domestic, or environmental exposure to asbestos. Unilateral pleural effusion associated with diffuse pleural thickening is the most common finding on initial examination (90%). The presence of a pleural-based or nodular mass within the lung favors a primary lung or metastatic carcinoma rather than MM.

3.3 Gross Findings

Macroscopically, the pleura are thickened. In early disease, discrete nodules and plaques of different sizes and consistency are seen. As the disease progresses, the pleural cavity becomes obliterated. Invasion into the lung parenchyma, chest wall, mediastinum, pericardium, and diaphragm are common in advanced disease.

3.4 Histologic Types

Forty-eight percent are epithelial, 18% mixed, 11% sarcomatous, 13% unusual variants and 10% poorly differentiated. (see Figures 2 and 3) The epithelial subtype consists of neoplastic cells with variable degree of atypia. Cytoplasm often appears squamoid. Epithelial MM can exhibit a variety of growth patterns including sheets, tubulo-papillary, and glandular. Intracellular vacuoles, similar to those seen in signet ring adenocarcinomas, may be present in epithelial mesothelioma. Unlike mucin-producing adenocarcinoma, these vacuoles do not contain epithelial (neutral) mucin but instead contain hyaluronic acid (acidic mucin) which is mucicarmine negative and PAS positive and disappear after application of hyaluronidase. Other histologic variants of MM include large/giant cell, small-cell, clear cell, and lymphohistiocytic.

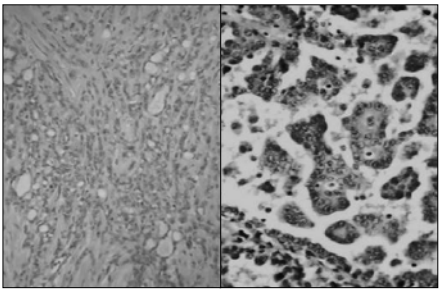

Figure 2. Epithelial MM. Left: tubular pattern. Right: papillary pattern. Notice the low cuboidal uniform cells with a small nucleioli. (H&E)

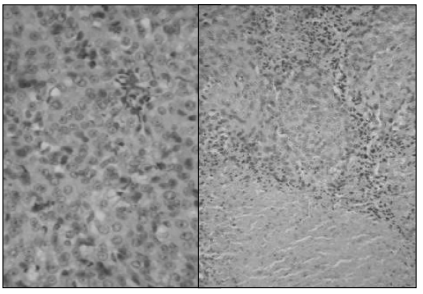

Figure 3. Poorly differentiated MM. Medium- (right) and high-power (left) view showing sheets of cells with high N/C ratio, prominent nucleioli, abundant mitotic figures and extensive necrosis. (H&E)

3.5 Differential Diagnosis

Differential diagnosis of MM is based on the histologic pattern (see Table 1). MM are diffuse tumors and adenocarcinomas are usually nodular pleural-based masses. Intranuclear inclusions and tall columnar cells with hobnail appearance favor primary lung cancer. Psammoma bodies may be seen in MM but are more common in lung adenocarcinoma. Papillary carcinoma of thyroid rarely metastasizes to the pleura. Lobular carcinoma of the breast is the most common metastasis to involve the pleura in women and closely mimics early invasive mesothelioma. Estrogen and progesterone receptor status is helpful in this context because both tumors are CK 7 positive. Pseudomesotheliomatous carcinoma clinically and histologically mimics MM. The presence of CEA, CD15, Ber-EP4 and/or MOC-31 expression are helpful to rule out MM. When clear cell features are present in MM, one should exclude a benign xanthomatous pleuritis (clear cells are macrophages, positive for KP-1 and negative for cytokeratin) and clear cell carcinoma of the lung or metastatic renal cell carcinoma. Small-cell variant of MM does not express chromogranin A or synaptophysin. Rare cases of mucicarmine positive MM have been reported.

Table 1. Differential diagnosis of MM based on histologic pattern

Mesothelioma	Metastatic tumors	Benign lesions
Tubulopapillary	Lung, ovarian, thyroid, bladder	Hyperplasia, AMH*
Epitheloid	Bladder, EH†	
Glandular	Lung, breast, gallbladder	
Large-cell solidus giant cell	Pleomorphic carcinoma	
Small-cell	Small-cell carcinoma, PNET	
Signet ring cell	GI‡, lobular carcinoma, EH	Adenomatoid tumor
Clear cell	Renal cell carcinoma	Xantomatous pleuritis
Lymphohistiocytic	Lympho-epithelial like arcinoma	Lymphoid pleuritis

* AMH: atypical mesothelial hyperplasia.
† EH: epithelial hemangioendothelioma.
‡ GI: gastrointestinal tract carcinomas.

If the tumor involving the pleura is poorly differentiated, the initial antibody panel should include pan-keratin, S-100 protein, HMB-45 (to rule out melanoma), CD31 and C34 (to rule out epitheloid angiosarcoma or hemangioendothelioma). Epitheloid angiosarcomas and hemangioendotheliomas may resemble mesothelioma with a tubulopapillary growth pattern or a bimorphic growth pattern. Epitheloid angiosarcoma usually expresses CD31 and CD34. However, aberrant expression of cytokeratin has been noted in 10% of angiosarcomas. If the tumor is diffusely and strongly positive for cytokeratin, the differential diagnosis is between mesothelioma and adenocarcinoma.

3.6 Cytology

To correctly diagnose mesothelioma on cytology, one needs to recognize its mesothelial origin and its malignant nature. Table 2 summarizes the differential diagnosis between reactive mesothelial cells and mesothelioma. Unfortunately, there is much overlap in the morphology between mesothelioma and reactive mesothelial cells. One important clue in diagnosing mesothelioma is the presence of “more and bigger cells in

Table 2. Differential diagnosis between reactive mesothelial cells and mesothelioma in cytology.

Cytologic features	Reactive mesothelial cells	Mesothelioma
Cellularity	Variable	Highly cellular
Cell arrangement		
Flat, monolayered sheets	Frequent	Infrequent
3-dimensional cell groups	Fewer, smaller, and flatter	Abundant, large, and more complex
Papillae	Less frequent	More frequent
Cells		
Size		Larger and more variable
Spindle-shaped cells	Absent	Sometimes[‡]
Giant and multinucleated cells	Rare	Frequent
Nuclear membrane	Smooth	Irregular
Macronucleoli	Absent	Present
Immunophenotyping		
EMA (membranous)	16%	75%
Desmin (cytoplasmic)	84%	22%
p53 (nuclear)	8% (weak and few)	57%
Aneuploidy	0%	53%

[*] in biphasic and sarcomatoid variants of mesothelioma.

more and bigger clusters" at low-power magnification. In some instances, the differences between the two entities can be quite subtle.

Ancillary studies are often employed to differentiate reactive mesothelial cells from mesothelioma, particularly a well-differentiated one. These studies include electron microscopy (EM), DNA ploidy measurement, and immunohistochemistry. EM is helpful in differentiating adenocarcinoma from mesothelial cells. However, it cannot separate benign from neoplastic mesothelial cells. In a study comparing the ploidy of benign effusions with that of mesothelioma, all benign effusions were diploid, whereas 53% of mesotheliomas were aneuploid. However, the current literature does not support the routine use of ploidy measurement in a clinical setting.

Immunohistochemistry is the most commonly employed ancillary studied in a clinical setting. The majority of the antimesothelial antibodies such as calretinin, thromobomodulin, N-cadherin, and HBME-1 stain both benign and neoplastic mesothelial cells. Mesothelioma cells often demonstrate strong membrane staining for EMA but not in reactive mesothelial cells. Desmin positivity is noted in 84% cases of benign/reactive effusion but in only 22% of mesothelioma. Others have reported that over 50% of mesotheliomas and less than 10% of the reactive mesothelial cells demonstrate nuclear staining with p53. The staining in reactive mesothelial cells is often weak and limited to occasional cells.

The accuracy of diagnosing mesothelioma by either cytology or pleural biopsy alone ranges from 40% to 66%. However, the two techniques are complementary: the accuracy increases to 80% using a combination of cytologic and histologic examination. False negative diagnoses of mesothelioma are not uncommon and are often due to scant

.

cellularity or obscuring blood and/or inflammatory cells. In addition, it may be misclassified as adenocarcinoma. False positive diagnoses of mesothelioma are rare.

3.7 Prognosis

The prognosis of MM is very poor with a median survival of 12 months. The overall survival rate is 36% at 2 years and 14% at 5 years. Pleural mesotheliomas tend to spread locally within the chest cavity, invading major structures. Metastases can occur to the lung parenchyma, mediastinal lymph nodes, and extrathoracic sites such as the liver, bones peritoneum, and adrenal glands. MM with sarcomatoid component (biphasic or pure sarcomatoid) have a worse prognosis than other types.

3.8 Treatment

The treatment options include a single mode of therapy (surgery, radiotherapy, and chemotherapy) or multimodal therapy. The role of surgery is controversial. There are two types of procedures: pleurectomy and extrapleural pneumonectomy. In pleurectomy, the pleura and pericardium are stripped and removed form the apex of the lung to the diaphragm. Pleurectomy can reduce the recurrence of effusion. Extrapleural pneumonectomy is a more extensive procedure in which the parietal and visceral pleura, the lung, the pericardium and the diaphragm are resected and the diaphragmatic defect is repaired by a graft. Multimode-therapy with pleuro-pneumonectomy followed by chemotherapy and radiotherapy has shown a significant improvement in patient survival. The overall survival rate is 36% at 2 years and 14% at 5 years.

4 METASTATIC ADENOCARCINOMA

4.1 Pseudomesotheliomatous Carcinoma of the Lung

Pseudomesotheliomatous carcinoma of the lung (PMC) is primary lung tumors that have the clinical, radiologic, macroscopic and microscopic appearance of pleural mesotheliomas. The most common histologic variety is adenocarcinoma. To date, about 119 cases have been described in the literature.

Clinically, PMC share clinical features with mesotheliomas. They both occur in older men (age range of 31-78 years with a mean age of 63 years). Men outnumber women by at least 5:1 and 90% of the patients are 40 years and older. Similar to mesothelioma, 21% of the patients with PMC have a possible or definite occupational exposure to asbestos (compared to 80% in mesothelioma). Main clinical complaints are chest pain, dyspnea, cough, and weight loss (symptoms due to pleural effusion). Mean duration of symptoms is usually 2 months. CXR show a pleural effusion in 80% of the cases, which is typically unilateral. Pleural effusion cytology is positive in 44% of the cases. The most effective diagnostic procedure is a thoracotomy with pleural biopsy, which is diagnostic in 77% of the cases.

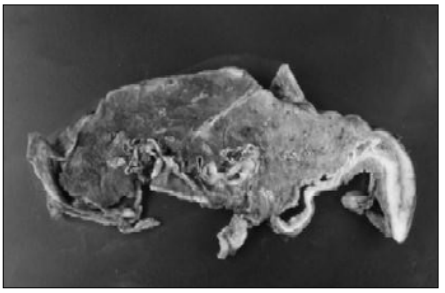

Figure 4. PMC. Gross picture showing involvement of the entire visceral pleura, the interlobular fissure and with invasion into the diaphragm.

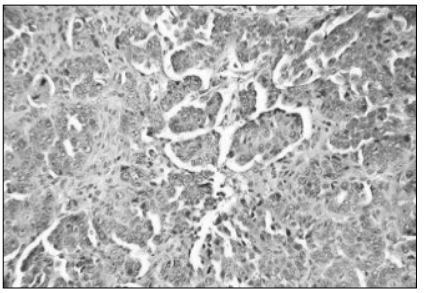

Figure 5. PMC. Medium-power view showing papillary and glandular pattern. (H&E)

The macroscopic criteria for diagnosis PMC include a diffuse neoplasm growing in a pleural distribution and the absence of a nodular or pneumonic tumor involving the lung parenchyma. Grossly, most of the PMC show small nodules, a cobblestone or thick white, firm rubbery pleural thickening measuring up to 2.5 cm in thickness. The tumor usually involves diffusely the visceral and parietal pleura, surrounding the lung, obliterating the pleural space. (see Figure 4) No intrapulmonary tumor is identified. The tumor also may invade the diaphragm and the intercostals muscles. Metastasis to regional (hilar/mediastinal) lymph nodes, adrenal glands, vertebra, pericardium and liver usually occur at a later stage.

Microscopically, most are adenocarcinomas forming glands, nest, cords, papillary or tubulo-papillary patterns (see Figure 5). Some of the reported cases have shown poorly differentiated adenocarcinoma with a focal sarcomatoid component, making the distinction from mesothelioma difficult. A finding of a subpleural bronchioloalveolar carcinoma is seen in 20% of the cases. Additional microscopic findings in the lung parenchyma include ferruginous bodies in the lung tissue (21% of cases) and asbestosis (14% of cases).

Similar to mesothelioma, the median survival in cases of PMC is poor and ranges from 4 to 10 months. The one- year survival of patients of PMC is 39% and 18 months survival is 13%. Most patients are treated with pleural stripping, adjuvant radiation therapy, chemotherapy, and immunotherapy.

4.2 Cytology of Metastatic Adenocarcinoma

The key to diagnosing a metastatic adenocarcinoma in fluid specimens is the finding of foreign cells with malignant features. At low magnification, tumor cells form large aggregates, cell balls, papillae, and acini. Cell balls, often multiple, are round cellular aggregates with smooth, community borders. “Cannonballs” refer to the presence of 3-dimensional cell balls and are diagnostic of a metastatic malignancy (see Figure 6). Acini are 3-dimensional clusters with hollow center. Papillae are 3-dimensional clusters that are longer in one dimension than in the others. Neoplastic cells can also arrange in chains or “Indian file.” Single cells are frequent. Rarely, signet ring cells may be present. The background is usually nonspecific.

Individual malignant cells appear round to oval with nuclear enlargement, high N/C ratio, irregular nuclear membranes, and prominent nucleoli. However, hyperchormasia may not be obvious. The cell borders are poorly defined and the cytoplasm is often basophilic and may contain vacuoles. Giant cells and multinucleated cells can be seen.

Mesothelial cells, both reactive and malignant, can mimic metastatic adenocarcinoma and therefore, can result in both false positive and negative diagnoses. Table 3 summarizes the differential features for adenocarcinoma and mesothelial cells in fluids.

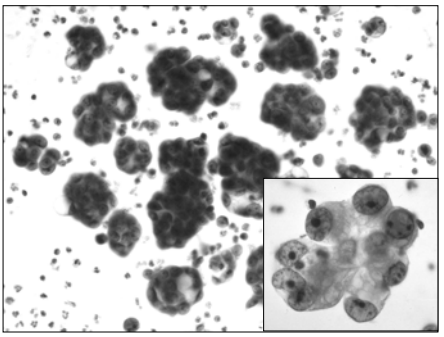

Figure 6. Metastatic ovarian carcinoma in pleural effusion. Cellular specimens with numerous cell balls—cannon ball appearance. Insert: individual cells show marked atypia. (Papanicolaou stain)

Table 3. Differential diagnosis of adenocarcinomas and mesothelial cells in fluid

Cytologic features	Mesothelial cells	Adenocarcinoma
Presentation	No foreign cells	Foreign cells with malignant features
Cell arrangement		
Cell balls	Lobulated, knobby borders	Smooth, community borders
Acinar pattern	Absent (intercellular window may mistaken as lumen)	Present
Cell-in-cell pattern	Present	Absent
Intercellular window	Present	Absent
Signet ring cells	Rare	Sometimes
Cytoplasm		
Borders	Well-defined	Variable
Texture	Dense center, with pale periphery	Homogeneous
Staining	two-tone	Uniform
Cytoplasmic blebs	Present	Absent
Nuclei		
Location	Central or paracentral	Eccentric
Bi- and multinucleation	Common	Rare
N/C ratio	Variable	Usually increase

The common primary sites of adenocarcinomas include the lung, breast (in women), and GI tract. Clinical history is the most useful information in determining the primary site of a tumor. Malignant effusion with an unknown primary site can be a diagnostic challenge. Certain cytologic features can sometimes provide clues as to the possible primary site. Table 4 summarizes the cytologic features and possible primary sites.

Table 4. Possible primary sites based on cytologic features

Cytologic features	Most likely primary site(s)	Other consideration
Cannonballs	Breast (ductal)	Ovary, lung (non-small cell)
Papillae	Lung and breast	Ovarian, uterine, GI tract
Signet ring cells	Stomach, breast, lobular (small)	Ovarian, lung (non-small cell)
Predominantly single cells	Breast (lobular), stomach	
"Indian files"	Breast (ductal and lobular)	Pancreas, stomach, lung (small cell)
Bizarre or giant cells	Lung, pancreas	
Columnar cells	Colorectal	Lung

4.3 Ancillary Studies

Various ancillary studies are often used to help in the distinction between mesothelial cells and adenocarcinomas. Demonstration of neutral mucin production by cytochemistry, particularly mucicarmine, differentiates adenocarcinoma from mesothelial cells. However, cytochemical stains are relatively insensitive. In addition, up to 2–5% of well to moderately differentiated mesotheliomas are mucicarmine positive, which usually disappears after treatment with hyaluronidase.

Electron microscopy has also been used in differentiating mesothelial cells from adenocarcinoma by demonstrating long, thin "bushy" microvilli in the mesotheliomas. Because certain adenocarcinomas can possess short microvilli, some authors suggested that only microvilli with a length/diameter ratio of 15 or above should be considered to be strongly supportive of mesothelioma. However, poorly differentiated epithelial and sarcomatous mesotheliomas may lack microvilli. Furthermore, the availability of adequate material, sizable costs, and long turnaround times limit the universal implementation of this technique.

Immunohistochemistry is the most commonly employed ancillary technique. Table 5 summarizes markers for mesothelial cells and adenocarcinoma.

Table 5. Markers for mesothelial cells and adenocarcinoma

Positive mesothelial markers	Positive adenocarcinoma markers
Calretinin	CEA
CK 5/6	B72.3
Wilm's tumor gene (WT-1)	CD15 (leu -M1)
Cytokeratin 5	BER-EP4
N-cadherin	MOC-31
HBME-1	TTF-1.
Thrombomodulin	E-cadherin

4.4 Positive Mesothelial Markers

Calretinin, a 29 kDa protein, is a member of a large family of calcium-binding proteins. It is the best and most frequently used marker for mesothelioma available to date. It stains, not only most epithelial MM but also some sarcomatoid MM. Calretinin is positive in 80–100% of the epithelial mesotheliomas and 8% of adenocarcinomas of various origins (usually weak and focal). The type of staining found in MM by calretinin varies according to the different studies from finely granular and cytoplasmic staining (nuclei negative) to positive nuclear and cytoplasmic staining. In most recent reports, the

staining in MM is strong and diffuse and occurs in both the cytoplasm and the nucleus. Calretinin expression also occurs in squamous cell carcinomas.

Cytokeratin 5/6 is one of the most sensitive of the positive mesothelioma markers. It is expressed in over 90–100% of the epithelial mesotheliomas, but is absent in sarcomatoid mesotheliomas. Cytokeratin 5/6 expression commonly occurs in squamous carcinomas and can be seen in a minority of adenocarcinomas where the staining if focal and limited to few cells (less than 5% of the tumor cells). In MM, the staining of CK 5/6 is strong and diffuse throughout the cytoplasm.

Wilm's tumor gene (WT-1) is a nuclear DNA-binding protein. It is a tumor suppressor gene and is expressed in mesangial cells of the kidney, Sertoli cells of the testes, ovarian stromal cells and surface epithelium, and reactive mesothelial cells, as well as in some adenocarcinomas, particularly papillary serous carcinomas. Positive nuclear staining is in seen in 75–93% of the MM. WT-1 is usually negative in pulmonary adenocarcinomas and therefore is very helpful in distinguishing between lung adenocarcinoma and mesothelioma. However, in the peritoneal cavity, it is not useful in separating MM form serous carcinomas of the ovary and peritoneum.

Thrombomodulin (TM) is a receptor for thrombin and plays an important role as a natural anticoagulant by inhibiting the activity of thrombin. It is expressed in endothelial cells of blood vessels and lymphatic, syncytiotrophoblast of the placenta, and in squamous, urothelial, and mesothelial cells. TM expression has been reported in angiosarcomas, syncytiotrophoblastic tumors, mesotheliomas, transitional cell carcinomas, squamous cell carcinomas of the lung, skin, esophagus, and oral cavity, and in a small number of adenocarcinomas of the lung, pancreas, liver, ovary, and breast. The literature varies regarding the percentage of TM-positive mesotheliomas and lung adenocarcinomas—ranging between 29% and 100% for mesotheliomas and 6% and 42% for lung adenocarcinomas. Although the cause of these discrepancies is unclear, this marker has no value for separating epithelioid MM and pulmonary adenocarcinoma. Strong cytoplasmic and membrane staining is characteristic of this marker.

Mesothelin is a 40-kDa surface glycoprotein of unknown function that is strongly expressed in normal mesothelial cells and MM. Meosthelin is a very sensitive positive marker for MM (100%), but the specificity is low (positivity in 38% of pulmonary adenocarcinomas). In addition, it has been shown that mesothelin is strongly expressed in serous carcinoma of the ovary, pancreatic adenocarcinoma, and some squamous carcinomas. Despite these limitations and because of the common and strong mesothelin expression in MM a negative staining for this marker can be regarded as a strong indication against such a diagnosis.

N-cadherin is one of the most recently recognized positive markers for MM. It is an adhesion protein that is found in nerve cells, developing muscle cells, and mesothelial cells. Positive staining is usually noted along the cell membrane. Reported positivity with N-cadherin for MM varies 77–100%, whereas only 19–30% of the adenocarcinomas are positive. N-cadherin is commonly expressed in papillary serous and endometroid carcinomas of the ovary. This marker has no value in differentiating these two tumors from mesotheliomas.

HBME-1 is one of the most controversial of the positive mesothelioma markers. It reacts with an unknown antigen present on the villous surface of the mesothelioma cells, producing a characteristic membranous staining pattern, whereas adenocarcinomas usually demonstrate cytoplasmic staining. According to a study by Ordonez, HBME-1 is noted in 85% and 68% of MM and lung adenocarcinomas, respectively. In addition, a

mixed membranous and cytoplasmic staining pattern is observed in 18 of 60 and in 21 of 50 of the MM and lung adenocarcinomas, respectively. Therefore, the value of this marker in the differential diagnosis of MM is very limited.

CD44 is a broadly distributed family of glycoproteins with molecular weights ranging from 80 to 250 kDa. Its functions include cell adhesion, cell matrix interaction lymphocyte homing and activation, and metastasis formation. The most abundant form of CD44 is the standard CD44S, which is the principal receptor for hyaluronic acid, a substance produced by mesotheliomas. It has been reported that 75–83% of mesotheliomas are positive for CD44, while 15–48% of the lung adenocarcinomas are positive. Therefore, this marker lacks specificity for mesotheliomas and has no practical utility.

4.5 Positive Adenocarcinoma Markers

CEA is the first marker to be accepted as being useful in distinguishing MM from adenocarcinoma. Eighty-eight percent of the lung adenocarcinomas express CEA, while mesotheliomas are almost invariably negative. The staining is cytoplasmic with accentuation of the cell membrane. It should be emphasized that this marker is expressed in only 20% of the serous carcinomas. The best results are obtained with monoclonal antibodies. Antigen retrieval results in stronger and more diffuse staining of the adenocarcinomas. CEA is a highly sensitive and specific marker for adenocarcinoma and continues to be one of the best negative mesothelioma markers. Its value is limited for discriminating MM form serous carcinoma of the ovary and peritoneum because less than half of these tumors expressed this marker.

MOC-31 is a monoclonal antibody against a glycoprotein generated using the GLS-1 small-cell lung carcinoma cell line. It is the best marker currently available for distinguishing MM from adenocarcinoma. Strong and diffuse (>50% of the tumor cells) cytoplasmic staining is seen in 100% of colon adenocarcinomas, 95% of ovary adenocarcinomas, 95% of breast, 90–100% of lung adenocarcinomas, and 38% of the renal cell carcinoma. Positive staining for MOC-31 has been reported in 5–10% of the MM; however, staining is usually focal and weak. MOC-31, therefore, is a very helpful marker and a strong diffuse positive staining argues against the diagnosis of MM.

B72.3 is a monoclonal antibody against a glycoprotein (TAG-72) present in breast cancer cells and is present in 84% of the lung adenocarcinomas and 87% of the serous carcinomas. Positive staining has been reported in 2–5% of the MM. When it occurs in MM, it is usually focal and confined to a few cells. Approximately 20% of the lung adenocarcinomas are negative for this marker. A coarse granular cytoplasmic staining with apical intensification is characteristic for this marker.

LeuM1 (CD15) is one the earliest markers in the diagnosis of mesothelioma. It is reported to bind to a specific sugar moiety also known as X-hapten that is found in the glycolipids. There is disagreement regarding the percentage of Leu-M1 positivity in pulmonary adenocarcinomas and MM. Positive staining has been reported in 50–72% of lung adenocarcinomas and 0–5% of MM. Most adenocarcinomas exhibit a granular cytoplasmic staining with occasional membrane accentuation. Staining in MM is usually focal and weak.

Ber-EP4 is a monoclonal antibody that was raised using breast cancer cell lines MCF-7 as immunogen. It recognizes two glycoproteins present on the cell membrane of

most normal and neoplastic epithelial cells. Most adenocarcinomas of the lung are positive for Ber-EP4 and show a strong and diffuse cytoplasmic and cell membrane staining. There is controversy in the literature regarding the value of Ber-EP4 in distinguishing lung adenocarcinoma and MM. The positive staining in MM varies according the series from 7% to 26%. This difference derived from differences in interpreting the stains rather than due to technical issues. Some studies considered Ber-EP4 positive only when there is typical lateral membrane staining in at least 2% of the cells. Other studies considered it positive when the staining affected the entire membrane of the tumor cells (membranous staining). Ordonez found that in well differentiated adenocarcinomas the staining was along the basolateral membranes and in poorly differentiated adenocarcinomas (solid areas) the Ber-EP4 staining was circumferential. Usually the staining Ber-EP4 in MM is focal and restricted to a limited number of cells in contrast to that seen in pulmonary adenocarcinomas which is invariably diffuse. The value of Ber-EP4 for discriminating nonpulmonary adenocarcinomas from MM is limited. The percentage of positivity for Ber-EP4 in nonpulmonary adenocarcinomas is 30–50%. In addition, the basolateral staining pattern that is often reported in lung adenocarcinomas can be absent in some of the nonpulmonary adenocarcinomas.

TTF-1 is a tissue-specific transcription factor that is expressed in the normal lung and thyroid as well as in the tumor derived from these organs. It is highly specific for lung adenocarcinomas. Up to 74% of lung adenocarcinomas and none of the MM demonstrate nuclear staining with TTF-1.

4.6 Conclusions

In the literature there in no unanimity about which antibodies to include in the diagnostic panel. The sensitivity and specificity of mesothelial and adenocarcinoma markers in diagnosing MM and adenocarcinomas are listed in Tables 6 and 7, respectively.

Table 6. Sensitivity and specificity of mesothelial markers in diagnosing mesothelioma

Mesothelial marker	Sensitivity	Specificity
Calretinin	87–100%	92%
WT-1	72–100%	100%
Cytokeratin 5/6	89–100%	95–100%
Thrombomodulin	63–100%	63–95%

Table 7. Sensitivity and specificity of adenocarcinoma markers in diagnosing adenocarcinoma

Adenocarcinoma marker	Sensitivity	Specificity
CEA	79–86%	90–100%
B72.3	81%	98–100%
CD15 (Leu -M1)	71–86%	97–100%
Ber-EP4	87–100%	82–100%
MOC-31	90–100%	89–100%
TTF-1	75%	100%

Calretinin, CK 5/6, and WT-1 are the mot sensitive and specific positive markers for distinguishing MM from adenocarcinomas. Calretinin and cytokeratin 5/6 are more sensitive than WT-1. Thrombomodulin, HBME-1, N-cadherin and CD44S are less sensitive and less specific and are not recommended. Mesothelin is a highly sensitive marker for epithelioid MM but is less specific and if needed can be used as an additional marker.

CEA, MOC-31, and B72.3 are the most sensitive and specific markers for discriminating between epithelioid MM and pulmonary adenocarcinoma. The secondary markers include CD15 and Ber-EP4. TTF-1 is highly specific for pulmonary adenocarcinoma and can be used when the latter is in the differential diagnosis.

From a practical point of view, a panel of four markers (two positive and two negative) usually allow for the distinction between epitheloid MM and adenocarcinoma. In our experience we use calretinin and CK 5/6 as the positive markers for MM and the CEA, B72.3, and/or MOC-31 as the adenocarcinoma markers. If lung adenocarcinoma is a main differential diagnosis we will include TTF-1. For cytology specimen, cytokeratin is also included to highlight cells of interest.

5 REFERENCES

5.1 Malignant Mesothelioma

1. Whitaker D, Shilkin KB, Diagnosis of pleural malignant mesothelioma in life—a practical approach. *Journal of Pathology*, 143(3), 147-75 (1984).
2. Attanoos RL, Gibbs AR, Pathology of malignant mesothelioma. *Histopathology*, 30(5), 403-18 (1997).
3. Antman KH, Clinical presentation and natural history of benign and malignant mesothelioma. *Seminars in Oncology*, 8(3), 313-20 (1981).
4. Grondin SC, Sugarbaker DJ, Malignant mesothelioma of the pleural space. *Oncology (Huntington)*, 13(7), 919-26; discussion 26, 31-2 (1999).
5. Sugarbaker DJ, Flores RM, Jaklitsch MT, et al., Resection margins, extrapleural nodal status, and cell type determine postoperative long-term survival in trimodality therapy of malignant pleural mesothelioma: results in 183 patients. *Journal of Thoracic and Cardiovascular Surgery*, 117(1), 54-63; discussion -5 (1999).
6. Mark EJ, Shin DH, Diffuse malignant mesothelioma of the pleura: a clinicopathological study of six patients with a prolonged symptom-free interval or extended survival after biopsy and a review of the literature of long-term survival. *Virchows Archiv - A, Pathological Anatomy and Histopathology*, 422(6), 445-51 (1993).
7. Sterman DH, Kaiser LR, Albelda SM, Advances in the treatment of malignant pleural mesothelioma. *Chest*, 116(2), 504-20 (1999).
8. Chang HT, Yantiss RK, Nielsen GP, McKee GT, Mark EJ, Lipid-rich diffuse malignant mesothelioma: a case report. *Human Pathology*, 31(7), 876-9 (2000).
9. Shimazaki H, Aida S, Iizuka Y, Yoshizu H, Tamai S, Vacuolated cell mesothelioma of the pericardium resembling liposarcoma: a case report. *Human Pathology*, 31(6), 767-70 (2000).
10. MacDougall DB, Wang SE, Zidar BL, Mucin-positive epithelial mesothelioma. *Archives of Pathology and Laboratory Medicine*, 116(8), 874-80 (1992).
11. Hammar SP, Bockus DE, Remington FL, Rohrbach KA, Mucin-positive epithelial mesotheliomas: a histochemical, immunohistochemical, and ultrastructural comparison with mucin-producing pulmonary adenocarcinomas. *Ultrastructural Pathology*, 20(4), 293-325 (1996).
12. Ordonez NG, Mackay B, Glycogen-rich mesothelioma. *Ultrastructural Pathology*, 23(6), 401-6 (1999).
13. Yousem SA, Malignant mesothelioma. *Archives of Pathology and Laboratory Medicine*, 111(6), 503 (1987).
14. Mayall FG, Gibbs AR, The histology and immunohistochemistry of small-cell mesothelioma. *Histopathology*, 20(1), 47-51 (1992).
15. Matsukuma S, Aida S, Hata Y, Sugiura Y, Tamai S, Localized malignant peritoneal mesothelioma containing rhabdoid cells. *Pathology International*, 46(5), 389-91 (1996).
16. Nascimento AG, Keeney GL, Fletcher CD, Deciduoid peritoneal mesothelioma: an unusual phenotype affecting young females. *American Journal of Surgical Pathology*, 18(5), 439-45 (1994).

17. Khalidi HS, Medeiros LJ, Battifora H, Lymphohistiocytoid mesothelioma: an often misdiagnosed variant of sarcomatoid malignant mesothelioma. *American Journal of Clinical Pathology*, 113(5), 649-54 (2000).
18. Orosz Z, Nagy P, Szentirmay Z, Zalatnai A, Hauser P, Epithelial mesothelioma with deciduoid features. *Virchows Archiv*, 434(3), 263-6 (1999).
19. Shanks JH, Harris M, Banerjee SS, et al., Mesotheliomas with deciduoid morphology: a morphologic spectrum and a variant not confined to young females. *American Journal of Surgical Pathology*, 24(2), 285-94 (2000).
20. Lin BT, Colby T, Gown AM, et al., Malignant vascular tumors of the serous membranes mimicking mesothelioma: a report of 14 cases. *American Journal of Surgical Pathology*, 20(12), 1431-9 (1996).
21. Attanoos RL, Suvarna SK, Rhead E, et al., Malignant vascular tumours of the pleura in "asbestos" workers and endothelial differentiation in malignant mesothelioma. *Thorax*, 55(10), 860-3 (2000).
22. Carella R, Deleonardi G, D'Errico A, et al., Immunohistochemical panels for differentiating epithelial malignant mesothelioma from lung adenocarcinoma: a study with logistic regression analysis. *American Journal of Surgical Pathology*, 25(1), 43-50 (2001).
23. Ordonez NG, Value of calretinin immunostaining in differentiating epithelial mesothelioma from lung adenocarcinoma. *Modern Pathology*, 11(10), 929-33 (1998).
24. Ordonez NG, Value of cytokeratin 5/6 immunostaining in distinguishing epithelial mesothelioma of the pleura from lung adenocarcinoma. *American Journal of Surgical Pathology*, 22(10), 1215-21 (1998).
25. Ordonez NG, Role of immunohistochemistry in differentiating epithelial mesothelioma from adenocarcinoma: review and update. *American Journal of Clinical Pathology*, 112(1), 75-89 (1999).
26. Ordonez NG, The immunohistochemical diagnosis of epithelial mesothelioma. *Human Pathology*, 30(3), 313-23 (1999).
27. Ordonez NG, The immunohistochemical diagnosis of mesothelioma: a comparative study of epithelioid mesothelioma and lung adenocarcinoma. *American Journal of Surgical Pathology*, 27(8), 1031-51 (2003).
28. Riera JR, Astengo-Osuna C, Longmate JA, Battifora H, The immunohistochemical diagnostic panel for epithelial mesothelioma: a reevaluation after heat-induced epitope retrieval. *American Journal of Surgical Pathology*, 21(12), 1409-19 (1997).
29. Moran CA, Wick MR, Suster S, The role of immunohistochemistry in the diagnosis of malignant mesothelioma. *Seminars in Diagnostic Pathology*, 17(3), 178-83 (2000).
30. Comin CE, Novelli L, Boddi V, Paglierani M, Dini S, Calretinin, thrombomodulin, CEA, and CD15: a useful combination of immunohistochemical markers for differentiating pleural epithelial mesothelioma from peripheral pulmonary adenocarcinoma. *Human Pathology*, 32(5), 529-36 (2001).
31. Foster MR, Johnson JE, Olson SJ, Allred DC, Immunohistochemical analysis of nuclear versus cytoplasmic staining of WT1 in malignant mesotheliomas and primary pulmonary adenocarcinomas. *Archives of Pathology and Laboratory Medicine*, 125(10), 1316-20 (2001).
32. Oates J, Edwards C, HBME-1, MOC-31, WT1 and calretinin: an assessment of recently described markers for mesothelioma and adenocarcinoma. *Histopathology*, 36(4), 341-7 (2000).
33. Doglioni C, Tos AP, Laurino L, et al., Calretinin: a novel immunocytochemical marker for mesothelioma. *American Journal of Surgical Pathology*, 20(9), 1037-46 (1996).
34. Gaffey MJ, Mills SE, Swanson PE, Zarbo RJ, Shah AR, Wick MR, Immunoreactivity for BER-EP4 in adenocarcinomas, adenomatoid tumors, and malignant mesotheliomas. *American Journal of Surgical Pathology*, 16(6), 593-9 (1992).
35. Sosolik RC, McGaughy VR, De Young BR, Anti-MOC-31: a potential addition to the pulmonary adenocarcinoma versus mesothelioma immunohistochemistry panel. *Modern Pathology*, 10(7), 716-9 (1997).
36. Koukoulis GK, Shen J, Monson R, Warren WH, Virtanen I, Gould VE, Pleural mesotheliomas have an integrin profile distinct from visceral carcinomas. *Human Pathology*, 28(1), 84-90 (1997).

5.2 Pseudomesotheliomatous Carcinoma and Metastatic Adenocarcinoma to the Lung

1. Harwood TR, Gracey DR, Yokoo H, Pseudomesotheliomatous carcinoma of the lung: a variant of peripheral lung cancer. *American Journal of Clinical Pathology*, 65(2), 159-67 (1976).
2. Koss M, Travis W, Moran C, Hochholzer L, Pseudomesotheliomatous adenocarcinoma: a reappraisal. *Seminars in Diagnostic Pathology*, 9(2), 117-23 (1992).
3. Koss MN, Fleming M, Przygodzki RM, Sherrod A, Travis W, Hochholzer L, Adenocarcinoma simulating mesothelioma: a clinicopathologic and immunohistochemical study of 29 cases. *Annals of Diagnostic Pathology*, 2(2), 93-102 (1998).
4. Hartmann CA, Schutze H, Mesothelioma-like tumors of the pleura: a review of 72 autopsy cases. *Journal of Cancer Research and Clinical Oncology*, 120(6), 331-47 (1994).

5. Dessy E, Pietra GG, Pseudomesotheliomatous carcinoma of the lung. An immunohistochemical and ultrastructural study of three cases. *Cancer*, 68(8), 1747-53 (1991).
6. Shah IA, Salvatore JR, Kummet T, Gani OS, Wheeler LA, Pseudomesotheliomatous carcinoma involving pleura and peritoneum: a clinicopathologic and immunohistochemical study of three cases. *Annals of Diagnostic Pathology*, 3(3), 148-59 (1999).
7. Ko EC, Jhala NC, Shultz JJ, Chhieng DC, Use of a panel of markers in the differential diagnosis of adenocarcinoma and reactive mesothelial cells in fluid cytology. *American Journal of Clinical Pathology*, 116(5), 709-15 (2001).

CHAPTER 8
CYTOLOGY AND SURGICAL PATHOLOGY OF NEOPLASMS OF THE LUNG

Claudia Y. Castro, M.D.,[*] and David C. Chhieng, M.D., M.B.A.[†]

1. INTRODUCTION

In this chapter, we are going to discuss the morphology and differential diagnosis of neuroendocrine tumor, bronchioalveolar carcinoma, non-small-cell lung carcinoma, metastatic tumors to the lung, and spindle cell neoplasm.

2. NORMAL CYTOLOGY

The cytologic specimens obtained from the lung and respiratory tract can be divided into two categories: exfoliative and aspiration. The former include sputum, bronchial brushings and washings, and bronchoalveoloar lavage. The number of specimens, the location, the size, the histologic subtype, and the degree of differentiation of tumor affect the diagnostic accuracy of exfoliative respiratory cytology.

Normal bronchial cells, occurring singly or in tissue fragments such as strips and honeycomb, are tall columnar cells with terminal bars and/or cilia. When the bronchial cells are irritated, they can become atypical and/or multinucleated. The finding of cilia and/or terminal bars speaks for benignancy. Goblet cells are characterized by the presence of vacuolated cytoplasm, often above the nucleus. Reserve cells refer to small, round, lymphocyte-like cells with central, hyperchromatic, uniform nuclei and scant cytoplasm often seen attached to benign columnar cells. They may be mistaken to be small-cell carcinoma.

[*] Assistant Professor and Director of Immunohistochemistry Laboratory, Department of Pathology, University of Texas, Galveston, TX.

[†] Associate Professor and Director of Immunohistochemisty Laboratory, Department of Pathology, University of Alabama, Birmingham, AL.

Pneumocytes or alveolar cells are not readily apparent in respiratory cytology unless they are hyperplastic. They occur singly and in clusters. They have cyanophilic, often vacuolated, cytoplasm. Alveolar macrophages are readily recognized by the presence of phagocytosed carbon and other pigments in their cytoplasm. Multinucleation is common. Cells from the chest wall, mesothelial cells, and, rarely, hepatocytes can be seen in precutaneous FNA of the lung.

3. NEUROENDOCRINE NEOPLASMS

Pulmonary neuroendocrine tumors can be classified into four categories: typical carcinoid, atypical carcinoid, small-cell lung carcinoma, and large-cell neuroendocrine carcinoma. The presene of mitotic activity and necrosis are the most important morphologic features to distinguish typical, atypical carcinoid, and high-grade neuroendocrine carcinomas such as small-cell lung carcinoma (SCLC) and large-cell neuroendocrine carcinoma (LCNE).

3.1 Typical Carcinoid

Typical carcinoids are low-grade malignancies. The majority of them are centrally located, whereas 20% are peripheral. Histologically, a typical carcinoid is characterized by an organoid, trabecular, ribbon of rosette-like arrangement, with uniform nuclei and moderately eosinophilic cytoplasm. Nucleoli may be present. The tumors should have fewer than two-mitoses/10 HPF and no necrosis. In addition, some carcinoid may have a papillary, sclerosing, follicular, or glandular features. Unusual types include mucin- and melanin-producing carcinoids, carcinoids with prominent nuclear convolutions, stroma with bone and cartilage formation, and hyalinization or amyloid deposition.

The aspirates consist of a loosely cohesive population of round to oval, uniform cells. Rosette formation may be seen. There is scant to moderate granular cytoplasm. The nuclei are often eccentrically located, uniformly round, with “salt-and-pepper” chromatin. Occasional larger cells with conspicuous nucleoli may be seen. However, nuclear molding and mitotic figures are infrequent. Necrosis and crush artifact is uncommon. The differential diagnosis includes well-differentiated adenocarcinoma including bronchioalveolar carcinoma (BAC). The cells from the latter tend to be more cohesive, have more abundant cytoplasm, and display a greater degree of pleomorphism. Typical carcinoid should also be distinguished from other neuroendocrine neoplasms. Table 1 summarizes the differential diagnosis of all neuroendocrine neoplasm cytologically.

About 10% to 20% of typical carcinoids demonstrate a population of spindle cells. They are usually peripherally located in the lung. The cells appear elongated with “salt-and- pepper” chromatin. They may display more atypia such as nuclear molding, few mitotic figures, and irregular membrane. The differential diagnosis includes other spindle cell neoplasms.

3.2 Atypical Carcinoids

The morphology of atypical carcinoids is somewhat between that of typical carcinoids and small-cells undifferentiated carcinoma. Histologically, atypical carcinoids exhibit 2–10 mitoses/10 hpf and frequently show focal areas of punctuate necrosis.

Table 1. Differential diagnosis of pulmonary neuroendocrine neoplasms

Cytologic features	Typical carcinoid	Atypical carcinoid	SCLC*	LCNEC†
Arrangement	Loosely cohesive groups, single cells, +/- rosettes	Single cells, small aggregates, and syncytial tissue fragments, +/- rosettes	Single cells, small aggregates, and syncytial tissue fragments	Single cells, small aggregates, and tissue fragments with peripheral palisading
Cells				
Size	2-2.5 that of normal lymphocytes,	Larger than that of typical carcinoid and SCLC	2–4 times that of normal lymphocytes	Larger than that of SCLC
Pleomorphism	Relatively uniform cells with occasional atypia	Mild to moderately pleomorphism	Highly pleomorphism	Highly pleomorphism
Shape	Round to oval, can be plasmacytoid, spindle-shaped in 10% to 20%	Polygonal or spindle-shaped	Irregular, polygonal, and spindle-shaped	Polygonal, spindle-shaped, and irregular
N/C ratio	Lower	Intermediate	Higher	Intermediate
Cytoplasm	Discernible	Discernible	Scant, indiscernible	Discernible
Nuclei				
Nuclear memb rane	Smooth	Smooth, rarely irregular	Smooth to irregular	Smooth to irregular
Chromatin	Salt-and-pepper	Coarsely granular	Finely granular	Fine to coarsely granular
Nucleoli	Usually absent	Inconspicuous	Inconspicuous	Frequent
Molding	Absent	Occasional	Frequent	Occasional
Mitotic figures	Absent	Rare	Present	Present
Apoptotic bodies	Absent	Rare	Present	Present
Necrosis	Absent	Sometimes	Frequent	Frequent

* SCLC: small-cell lung carcinoma

† LCNEC: large-cell neuroendocrine carcinoma

Cytologically, they differ from typical carcinoids by having larger nuclei, more pleomorphism, higher N/C ratio, and the presence of necrosis. Nuclear molding may be more conspicuous. to small-cell carcinoma, the cells of atypical carcinoids are more or less the same size.However, the latter have more abundant cytoplasm and prominent nucleoli. It may be very difficult to distinguish atypical carcinoids from SCLC. The diagnosis may have to be resolved by histologic examination. In practice, the more closely an atypical carcinoid resembles a SCLC, the more aggressive the tumor, and the less important clinically their distinction.

3.3 Small-Cell Lung Carcinoma (SCLC)

SCLC consists of small-cells with scant cytoplasm, ill-defined cell borders absent of faint nucleoli, and finely granular nuclear chromatin. The cells are round, oval, and spindle-shaped; nuclear molding is usually prominent and the mitotic count is high (average 60–70 per square millimeter). How small should the cells of a tumor be to classify the tumor as small-cell carcinoma? The answer is an arbitrary cut-off of no more than three times the size of a small resting lymphocyte nucleus, acknowledging that the absolute upper limit in nuclear size is currently under debate and may be larger if all other nuclear features are typical (nuclear molding, fine chromatin, indistinct nucleoli, high N/C ratio, high mitotic activity, abundant crush artifact). Non-small-cell carcinoma may simulate small-cell carcinoma, particularly in transbronchial biopsies when the tissue is ischemic, demonstrate the effects of therapy or poor fixation.

In sputum, the cells are often arranged in a linear array in mucus strands. Apoptotic bodies and a necrotic background are frequent. Crush artifact is characteristic of small-cell carcinoma in FNA. The differential diagnosis includes both benign lesions and malignant neoplasms, and depends on the type of cytologic specimen (see Table 2). For example, reserve cell hyperplasia and follicular bronchitis are not on the list of differential diagnosis for specimens obtained by percutaneous FNA.

Table 2. Differential diagnosis of small-cell lung carcinoma on cytology

Entity	Differential features
Reserve cell hyperplasia	No single cells, no atypia, minimal nuclear molding, no apoptotic bodies, often associated with ciliated bronchial cells
Follicular bronchitis/lymph node	Single-cell pattern, mixed small and large lymphocytes mixed with tingible macrophaages and plasma cells, no nuclear molding
Lymphoma	Single-cell pattern, monotonous population of lymphocytes, no nuclear molding
Non-small-cell lung carcinoma, poorly differentiated	Large-cells, discernible cytoplasm, prominent nucleoli, minimal nuclear molding
Metastatic small-cell malignancies	Known history of previous malignancy, patient's age, ancillary studies

Other issues with SCLC include marked crush artifact that may preclude a definitive diagnosis, as this may be seen in other highly cellular tumors and inflammatory conditions. In this case an immunohistochemical stain for keratin may be useful for suggesting the diagnosis. Immunohistochemical stain for chromogranin and synaptophysin are not required for the diagnosis of small-cell carcinoma, but they may be

useful if they are positive. It is important to remember that up to 25% of small-cell carcinomas are negative for chromogranin, synaptophysin, and Leu-7.

Variants of small-cell carcinoma include combined small-cell carcinoma in which the small-cell carcinoma has an additional component that include any other type of non-small-cell carcinoma (adenocarcinona, squamous cell carcinoma, large-cell carcinoma, large-cell neuroendocrine carcinoma, sarcomatoid carcinoma) or heterologous sarcomatous elements (osteosarcoma, chondrosarcoma, etc.). The histologic type of the second component should be always noted in the diagnosis, that is, combined small-cell carcinoma (80%) with adenocarcinoma (20%), combined small-cell carcinoma (95%), and chondrosarcoma (5%). Variants of small-cell carcinoma, despite the nature of the second component (adenocarcinoma, osteosarcoma, etc.), are treated as small-cell carcinoma.

3.4 Large-cell Neuroendocrine Carcinoma (LCNEC)

This is a recently described entity. Affected patients are usually heavy cigarette smokers. The lesions tend to locate peripherally. LCNEC exhibits greater than 11 mitoses/10 hpf and larger areas of necrosis than atypical carcinoid tumors. LCNE show organoid, nesting, trabecular, rosette-like, palisading patterns, usually prominent nucleoli, vesicular or fine chromatin and more cytoplasm than small-cell carcinoma (see Figures 1 and 2). The 1999 WHO criteria for the diagnosis of LCNE include a neuroendocrine morphology and positivity for one or more of the neuroendocrine markers including chromogranin and/ or synaptophysin (see Figure 3).

However, LCNEC are often diagnosed cytologically as non-small-cell lung carcinoma, NOS (see Figure 4). In one study, the neuroendocrine nature of these tumors was not suggested initially on cytology in 80% of the cases. Non-small-cell lung carcinomas tend to display more marked nuclear pleomorphism and lack nuclear molding. To diagnose LCNEC, one should have a high degree of suspicion and then perform immunocytochemical staining to confirm the neuroendocrine differentiation.

Cell size is the most important diagnostic criteria to distinguish SCLC from LCNE. However, size can be difficult to recognize because both neoplasms usually exhibit a

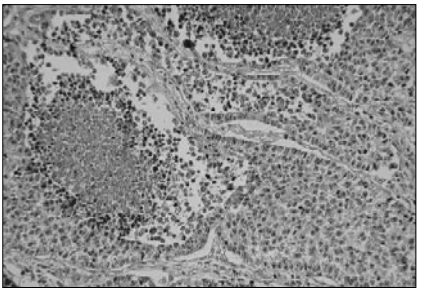

Figure 1. Large-cell neuroendocrine carcinoma Low-power magnification showing nesting pattern and central comedo necrosis. (H&E)

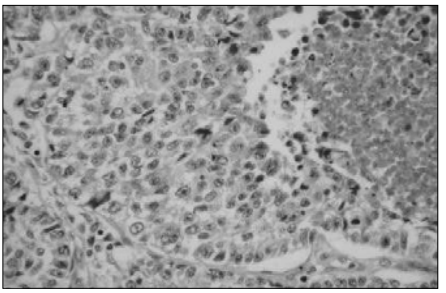

Figure 2. Large-cell neuroendocrine carcinoma Medium-power showing large-cells with abundant pink cytoplasm and prominent nucleoli. (H&E)

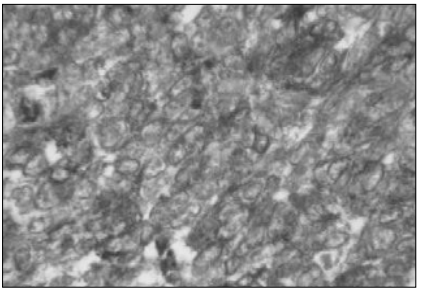

Figure 3. Large-cell neuroendocrine carcinoma. Positive chromogranin stain.

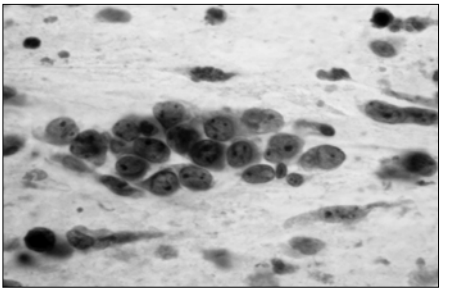

Figure 4. FNA of large-cell neuroendocrine carcinoma. Cohesive group of large neoplastic cells with fine chromatin and prominent nucleoli. (Papanicolaou stain)

spectrum of nuclear sizes and the nuclear size vary according to the specimen size and the degree of tissue crushing. In certain instances, attempts to classify a particular case is difficult. According to a study by Travis et al., the authors reported that the interobserver agreement in the diagnosis of SCLC and LCNEC among pulmonary pathologists was 70% and 40%, respectively.

Is the differentiation of SCLC and LCNEC prognostically significant? The answer is no. LCNEC have a slightly better prognosis. The 5-year and 10-year survival of LCNE are 27% and 9%, respectively, compared to 9% and 5%, respectively for SCLC (the difference is not statistically significant). Therefore, it is controversial if the distinction between SCLC and LCNE has clinical value. Surgery is advocated for the treatment of patients with LCNEC and limited-stage SCLC. Chemotherapy has a limited value for early-stage LCNEC.

4. BRONCHIOALVEOLAR CARCINOMA (BAC)

BAC is a well-differentiated type of adenocarcinoma in which the cells grow over the intact alveolar architecture of the lung with little septal inflammation or fibrosis. The 1999 WHO classification currently proposes a very strict definition for bronchioloalveolar carcinoma, including only the noninvasive tumors with lepidic spread and excluding all the tumors that show stromal, vascular, or pleural invasion. A tumor with bronchioloalveolar pattern with focal stromal, vascular, or pleural invasion should be classified as a mixed adenocarcinoma with brochioloalveolar features. This strict definition only allows the pathologist to make a diagnosis of bronchioloalveolar carcinoma in a complete resection and not on material obtained in a transbronchial biopsy, needle biopsy, or cytology specimens, because the presence of invasion in this limited material cannot be excluded. The diagnosis in this limited sample should be "adenocarcinoma, favor bronchioloalveolar carcinoma."

The incidence of BAC is 3% to 5% of all the primary lung carcinomas. Clinically, BAC presents as a solitary nodule or diffuse pneumonic infiltrate. Histologically, there are three subtypes: mucinous (25%), nonmucinous (50%), and mixed types (25%). The mucinous type is composed by tall columnar or cuboidal cell with abundant clear

cytoplasm, filled with mucin, associated with a basal nuclei, showing little atypia (see Figure 5). This subtype has a marked propensity to spread aerogenously, forming satellite nodules and producing copious mucin resulting in a pneumonia-like picture. The nonmucinous type is composed of columnar or cuboidal cells with pink cytoplasm, high nuclear cytoplasmic ratio, marked variation of nuclear atypia, the presence of intranuclear inclusions, and hobnail appearance—apical cytoplasmic snouts (see Figure 6).

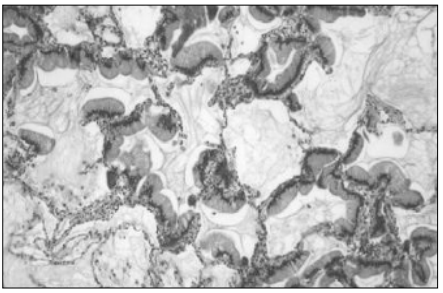

Figure 5. BAC mucinous type. Abundant mucin material present in the alveolar spaces and tall columnar cells with basal nuclei and little pleomorphism. (H&E)

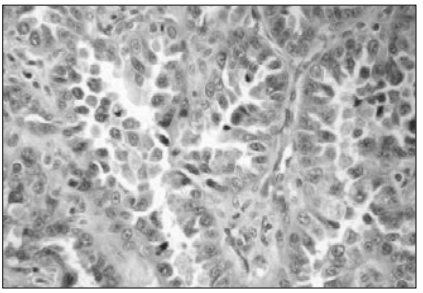

Figure 6. BAC nonmucinous type. Tall columnar cells with marked variation in size and shape and nuclear pleomorphism. (H&E)

Indentation of the pleura associated with subpleural or central anthracotic and fibrotic foci may be seen in some BAC and are not considered as evidence of stromal invasion. Stromal invasion is suggested by tumor cells arranged in acinic or solid nests in a background of fibroblastic stroma. Papillary growth with complicated secondary and tertiary branches is classified as papillary adenocarcinoma and not as BAC. Before a diagnosis of BAC can be made with certainty, cytologicially or histologically, metastatic adenocarcinoma must be excluded. Metastatic carcinomas from the pancreas, biliary tree, stomach, and ovary may simulate a BAC. These tumors share the histopathologic features of BAC including low nuclear grade and the ability to grow in a lepidic fashion over the normal architecture of the lung parenchyma. Whether the lesion is solitary or multiple (metastatic-appearing) is not useful because BAC may be multifocal and metastasis, particularly the ones from the colon, may present as a single lung lesion. In this instance comparison with the known primary is helpful as well as the use of immunohistochemistry. In the case of a nonmucinous BAC the tumor cells are positive for CK7 (75–92%) and TTF-1 (96%) and negative for CK20 (100%). In the case of a mucinous BAC, most are positive for CK7 (83–86%) and for CK20 (25–79%). The tumor cells are negative for TTF-1, and rarely positive for villin in a cytoplasmic pattern, while metastatic colon carcinomas are positive for CK20 and villin (with a brush border pattern) and negative for TTF-1 and CK7.

Other differential diagnosis for nonmucinous BAC includes atypical adenomatous hyperplasia on histology. Atypical adenomatous hyperplasia (AAH) is characterized by a proliferation of cuboidal to low columnar cells with mild to moderate atypia, increased N/C ratio, hyperchromatic nuclei and prominent nucleoli. Mitotic figures are rare. Between the atypical cells, one can find empty looking spaces, which is characteristic of AAH. No high cellularity amd tufting or papillary structures are seen. Often, the

distinction between AAH and BAC is an arbitrary one and is based on the size of the lesion. A lesion of 0.5 cm or less is classified as AAH and a lesion > 0.5 cm is BAC.

4.1 Cytology

The cytology of BAC is characterized by the presence of numerous groups of relativdy uniform, bland appearing glandular cells. The cells can also arrange in monolayered flat sheets, 3-dimensional cell balls, and papillae The tumor cells within the cell balls often have a hobnailed appearance. Acinar formation may be seen. The background is usually clean with scattered single cells. Psammoma bodies are rarely noted. The appearance of individual cells depends on whether they are mucinous or nonmucinous (see Figures 7 and 8). Table 3 lists the cytologic features that are seen in both subtypes. Poorly differentiated BAC has been reported. The tumor cells display more pronounced pleomorphism. They are often indistinguishable from primary adenocarcinoma, NOS.

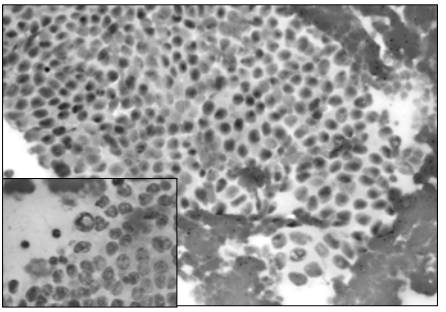

Figure 7. FNA of nonmucinous BAC. 2-dimensional sheets of relatively uniform neoplastic cells. Insert: Intranuclear inclusions. (Diff Quik stain)

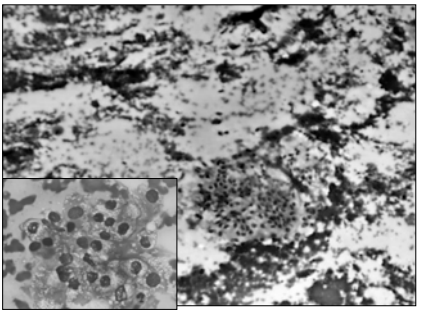

Figure 8. FNA of mucinous BAC. Cohesive group of neoplastic cells in a mucinous background. Insert: Neoplastic cells show vacuolated cytoplasm. (Diff Quik stain)

One of the major differential diagnoses of BAC is from non-neoplastic processes that induce hyperplasia and reparative changes of the respiratory epithelium. These non-neoplastic processes include infection, asthma, infarcts, exposure to chemical toxins, ARDS, and bronchiectasis. BAC may be difficult to differentiate from primary lung adenocarcinoma NOS, and certain metastatic adenocarcinoma such as breast, thyroid, prostate, colon, and kidney.

Nonmucinous BAC also needs to be differentiated from mesothelial cells aspirated during percutaneous FNA. The latter often present as 2-dimensional sheets. An intercellular window may be seen between adjacent mesothelial cells. Individual cells have low N:C ratio, uniform nuclei, fine granular chromatin, and sometimes small, distinct nucleoli.

BAC may be mistaken cytologically as sclerosing hemangioma. The latter is a rare, benign tumor of the lung which is derived from type II pneumocytes. The tumor cells form 2-dimensional sheets and scattered single cells in a bloody background. The presence of papillary fragments with a fibrovascular core is a characteristic finding of

Table 3. Cytologic features of the two subtypes of BAC

Cytologic features	Nonmucinous BAC	Mucinous BAC
Arrangement	Monolayered sheets	3-dimensional clusters, honeycomb sheets
Cell	Resemble alveolar pneumocytes or histiocytes	Resemble goblet cells
Shape	Columnar	Cuboidal
Cytoplasm	Scant, granular/ non-descriptive	Abundant, clear/vacuolated
Terminal bars—like borders	Absent	Present
Nuclei	Centrally located	Basally located
Intranuclear cytoplasmic inclusions	Frequent	Rare
N:C ratio	High	Low
Background	Clean	Mucinous

sclerosing hemangioma. Individual cells resemble reactive alveolar pneumocytes and have a moderate amount of nondescript cytoplasm. The nuclei are uniform, round to oval, and lack atypia. Nucleoli are indistinct but intranuclear cytoplasmic inclusions are frequently noted. Hemosiderin-laden macrophages are also present.

5. NON-SMALL-CELL LUNG CARCINOMA (NSCLC)

The cytology of NSCLC consists of neoplastic cells arranging singly, in 3-dimensional aggregates and syncytial tissue fragments. The nuclei are much larger than that of normal bronchial cell nuclei. The cells often demonstrate obvious malignant features such as high N:C ratio, variation in size and shape, hyperchromasia, irregular nuclear membrane, and prominent nucleoli. Giant cells and multinucleation may be noted. The diagnosis is usually straightforward when there are abundant malignant cells.

Based on their differentiation, NSCLC can be further subdivided into several types—squamous cell carcinoma, adenocarcinoma, and large-cell undifferentiated. However, many lung cancers are mixture of cell types. In practice, the cytologic distinction between SCLC and NSCLC in primary lung cancer is sufficient to guide subsequent management.

5.1 Squamous Cell Carcinoma (SCC)

Squamous cell carcinomas can arise anywhere in the lung although the majority are located centrally. Therefore, they are more readily diagnosed with sputum and bronchial cytology. They can range from well-differentiated (keratinizing) to poorly differentiated (non-keratinizing) and anywhere in between. The cytology of keratinizing and nonkeratinizing SCC is summarized in Table 4. Granulomatous reaction may be noted in either subtype.

Table 4. Cytology of squamous cell carcinomas

Cytologic features	Keratinizing SCC	Nonkeratinizing SCC
Arrangement	Single cells more frequent; pearl formation	Syncytial fragments more frequent; no pearl formation
Cells	Marked pleomorphism, bizarre forms frequent	More uniform, bizarre forms rare
Cytoplasm	Dense, orangeophilic (PAP statin)	Dense, cyanophilic (PAP stained)
N : C ratio	Variable	High
Chromatin	Coarse and dense to pyknotic	Coarse, but more open
Nucleoli	Absent or inconspicuous	More prominent
Background	Necrosis, keratinized debris, +/- cystic degeneration	Necrosis

The differential diagnosis of keratinizing SCC includes various non-neoplastic processes that can cause atypical squamous metaplasia. These processes include necrotizing pneumonia (particularly aspergillosis), abscess, and pulmonary infarct. The squamous cells often form cohesive sheets in mosaic pattern and show varying degrees of atypia. However, single atypical cells are rare. One needs to exercise caution when diagnosing SCC in an inflammatory background, although SCC can be quite inflamed. Squamous dysplasia and CIS, which is more frequently encountered in sputum and bronchial cytology, can be indistinguishable from invasive SCC. The finding of a necrotic background and conspicuous single cells favors an invasive squamous cell carcinoma. Vegetable cells often present with orangeophilic cytoplasm and pyknotic nuclei, mimicking keratinizing SCC. The former often have refractile cell walls and odd shape. Radiation and/or chemotherapy often result in nuclear enlargement and varying degree of cytoplasmic and nuclear pleomorphism. However, the N:C ratio is often within normal limits and the chromatin appears smudgy.

Poorly differentiated SCC composed of predominantly small-cells should be differentiated from SCLC. Evidence of keratinization and lack of nuclear molding favor the former.

5.2 Adenocarcinoma (Excluding Bronchioalveolar Carcinoma)

Adenocarcinomas often arise peripherally and are less readily detected by sputum cytology. Depending on the degree of differentiation, the neoplastic cells can form crowded sheets, cell balls, papillae, and acini. Single cells are common. Individual cells can be cuboidal or columnar. Cytoplasm is often delicate, poorly defined, and often vacuolated. Chromatin is more open and macronucleoli are common.

Table 5 summarizes the differential diagnosis between nonkeratinizing SCC and poorly differentiated adenocarcinoma. However, the distinction between the two may not always be possible. If the tumor does not show definite evidence of either squamous or glandular diffferentiation, the tumor can be designated as undifferentiated large-cell lung carcinoma. Furthermore, it is not uncommon for primary lung carcinoma to show both squamous and glandular differentiation. In addition, one study shows that the concordance between cytologic and histologic typing ranges from poor to fair. This is especially the case for tumors that are poorly differentiated, mixed patterns, and peripherally located. In our institute, a cytologic diagnosis of non-small-cell lung carcinoma is sufficient; our clinicians do not require us to further classify these tumor based on differentiation.

Table 5. Differential diagnosis between nonkeratinizing squamous cell carcinoma and adenocarcinoma

Cytologic features	Squamous cell carcinoma	Adenocarcinoma
Acini formation	Absent	Present
Cytoplasm	Dense and thick, well defined borders	Delicate, indistinct cell borders
Cytoplasmic vacuoles	Usually absent *	Frequent
Nucleus	Central	Eccentric
Chromatin	More coarse	More fine
Nucleoli	Small	Large and prominent
Mucin	Negative	Positive in 25% of cases

* Squamous cells can display degenerative vacuoles.

5.3 Differential Diagnosis

The differential diagnosis of NSCLC includes various reactive conditions that results in marked atypia in bronchial and alveolar epithelial cells. These conditions include infectious processes, pulmonary infarct, and therapeutic effects. Cytologic clues that favor a benign process include paucity of the atypical cells, lack of single atypical cells, inflammatory background, and the findings of specific organisms. Another helpful clue is the presence of a continuum spectrum of atypia from normal to bizarre. In case of therapy-induced atypia, cytoplasmic vacuolation, nuclear enlargement, and multinucleation, prominent nucleoli may be seen. However, the N:C ratio is often maintained. Viral cytopathic changes secondary to CMV and HSV infections can be mistaken for non-small-cell carcinoma.

Metastatic carcinomas are more common than primary bronchogenic carcinomas. The most common primary sites of lung metastases are breast, colon, pancreas, stomach, melanoma, kidney, and sarcomas. However, any malignant tumor can metastasize to the lung. There are no reliable cytology features that can differentiate primary form metastatic carcinoma. When differentiating between primary and metastatic lesions, one must take into account the clinical history, radiologic findings, previous pathologic materials, and ancillary studies. One should keep in mind that patients with other cancers can also develop primary lung cancer.

6. METASTATIC CARCINOMA TO THE LUNG

Metastasis may reach the lung parenchyma through hematogenous or lymphatic routes. The classical presentation of metastatic tumors to the lung is in the form of multiple bilateral peripheral nodules. Metastases that present as a single lesion in the lung are not rare; according to the International Registry of Lung report analyzing 5,206 cases of lung resection due to metastasis, single metastases accounted for 46% and multiple metastases for 52% of the cases. The incidence of metastases based of the type of tumor was as follows: 44% carcinomas, 42% sarcomas, 7% germ cell tumors, 6% melanomas and 2% were others (including Wilm's tumors, etc.). The most common primary site of the carcinoma included colorectal (33%), breast (20%), kidney (19%), head and neck (12%), uterus (7%), lung (3%), and others (7%).

In the great majority of the cases, a clinical history of a primary site outside of the lung is known and the reason for biopsy or surgical excision of a metastasis of the lung is to determine if there is a second primary of the lung or to improve survival. Only in 6% of the cases is the lesion a manifestation of nonpulmonary occult primary. Clinical variables such as inadequate clinical history and occurrence of late metastasis of a tumor presumed to have been cured complicate the evaluation of these lesions.

The approach of the a metastasis of the lung from another site includes comparing the morphology of the known primary if the slides from the previous primary are available. If they are not available, the histologic patterns of the lesion and immunohistochemical studies may be helpful in determining if the lesion is a primary lung or a metastasis. Primary adenocarcinomas of the lung are positive for cytokeratin 7, TTF-1, EMA, CEA, B72.3, and CD15. They are sometimes positive for CA19.9, CA-125, and BCA 225.

6.1 Adenocarcinomas

Both primary and metastatic adenocarcinomas may have acinar or solid patterns. The use of immunohistochemical stain is helpful in this context. Findings that are in favor of a primary lung adenocarcinoma include mixed patterns with solid, acinar and/or bronchioloalveolar components, metastasis of hilar lymph nodes, and positivity for Ck7 and TTF-1 but negative for CK 20. Findings that are in favor of a metastasis include complex cribriform architecture, a nest of very uniform or bland cells, signet ring cells, positivity for PSA and PAP for prostate carcinoma, and positivity for GCDFP, ER, and PR for breast carcinoma. The finding of dirty necrosis and complex or cribriform patterns suggests metastatic colon carcinoma.

Metastatic adenocarcinoma with a “bronchioloalveolar pattern” occurs in 15% of the cases of metastatic cancer to the lung. The primaries include colon, rectum, gallbladder, breast, pancreas, stomach, prostate, thyroid, and kidney. Usually, examination of multiple tissue sections will show more conventional features of the primary lesion. In cases simulating a non-mucinous bronchioloalveolar pattern (metastasis of thyroid and kidney, prostate, papillary serous carcinomas), immunohistochemical stains are helpful.

Metastasis with a “mucinous bronchioloalveolar-like pattern” may be seen in primaries of the colon, rectum, gallbladder, pancreas, and stomach (see Figure 9). However, the use of immunohisto-chemistry is of limited value as both primary lung (mucinous bronchioloalveolar) and metastatic mucinous tumor from colon, pancreas, and ovaries are positive for CEA, variable positive for CK20, CK7, and CA19.9. The only marker helpful that may be helpful is TTF-1, which when positive favors a lung primary; when TTF-1 is negative, one has to rely on histologic grounds.

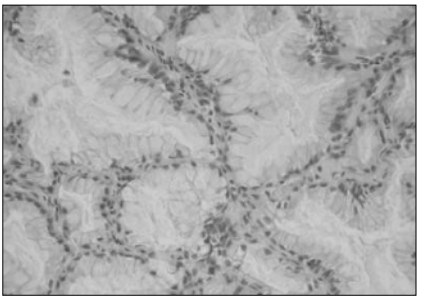

Figure 9. Metastatic adenocarcinoma of the gallbladder to lung, simulating a mucinous BAC. The tumor is positive for CK 7 and CK 20 but negative for TTF-1. (H&E)

6.2 Papillary Carcinoma

Primary papillary adenocarcinomas occur in the lung and their classification is subject to some controversy. Whether these tumors are papillary variants of bronchioloalveolar carcinomas or a separate subtype of carcinoma is still being debated.

- Favor lung primary: CEA +, TTF-1 +, thyroglobulin negative. Finding a second component: acinar, bronchioloalveolar.
- Favors thyroid: TTF-1 +, thyroglobulin +. History of metastasis to lymph node of neck.
- Favor ovary: CA-125 +, WT-1 +, TTF-1 negative
- Favors GI: CA19.9, TTF-1 negative.
- Favor kidney: negative for TTF-1, positivity for CD10.

6.3 Clear Cell Carcinoma

Metastatic renal cell carcinoma is one of the most frequent metastasis surgically excised from the lungs and when solitary the survival improves by surgical resection. It may present as a solitary lesion that develops many years after its resection (10–30 years). Primary clear cell carcinomas of the lung are variants of adenocarcinomas or squamous carcinomas. Table 6 summarizes the features that help in the differentiation between a primary and a metastatic clear cell carcinoma

Renal cell carcinoma may also show sarcomatoid, oncocytic, or papillary patterns that my lead to confusion with other primary and metastatic lung tumors.

Table 6. Differential diagnosis of primary clear cell lung carcinoma and metastatic renal cell carcinoma

Markers	Metastatic renal cell carcinoma	Primary clear cell lung carcinoma
Cytokeratin	Variable	Positive
EMA	Positive	Positive
Vimentin	Positive	Negative
CEA	Negative	Positive
CD10	Variable	Negative
RCC marker	Positive	Negative
Lipid	Positive	Negative
Glycogen	Positive	Positive

6.4 Squamous Cell Carcinoma

Metastatic head and neck carcinomas cannot be differentiated from primary lung carcinoma on histologic grounds alone. Features that favor a primary include association of the invasive tumor with squamous carcinoma in-situ and/or the presence of positive hilar lymph nodes. Most head and neck carcinomas will metastasize first to regional lymph nodes and then to the lung.

6.5 Melanoma

Like renal cell carcinoma, melanoma is notorious for its ability to mimic a variety of histologic patterns. The lung is the most frequent site of metastases from melanoma. The primary site of melanoma may spontaneously regress or may have been surgically excised years previously. Melanoma is positive for HMB-45, S-100, and Mart-1.

6.6 Unusual Patterns of Metastasis

Metastatic tumors of the lung may adopt unusual growth patterns that can be confused with primary lung diseases. For example, miliary spread of tumor nodules simulates an infectious process such as tuberculosis or sarcoidosis. It is usually seen in metastasis of carcinoma of the breast, pancreas, or kidney and angiosarcoma from the heart. The lesion is characterized by multiple microscopic foci, measuring 2–3 mm in dimension, usually involving both lungs.

Lymphangitic spread of carcinoma is frequently seen in metastatic carcinoma of the stomach, pancreas, breast, or prostate. Microscopically, it is characterized by multiple tumor emboli in bronchial, septal, and pleural lymphatics. CXR show a reticulo-nodular infiltrate simulating interstitial lung disease or embolic phenomenon.

Endobronchial metastasis is often from kidney, malignant melanoma, colon, rectum, biliary tract, pancreas, breast, cervix, uterus, bladder, and sarcomas. The latter include fibrosarcoma, angiosarcoma, leiomyosarcoma, MPNST, and osteosarcoma. Endobronchial metastases from sarcomas usually appear after a long latency period between the initial diagnosis of the primary and the metastasis.

The morphologic appearance of the pulmonary metastasis may be different from their primary counterpart. For example, the metastasis of melanoma is often amelonotic and may show a different histology pattern including a spindle cell pattern simulating neural or smooth muscle; uniform cell population with low mitotic activity, simulating atypical carcinoid; extensive areas of hyalinization and/or myxoid change mimicking low-grade neural or fibroblastic proliferation; abundant osteoclast giant cells simulating MFH; heavy neutrophilic infiltrate simulating an anaplastic large-cell carcinoma primary of lung; a signet ring cell configuration, simulating metastasis form GI primary. Sarcomas may show a “maturation” effect. For example, in osteosarcoma there may be heavy chondroid differentiation, heavy collagenization forming a paucicellular mass, or massive osteoclast giant cells simulating an aneurismatic bone cyst. MFH may show muscular, bone or cartilage differentiation. Leiomyosarcoma may demonstrate marked hemagiopericytic pattern.

6.7 Pulmonary Metastases from “Benign” Tumors

Secondary deposits in the lung from tumors that are believed to be benign have been described in the literature. Benign metastasizing leiomyoma presents a single or multiple histologically benign nodules of smooth muscle in the lung parenchyma. The majority of the patients are women with a history of removal of a leiomyoma. Review of the sections of previous hysterectomy is usually unrevealing. The clinical evolution is indolent. Benign mestasizing meningioma presents with multiple meningothelial nodules in the lung secondary to an intracranial meningioma displaying a benign histologic appearance.

Generally, the lesions appear after a long latency period. Benign metastasizing giant-cell tumor of the bone is rare. Only 45 cases have been described in the literature. Lesions respond well to resection and a combination of chemotherapy and radiation therapy. Metastases from thymoma in the absence of cytologic atypia or evidence of invasion have been well documented. Although it happens with any histologic type of thymoma, it is more common in thymomas composed of round or polygonal epithelial cells but rarely in spindle cell thymomas.

6.8 Miscellaneous

Metastases to hilar or mediastinal lymph nodes from an extra-pulmonary primary tumor can occur either with or without lung parenchymal metastasis. The incidence of nodal metastasis reported by the International Registry of Lung Metastasi's is 5%, with the highest incidence (11%) in germ cell tumors, followed by melanoma (8%), carcinomas (6%), and sarcomas (2%). The presence of nodal involvement in the absence of lung metastasis is rare and is usually due to germ cell tumors and breast carcinomas.

6.9 Prognosis

According to the International Registry of Lung Metastases report, the 5-year survival after resection of solitary nonpulmonary metastases averages about 30% in most series. Patients with germ cell tumors had the best survival (68% at 5 years and 63% at 10 years) and melanoma the worse (21% at 5 years and 14% at 10 years). The survival of metastases from carcinomas (37% at 5-year, 21% at 10-years, median 40 months) and for sarcomas (31% at 5-year, 26% at 10-years, median 29 months) did not differ significantly. In other studies, the 5-year survival for patients that underwent resection of the metastatic carcinomas is 33–50%, 39–62%, 36–38%, and 27–38% for kidney, colorectal, breast, and soft tissue sarcomas, respectively.

7. SARCOMATOID CARCINOMA AND OTHER SPINDLE CELL LESIONS

Sarcomatoid carcinoma is the most common spindle cell malignancy of the lung, while primary true sarcomas of the lung are exceptionally rare. Names used in the past include spindle cell carcinoma, squamous cell carcinoma with pseudosarcomatous stroma, pseudosarcoma, carcinosarcoma and teratocarcinoma. Some of the new proposed names include biphasic sarcomatoid carcinoma and monophasic sarcomatoid carcinoma. In this text, we will use the term sarcomatoid carcinoma, which should be viewed as an epithelial neoplasm with divergent mesenchymal differentiation, in which the carcinoma cells have acquired the potential to express a mesenchymal phenotype.

Clinically, most patients are men and most are smokers. The male to female ratio is 3 to 1 and the mean age is 60 years. Most sarcomatoid carcinomas are located in a large bronchus followed by peripheral lung tissue. The bronchial lesions are usually a polypoid mass associated with a bacterial pneumonia or other symptoms like cough, hemoptysis, and dyspnea. The peripheral lesion is usually asymptomatic. The mean size for endobronchial lesions is 6 cm while for peripheral lesions it can be up to 10.0 cm.

Microscopically, the central tumors are polypoid endobronchial masses that occlude the bronchi and may be associated with adjacent squamous dysplasia or carcinoma in-situ. Broad areas of geographic and hemorrhagic necrosis are typically identified. In most cases, a poorly differentiated squamous carcinoma is admixed with sarcoma-like areas. The sarcomatoid component is composed by anaplastic fusiform and pleomorphic cells (see Figure 10). Rarely, the sarcomatoid component has a myxoid stroma with limited cytologic atypia associated with inflammation, simulating a myofibroblastic tumor (inflammatory pseudotumor). Other mesenchymal components include osteosarcoma, chondrosarcoma, and rhabdomyosarcoma (see Figure 11); the last two are by far the most common. By immunohistochemistry the sarcomatoid component is variably positive for cytokeratin and EMA (25–75% of the cases). The staining pattern is usually focal.

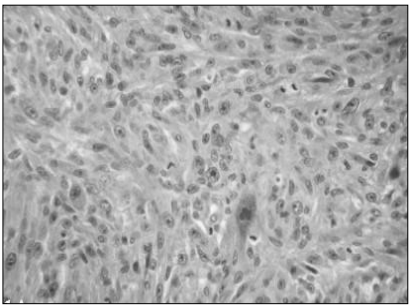

Figure 10. Sarcomatoid carcinoma. The sarcomatoid component consists of anaplastic fusiform cells. (H&E)

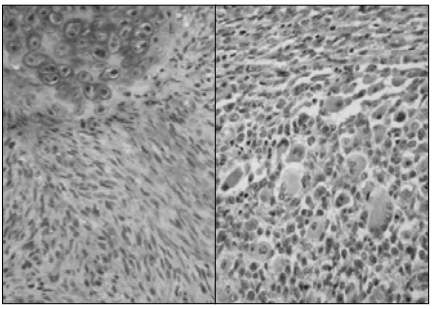

Figure 11. Sarcomatoid carcinoma with chondrosarcoma (left) and rhabdomyosarcoma (right) component. (H&E)

The main differential diagnosis is primary or metastatic sarcomas of the lung including leimyosarcoma, rhabdomyosarcoma, osteosarcoma, chondrosarcoma, angiosarcoma, Kaposi's sarcoma, malignant fibrous histiocytoma, malignant peripheral nerve sheath tumor, melanoma, and synovial sarcoma (SS). In most instances the histology and immunohistochemistry would be of help (see Table 7).

The only tumor in which immunohistochemistry is not helpful is SS, as both tumors stain with keratin and EMA. Features that help differentiate them are the marked propensity of SS to affect children, adolescents, and young adults (the average age of patients with synovial sarcoma is 25 years compared to 60 with sarcomatoid carcinoma) and the cytogenetic analysis, which in the case of SS will show the t (X;18)(p11;q11) chromosomal translocation. Patients with synovial sarcoma also have a better prognosis with a survival ranging from 1 to 6 years.

Sarcomatoid mesothelioma is also in the differential diagnosis particularly in a limited sample and when the sarcomatoid carcinoma has spread to the pleura. The presence of an intrapulmonary mass favors primary sarcomatoid carcinoma. The presence of diffuse pleural thickening, a history of asbestos exposure, and the presence of calretinin or WT-1 positivity will favor a sarcomatoid malignant mesothelioma.

Although 50% of the sarcomatoid carcinomas are only stage I, the postoperative survival at 5 years is only 20%. Metastasis usually occurs in the opposite lung, liver, bones, adrenal glands, and brain.

7.1 Approach to Diagnosis of Spindle Cell Lesions on FNA

The reported incidence of spindle cell and mesenchymal lesions encountered in a large series of transthoracic pulmonary FNAs ranges from less than 1% to 8%. Less than half are malignant lesions. These spindle cell lesions consist of a heterogeneous group of inflammatory/reactive and neoplastic conditions. The diagnostic considerations include the distinction between reactive/inflammatory conditions and neoplasms, soft tissue neoplasms and nonmesenchymal lesions, and benign and malignant soft tissue neoplasms. We classify spindle cell and mesenchymal pulmonary lesions into three general categories based on the cytologic morphology along with the radiologic and clinical findings.

The first group of lesions consists of spindle cells that are inflammatory/reactive in nature. The most frequent lesion encountered in this category is granulomatous disease. Radiologically, the findings of granulomatous inflammation are nonspecific and may resemble a neoplasm. Cytologically, the epithelioid histiocytes often assume a spindle cell morphology and form loosely cohesive aggregates that may mimic a mesenchymal proliferation. The presence of acute or chronic inflammation and multinucleated giant cells should suggest an inflammatory process. Additional material should be obtained for culture and cytochemical stains to rule out an infectious etiology such as mycobacteria or fungal organisms. After an infectious etiology is ruled out, other causes including sarcoidosis should be considered. A potential pitfall in diagnosing granulomatous inflammation is the presence of reactive bronchial and alveolar cells as well as metaplastic squamous cells that may be mistaken as carcinoma. They are usually few in number. On the other hand, granulomatous inflammation may coexist with cancers. Other inflammatory/reactive pulmonary lesions are encountered infrequently in FNA

The lesions in the second category consist of benign neoplasms and often present radiologically as a solitary, well-circumscribed, stable or slow-growing pulmonary nodule. The majority of these patients are asymptomatic and the lesions are often detected incidentally. Pulmonary hamartomas are the most common benign neoplasm of the lung, accounting for 6% of all solitary pulmonary nodular lesions. Popcorn-like calcification is rarely noted, but when present in a well-circumscribed pulmonary nodule, is diagnostic of pulmonary hamartoma. The cytologic findings are characterized by the presence of cartilage, fibromyoxid stroma, smooth muscle, and bronchial cells in varying proportions (see Figure 12). When the aspirated materials are sparse, the cellular components may be mistaken as the normal constituent of the bronchial wall or chest wall and the aspirate may be classified as nondiagnostic. On the other hand, bronchial cells with reactive atypia may be a potential source of false positives. Some authors advocate the use of immunocytochemical staining for S-100 protein to highlight the chondroid and fibromyxoid stroma of pulmonary hamartomas. A wide variety of benign mesenchymal tumors can occur in the lung including leiomyomas, fibromas, and nerve sheath tumors. There are considerable overlaps in the cytologic findings among these lesions. Because the choice of treatment, that is, wedge resection, would be the same, it may be less critical to differentiate among various benign soft tissue neoplasms after the benign nature of the lesion has been determined.

The third category consists of malignant spindle cell and mesenchymal lesions. It comprises an uncommon and heterogeneous group including primary and secondary, mesenchymal and nonmesenchymal malignancies. The nonmesenchymal spindle cell

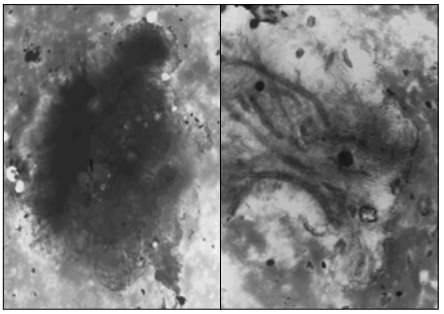

Figure 12. FNA of pulmonary hamartoma. Chrondoid (left) and fibromyxoid (right) stromal fragments. (Diff Quik stain)

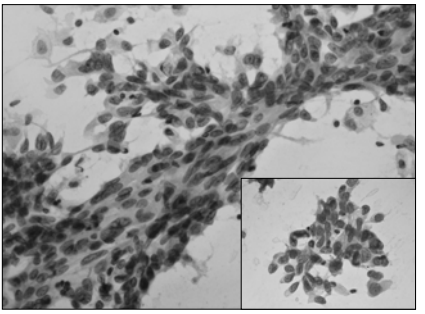

Figure 13. FNA of sarcomatoid carcinoma. Tissue fragment of spindle cells. Insert: individual cells display obvious malignant features. (Papanicolaou stain)

metastatic carcinomas with a spindle cell or sarcomatoid component (see Figure 13) and metastatic malignant melanomas. Primary pulmonary sarcomas are relatively infrequent. Virtually, any soft tissue sarcomas can arise in the lung, resulting in widely diverse histologic and cytologic features. The use of ancillary studies such as immunocytochemistry and electron microscopy is helpful in narrowing the differential diagnosis. The lung is also a common site of metastasis from a sarcoma. In fact, metastatic sarcomas are far more common than primary lung sarcomas. In most instances, a prior history of sarcoma is present at the time of FNA. Comparison with the original material helps to confirm the metastatic nature of the pulmonary lesion.

8. REFERENCES

8.1 General

1. Colby TV, Koss MN, Travis WD, *Tumors of the Lower Respiratory Tract* (Armed and Forces Institute of Pathology, Washington, DC, 1995).
2. Travis WD, Colby TV, Corrin B, Shimostao Y, Brambilia E, *Histological Typing of Lung and Pleural Tumours* (Springer-Verlag, New York, NY, 1999).
3. Raab SS, Silverman J, Clinical utility of cytologic typing of lung tumors. *Diagnostic Cytopathology*, 10(4), 376-82 (1994).

8.2 Neuroendocrine Neoplasms

1. Beasley MB, Thunnissen FB, Brambilla E, et al., Pulmonary atypical carcinoid: predictors of survival in 106 cases. *Human Pathology*, 31(10), 1255-65 (2000).
2. Dresler CM, Ritter JH, Patterson GA, Ross E, Bailey MS, Wick MR, Clinical-pathologic analysis of 40 patients with large-cell neuroendocrine carcinoma of the lung. *Annals of Thoracic Surgery*, 63(1), 180-5 (1997).
3. Junker K, Wiethege T, Muller KM, Pathology of small-cell lung cancer. *Journal of Cancer Research and Clinical Oncology*, 126(7), 361-8 (2000).
4. Lee TK, Silverman JF, Horner RD, Scarantino CW, Overlap of nuclear diameters in lung cancer cells. *Analytical and Quantitative Cytology and Histology*, 12(4), 275-8 (1990).
5. Lee TK, Horner RD, Silverman JF, Jackson DV, Jr., Anderson-Goetz D, Scarantino CW, Implications of nuclear diameter in small-cell lung carcinoma. *Analytical and Quantitative Cytology and Histology*, 12(2), 78-84 (1990).

6. Lee TK, Esinhart JD, Blackburn LD, Silverman JF, The size of small-cell lung carcinoma cells: ratio to lymphocytes and correlation with specimen size and crush artifact. *Analytical and Quantitative Cytology and Histology*, 14(1), 32-4 (1992).
7. Ordonez NG, Value of thyroid transcription factor-1 immunostaining in distinguishing small-cell lung carcinomas from other small-cell carcinomas. [see comment]. *American Journal of Surgical Pathology*, 24(9), 1217-23 (2000).
8. Travis WD, Linnoila RI, Tsokos MG, et al., Neuroendocrine tumors of the lung with proposed criteria for large-cell neuroendocrine carcinoma: an ultrastructural, immunohistochemical, and flow cytometric study of 35 cases: a*merican Journal of Surgical Pathology*, 15(6), 529-53 (1991).
9. Travis WD, Rush W, Flieder DB, et al., Survival analysis of 200 pulmonary neuroendocrine tumors with clarification of criteria for atypical carcinoid and its separation from typical carcinoid. *American Journal of Surgical Pathology*, 22(8), 934-44 (1998).
10. Travis WD, Gal AA, Colby TV, Klimstra DS, Falk R, Koss MN, Reproducibility of neuroendocrine lung tumor classification. *Human Pathology*, 29(3), 272-9 (1998).
11. Vollmer RT, The effect of cell size on the pathologic diagnosis of small- and large-cell carcinomas of the lung. *Cancer*, 50(7), 1380-3 (1982).
12. Wick MR, Immunohistology of neuroendocrine and neuroectodermal tumors. *Seminars in Diagnostic Pathology*, 17(3), 194-203 (2000).
13. Wick MR, Neuroendocrine neoplasia. Current concepts. *American Journal of Clinical Pathology*, 113(3), 331-5 (2000).
14. Wick MR, Ritter JH, Neuroendocrine neoplasia of the lung. *Annals of Thoracic Surgery*, 69(1), 307-8 (2000).
15. Anderson C, Ludwig ME, O'Donnell M, Garcia N, Fine needle aspiration cytology of pulmonary carcinoid tumors. *Acta Cytologica*, 34(4), 505-10 (1990).
16. Collins BT, Cramer HM, Fine-needle aspiration cytology of islet cell tumors. *Diagnostic Cytopathology*, 15(1), 37-45 (1996).
17. Craig ID, Finley RJ, Spindle cell carcinoid tumor of lung: cytologic, histopathologic, and ultrastructural features. *Acta Cytologica*, 26(4), 495-8 (1982).
18. Delgado PI, Jorda M, Ganjei-Azar P, Small-cell carcinoma versus other lung malignancies: diagnosis by fine-needle aspiration cytology. *Cancer*, 90(5), 279-85 (2000).
19. Fekete PS, Cohen C, DeRose PB, Pulmonary spindle cell carcinoid. Needle aspiration biopsy, histologic and immunohistochemical findings. *Acta Cytologica*, 34(1), 50-6 (1990).
20. Frierson HF, Jr., Covell JL, Mills SE, Fine needle aspiration cytology of atypical carcinoid of the lung. *Acta Cytologica*, 31(4), 471-5 (1987).
21. Kim K, Mah C, Dominquez J, Carcinoid tumors of the lung: cytologic differential diagnosis in fine-needle aspirates. *Diagnostic Cytopathology*, 2(4), 343-6 (1986).
22. Miyamoto H, Inoue S, Abe S, Murao M, Yasuda S, Sakai E, Relationship between cytomorphologic features and prognosis in small-cell carcinoma of the lung. *Acta Cytologica*, 26(4), 429-33 (1982).
23. Nguyen GK, Cytopathology of pulmonary carcinoid tumors in sputum and bronchial brushings. *Acta Cytologica*, 39(6), 1152-60 (1995).
24. Nicholson SA, Ryan MR, A review of cytologic findings in neuroendocrine carcinomas including carcinoid tumors with histologic correlation. *Cancer*, 90(3), 148-61 (2000).
25. Wiatrowska BA, Krol J, Zakowski MF, Large-cell neuroendocrine carcinoma of the lung: proposed criteria for cytologic diagnosis. *Diagnostic Cytopathology*, 24(1), 58-64 (2001).
26. Zaharopoulos P, Wong JY, Stewart GD, Cytomorphology of the variants of small-cell carcinoma of the lung. *Acta Cytologica*, 26(6), 800-8 (1982).
27. Yang YJ, Steele CT, Ou XL, Snyder KP, Kohman LJ, Diagnosis of high-grade pulmonary neuroendocrine carcinoma by fine-needle aspiration biopsy: non-small-cell or small-cell type? *Diagnostic Cytopathology*, 25(5), 292-300 (2001).

8.3 Bronchioalveolar Carcinoma

1. Cagle PT, Fraire AE, Greenberg SD, Cox A, Brown RW, Potential utility of p53 immunopositivity in differentiation of adenocarcinomas from reactive epithelial atypias of the lung. *Human Pathology*, 27(11), 1198-203 (1996).
2. Goldstein NS, Thomas M, Mucinous and nonmucinous bronchioloalveolar adenocarcinomas have distinct staining patterns with thyroid transcription factor and cytokeratin 20 antibodies. *American Journal of Clinical Pathology*, 116(3), 319-25 (2001).

3. Miller RR, Nelems B, Evans KG, Muller NL, Ostrow DN, Glandular neoplasia of the lung: a proposed analogy to colonic tumors. *Cancer*, 61(5), 1009-14 (1988).
4. Kitamura H, Kameda Y, Ito T, Hayashi H, Atypical adenomatous hyperplasia of the lung: implications for the pathogenesis of peripheral lung adenocarcinoma.[see comment]. *American Journal of Clinical Pathology*, 111(5), 610-22 (1999).
5. Mori M, Rao SK, Popper HH, Cagle PT, Fraire AE, Atypical adenomatous hyperplasia of the lung: a probable forerunner in the development of adenocarcinoma of the lung. *Modern Pathology*, 14(2), 72-84 (2001).
6. Auger M, Katz RL, Johnston DA, Differentiating cytological features of bronchioloalveolar carcinoma from adenocarcinoma of the lung in fine-needle aspirations: a statistical analysis of 27 cases. *Diagnostic Cytopathology*, 16(3), 253-7 (1997).
7. Kaw YT, Nayak RN, Fine needle aspiration biopsy cytology of sclerosing hemangioma of the lung: a case report. *Acta Cytologica*, 37(6), 933-7 (1993).
8. Lozowski W, Hajdu SI, Cytology and immunocytochemistry of bronchioloalveolar carcinoma. *Acta Cytologica*, 31(6), 717-25 (1987).
9. MacDonald LL, Yazdi HM, Fine-needle aspiration biopsy of bronchioloalveolar carcinoma. *Cancer*, 93(1), 29-34 (2001).
10. Ng WK, Fu KH, Wang E, Tang V, Sclerosing hemangioma of lung: a close cytologic mimicker of pulmonary adenocarcinoma. *Diagnostic Cytopathology*, 25(5), 316-20 (2001).
11. Scoggins WG, Smith RH, Frable WJ, O'Donohue WJ, Jr., False-positive cytological diagnosis of lung carcinoma in patients with pulmonary infarcts. *Annals of Thoracic Surgery*, 24(5), 474-80 (1977).
12. Silverman JF, Finley JL, Park HK, Strausbauch P, Unverferth M, Carney M, Fine needle aspiration cytology of bronchioloalveolar-cell carcinoma of the lung. *Acta Cytologica*, 29(5), 887-94 (1985).

8.4 Non-Small-cell Lung Carcinoma

1. Zusman-Harach SB, Harach HR, Gibbs AR, Cytological features of non-small-cell carcinomas of the lung in fine needle aspirates. *Journal of Clinical Pathology*, 44(12), 997-1002 (1991).
2. Schulte MA, Ramzy I, Greenberg SD, Immunocytochemical characterization of large-cell carcinomas of the lung: role, limitations, and technical considerations. *Acta Cytologica*, 35(2), 175-80 (1991).
3. Truong LD, Underwood RD, Greenberg SD, McLarty JW, Diagnosis and typing of lung carcinomas by cytopathologic methods: a review of 108 cases. *Acta Cytologica*, 29(3), 379-84 (1985).

8.5 Metastatic Tumors to the Lung

1. Anonymous, Long-term results of lung metastasectomy: prognostic analyses based on 5206 cases. The International Registry of Lung Metastases. *Journal of Thoracic and Cardiovascular Surgery*, 113(1), 37-49 (1997).
2. Cagle PT, Philip T. Differential diagnosis between primary and metastatic carcinomas. In: Brambilia C, Brambilla E, eds. *Lung Tumors: Fundamental Biology and Clinical Management*. New York, NY: Marcek Dekker Inc., 1999.
3. DeYoung BR, Wick MR, Immunohistologic evaluation of metastatic carcinomas of unknown origin: an algorithmic approach. *Seminars in Diagnostic Pathology*, 17(3), 184-93 (2000).
4. Friedel G, Pastorino U, Ginsberg RJ, et al., Results of lung metastasectomy from breast cancer: prognostic criteria on the basis of 467 cases of the International Registry of Lung Metastases. *European Journal of Cardio-Thoracic Surgery*, 22(3), 335-44 (2002).
5. Johnston MR, Grondin S, The role of endoscopy in the staging and management of lung metastases. *Chest Surgery Clinics of North America*, 8(1), 49-58 (1998).
6. Koodziejski L, Goralczyk J, Dyczek S, Duda K, Nabiaek T, The role of surgery in lung metastases. *European Journal of Surgical Oncology*, 25(4), 410-7 (1999).
7. Pastorino U, McCormack PM, Ginsberg RJ, A new staging proposal for pulmonary metastases: the results of analysis of 5206 cases of resected pulmonary metastases. *Chest Surgery Clinics of North America*, 8(1), 197-202 (1998).
8. Suster S, Moran CA, Unusual manifestations of metastatic tumors to the lungs. *Seminars in Diagnostic Pathology*, 12(2), 193-206 (1995).
9. Chhieng DC, Cangiarella JF, Zakowski MF, Goswami S, Cohen JM, Yee HT, Use of thyroid transcription factor 1, PE-10, and cytokeratins 7 and 20 in discriminating between primary lung carcinomas and metastatic lesions in fine-needle aspiration biopsy specimens. *Cancer*, 93(5), 330-6 (2001).
10. Pilotti S, Rilke F, Gribaudi G, Damascelli B, Fine needle aspiration biopsy cytology of primary and metastatic pulmonary tumors. *Acta Cytologica*, 26(5), 661-6 (1982).

8.6 Sarcomatoid Carcinoma and Other Spindle Cell Lesions

1. Berho M, Moran CA, Suster S, Malignant mixed epithelial/mesenchymal neoplasms of the lung. *Seminars in Diagnostic Pathology*, 12(2), 123-39 (1995).
2. Humphrey PA, Scroggs MW, Roggli VL, Shelburne JD, Pulmonary carcinomas with a sarcomatoid element: an immunocytochemical and ultrastructural analysis. *Human Pathology,* 19(2), 155-65 (1988).
3. Koss MN, Hochholzer L, Frommelt RA, Carcinosarcomas of the lung: a clinicopathologic study of 66 patients. *American Journal of Surgical Pathology*, 23(12), 1514-26 (1999).
4. Nappi O, Glasner SD, Swanson PE, Wick MR, Biphasic and monophasic sarcomatoid carcinomas of the lung: a reappraisal of 'carcinosarcomas' and 'spindle-cell carcinomas'. *American Journal of Clinical Pathology*, 102(3), 331-40 (1994).
5. Ro JY, Chen JL, Lee JS, Sahin AA, Ordonez NG, Ayala AG, Sarcomatoid carcinoma of the lung. Immunohistochemical and ultrastructural studies of 14 cases. *Cancer*, 69(2), 376-86 (1992).
6. Dunbar F, Leiman G, The aspiration cytology of pulmonary hamartomas. *Diagnostic Cytopathology*, 5(2), 174-80 (1989).
7. Hummel P, Cangiarella JF, Cohen JM, Yang G, Waisman J, Chhieng DC, Transthoracic fine-needle aspiration biopsy of pulmonary spindle cell and mesenchymal lesions: a study of 61 cases. *Cancer*, 93(3), 187-98 (2001).
8. Silverman JF, Marrow HG, Fine needle aspiration cytology of granulomatous diseases of the lung, including nontuberculous Mycobacterium infection. *Acta Cytologica*, 29(4), 535-41 (1985).
9. Wiatrowska BA, Yazdi HM, Matzinger FR, MacDonald LL, Fine needle aspiration biopsy of pulmonary hamartomas: radiologic, cytologic, and immunocytochemical study of 15 cases. *Acta Cytologica*, 39(6), 1167-74 (1995).

CHAPTER 9
ENDOSCOPIC ULTRASOUND GUIDED FINE NEEDLE ASPIRATION OF THE PANCREAS

Darshana Jhala, M.D, B. Mus.,[*] and Nirag C. Jhala, M.D, MIAC[†]

1. INTRODUCTION

Currently, pancreatic cancer is the fourth leading cause of cancer-associated deaths in the United States and ranks ninth in its incidence. Increased mortality from this tumor results from multiple factors including detection at advanced stages, aggressive biology, and relative resistance to available therapy. It is reported that resection of early (size <3.0 cm) organ-confined tumors provide significantly improved patient survival in comparison to large tumors.[1] It is, therefore, important to detect these tumors early. Imaging studies (percutaneous ultrasound and CT scan) have provided a valuable support in detection of these tumors for a long time. Endoscopic ultrasound (EUS) is a relatively new imaging modality and is reported to be superior to both CT scans and MRI in detecting pancreatic lesions, especially when lesions are smaller than 3.0 cm. [2]

While imaging studies are important to detect the lesion, tissue diagnosis still remains the gold standard to determine an accurate diagnosis and begin disease-specific intervention. For a long time needle biopsies and frozen section diagnosis remained as initial modalities to provide tissue diagnosis. Due to its success, fine needle aspirates (FNA) from the pancreas obtained percutaneously under image guidance (ERCP, angiography, CT scan, or ultrasound) or intraoperatively became the standard practice in some centers.[3-7] Studies have also shown that both percutaneous and intraoperative FNA from the pancreas have comparable sensitivity and specificity.[8] EUS-guided FNA of the pancreas is a relatively new modality to obtain preoperative diagnosis and staging for pancreatic malignancies.[9,10] This modality improves cellular yield and, in turn, the diagnostic performance for both small and large lesions. The success of EUS-FNA in diagnosing pancreatic lesions has changed the practice for obtaining preoperative

[*]Assistant Professor, Department of Pathology, University of Alabama, Birmingham, AL.
[†]Associate Professor, Department of Pathology, University of Alabama, Birmingham, AL.

diagnosis and staging for pancreatic cancer in large referral centers such as ours.[9, 11] This increasing trend will soon be considered as the standard of practice. It is, therefore, important to understand the cytologic features and possible factors that may play a role in avoiding misinterpretations on samples obtained under EUS guidance.

2. EUS-FNA SERVICE AND SAMPLE PREPARATION

Success of EUS-FNA service rests upon several critical factors that have been highlighted in our previous publication.[9] In addition to the experience of the endosonographer, good lines of communication between the cytopathologist and the endosonographer, adequate sampling, optimal sample processing, accurate interpretation, and the ability to determine the need for additional samples required for ancillary studies are needed for effective diagnosis. Cost–benefit parameters in individual laboratories dictate whether a cytopathologist/advanced trainee/or a trained cytotechnologist is present in the endoscopy suite.[9] We, like many other observers, propose that the cytopathologist's presence in the endoscopy suite improves sample adequacy for EUS-FNA. In cases where a cytopathologist cannot go to the endoscopy suite, it is beneficial if at least six passes from the pancreas are made and the specimen are placed in a transport media to obtain adequate samples.[12] It is also imperative that universal precaution be taken by any personnel handling needles and samples in the endoscopy suite to prevent the introduction of any iatrogenic infections into or from the patient.

3. OBJECTIVE

The objectives for performing EUS-FNA of lesions of the pancreas are (1) to detect and determine the extent of the lesions, and (2) to obtain preoperative tissue diagnosis for a clinically suspicious malignancy and stage malignancies.

4. NORMAL CELLULAR ELEMENTS

While reviewing FNAs one should also consider the modality by which the sample was obtained. For samples obtained under EUS guidance one should also consider the tumor location and the organ site through which the needle enters the pancreas. One should also recognize normal cellular elements that could be obtained on FNA samples to avoid misinterpretations.[13] Table 1 describes the normal cellular elements that are important to be recognized as normal elements in EUS-FNA of the pancreas. In addition to the native cellular elements of the pancreas, additional normal cells that can form part of the EUS-FNA samples are noted (see Figure 1 and Table 2).

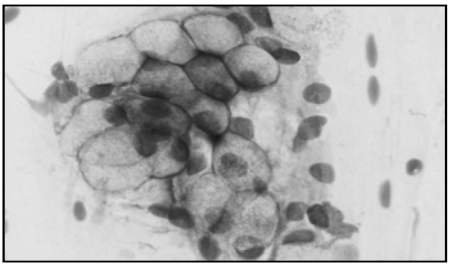

Figure 1. Smear from transduodenal aspirate for pancreatic head mass reveals tightly cohesive group of surface duodenal mucosa. (Papanicolaou)

Table 1. Normal cellular elements from the pancreas which may be noted on FNA

	Acinar cells	Ductal cells	Islet cells
Arrangement	Acinar pattern, rarely isolated	Cohesive, honey comb, picket-fenced	Isolate, groups, rarely seen
Cells	Pyramidal/polygonal	Cubodial to columnar	Round to oval
Cell borders	Well-defined	Well-defined	Poorly-defined
Cytoplasm	Abundant, granular	Delicate, pale, vacuolated, ±mucin	Moderate, pale, wispy
Nucleus	Round/oval,	Round/oval, uniform	Round/oval, eccentrically located ±pleomorphism
Nucleolus	Distinct or prominent	Tiny and inconspicuous	Inconspicuous
Chromatin	Finely granular	Finely granular	Salt-and-pepper

Table 2. Approaches to perform EUS-FNA for lesions located at different sites in pancreas

Location of lesion	Approach	Additional cells
Head/uncinate	Transduodenal	Tightly cohesive glandular cells with honey comb appearance and goblet cells from duodenum
Body/tail	Transgastric	Parietal cells, chief cells, superficial gastric glandular cells

5. IMAGING STUDIES

Imaging studies help determine whether the lesion is solid, solid and cystic, or predominantly cystic.

6. SOLID PANCREATIC MASSES

Table 3 summarizes the differential diagnosis of solid pancreatic masses on FNA.

6.1 Chronic Pancreatitis

Smears from chronic pancreatitis often are paucicellular and include more than one cell type in the aspirate. Reactive ductal epithelium usually is in tight 2-dimensional cohesive groups (see Figure 2) with rare single atypical cells. Cells in groups show preserved polarity and may show enlarged nuclei with a preserved nuclear-to-cytoplasmic ratio. Reactive ductal cells may show enlarged nuclei, prominent nucleoli, and anisocytosis. In addition, these smears may also show acinar cells, dense collagenous fibrosis, chronic inflammation, occasional necrosis and normal mitoses.

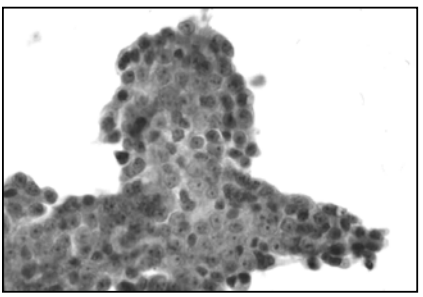

Figure 2. Chronic pancreatitis. Cohesive 2-dimensional cluster of pancreatic ductal epithelial cells. (Papanicolaou)

6.2 Pancreatic Adenocarcinoma

Smears from pancreatic adenocarcinoma are usually cellular and show many single atypical cells with anisocytosis and anisonucleosis. These atypical nuclei show an

Table 3. Differential diagnoses for solid pancreatic masses

Benign	Malignant
Chronic pancreatitis	Carcinoma
Islet cell tumor	Ductal adenocarcinoma and its variants
Abscess	Metastatic carcinomas
Infections	Acinar cell carcinoma (rarely)
	Malignant islet cell tumor
	Metastatic nonepithelial malignancies

increased nuclear-to-cytoplasmic ratio, markedly irregular nuclear membrane, coarse chromatin, prominent nucleoli, and occasionally abnormal mitoses (see Figure 3 and 4). Individual cells may also show multinucleation and foamy, finely granular cytoplasm with sharp cytoplasmic membrane. Tumor diathesis may be seen. When in groups,

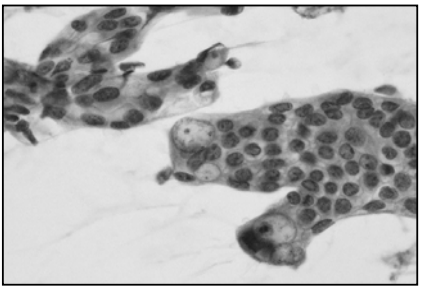

Figure 3. Pancreatic carcinoma, well-differentiated. Cohesive group with drunken honey comb appearance. (Papanicolaou)

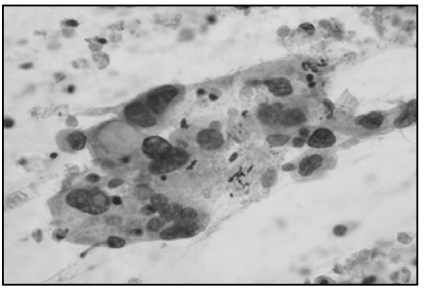

Figure 4. Pancreatic carcinoma, well-differentiated**.** Markedly atypical cells in loose aggregate. Atypical mitosis is noted. (Papanicolaou)

smears from well-differentiated carcinoma may show large folded sheets in which nuclei are crowded and 3-dimensional, or may demonstrate a drunken honey comb appearance. In the later pattern, cell groups show irregularly spaced nuclei with moderate cytoplasm and show altered polarity. Individual nuclei may be enlarged at least about 1.5 to 2 times the size of a red cell and show marked nuclear membrane irregularity, coarse chromatin clumping, and, frequently, prominent nucleoli. In comparison, cell groups in moderate to poorly differentiated tumors are fewer in number, and they show many 3-dimensional clusters with loose cohesion. The nuclei in these cell groups show obvious features of malignancy.

6.3 Variants of Ductal Adenocarcinoma

These include adenosquamous carcinoma, giant cell carcinoma, signet ring cell carcinoma, colloid carcinoma, and foam cell carcinoma. Cytologic features will show the prominence of cells as reflected in the names of these tumors. These tumors must also be separated from metastatic carcinomas which may have similar cytologic features.

For example, both malignant squamous and adenocarcinoma cells may be noted in adenosquamous carcinoma. The differential diagnosis for this tumor, especially, on an EUS-FNA sample, will include chronic pancreatitis with an admixture of reactive squamous cell contamination from esophageal mucosa.

6.4 Differential Diagnosis of Pancreatic Adenocarcinoma Versus Chronic Pancreatitis

Increased cellularity is one of the criteria used to distinguish well-differentiated adenocarcinoma from chronic pancreatitis. The cellularity of a sample is influenced by several factors including the technique, operator expertise, onsite adequacy checks, and the anatomic location of the tumor.[12,14] The use of cellularity as a criterion in the differentiation of chronic pancreatitis and well-differentiated adenocarcinoma should be used with caution especially when the samples have been obtained using EUS-FNA.

Hypocellularity of the sample may result in a false-negative diagnosis. False-negative diagnoses may occur due to technical difficulties, sampling errors, or interpretive errors. A sampling error may result from the technical difficulty associated with reaching a lesion. It also is possible that the marked desmoplasia of pancreatic adenocarcinoma may result in an inadequate specimen and /or an inconclusive diagnosis (i.e., atypical or suspicious for malignancy), both of which require further investigations or a repeat FNA.[12,15-17] As discussed above, we believe that the presence of a cytopathologist in the endoscopy suite at the time of the procedure is helpful in ensuring adequate diagnostic samples.

6.5 Acinar Cell Carcinoma

This is a rare tumor and is not very commonly detected on cytology samples. These tumors, when aspirated, show increased cellularity. The smears show many loosely cohesive sheets with acini formation. Many single cells and nuclei without cytoplasm are also observed. Individual cells resemble pancreatic acinar cells and have centrally placed nuclei with prominent nucleoli. They have moderate granular amphophilic cytoplasm. The granular cytoplasm of the enzyme secreting zymogen granules are best visualized on Romanowsky stains and PAS with and without diastase stains. Immunohistochemical stains that highlight these cells include trypsin, amylase, and alpha 1 anti-chymotrypsin.

6.6 Metastatic Malignancies

This group comprises a variety of malignancies that can involve the pancreas. Some of the more common malignancies include renal cell carcinoma (see Figure 5), pulmonary adenocarcinoma, and breast carcinoma. In addition, other malignancies such as non–Hodgkin's lymphoma and melanoma have also been recognized. These tumors have been well-characterized and patient history and cytologic features in conjunction with pertinent immunohistochemical stains are useful to differentiate primary from metastatic malignancies.

6.7 Pancreatic Neuroendocrine Cell Tumors (Islet Cell Tumors)

Islet cell tumors (ICT) of the pancreas are rare. On FNA they are noted with a frequency ranging from 3% to 5%.[14,18] A higher frequency of 8.8% is noted when only solid pancreatic lesions are aspirated.[16]

Aspirates from ICT demonstrate cellular, predominantly dyscohesive single cells with plasmacytoid appearance. Rosette formation is also frequently identified. Neoplastic

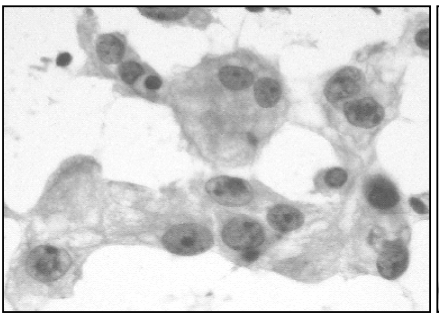

Figure 5. Metastatic renal cell carcinoma to the pancreas. Loosely cohesive group of cells with foamy cytoplasm and nuclei with prominent nucleoli. (Papanicolaou)

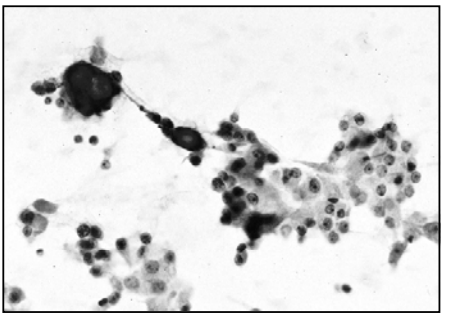

Figure 6. Glucagonoma. Neoplastic cells with occasional acini, eccentrically placed nuclei with conspicuous nucleoli, and calcification. (Papanicolaou)

cells have moderate cytoplasm and predominantly eccentrically placed nuclei with regular nuclear membrane; finely granular, evenly distributed chromatin pattern; and inconspicuous nucleoli. Other features that may be observed include cytoplasmic pigment, anisocytosis, anisonucleosis, conspicuous nucleoli, and calcification (see Figure 6). Mitoses and necrosis might occasionally be noted. Such tumors should be investigated to further rule out metastasis. Psammomatous calcifications have been reported with somatostatinoma arising from the duodenum. In the pancreas, calcification may be noted with other ICTs and are not characteristic of somatostatinoma. Cytologic features alone, however, should not be used to separate benign from malignant tumors. These tumors, therefore, should be closely followed and further investigated to determine possible malignancy.

Immunohistochemical stains are important for confirming ICT and ruling out other tumors from other entities in the differential diagnosis. In addition, immunohistochemical stains may further help to characterize the cell with the ability to produce hormones. Immunohistochemical stains that help to determine the neuroendocrine nature of cells include chromogranin, synaptophysin, and neuron-specific enolase. In addition, focal keratin positivity may also be noted. Increased proliferative activity, as noted by Ki-67, is a helpful tool to predict aggressiveness of the tumor. Functional tumors show characteristic clinicopathologic changes. Immunoperoxidase stains further help to characterize the hormonal status of these tumor cells. If enough cells are available, additional stains such as gastrin, insulin, glucagon, vasoactive intestinal peptide, serotonin, and somatostatin, etc., may be helpful.

ICTs should be differentiated from other morphologic mimickers. It should be differentiated from pancreatic adenocarcinoma, acinar cell carcinoma, solid cystic pancreatic neoplasms, and non-Hodgkin's lymphoma (see Table 4). This, however, requires correlation with clinical symptoms, morphologic characteristics, and ancillary studies.[14,19-23] We believe that an on-site assessment increases the diagnostic accuracy by allowing immediate collection of additional material for ancillary studies.[14] When on-site assessment has not been performed, the sensitivity of EUS-FNA for detecting ICT is reduced.[16]

Table 4. Salient features that differentiate islet cell tumor and its morphologic mimickers

	Islet cell tumor	Adenocarcinoma	Acinic cell carcinoma	Solid and cystic tumor	Lymphoma
Cellularity	Cellular	Variable	Mostly cellular	Variable	Cellular
Cohesiveness	Dyscohesive	Loosely cohesive with single cells*	Mostly cohesive overlapping groups	Mostly cohesive groups	Dyscohesive
Cell pleomorphism	Usually absent	Marked in poorly diff.	Minimal	Minimal	Minimal
Cell arrangement	Rosette formation	Cellular pleomorphism	Acini formation	Papillary groups with fibrovascular cores	Single cells
Nuclei	1. Regular membrane 2. Eccentrically placed (plasmacytoid)	Membrane irregularity	1. Mild nuclear membrane irregularity 2. Lack of plasmacytoid appearance	Nuclear grooves	Characteristic nuclei with margination of chromatin
Nucleoli	Inconspicuous†	Prominent	Prominent	Conspicuous	Absent/ inconspicuous
Useful Special stains	Chromogranin, Neuron-specific enolase, Synatophysin.	Keratin, CA19-9, DuPan4	Trypsin + Chymotrypsin +, PAS/PASD +	PAS + cytoplasmic globules	LCA, L26, CD3, etc.
Other features	Calcification	Mucin, necrosis, Mitoses, squamoid cells	Granular cytoplasm	Metachromatic matrix material	Lymphoglandular bodies

* Three-dimensional groups, with drunken honey comb appearance (well-differentiated) and many atypical pleomorphic single cell (poorly differentiated adenocarcinoma).

† Rarely conspicuous nucleoli; anisonucleosis may be noted.

7. CYSTIC PANCREATIC LESIONS

The evaluation of cystic lesions of the pancreas poses an equal challenge for the radiologist, the endoscopist, and the pathologist.[24-29] Table 5 summarizes the differential diagnosis of cystic pancreatic lesions.

7.1 Pseudocyst of Pancreas

This is the most common type of cyst noted in the pancreas.[30] It occurs as one of the sequelae of chronic pancreatitis.

Aspirates from pseudocysts usually show abundant turbid brown fluid. It shows hemosiderin-laden macrophages, multinucleated giant cells, and other inflammatory cells (see Figure 7). In addition, it may show a background of cellular debris, bile, and hematoidin pigment. No epithelial cyst lining is noted. When an epithelial cell is present, it usually represents contaminant from GI tract mucosa or other cellular elements from adjacent pancreas.

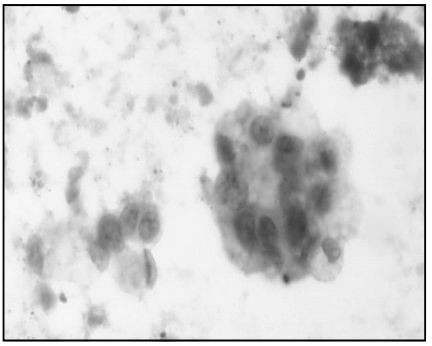

Figure 7. Pancreatic pseudocyst. Aspriate shows macrophages and giant cells in a background of necrotic debris of cyst contents. (Papanicolaou)

7.2 Lymphoepithelial Cyst

Lymphoepithelial cysts of the pancreas, unlike pseudo cysts of the pancreas are true cysts and are lined by epithelial lining.[31, 32] They are usually asymptomatic and on imaging could be either uni- or multilocular. Its preoperative identification on EUS-FNA may allow conservative management.

Aspiration from these cysts usually shows creamy paste-like material. Smears show nucleated squamous cells and may also show an admixture with goblet cells and mucus cells. In addition, they show keratinous debris, cholesterol crystals and chronic inflammatory cells.

7.3 Mucinous Cystic Neoplasm

These tumors occur more frequently in the body of the pancreas and almost exclusively in females.[33-35] These cysts are lined by nonpapillary mucinous epithelial cells. The epithelial cells may not have any atypia (cyst adenoma) or may have features of malignancy (cyst adenocarcinoma). One of the characteristic features for its recognition in histology is the presence of ovarian stroma. This feature is not readily identified in cytology samples.

Aspirated samples show viscous fluid. The smears reveal ample mucin which is better observed on Romanowsky stains (see Figure 8). Admixed amongst the mucin and occasional histiocytes are rare tightly cohesive groups or strips of cuboidal to columnar

Table 5. Differential diagnoses for pancreatic cyst

Non-neoplastic	Neoplastic
Pseudocyst	Mucinous cystic neoplasm
Lymphoepithelial cyst	Intraductal papillary mucinous neoplasm
Dermoid cyst	Solid cystic papillary neoplasms
	Islet cell tumors (rarely)
	Serous microcystic adenomas
	Macrocystic adenomas

epithelium with varying degree of atypia. Those with preserved nuclear:cytoplasmic ratio, round nuclei with smooth nuclear membrane, and inconspicuous nucleoli may most likely represent mucinous cystadenoma. Those aspirates that reveal increased cellularity, many single atypical epithelial cells, increased nuclear:cytoplasmic ratio, nuclear hyperchromasia, nuclear membrane irregularities, coarse chromatin clumping, and prominent nucleoli most likely represent mucinous cystadenocarcinoma. Cytology cannot always differentiate these subtle differences and a generic diagnosis of mucinous cystic neoplasm can be used in difficult cases. Furthermore, cytology also cannot differentiate between noninvasive and invasive mucinous cystadenocarcinoma.

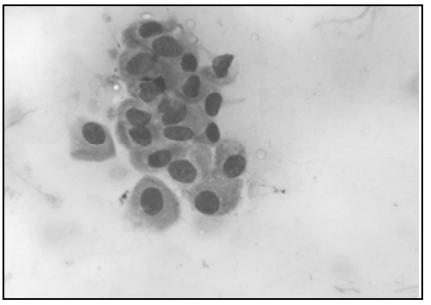

Figure 8. Cystic mucinous neoplasm. Aspirate shows background mucin with loose aggregates of cells with minimal pleomorphism, centrally placed nuclei, and inconspicuous nucleoli. (Diff Quik)

Mucinous cystic neoplasms cannot often be differentiated from intraductal papillary mucinous neoplasm. Many papillary groups with a fibrovascular core, however, would favor IPMN over mucinous cystic neoplasm. In addition, calcification, if noted would favor IPMN over mucinous cystic neoplasm.

Because the needle courses through mucosa of the GI tract EUS-FNA, it is very challenging and sometimes difficult to distinguish neoplastic epithelium from normal surface mucosal epithelial cells of the stomach.

7.4 Intraductal Papillary Mucinous Neoplasm

This is a recently characterized neoplasm with characteristic clinico pathologic changes.[36, 37] These tumors occurs more frequently in the head. Furthermore, they communicate with the main pancreatic duct, produce large quantities of mucin, and may be multifocal. On endoscopy the ampulla of vater may be dilated and may show abundant viscous mucous exuding out.

Cytologic features for this tumor are similar to mucinous cystic neoplasm and are variable. They are characterized by variable cellularity lying in a pool of mucin. Cases with characteristic features show many papillary epithelial groups with a fibrovascular core. Individual cells also show a wide spectrum of changes. When individual cells show oncocytic change it may represent intraductal oncocytic papillary neoplasm. Cytologic features may not be able to differentiate adenoma from adenocarcinoma (whether it is in situ or invasive carcinoma).

7.5 Serous Cystadenoma

Aspirates from these lesions show scant cellularity and may often be considered insufficient for evaluation if adequate history is not available. The aspirates show a proteinaceous background with flat sheets and small cuboidal cell groups. The nuclei are round, with evenly distributed chromatin. The cytoplasm is glycogen rich and cell borders are well-defined. PAS staining will highlight the cytoplasmic glycogen.

7.6 Ancillary Studies to Differentiate Cystic Lesions

Ancillary studies can be used to distinguish cystic lesions based on their tumor marker analysis. Analyses of cyst contents, especially carcinoembryonic antigen, amylase, CA125, and CA19-9, have been used in the hope of increasing the sensitivity and specificity of the diagnosis. These, however, have yet to become the standard of practice.[38-40] In a recent study, pancreatic tissues with noninvasive mucinous cystic neoplasms, irrespective of the degree of atypia, was found to be positive for MUC5AC and negative for MUC1. In contrast, those cases with an invasive component exhibited expression of MUC1. It is possible that the expression pattern of the MUC antigens may become useful to determine the invasive potential of a cystic mucinous lesion.[41] Serous cystadenomas usually have low levels of CEA and enzyme levels (trypsin and amylase). In comparison, pseudo cysts may have elevated levels of enzymes (trypsin and amylase). More studies are needed, however, to evaluate the expression patterns of MUC antigen in cytology samples and to assess their ability to differentiate between benign and malignant mucinous cystic lesions.

Recently a panel of following tumor markers in the cyst fluid were evaluated and found useful to differentiate mucinous from nonmucinous cystic lesions of the pancreas.[42]

8. FUTURE DIRECTIONS AND SUMMARY

FNAs are being utilized increasingly to perform biomarker studies on small samples obtained from the pancreas in order to detect and distinguish chronic pancreatitis from pancreatic malignancies. To date, some of the biomarkers that have been used on FNA samples for such an application include determinations of k-ras,[43,44] p53, DPC4 activity,[45] clusterin expression,[46] mesothelin and prostate stem cell factor,[47] MUC1 and MUC2,[48] and telomerase activity.[49,50] The increased utility of molecular techniques for the early

Table 6. Tumor markers that may help to differentiate mucinous pancreatic cysts from nonmucinous ones. (Adapted from Brugge et al., *Gastroenterology* 2004; 126:1330–1336.)

Tumor markers in cyst fluid	Sensitivity	Specificity	Accuracy	Cut-off Value	Significance
CEA	73%	84%	79%	192 ng/ml	<0.001
CA19-9	68%	62%	66%	2900 ng/ml	0.004
CA 72-4	80%	61%	72%	7 ng/ml	0.001

detection and prognostication of tumors will potentially increase the utility of powerful modalities, such as EUS-FNA, that can provide samples from deep-seated lesions.

In summary, EUS is a powerful modality that promises to change the practice patterns for patients with deep-seated malignancies in coming years. This modality requires that cytopathologists become an integral part of the patient management team, and the protocols concerning management will reflect this. While the diagnostic criteria for the majority of lesions are not affected, the cytopathologist should be aware of the limitations and pitfalls of this technique when evaluating samples obtained by EUS-FNA.

9. REFERENCES

1. Benassai G, Mastrorilli M, Quarto G, et al., Factors influencing survival after resection for ductal adenocarcinoma of the head of the pancreas. *J Surg Oncol*, 73(4), 212-8 (2000).
2. Muller MF, Meyenberger C, Bertschinger P, Schaer R, Marincek B, Pancreatic tumors: evaluation with endoscopic US, CT, and MR imaging. *Radiology*, 190(3), 745-51 (1994).
3. Celle G, Savarino V, Biggi E, et al., Fine-needle aspiration cytodiagnosis: a simple and safe procedure for cancer of the pancreas. *Gastroenterol Clin Biol*, 10(8-9), 545-8 (1986).
4. Hancke S, Holm HH, Koch F, Ultrasonically guided percutaneous fine needle biopsy of the pancreas. *Surg Gynecol Obstet*, 140(3), 361-4 (1975).
5. Hastrup J, Thommesen P, Frederiksen P, Pancreatitis and pancreatic carcinoma, diagnosed by peroperative fine needle aspiration biopsy. *Acta Cytologica*, 21(6), 731-4 (1977).
6. Clouse ME, Gregg JA, McDonald DG, Legg MA, Percutaneous fine needle aspiration biopsy of pancreatic carcinoma. *Gastrointest Radiol*, 2(1), 67-9 (1977).
7. Kocjan G, Rode J, Lees WR, Percutaneous fine needle aspiration cytology of the pancreas: advantages and pitfalls. *J Clin Pathol*, 42(4), 341-7 (1989).
8. Savarino V, Ceppa P, Biggi E, Arcuri V, Mansi C, Celle G, Comparative study of percutaneous and peroperative fine-needle aspirations in the diagnosis of pancreatic cancer. *Hepatogastroenterology*, 33(2), 75-8 (1986).
9. Jhala NC, Jhala DN, Chhieng DC, Eloubeidi MA, Eltoum IA, Endoscopic ultrasound-guided fine-needle aspiration. A cytopathologist's perspective. *Am J Clin Pathol*, 120(3), 351-67 (2003).
10. Chhieng DC, Jhala D, Jhala N, et al., Endoscopic ultrasound-guided fine-needle aspiration biopsy: a study of 103 cases. *Cancer*, 96(4), 232-9 (2002).
11. Steinhauer J, Jhala D, Lazenby A, et al., Impact of ultrasound-guided fine-needle aspiration on the diagnosis of pancreatic lesions. *Mod Pathol*, 16(82A (2003).
12. Jhala N, Jhala D, Eltoum I, et al., Endoscopic ultrasound guided fine needle aspiration biopsy: a powerful tool to obtain samples from small lesions. *Cancer*, In Press((2004).
13. Young NA, Mody DR, Davey DD, Misinterpretation of normal cellular elements in fine-needle aspiration biopsy specimens: observations from the College of American Pathologists Interlaboratory Comparison Program in Non-Gynecologic Cytopathology. *Arch Pathol Lab Med*, 126(6), 670-5 (2002).
14. Jhala D, Eloubeidi M, Chhieng DC, et al., Fine needle aspiration biopsy of the islet cell tumor of pancreas: a comparison between computerized axial tomography and endoscopic ultrasound-guided fine needle aspiration biopsy. *Ann Diagn Pathol*, 6(2), 106-12 (2002).
15. Klapman JB, Logrono R, Dye CE, Waxman I, Clinical impact of on-site cytopathology interpretation on endoscopic ultrasound-guided fine needle aspiration. *Am J Gastroenterol*, 98(6), 1289-94 (2003).
16. Voss M, Hammel P, Molas G, et al., Value of endoscopic ultrasound guided fine needle aspiration biopsy in the diagnosis of solid pancreatic masses. *Gut*, 46(2), 244-9 (2000).
17. Eloubeidi MA, Jhala D, Chhieng DC, et al., Yield of endoscopic ultrasound-guided fine-needle aspiration biopsy in patients with suspected pancreatic carcinoma. *Cancer*, 99(5), 285-92 (2003).
18. David O, Green L, Reddy V, et al., Pancreatic masses: a multi-institutional study of 364 fine-needle aspiration biopsies with histopathologic correlation. *Diagn Cytopathol*, 19(6), 423-7 (1998).
19. al-Kaisi N, Weaver MG, Abdul-Karim FW, Siegler E, Fine needle aspiration cytology of neuroendocrine tumors of the pancreas: a cytologic, immunocytochemical, and electron microscopic study. *Acta Cytol*, 36(5), 655-60 (1992).
20. Labate AM, Klimstra DL, Zakowski MF, Comparative cytologic features of pancreatic acinar cell carcinoma and islet cell tumor. *Diagn Cytopathol*, 16(2), 112-6 (1997).
21. Bardales RH, Centeno B, Mallery JS, et al., Endoscopic ultrasound-guided fine-needle aspiration cytology diagnosis of solid-pseudopapillary tumor of the pancreas: a rare neoplasm of elusive origin but characteristic cytomorphologic features. *Am J Clin Pathol*, 121(5), 654-62 (2004).

22. Chen KT, Workman RD, Efird TA, Cheng AC, Fine needle aspiration cytology diagnosis of papillary tumor of the pancreas. *Acta Cytol*, 30(5), 523-7 (1986).
23. Samuel LH, Frierson HF, Jr., Fine needle aspiration cytology of acinar cell carcinoma of the pancreas: a report of two cases. *Acta Cytol*, 40(3), 585-91 (1996).
24. Gress F, Gottlieb K, Cummings O, Sherman S, Lehman G, Endoscopic ultrasound characteristics of mucinous cystic neoplasms of the pancreas. *Am J Gastroenterol*, 95(4), 961-5 (2000).
25. Shiraishi M, Tokashiki H, Samura H, et al., Avoiding an overdiagnosis of pancreatic pseudocysts. *Hepatogastroenterology*, 48(42), 1758-61 (2001).
26. Jones EC, Suen KC, Grant DR, Chan NH, Fine-needle aspiration cytology of neoplastic cysts of the pancreas. *Diagn Cytopathol*, 3(3), 238-43 (1987).
27. Ahmad NA, Kochman ML, Lewis JD, et al., Endosonography is superior to angiography in the preoperative assessment of vascular involvement among patients with pancreatic carcinoma. *J Clin Gastroenterol*, 32(1), 54-8 (2001).
28. Ahmad NA, Kochman ML, Lewis JD, Ginsberg GG, Can EUS alone differentiate between malignant and benign cystic lesions of the pancreas? *Am J Gastroenterol*, 96(12), 3295-300 (2001).
29. Bounds BC, Brugge WR, EUS diagnosis of cystic lesions of the pancreas. *Int J Gastrointest Cancer*, 30(1-2), 27-31 (2001).
30. Breslin N, Wallace MB, Diagnosis and fine needle aspiration of pancreatic pseudocysts: the role of endoscopic ultrasound. *Gastrointest Endosc Clin N Am*, 12(4), 781-90, viii (2002).
31. Bolis GB, Farabi R, Liberati F, Maccio T, Lymphoepithelial cyst of the pancreas: report of a case diagnosed by fine needle aspiration biopsy. *Acta Cytol*, 42(2), 384-6 (1998).
32. Liu J, Shin HJ, Rubenchik I, Lang E, Lahoti S, Staerkel GA, Cytologic features of lymphoepithelial cyst of the pancreas: two preoperatively diagnosed cases based on fine-needle aspiration. *Diagn Cytopathol*, 21(5), 346-50 (1999).
33. Emmert GM, Bewtra C, Fine-needle aspiration biopsy of mucinous cystic neoplasm of the pancreas: a case study. *Diagn Cytopathol*, 2(1), 69-71 (1986).
34. Dodd LG, Farrell TA, Layfield LJ, Mucinous cystic tumor of the pancreas: an analysis of FNA characteristics with an emphasis on the spectrum of malignancy associated features. *Diagn Cytopathol*, 12(2), 113-9 (1995).
35. Gupta RK, Scally J, Stewart RJ, Mucinous cystadenocarcinoma of the pancreas: diagnosis by fine-needle aspiration cytology. *Diagnostic Cytopathology*, 5(4), 408-11 (1989).
36. Hara H, Suda K, Oyama T, Cytologic study of noninvasive intraductal papillary-mucinous carcinoma of the pancreas. *Acta Cytol*, 46(3), 519-26 (2002).
37. Bounds BC, Diagnosis and fine needle aspiration of intraductal papillary mucinous tumor by endoscopic ultrasound. *Gastrointest Endosc Clin N Am*, 12(4), 735-45, vii (2002).
38. Hammel P, Levy P, Voitot H, et al., Preoperative cyst fluid analysis is useful for the differential diagnosis of cystic lesions of the pancreas. *Gastroenterology*, 108(4), 1230-5 (1995).
39. Pinto MM, Meriano FV, Diagnosis of cystic pancreatic lesions by cytologic examination and carcinoembryonic antigen and amylase assays of cyst contents. *Acta Cytol*, 35(4), 456-63 (1991).
40. Lewandrowski KB, Southern JF, Pins MR, Compton CC, Warshaw AL, Cyst fluid analysis in the differential diagnosis of pancreatic cysts: a comparison of pseudocysts, serous cystadenomas, mucinous cystic neoplasms, and mucinous cystadenocarcinoma. *Ann Surg*, 217(1), 41-7 (1993).
41. Luttges J, Feyerabend B, Buchelt T, Pacena M, Kloppel G, The mucin profile of noninvasive and invasive mucinous cystic neoplasms of the pancreas. *Am J Surg Pathol*, 26(4), 466-71 (2002).
42. Brugge WR, Lewandrowski K, Lee-Lewandrowski E, et al., Diagnosis of pancreatic cystic neoplasms: a report of the cooperative pancreatic cyst study. *Gastroenterology*, 126(5), 1330-6 (2004).
43. Tada M, Komatsu Y, Kawabe T, et al., Quantitative analysis of K-ras gene mutation in pancreatic tissue obtained by endoscopic ultrasonography-guided fine needle aspiration: clinical utility for diagnosis of pancreatic tumor. *Am J Gastroenterol*, 97(9), 2263-70 (2002).
44. Shibata D, Almoguera C, Forrester K, et al., Detection of c-K-ras mutations in fine needle aspirates from human pancreatic adenocarcinomas. *Cancer Res*, 50(4), 1279-83 (1990).
45. van Heek T, Rader AE, Offerhaus GJ, et al., K-ras, p53, and DPC4 (MAD4) alterations in fine-needle aspirates of the pancreas: a molecular panel correlates with and supplements cytologic diagnosis. *Am J Clin Pathol*, 117(5), 755-65 (2002).
46. Jhala D, Jhala N, Eloubeidi M, Medeiros J, Eltoum I, Frost A, Clusterin expression in pancreatic adenocarcinoma and chronic pancreatitis. *Mod Pathol*, 15((2002).
47. McCarthy DM, Maitra A, Argani P, et al., Novel markers of pancreatic adenocarcinoma in fine-needle aspiration: mesothelin and prostate stem cell antigen labeling increases accuracy in cytologically borderline cases. *Appl Immunohistochem Mol Morphol*, 11(3), 238-43 (2003).

48. Chhieng DC, Benson E, Eltoum I, et al., MUC1 and MUC2 expression in pancreatic ductal carcinoma obtained by fine-needle aspiration. *Cancer*, 99(6), 365-71 (2003).
49. Suehara N, Mizumoto K, Kusumoto M, et al., Telomerase activity detected in pancreatic juice 19 months before a tumor is detected in a patient with pancreatic cancer. *American Journal of Gastroenterology*, 93(10), 1967-71 (1998).
50. Suehara N, Mizumoto K, Tanaka M, et al., Telomerase activity in pancreatic juice differentiates ductal carcinoma from adenoma and pancreatitis. *Clinical Cancer Research*, 3(12 Pt 1), 2479-83 (1997).

CHAPTER 10
USING IMAGING DATA IN MAKING ORTHOPEDIC DIAGNOSES

Michael J. Klein, M.D.*

1. INTRODUCTION

At some point in their training, pathologists learn that the diagnosis of bone lesions should not be undertaken without first reviewing the clinical radiographs. If a pathologist strictly adheres to this philosophy, the orthopedic surgeon will eventually provide the patient's x-rays (better to share x-rays than get no diagnosis). When this happens, a pathologist who knows little about x-ray interpretation may begin to feel like a dog running and barking at passing cars (if the car ever stopped and the dog jumped inside, what would the dog do with it?). This is because pathologists are seldom taught in their residencies how radiographic data are actually incorporated into the formulation of histological diagnosis.

The aim of this chapter is to emphasize the reasons why characteristic biological alterations of bone give rise to reproducible radiographic findings. While the discussion cannot teach one to be a radiologist or an orthopedic pathologist, its intent is to make you appreciate some of the logic in pathoradiologic correlation. More importantly, you will understand the limitations and potential danger of histodiagnosis of bone lesions without radiographic information.

2. X-RAYS

X-rays are electromagnetic waves of about one Angstrom in length. The degree of their ability to penetrate matter is related to their energy level and the electron density of the matter being x-rayed; the energy is absorbed or scattered by electron clouds. Substances of lower electron densities are thus more easily penetrated. Nuclei can also absorb x-rays; however, the nucleus occupies so little space in the atom ($1/100{,}000^{th}$) that

* Professor and Director of Surgical Pathology, Department of Pathology, University of Alabama, Birmingham, AL.

even in atoms with many nuclear particles (lead, osmium, etc.) the nuclei play practically no role in x-ray absorption. The state of matter of the substance also plays a role in radiodensity. For example, while the atoms of the heavier Noble gases (e.g., Krypton, Radon) are capable of electron absorption, their wide spacing in a gas renders them completely radiolucent. X-rays also have the ability to sensitize a photographic emulsion, but they do so much more slowly than visible light because this reaction is photochemical and x-rays are in the wrong part of the electromagnetic spectrum to produce photochemical energy. In order to accelerate this process, the photographic film used in x-rays is placed in a cassette, which has a fluorescent coating inside. When x-rays strike this coating, there is secondary emission of light, which then strikes the film, making a contact print inside the light tight cassette. Precipitation of silver in the emulsion takes place as a result of this secondary photochemical reaction, which results in exposure of the film.[1]

A radiographic image results from the absorption, scatter, and transmission of the primary x-ray beam emitted from the tube as it passes through tissues to strike the fluorescent screen of the cassette and the secondary exposure of the photographic emulsion. The image generated is essentially a large photographic negative that results from different degrees of exposure of the photographic emulsion by x-ray and light photons. Because bone, calcium salts, and heavy metals (being of higher electron density/atomic number) permit fewer photons to pass through to the film, the areas of the processed film in the paths of these objects remain clear (or white). Because soft tissues are lower in electron density, fewer x-ray photons are absorbed. Because of this, the corresponding areas of the radiographs are proportionately darkened. Soft tissues can further be divided into those of water density (including cartilage, tendon and ligament, blood, and muscle) and fat. The tissues with water density absorb more x-ray energy than fat, and this can often be seen when the two are contrasted with one another in soft-tissue x-rays (fat planes are more radiolucent than muscles). Gases absorb even less x-radiation, and film exposure is even darker under areas with gas or air in the x-ray path. Radiographic examination of a joint, for example, shows bones as white structures separated by a thin dark space and surrounded by indistinct zones of grey. While the soft tissues of the joint cannot be distinguished from one another, changes in the adjacent ossified tissues may be observed, and those alterations in the interposed tissues can be evaluated indirectly. For example, if articular cartilage in a joint is destroyed, there is usually closer approximation of adjacent bony structures and secondary changes in the articular surfaces or their margins.

When observing a radiograph, one must remember to think in three dimensions. While a radiographic image is a two-dimensional representation of anatomy and pathophysiology taking place in three dimensions, this fact is easily forgotten. For example, an x-ray of a long bone appears to have two compact outer zones corresponding to the cortex and a lace-like or hazy central portion corresponding to the medullary cavity. A 3-dimensional construct, however, reminds us that the x-ray beam transects two thicknesses of cortex in the region our mind's eye assumes is medullary. The reason that we perceive the outer regions as denser is because the x-ray beam path crosses a greater thickness of compact bone in traveling through this region of the cortex. Most of the radiographic image that we infer as medullary, therefore, is derived from a stream of photons passing through two cortices. Consequently, a lesion confined to the medullary cavity that is less radiodense than bone is virtually invisible on a plain x-ray. In fact, routine radiographic studies are so insensitive that a lesion that is purely destructive must

destroy about 40% of the bone in the beam path in order to be perceived. In other words, almost an entire cortical thickness must be absent to see a bone-destroying lesion. The same 40% loss relationship holds true for cancellous bone volume in the metaphyseal portions of long bones. Lesions with associated calcification or production of radiodense bone matrix are additive with bone that is already present and are more easily visualized on an ordinary x-ray.[2, 3]

Other factors also add to confusion in routine radiographs. The radiographic image is due to a photon beam projected onto a cassette. Even if a patient is in contact with the cassette, the portions of the patient facing away from the cassette are magnified on the film. In addition, a large proportion of soft-tissue shadows on plain x-rays are produced by Compton scattering, which results when electrons give off secondary photons at varying angles. These magnification effects and extra emissions contribute to a loss of sharpness, or "image blur."[4]

It is also important to remember that a radiographic image is influenced by conditions that can be technically controlled. For example, if voltage potential to the cathode ray tube is increased, photons of higher energy are produced. The resulting radiographs will accentuate the bony structures and over-penetrate the soft tissues. The same effect may be achieved by increasing the exposure time at a given voltage; however, this effect is limited by the amount of time a subject can remain motionless.[1, 4]

Several general considerations need to be weighed when examining bone radiographs. Bacause bone lesions tend to follow reproducible patterns in age, skeletal distribution, and radiographic appearance, a few questions must be answered when examining x-ray studies.[2]

The bone containing the lesion as well as that part of the bone actually involved in the process should be identified, because specific types of lesions not only predilect certain bones but certain parts of bones. The patient's age is an important consideration. Primary tumors such as osteosarcoma and Ewing’s sarcoma primarily affect young individuals. Giant-cell tumor and chondrosarcoma have a predilection for the mature skeleton. Metastatic carcinoma seldom occurs prior to the fifth decade. Clinically uninvolved bones should also be examined, because metabolic diseases, which may mimic tumors, usually affect the entire skeleton to some extent. Other factors, such as whether a lesion is solitary or multifocal, involves the joint, or possesses features characteristic for matrix production are also important considerations.

The radiographic assessment of bone lesions depends upon a consideration of bone structure and the manner in which osseous tissues respond to the presence of a pathological process. Bone reacts to structural abnormalities in a similar manner whether the lesion is a space-occupying neoplasm, an inflammatory disease, or a metabolic process; the variations are those of degree.[5] In general, the response of osseous tissue to a pathologic process is some combination of bone reabsorption and new bone formation.[6] The radiographic appearance depends upon the relative dominance of each process in the bone in addition to any characteristics unique to the lesional tissue itself.

The most important radiographic assessment of the biologic potential of a pathological process is the definition of its border and that of the surrounding normal bone. The area between the lesion and where the bone is obviously normal is sometimes referred to as the transition zone.[7] In general, better-demarcated transition zones are indicative of more benign processes because a slowly progressing process enables the host bone to remodel in response to the lesion. A process indolent enough to produce a well-demarcated transition zone will not penetrate the intertrabecular marrow spaces of

the cancellous bone adjacent to the advancing edge of the lesion. In the same way, a benign lesion may push up against the endosteal cortex. Over time, there may be erosion of the inner cortex due to osteoclast activity; however, benign lesions do not have the ability to penetrate the cortex nor to extend into its vascular canals.

The radiographic-appearance of a lesion is described as geographic if its transition zone is well-defined.[8] This type of intraosseous extension implies that osteoclastic reabsorption of bone at the periphery of the lesion destroys bone at about the same rate as the lesion grows. Because osteoclast activity is a slow phenomenon, this infers that the lesion is slowly growing and probably benign. Examination of the interface between the tumor and adjacent normal bone reveals an abrupt transition between lesional tissue and normal bone and marrow. A geographic appearance is described as marginated if there is, in addition, surrounding bony sclerosis.[9] Ability of the host bone to produce bony sclerosis at the periphery of a destructive lesion implies an even more benign behavior. The histological interface between the lesion and adjacent bone reveals a variable amount of bone between the two. If the lesion is aggressive or a low-grade malignancy, it grows at a faster rate and has the capacity to penetrate the marrow of the intertrabecular spaces and the Haversian and Volkmann canals of the cortex. In addition, the bone parts associated with slower tumor growth respond by osteoclastic activity resulting in irregular areas of radiolucency with less-defined borders. The x-ray appearance of such lesions of intermediate and irregular growth has been described as moth-eaten.[8] The most highly malignant neoplasms infiltrate intertrabecular spaces and cortical vascular canals at so rapid a rate that reabsorption of large foci by osteoclastic activity does not have time to proceed, except near the oldest areas of the lesion. Radiographs of this type of bone destruction are termed permeative.[8] The tumor occupies areas in the bone that normally contain structures of the same radiodensity as the tumor cells, often without a significant degree of osseous reabsorption. Bony abnormalities may be subtle, but there is usually a large tumor volume present; often it is associated with a large soft-tissue mass. Later in its evolution, there will be diffuse linear or lenticular defects, which coalesce, and the extensive nature of the process becomes obvious.

The presence and type of periosteal reaction also influence general radiographic assessment of the biological behavior of bone lesions. The periosteum is loosely connected to the bone during childhood and adolescence. Its Sharpey fibers shorten and become less lax as the skeleton matures, resulting in its tighter adherence to the cortex in adulthood. The periosteum consists of an outer, tough fibrous layer and an inner germinative layer, or cambium layer. Even though the periosteum is invisible on routine x-rays, any process that causes the separation of the cambium layer from the underlying cortex stimulates osteoblastic activity by the periosteum. When subperiosteal new bone is formed by these osteoblasts, a radiodense periosteal reaction begins to appear on routine x-rays. The character of this periosteal reaction depends upon the patient's age and the nature of the underlying process. In general, more continuous and solid periosteal reactions indicate more indolent underlying lesions because it takes time to form an organized and continuous periosteal reaction.[7] If the continuous periosteal reaction is solid, it results in the formation of a thickened cortex, which may be linear or fusiform depending upon the overall manner of periosteal new bone formation. In the case of some small benign lesions that cause disproportionate periosteal irritation such as osteoid osteoma, the periosteal new bone may actually obscure the lesion in the plain radiographs.

Interrupted periosteal reactions are more often indicative of a malignant process. The most important of these is the Codman angle, in which the periosteal reaction is single-layered, attached to the cortical surface at one end, and extends away from the cortex at the other end. This configuration forms an open radiodense angle without ossification being visible in the plain x-rays at its other end. While Codman angles may occasionally be indicative of benign lesions, they are often characteristic of processes having rapid expansion and are usually associated with sarcomas. Multiple layers of continuous periosteal bone reactions consisting of concentric strata of periosteal new bone often separated by loose, vascular connective tissue produce a type of reaction, termed "onionskin" by radiologists.[10] While this type of reaction is associated with benign conditions if the new bone layers are continuous, it may be associated with malignant tumors such as Ewing's sarcoma if it is discontinuous. Complex periosteal reactions such as a "hair-on-end" or "sunburst" patterns are also indicative of very rapid growth if they are interrupted,[2] and may consist of a mixed combination of reactive and neoplastic bone. The same complex periosteal reactions may be indicative of benign processes if they are continuous. Regardless of its periosteal reaction, any lesion thought to be a bone neoplasm should be considered malignant if there is a soft-tissue mass associated with an intraosseous tumor without visible physical disruption of the cortex.

Sensitivity of routine x-rays may be increased with the use of conventional (plane) tomography and with computer-assisted tomography (CT scan). In plane tomography, the x-ray source and x-ray films are moved in opposite directions about a stationary point calculated to fall in the desired plane of a patient to be studied. Taking successive images and continually moving the pivot point between source and film results in a series of planes or slices in which objects in a given plane are in focus but in which structures not in the plane of interest are intentionally blurred.[1] The same effect is achieved by "panning" in general photography. When objects in a photograph are moving in a linear direction, a still photograph with the camera on a tripod will result in the moving object appearing blurred and the background appearing sharply focused. If the camera is “panned,” the camera is moved in the same linear direction as the moving object at approximately the same rate of speed while the shutter is opened. This results in the object appearing relatively sharp while the background is intentionally blurred due to camera motion. This technique is very useful in identifying subtle fracture lines, particularly when an exuberant fracture callus associated with undisplaced fractures may masquerade clinically as osteosarcoma.[11] The use of plane tomography has been limited by the advent of computerized axial tomography.

3. COMPUTERIZED AXIAL TOMOGRAPHY

In computerized axial tomography, multiple x-ray sources pass through the patient in an axial direction. Each source of x-rays usually has its own corresponding x-ray detector. A computer calculates the difference between the energy leaving the source and that reaching the detector and plots the difference by Fourier transform into a 2-dimensional image, which is essentially a map of radiodensity.[12] A CT scan is essentially what one would get if the body could be frozen solid, sliced into one-centimeter-thick slices, and a plain x-rays could then be prepared by placing each slice on a cassette and making a contact radiograph of each slice.[13] Moreover, the thickness of each slice can be manipulated to as thin as one millimeter. In addition, the computer can be manipulated to

preferentially examine the soft tissue or bone selectively from the same data obtained in one scan.[14] The density of any area of a CT study can be measured to the accuracy of 1/10 of the density of a cubic centimeter of water, or a Hounsfield unit.[13] This means that CT scanning is extremely sensitive when compared to conventional x-rays. Keep in mind, however, that CT is not specific; that is, it does not give a picture of the process as a whole in the same way as a radiograph. The techniques are complementary and one should not serve as a substitute for the other. This is one reason that scout x-rays are done prior to the performance of a CT scan. The technique insures that the areas of interest are included in the areas sliced by the CT scans. In addition, the gantry of earlier CT scanners essentially limited the planes of body imaging to axial (crosswise). In these machines, in order for a CT scan to be displayed in any other plane, many axial slices must be reconstructed indirectly by computer in the desired view subjecting a patient to an increased total radiation dose. In the newer CT scanners, the sources and detectors can move opposite to one another not only axially, but also helically, which gives more recent CT scanners a greater capability to produce scans in sagittal, coronal, or other nonaxial views.

4. MAGNETIC RESONANCE IMAGING

Magnetic resonance imaging (MRI) is the newest imaging technique to come into use in bone radiology. Although the images produced resemble CT, there is no ionizing radiation used in the technique, because the portion of the electromagnetic spectrum used to generate these images is in its radiofrequency portion. Resonance is a physical phenomenon in which an object absorbs energy from an external energy source. The energy absorption is most efficient when the frequency of the external energy source matches the natural frequency of the object absorbing the energy. The object, in turn, gives off this energy at the same natural frequency. The phenomenon of resonance is easily demonstrated by juxtaposing two tuning forks with the same natural frequency. When one tuning fork is struck and placed in proximity to the other tuning fork, the oscillating sound waves of the first tuning fork are absorbed by the second. In turn, the same note may be heard coming from the second tuning fork. Nuclear magnetic resonance uses the same principle; however, radio waves rather than sound waves induce the resonance signal, and the resonance signal itself is derived from the spin of nuclear particles.

While nuclear magnetic resonance can be induced in any substance with an odd number of protons or neutrons,[13] most of the magnetic resonance imaging performed on patients effectively reflects their tissue content of hydrogen nuclei.[14] If one were to imagine protons as minute spinning tops, the spinning of each top would create a unique spin axis or dipole moment for each proton. The motion of this axis is wobbly and referred to as precession.[13] Because the protons spin in more or less random directions, the net dipole moments in numerous directions normally cancel one another under ordinary natural conditions. In a magnetic resonance imager, a patient is placed inside a very strong magnetic field, which causes alignment of the dipole moments along the axis of the magnetic field lines. A pulse of radiofrequency is then given to the patient at the Larmor frequency.[13] This frequency is that necessary to make protons resonate at any given magnetic field strength, and is directly proportional to the field strength. In general, this frequency is 42.6 MHz (million cycles per second) per one Tesla of field strength. When this frequency is given to the patient in a magnetic field, the protons acquire this

energy and resonate at the same frequency. While they resonate, the protons give off radio waves at the Larmor frequency, and a radiofrequency detector is able to record this radio signal. In addition, the extra energy imparted to the protons from the radiofrequency pulse momentarily deflects their magnetic dipoles out of the plane of the strong magnetic field. The resonance signal can only come from those atoms having an odd number of protons. This is because nuclei with even numbers of protons have half their dipole moments pointing in opposite directions. The net effect is that the net resonance signal of atoms with even numbers of protons and neutrons is exactly cancelled out. Because the resonance signal from each nucleus is produced by the one extra odd nuclear particle, hydrogen, with a single proton, is the ideal atom for MRI measurements. When the radiofrequency pulse is discontinued, resonance diminishes because the proton dipole moments soon return to the prevailing direction of the magnetic field without an additional burst of energy. The time necessary for the return of the protons to the direction of the magnetic field is the relaxation time. The measurement of the intensity of this resonance (signal intensity) with respect to various relaxation time constants yields certain characteristics, which help to differentiate different kinds of tissue from each other. The most common of these time constants are known as T_1 and T_2. T_1 is defined as the time it takes for the loss of 63% of the radiofrequency signal energy. T_2 is defined as the time it takes for 63% of signal loss due to dephasing. The net resonance signal is derived from a very large number of subatomic particles. At the instant of the radiofrequency pulse, all of these particles are synchronized in terms of their magnetic dipole moment. As time progresses, the processing of the particles becomes asymmetric. This results in radio waves that arrive out of phase at the signal detector. The addition of the peaks and troughs of these waves tends to dampen the received signal and makes the apparent signal loss greater. As a result, T_2 is almost always shorter than T_1. As in CT scanning, the signals from the tissue are plotted by Fourier transform, but because there are no x-rays, the shades of grey are not imparted by absorption, scatter, and penetration. Instead, brightness is directly related to the strength of the detected signal. Because the signal is externally detected instead of absorption of x-ray energy measured, MRI can image directly in any plane chosen by the operator without having to scan many sections and indirectly reconstruct them (as in CT scanning). Interpreting MRI in a simple diagnostic fashion does not require that a physician must understand the physical principles of MRI, just as to drive an automobile one does not have to be an auto mechanic. What is required is a general knowledge of anatomy combined with an awareness of the typical signals generated by various tissues in MRI. Adipose tissue, for example, generates a bright signal in T_1 weighted images and a slightly less bright signal in T_2 weighted images. Fluid generates a slight signal in T_1 weighted images and a bright signal in T_2 weighted images. Muscle generates a slight signal in T_1 weighted images and very slightly increased signal in T_2 weighted images. Significantly, because cortical bone does not contain free water, it fails to generate a significant signal regardless of the sequence of radiofrequency energy measured, so cortical bone always appears black on MRI studies. On the other hand, becuase the medullary cavity of the bone contains adipose tissue and marrow, the signal inside the bone can be very bright, but varies according to the proportion of adipose tissue to hematopoietic marrow. This means that the borders of intramedullary tumors can often be well demarcated by MRI, but that cortical destruction cannot. The spatial resolution is not as good for MRI as it is in CT scanning, but this is likely to improve as the technology is refined.[14] On the other hand, the degree of contrast is much better in MRI than it is in

CT.[15] Consequently, MRI is useful for the imaging of soft-tissue abnormalities associated with bone lesions as well as demonstrating their intramedullary extent, but it gives little information about the bone itself.

5. REFERENCES

1. Squire LF, *Fundamentals of Radiology* (Harvard University Press, Cambridge, MA, 1988).
2. Fechner R, Mills S, *Tumors of the Bones and Joints* (Armed Forces Institute of Pathology, Washington, DC, 1993).
3. Sweet DE, Madewell JE, Ragsdale BD, Radiologic and pathologic analysis of solitary bone lesions. Part III: matrix patterns. *Radiologic Clinics of North America*, **19**(4), 785-814 (1981).
4. Sprawls P, *The Physical Principles of Diagnostic Radiology* (University Park Press, Baltimore, MD, 1977).
5. Spjut HJ, Dorfman HD, Fechner R, Ackerman LV, *Tumors of Bones and Cartilage* (Armed Forces of Institute of Pathology, Washington, DC, 1981).
6. Milch RA, Changus GW, Response of bone to tumor invasion. *Cancer*, **9**(2), 340-51 (1956).
7. Greenspan A, Klein MJ. Radiology and pathology of bone tumors. In: Lewis MM, ed. *Musculoskeletal Oncology: An Interdisciplinary Approach.* Philadephia, PA: W.B. Saunders Co, 1992; 13-72.
8. Lodwick GS, Predictor Variables in bone tumors. *Seminars in Radiology*, **1**(293 (1966).
9. Madewell JE, Ragsdale BD, Sweet DE, Radiologic and pathologic analysis of solitary bone lesions. Part I: internal margins. *Radiologic Clinics of North America*, **19**(4), 715-48 (1981).
10. Ragsdale BD, Madewell JE, Sweet DE, Radiologic and pathologic analysis of solitary bone lesions. Part II: periosteal reactions. *Radiologic Clinics of North America*, **19**(4), 749-83 (1981).
11. Kahn LB, Wood FW, Ackerman LV, Fracture callus associated with benign and malignant bone lesions and mimicking osteosarcoma. *American Journal of Clinical Pathology*, **52**(1), 14-24 (1969).
12. Sprawls P, *Physical Principles of Medical Imaging* (University Park Press, Baltimore, MD, 1987).
13. Olendorf W, Olendorf WJ, *MRI Primer* (Raven Press, New York, NY, 1991).
14. McLeod RA, Berquist TH. Bone tumor imaging: contribution of C.T. and M.R.I. In: Unni KK, ed. *Bone Tumors.* New York, NY: Churchill Livingston Co., 1988; 1-34.
15. Gilkey F, Sweet DE, Mirra J. Radiologic/Pathologic Correlation of Bone Tumors. In: Mirra J, ed. *Bone Tumors, Clinical, Radiologic, and Pathologic Correlations,* 2nd ed., Philadelphia, PA: J.B. Lippincott Co., 1989; 1803-31.

CHAPTER 11
SELECTED CASE STUDIES IN HEMATOPATHOLOGY
Application of Current Ancillary Techniques in Diagnosis

Vishnu V. B. Reddy, M.D.*

1. HIGH-GRADE B-CELL LYMPHOMA WITH PLASMACYTIC DIFFERENTIATION

1.1 Case History

The patient was a 59-year-old male with 1.5 months of diarrhea, cramping, and 5-lb weight loss. On physical examination he was found to have a mobile 4 x 6 cm RUQ mass. He underwent a colonoscopy and biopsy. Later, a right colectomy with attached segment of small bowel was done. On opening the specimen a circumferential mass was seen in the small bowel extending into the proximal cecum. The mass itself occupied approximately 20 cm segment of the bowel and on sectioning it displayed a homogenous solid, white-tan, fleshy appear-ance. Few peri-colonic lymph nodes were found (0.8–2.0 cm).

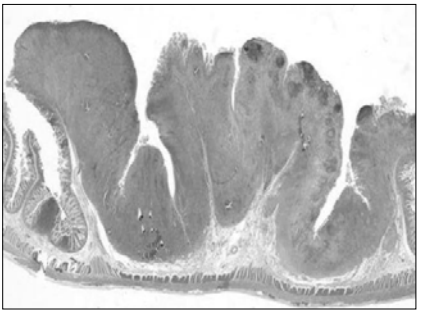

Figure 1. Lymphoma confined to the colonic mucosa.

1.2 Morphology

Biopsy from the small bowel showed the lesion confining to the mucosa (see Figure 1). The cells ranged from plasmacytoid to large lymphocytic. Most of the cells were large with moderate to

* Professor and Director of Hematopathology and Hematology Lab, Department of Pathology, University of Alabama, Birmingham, AL.

abundant pink-blue cytoplasm containing hyperchromatic nuclei with prominent nucleoli (see Figure 2). Mitotic activity was brisk. No definite lymphoepithelial islands (LELs) were found. Partial involvement of the lymph nodes with sharp demarcation between normal and tumor was seen (see Figure 3). Mucin and PAS stains were negative.

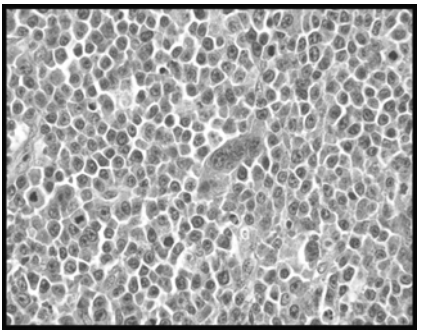

Figure 2. Cells have distinct plasmacyte morphology and several large multinucleated cells noted.

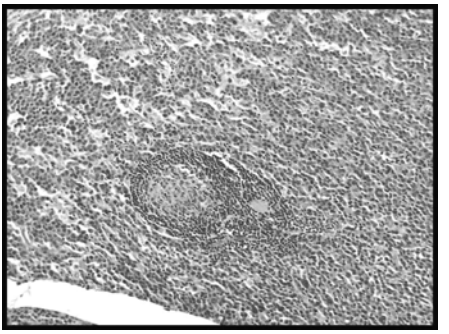

Figure 3. Partial involvement of the lymph node with residual germinal centers (B-cell areas).

1.3 Immunohistochemical Stains

CD45 neg, S100 neg, CD20 neg, kappa/lambda with high background, CD3 neg, EBV neg, EBNA neg and CD79a positive.

1.4 Differential Diagnosis

Poorly differentiated carcinoma, melanoma, neuroendocrine carcinoma, MALT lymphoma, large B-cell lymphoma, plasmacytoma, plasmacytoid lymphoma.

1.5 Diagnosis

High-grade B-cell lymphoma with plasmacytic differentiation.

1.6 Discussion

Morphology was variable, lymphocytic to plasmacytoid, and most of the hematopoietic markers were negative. Only CD79a was positive. Most plasmacytoid B-cell lymphomas are usually negative for CD20 and LCA and are positive with CD79a and CD138. The lymphoma in the involved nodes was not “homing” into B-cell regions, and there was a sharp demarcation from the uninvolved lymph node mimicking “metastatic tumor.” Immunohistochemical stains CD79a and CD138 (Syndecan-1) are helpful in identifying B-cell lymphomas with plasmacytoid morphology (see Figure 4).

There is some morphologic overlap between lymphoplasmacytic/ immunocytoma, marginal zone and MALT lymphomas. These tumors express CD20, CD79a and CD43. However, MALT lymphomas usually have lymphoepithelial islands (LEL) and pleomorphic cell components (small and large lymphoid cells mixed with plasma cells).

CLL/SLL with plasmacytoid features usually express CD5 and CD20. Immunocytoma (Waldenström's) is associated with IgM monoclonal gammopathy and has systemic involvement. Some immunoblastic lymphomas may have significant plasma cell differentiation. The case presented here is most consistent with large B-cell lymphoma (high-grade) with focal plasmacytic differentiation.

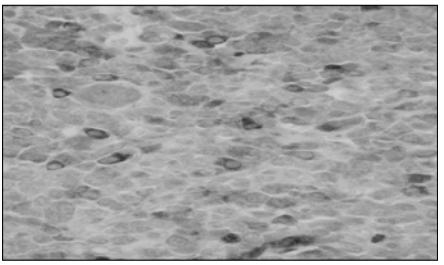

Figure 4. Most of the tumors are positive for CD 138.

2. FOLLICULAR B-CELL LYMPHOMA WITH ABERRANT T-CELL ANTIGEN EXPRESSION

2.1 Case History

The patient was 38-year-old female with massive lymphedema of the left leg. She noted gradual swelling over a period of 2–3 months. Past medical history was unremarkable. Imaging studies showed inguinal and some retroperitoneal lymphadenopathy. CBC and bone marrow biopsy were within normal limits with a slight increase of platelets. Later, two separate groin lymph node biopsies were done, one outside and at UAB.

2.2 Morphology

Lymph node biopsy #1—Lymph nodes showed partial replacement by fibrosis, vascular proliferation, in the uninvolved area, several residual germinal centers and mantle zones were seen. In some areas thick fibrotic capsule with edematous fluid in the subcapsular sinuses was seen. Also, a single collection of large lymphoid cells without mantle zone was found.

Lymph node biopsy #2 — Part of the node was similar to the first biopsy. However, a distinct nodular (follicular) area composed of large lymphoid cells was found (see Figures 5 and 6). No necrosis, granulomas, or Reed-Sternberg cells were found.

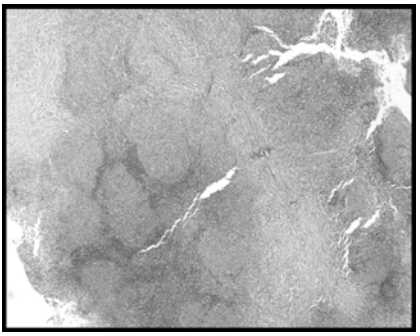

Figure 5. Lymph node biopsy #2 showing lymphoma with a follicular pattern. (H&E)

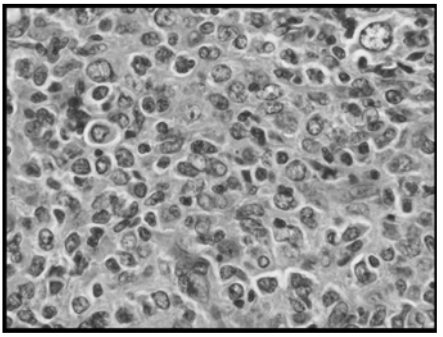

Figure 6. Lymph node biopsy #2 showing a predominant population of large lymphoid cells (H&E)

2.3 Immunohistochemical Stains

Lymph node biopsy #1: Fibrotic area contained both T & B cells (CD20, CD3, and CD5) and few large-cells were CD30 positive (reactive lymphoid cells). Negative for CD15, S100, desmin, and muscle-specific actin.

Lymph node biopsy #2: Follicular areas were positive for CD20, CD79a, and CD22 (see Figure 7). Few T-cells are seen around the nodular areas; rare CD3 positive cells were seen within the follicular areas (see Figure 8). CD30, CD15, HSV8, and EBV (LMP, EBNA-2) were negative.

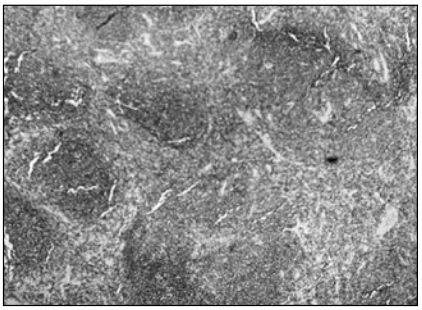

Figure 7. Lymph node biopsy #2 showing most of the follicular areas stained with CD 20.

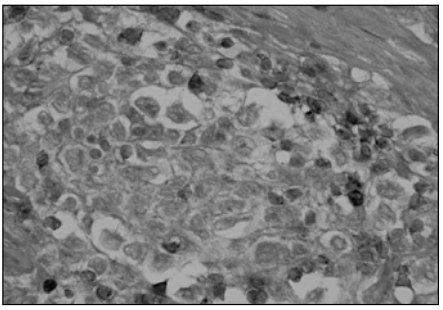

Figure 8. Lymph node biopsy #2 showing scattered CD3 +ve ells around the nodular area.

2.4 Flow Cytometry (Lymph Node #2)

An aberrant lymphoid population expressing CD3, CD4, CD5, CD7, CD20, CD30, and HLA-DR was found and these cells were negative for CD19, CD11c, CD22, CD23, and CD10.

2.5 Gene Rearrangement Studies

Positive clonal light chain (kappa) rearrangement (PCR). T-cell beta/gamma gene and heavy chain Ig gene rearrangement were negative.

2.6 Differential Diagnosis

B-cell lymphoma (follicular center cell origin), T-cell lymphoma with aberrant CD20 expression, B-cell lymphoma with aberrant T-cell markers and composite T&B cell lymphoma and nodular variant of T-cell lymphoma.

2.7 Diagnosis

Lymph node #1— Reactive node with fibrosis.

Lymph node #2— Follicular B-cell lymphoma with aberrant T-cell antigen expression.

2.8 Discussion

The initial lymph node biopsy was nondiagnostic with a small focus of large-cells. Flow cytometry on the second node (results available before H&E sections) was consistent with peripheral T-cell lymphoma with aberrant CD20 expression. H&E sections showed a distinct follicular pattern composed of B-cells (CD20+, CD-, CD5-, CD30- and CD4-). This discordance between flow and immunohistochemistry (IPOX) is not uncommon, and to some extent is based on "surface" vs. "cytoplasmic" staining properties (flow is more sensitive in detecting surface antigens and IPOX detects cytoplasmic antigens). Gene rearrangement studies confirmed a B-cell clonal process. Table 1 summarizes the performance of gene rearrangement studies for T- and B-cell lymphomas.

Table 1 Performance for gene rearrangement studies

T-cell gene rearrangement studies	B-cell gene rearrangement studies
Fresh tissue (high quality DNA) is more sensitive in identifying clonal population	Both PCR and southern blots are sensitive in identifying clonal population (IgH or light chain)
False PCR negative rate: 15–30%	

3. HIGH-GRADE B-CELL LYMPHOMA

3.1 Case History

The patient was a 63-year-old female who presented to an outside hospital with back pain and weakness in both legs. Routine CBC showed normal WBC/platelet count with mild anemia (Hb 10.1 gm/dl) and other laboratory tests were noncontributory. A large epidural mass (L4-5) was found on CT scan. The mass was biopsied and this was followed by bone marrow biopsy.

3.2 Morphology

A diffuse infiltration by lymphoid cells into soft tissue and bone marrow was seen (see Figures 9 and 10). Most of the cells were medium to large, containing fine nuclear chromatin, minimal to moderate amount of pink/blue cytoplasm (see Figure 11). Nucleoli were small and mitotic figures were few. Bone marrow aspirate contained several large lymphoid cells with fine chromatin and cytoplasmic vacuoles, and interstitial infiltrates in the biopsy was also seen.

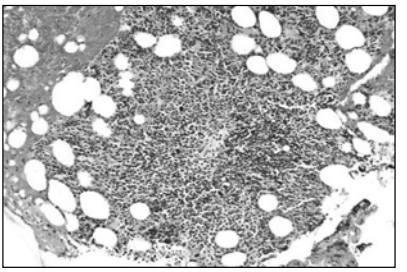

Figure 9. Bone marrow biopsy shows lymphomatous infiltrates. (H&E)

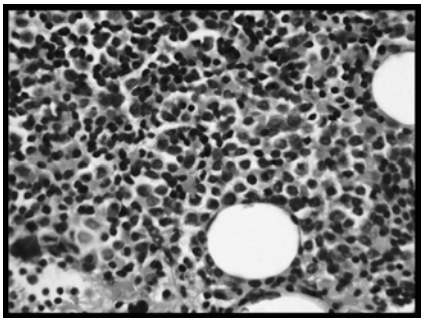

Figure 10. High power of lymphomatous infiltrates. (H&E)

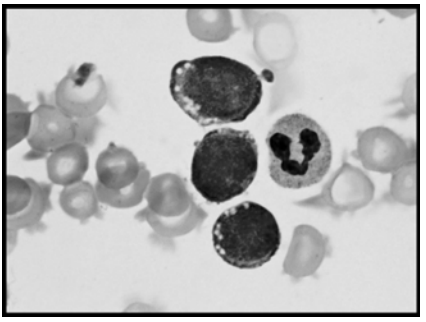

Figure 11. Bone marrow aspirate showing atypical lymphoid cells. (Romanosky)

3.3 Immunohistochemical Stains

Tumor was weakly positive with CD3, CD5, and CD43. CD20, CD7, EBV, and CD57 were negative.

3.4 Flow Cytometry

Bone marrow was repeated at UAB and was positive for CD45, CD19dim+, IgM/kappa dim+ and negative for CD5, CD20, CD20, CD4, CD8, CD33, CD34 (see Figure 12). *Note*: Outside IMMUNOHISTOCHEMICAL stains on bone marrow biopsy were positive for CD79a and CD138.

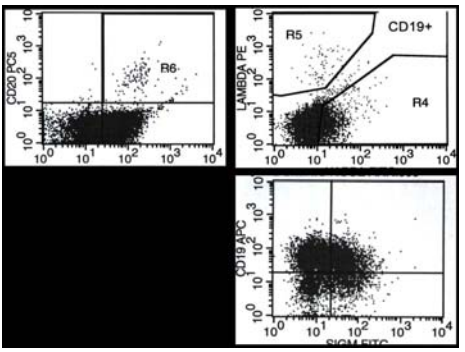

Figure 12. Flow cytometry. The lymphoid cells were positive for CD19dim+ (upper left), kappa light chain dim+ (upper right), and IgM+ (lower right).

3.5 Differential Diagnosis

Lymphoma, T-cell type (based on initial outside IPOX studies) vs. aberrant loss of CD20 on the cells.

3.6 Diagnosis

High-grade B-cell lymphoma (CD45+, CD19dim+, IgM/kappa dim+).

3.7 Discussion

This case illustrates variability of IPOX stains on formalin-fixed tissue vs. fresh tissue analyzed by flow cytometry. The majority of immature B-cell lymphomas are usually CD20 negative, and this limits the diagnosis of B-cell lymphomas on formalin-fixed tissue if only one B-cell (CD20, L-26) marker is used. Additional B-cell markers

that work in formalin-fixed tissues such as CD79a and CD138 (for plasmacytoid cells) may be more useful in identifying "immature/ aberrant B-cell" neoplasms. Flow is more sensitive in identifying both mature and immature B-cell tumors than IPOX stains.

4. PROGRESSIVE TRANSFORMATION OF GERMINAL CENTERS

4.1 Case History

The patient was a 31-year-old male who recently noted a mass in the right axilla. He reported no weight loss or constitutional symptoms. His past history was remarkable for Hodgkin's lymphoma diagnosed five years ago, for which he received treatment and later follow-up studies showed complete remission. His current CBC and other laboratory results were within a normal range. Imaging studies and physical examination were negative. He underwent an excisional biopsy.

4.2 Morphology

The excised node measured 4.3 cm and the cut surface was gray-tan and smooth with focal small nodules (see Figure 13). Multiple sections of the node showed large areas of confluent germinal centers with "merging of follicles and mantle areas" (progressive transformation) and adjacent areas of normal-appearing lymph nodes with secondary germinal centers and T-cell areas. Interfollicular areas contained macrophages and few plasma cells. No Reed-Sternberg cells or variants were found.

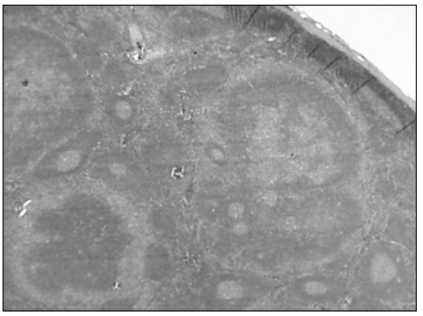

Figure 13. Low-power of PTGC. (H&E)

4.3 Immunohistochemical Stains

CD15, CD30, and EMA were negative. However, few transformed lymphoid cells were positive with CD30 (nonspecific staining). T- and B-cell stains revealed a normal pattern. Special stains for EBV, fungi and mycobacteria were negative.

4.4 Differential Diagnosis

Progressive transformation of germinal centers (PTGC), nodular lymphocyte predominant Hodgkin's disease (NLPHD), interfollicular Hodgkin's lymphoma and non-Hodgkin's lymphoma.

4.5 Diagnosis

Progressive transformation of germinal centers (PTGC); no evidence of malignancy.

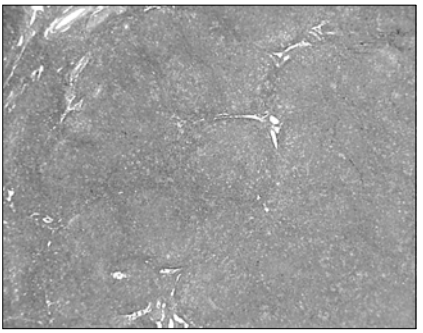

Figure 14. Low-power of NLPHL. (H&E)

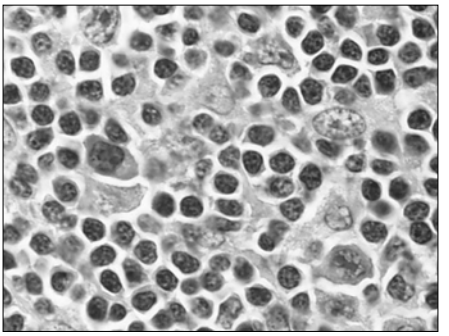

Figure 15. High-power showing RS cells variant in NLPHL. (H&E)

4.6 Discussion

PTGC is a distinctive type of follicular lymphoid hyperplasia (N. Harris et al.) seen focally in about 20% of nodes with nodular lymphocyte-predominant Hodgkin's lymphoma (NLPHL), and it can also be seen as isolated finding not associated with lymphoma. Morphologically this can manifest as enlarged follicles that contain several mantle zone type B cells mixed with germinal center cells (see Figures 14 and 15). Single or multiple foci are present in the nodes and usually there is lymph-adenopathy. Several studies have shown that de novo PTGCs in children are associated with some risk of subsequent development of NLPHL. This progression is infrequent and may occur after many years (10–15 years). In some cases the distinction between early Hodgkin's lymphoma and PTGC can be blurred.

Careful attention to the morphology and use of immunocytochemical stains (see Table 2) may resolve the dilemma. CD20+ cells and CD57 rosettes are common in NLPHD and are useful in diagnosis (see Figure 16).

Table 2. Immunocytochemical staining results with PTGC and Hodgkin's lymphoma

	PTGC†	NLPHD‡
CD20	Tight nodules	Irregular nodules
CD45RA	Tight nodules	Irregular nodules
CD3	Scattered cells	Large aggregates
CD57 rosettes	Absent	Present in most cases (>85%)
CD30	Variable staining	Negative

Modified from Phuong L et al. AJSP. 23(1):27-33, 1999.
†: PTGC: progressive transformation of germinal center.
‡: NLPHD: nodular lymphocyte-predominant Hodgkin's disease.

PTGC was first described by Lennert and Muller-Hermelink (1975) as large aggregates of germinal centers, which are 2–3 times the size of normal germinal centers. Earlier reports indicated diagnostic overlap with Hodgkin's disease. However, by using a combination of morphologic criteria and IPX stains these entities can be separated. In more recent times "microdissection" of suspected areas and IgH gene rearrangement by

PCR may provide additional help. Young patients with florid PTGCs should be followed closely for development of Hodgkin's lymphoma.

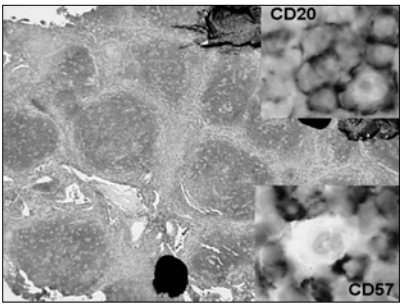

Figure 16. NLPHL. Positive CD20 staining showing irregular nodules. (main and upper insert). CD57 rosettes (lower insert).

5. BI-PHENOTYPIC LYMPHOMA/ LEUKEMIA

5.1 Case History

The patient was a 35-year-old female who presented to the hospital with skin rash, palpitation, and fevers. Initial physical examination revealed multiple nonpalpable ecchymosis and inguinal lymphadenopathy. A CBC revealed mild anemia and leukocytosis (15, 000/μl) with a mild monocytosis and occasional blasts. Past history was unremarkable. A lymph node biopsy was done.

5.2 Morphology

The inguinal lymph node measured 2.5 cm and the cut-surface was smooth pink-tan. Sections showed florid T-cell proliferation and rare preserved germinal centers (see Figure 16). Interfollicular areas also contained several macrophages with brown granular pigment (dermatopathic changes, see Figure 17)). The cellular infiltrates in the T-cell region ranged from small to large, and nuclear chromatin from fine to focally clumped, and few cells contained occasional large nucleoli (see Figure 19). Cytoplasm was minimal to moderate. Few plasma cells and rare eosinophils were also seen.

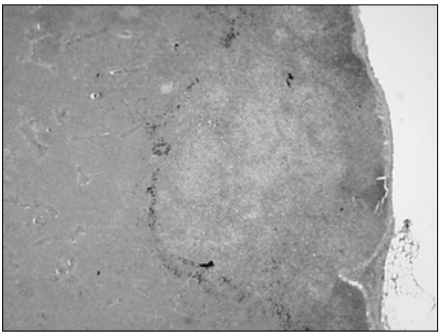

Figure 17. Low-power image showing expanded inter-follicular areas and rare preserved germinal center. (H&E)

5.3 Immunohistochemical Stains

CD3, CD5 (focal staining), UCHL-1 (T-cell), CD43, and myeloperoxidase (MPO) were strongly positive in the expanded T-cell region (see Figure 20). CD20 and CD21 showed few preserved and somewhat compressed germinal centers.

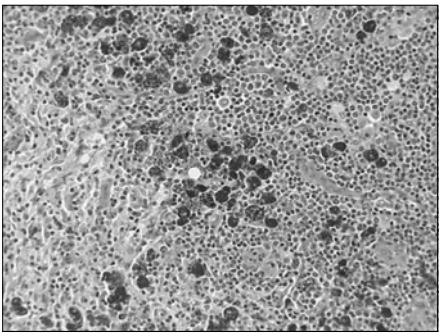

Figure 18. Higher power image of the interfollicular area showing pigment-laden macrophages and dermato-pathic changes. (H&E)

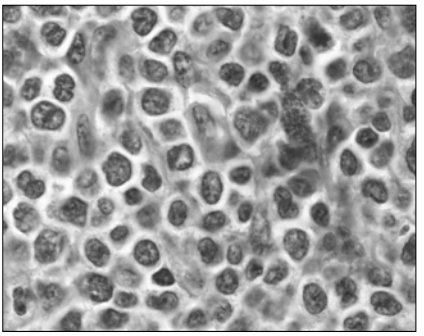

Figure 19. Small to large atypical lymphocytes with fine to focally clumped chromatin and occasional nucleoli. (H&E)

5.4 Flow Cytometry

Abnormal T-cell population expressed CD2, CD3, CD5, tDt and CD33 (myeloid marker). Also, some of the T-cells expressed dim CD10.

5.5 Differential Diagnosis

Abnormal T-cell response (secondary to viral infection), dermatopathic lymphadenopathy, peripheral T-cell lymphoma, cutaneous T-cell lymphoma (CTCL), angioimmunoblastic lymphadenopathy (AILD), granulocytic sarcoma, T-CLL, and acute leukemia infiltrates.

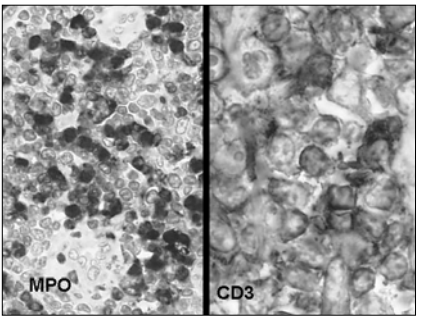

Figure 20. The atypical lymphoid cells are positive for MPO (left) and CD3 (right).

5.6 Diagnosis

Immature T-cell population, consistent with a bi-phenotypic lymphoma/ leukemia.

5.7 Discussion

Marked expanded T-cell regions and compressed (displaced) B-cell areas suggest a neoplastic process. In most viral infections, significant “transformed” lymphoid cells and vascular proliferation is common. Also, B-cell areas are preserved in most reactive conditions. Dermatopathic lymphadenopathy is often seen in lymph nodes draining chronic skin conditions (including CTCL). However, macrophages dominate the lymph node infiltrate and few clusters of immature T-cells may be seen. B-cell areas are usually preserved and secondary germinal centers are found. AILD is a clinical syndrome with hypergammaglobulinemia, hemolytic anemia and lymphadenopathy. Vascular proliferation with prominent endothelial cells is often seen.

Table 3. Immunophenotype and cytochemical features of acute and chronic leukemias

Cytochemical stains and markers	AML* M0-M4	AML M4-M5	AML M6†	AML M7	ALL (pre B)‡	ALL (preT)§	Burkitt's (L3)	CLL**/HCL††
Myeloperoxidase (MPO)	+++	+/–	++	–	–	–	–	CLL=
Sudan black (SBB)	+++	+/–	++	–	–	–	–	CD20+,
Naphthol AS-D Chloroacetate	+++	++/–	–	–	–	–	–	CD5+, CD23+
Nonspecific esterase (NSE)	+/–	+++	–	+/–	–	–	–	
PAS	–	+/–	+++	++	–	–	–	HCL=
Oil red O	–	–	–	–	–	–	+	CD20+,
CD13, CD33, CD34	+++	++/–	++	–	–	–	–	CD25+,
CD14, CD24, HLA-DR	–/+	+++	–	–	–	–	–	CD103+ &
CD19, CD10, tDt	–	–	–	–	+++	–	–	CD11c+
CD3, CD10, tDt	–	–	–	–	–	+++	–	
CD41 and CD61	–	–	–	++	–	–	–	
Cytoplasmic mu	–	–	–	–	–/+	–	+	+
Light chains (Kappa/lambda)	–	–	–	–	–	–	++	+

* Acute myelocytic leukemia.
† Erythroleukemia contains both erythroid and myeloid blasts.
‡ Precursor B ALL.
§ Precursor T ALL.
** Chronic lymphocytic leukemia.
†† Hairy cell leukemia.

Peripheral T-cell lymphoma and CTCL lymph node infiltration are similar and IPX/flow cytometry are needed for the diagnosis. Later, the patient's peripheral blood revealed several blasts with identical immunophenotype (immature T-cell with myeloid marker co-expression). Leukemic infiltrate of the lymph node (lymphadenopathy) is not uncommon; approximately 20–45% of acute lymphoblastic leukemias (ALL) can present with generalized lymphadenopathy. In myeloid leukemias, especially the myelomonocytic type can manifest with significant tissue infiltrates and lymphadenopathy. In pure acute myeloid leukemia (AML) initial lymph node enlargement is unusual. Mixed lineage leukemias (combination of T, B, and myeloid) have been known to present with lymphadenopathy. Based on current FAB classification criteria, leukemias are considered biphenotypic when leukemic cell express two markers of each lineage, e.g., CD13/CD33 (myeloid) and CD2/CD3 (T-lymphoid). This aberrant population is detected by cytochemical stains and by flow cytometry. In this case leukemic/lymphoma cells "homed" to a T-cell region mimicking a lymphoproliferative process.

CBC and bone marrow examination are often needed in evaluating lymph nodes with the above morphology. Table 3 summarizes the immunophenotype and cytochemical features of acute and chronic leukemias.

6. REFERENCES

6.1 High-Grade B-Cell Lymphoma with Plasmacytic Differentiation

1. Harris NL, Hodgkin's disease: classification and differential diagnosis. *Modern Pathology*, **12**(2), 159-75 (1999).
2. Jaffe ES, Harris NL, Stein H, Vardiman JM. *Pathology and Genetics of Tumors of Hematopoietic and Lymphoid Tissues:* World Health Organization Classification of Tumors. Lyons, Fr: IARC Press, 2001.
3. Andriko JA, Swerdlow SH, Aguilera NI, Abbondanzo SL, Is lymphoplasmacytic lymphoma/immunocytoma a distinct entity? A clinicopathologic study of 20 cases. *American Journal of Surgical Pathology*, **25**(6), 742-51 (2001).
4. Evans HL, Polski JM, Deshpande V, Dunphy CH, CD5+ true SLL/CLL with plasmacytic differentiation and an unusual 1p36 translocation: case report and review of the literature. *Leukemia and Lymphoma*, **39**(5-6), 625-32 (2000).
5. Hussong JW, Perkins SL, Schnitzer B, Hargreaves H, Frizzera G, Extramedullary plasmacytoma: a form of marginal zone cell lymphoma? *American Journal of Clinical Pathology*, **111**(1), 111-6 (1999).
6. Dunphy CH, Galambos C, Polski JM, et al., Extranodal posttransplant plasmacytic hyperplasia with subsequent posttransplant plasmacytic malignancy: six-year interval case report and review of the literature. *Archives of Pathology and Laboratory Medicine*, **126**(3), 351-6 (2002).
7. Van Huyen JP, Molina T, Delmer A, et al., Splenic marginal zone lymphoma with or without plasmacytic differentiation. *American Journal of Surgical Pathology*, **24**(12), 1581-92 (2000).

6.2 Follicular B-Cell Lymphoma with Aberrant T-Cell Antigen Expression

1. Kaleem Z, White G, Zutter MM, Aberrant expression of T-cell-associated antigens on B-cell non-Hodgkin lymphomas. *American Journal of Clinical Pathology*, **115**(3), 396-403 (2001).
2. Achten R, Verhoef G, Vanuytsel L, De Wolf-Peeters C, T-cell/histiocyte-rich large B-cell lymphoma: a distinct clinicopathologic entity. *Journal of Clinical Oncology*, **20**(5), 1269-77 (2002).

6.3 High-Grade B-Cell Lymphoma

1. Sapi Z, Antal I, Papai Z, et al., Diagnosis of soft-tissue tumors by fine-needle aspiration with combined cytopathology and ancillary techniques. *Diagnostic Cytopathology*, **26**(4), 232-42 (2002).

2. Wei SH, Sheen JM, Huang CB, Hsiao CC, Primary spinal epidural non-Hodgkin's lymphoma in a child. *Chang Gung Medical Journal*, **24**(12), 820-5 (2001).
3. Herrlinger U, Weller M, Kuker W, Primary CNS lymphoma in the spinal cord: clinical manifestations may precede MRI detectability. *Neuroradiology*, **44**(3), 239-44 (2002).
4. Durr HR, Muller PE, Hiller E, et al., Malignant lymphoma of bone. *Archives of Orthopaedic and Trauma Surgery*, **122**(1), 10-6 (2002).

6.4 Progressive Transformation of Germinal Centers

1. Harris NL, Hodgkin's disease: classification and differential diagnosis. *Modern Pathology*, **12**(2), 159-75 (1999).
2. Burns BF, Colby TV, Dorfman RF, Differential diagnostic features of nodular L & H Hodgkin's disease, including progressive transformation of germinal centers. *American Journal of Surgical Pathology*, **8**(4), 253-61 (1984).
3. Ferry JA, Zukerberg LR, Harris NL, Florid progressive transformation of germinal centers: a syndrome affecting young men, without early progression to nodular lymphocyte predominance Hodgkin's disease. *American Journal of Surgical Pathology*, **16**(3), 252-8 (1992).
4. Nguyen PL, Ferry JA, Harris NL, Progressive transformation of germinal centers and nodular lymphocyte predominance Hodgkin's disease: a comparative immunohistochemical study. *American Journal of Surgical Pathology*, **23**(1), 27-33 (1999).

6.5 Bi-Phenotypic Lymphoma/Leukemia

1. Matutes E, Morilla R, Farahat N, et al., Definition of acute biphenotypic leukemia. *Haematologica*, **82**(1), 64-6 (1997).
2. Nakase K, Sartor M, Bradstock, Detection of myeloperoxidase by flow cytometry in acute leukemia. *Cytometry*, **34**(4), 198-202 (1998).
3. Ogawa K, Shichishima T, Maruyama Y, Mixed-lineage leukemia/hybrid leukemia/biphenotypic leukemia. *Ryoikibetsu Shokogun Shirizu*, 22 Pt 3), 139-41 (1998).
4. Willman CL, Acute leukemias: a paradigm for the integration of new technologies in diagnosis and classification. *Modern Pathology*, **12**(2), 218-28 (1999).
5. Taguchi H, Morishita N, Murakami K, Kubota T, Kubonishi I, Miyoshi I, Biphenotypic leukemia with a new translocation, t(2;6)(q31;q23). *Cancer Genetics and Cytogenetics*, **91**(2), 104-5 (1996).
6. Bennett JM, Catovsky D, Daniel MT, et al., Proposed revised criteria for the classification of acute myeloid leukemia: a report of the French–American–British Cooperative Group. *Annals of Internal Medicine*, **103**(4), 620-5 (1985).
7. Bloomfield CD, Herzig GP, Caligiuri MA, Introduction: acute leukemia: recent advances. *Seminars in Oncology*, **24**(1), 1-2 (1997).

CHAPTER 12
AGGRESSIVE B-CELL LYMPHOMAS

Wei Yang, M.D., Ph.D.,* and Catherine M. Listinsky, M.D.†

1. INTRODUCTION

The aggressive B-cell lymphomas are surprisingly heterogeneous in morphologic and architectural features, despite their common cell lineage. There are, in addition, a variety of differences among these entities that have no morphologic correlates. These disorders were spotlighted in the XI Workshop of the European Association of Hematopathology in May 2002 in Siena, Italy, and reviewed in the symposium of the American Society for Hematopathology in March 2003 at the Annual Meeting of the US–Canadian Academy of Pathology.[1-3] Like the symposium, this presentation is derived from material presented at the XI European Workshop. Our intention is to provide a practical, illustrated update on the aggressive B-cell lymphomas for general pathologists in practice.

The WHO classification of hematopoietic neoplasms serves as the basic framework for discussion of the aggressive B-cell lymphomas, and the WHO publication *Pathology and Genetics of Tumours of Hematopoietic and Lymphoid Tissues* has become the standard reference.[4] John K. C. Chan's chapter, "Tumors of the Lymphoreticular System," provides a discussion of diagnostic considerations in the lymphomas, and is highly recommended as a comprehensive overview of the field.[5]

Before beginning the discussion, however, it is important to note that there are two clinical factors that are critical to consider in addition to WHO classification. (1) Is the lymphoma present as a de novo entity, or is it present as a result of transformation from a low-grade lymphoma? This is not always straightforward to determine, because a patient with low-grade lymphoma may first come to clinical attention during a high-grade transformation. In general, lymphomas that are transformations are relatively refractory to therapy. (2) Is the lymphoma present in a patient with normal immune function, or with an immune-deficient state? These special conditions, lymphomas (1) in transformation and (2) in the setting of immune deficiency, were given detailed

* Fellow in Hematopathology, Department of Pathology, Case Western Reserve University, Cleveland, OH.
† Associate Professor, Department of Pathology, Case Western Reserve University, Cleveland, OH.

consideration at a number of workshops and symposia, and are beyond the scope of this discussion.

In this limited presentation, we focus on the de novo aggressive B-cell lymphoma entities that are defined in the 2001 WHO classification (see Table 1), and we include one example of a transformed lymphoma type that can be confused with classical Burkitt lymphoma. The aims are to familiarize the reader with the application of the WHO terminology, and to provide a brief atlas of illustrative examples.

Table 1. WHO classification of aggressive B-cell lymphomas (extracted from WHO classification) [4]

Precursor B-cell neoplasms	Mature B-cell neoplasms
Precursor B-lymphoblastic lymphoma	Mantle cell lymphoma
	Diffuse large B-cell lymphoma
	Mediastinal (thymic) large B-cell lymphoma
	Intravascular large B-cell lymphoma
	Primary effusion lymphoma
	Burkitt lymphoma

2. PRECURSOR B-LYMPHOBLASTIC LYMPHOMA

Precursor B-lymphoblastic lymphoma is the tissue-based equivalent of B precursor acute lymphoblastic leukemia, and the diagnosis excludes cases with bone marrow involvement by 25% or more malignant cells. The cells are CD19+, CD79a+, and TdT +, and usually coexpress CD10 and CD24.[4-6]

If histologic sections are of good quality, precursor B lymphoblastic lymphoma presents as sheets of cells with fine nuclear chromatin, extremely scant cytoplasm, and a high rate of mitotic activity (see Figure 1). The morphologic differential diagnosis includes precursor T-lymphoblastic lymphoma, Burkitt's lymphoma, blastoid variant of mantle cell lymphoma, and extramedullary myeloid cell tumor. If the histological preparation is suboptimal (crush artifact, degenerative changes, poor preservation—obscuring the quality of the fine chromatin and the presence of mitotic activity, as in the Burkitt lymphoma) the differential diagnosis in adults will include the far commoner low-grade lymphomas. This could result in a serious delay in diagnosis of the aggressive entity. Immunohisto-chemical or flow cytometric analysis is required for the definite classification, as is the case for most non-Hodgkin lymphomas.

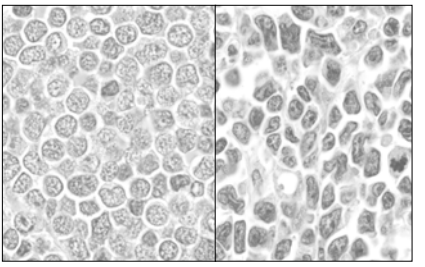

Figure 1. Two examples of precursor B lymphoblastic lymphoma — one with round nuclei (left) and one with convoluted nuclei (right). The cells in both examples exhibit fine chromatin distribution. (H&E)

3. MANTLE CELL LYMPHOMA

Diffuse mantle cell lymphoma is clinically aggressive, an intermediate-grade malignant lymphoma. However, because the cells are on the order of the size and chromatin texture of small lymphocytes or centrocytes, the differential diagnosis includes lymphocytic lymphoma and

follicular lymphoma—entities that require an entirely different clinical approach. Diffuse mantle cell lymphoma is often recognizable on H+E-stained sections even on low to intermediate magnification, because the monotonous sheets of cells contain a distinctive scattering of solitary epithelioid histiocytes in the background. [5] The diagnosis of mantle cell lymphoma is confirmed by the demonstration of the CD20+, CD19+, CD5+, CD23-, CD10- immunophenotype, and validated by the demonstration of increased nuclear Cyclin D1, which is the result of the upregulation of the bcl-1 gene that occurs in the presence of the t(11;14) chromosomal translocation.[4, 5, 7]

The more problematic blastoid variant of mantle cell lymphoma is a subject of ongoing investigation and discussion. Blastoid variant of mantle cell lymphoma, as the name implies, may morphologically resemble the highly aggressive B- or T-lymphoblastoid lymphomas (see Figures 2 and 3); however, the designation "blastoid mantle cell lymphoma" also encompasses cases which morphologically resemble diffuse large-cell lymphomas. Requisite for the diagnosis of the blastoid variant of mantle cell lymphoma is evidence of cyclin D1 amplification plus evidence of additional cytogenetic abnormalities,[4,5,7] and the morphologic features are of secondary consideration. The blastoid variant of mantle cell lymphoma may arise as a transformation from a known mantle cell lymphoma, or it may arise de novo.

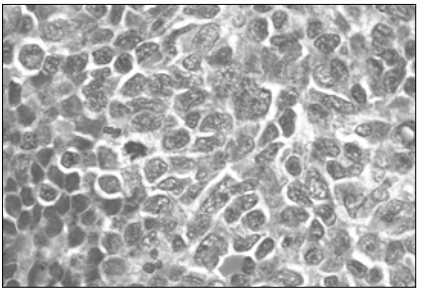

Figure 2. Blastoid variant of mantle cell lymphoma arising from a typical mantle cell lymphoma. Residual typical mantle cells are noted in the left corner. (H&E)

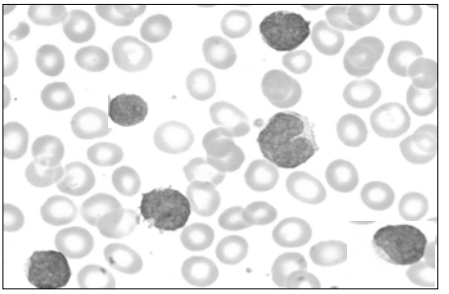

Figure 3. Blastoid variant of mantle cell lymphoma. Peripheral blood involvement by blastoid mantle cell lymphoma (Wright-Giemsa stain).

4. DIFFUSE LARGE B-CELL LYMPHOMA

"Diffuse large B-cell lymphoma," encompasses a morphologically heterogeneous mix of neoplasms (see Figures 4 and 5), and some morphologic overlap may blur the diagnostic distinctions among them.[4, 5, 8] Whether there are important clinical differences among these morphologically different tumors is controversial, and the use of these subsets in diagnosis is considered optional by the WHO panel.[4]

The commonest morphologic subtype of diffuse large B-cell lymphoma is "centroblastic"—resembling the large transformed cells of the B-cell follicle (see Figure 4). Classification into the "immunoblastic" subtype requires (by definition) cellular monotony, with sheets of cells with large vesicular nuclei, prominent central eosinophilic nucleoli and abundant eccentric amphophilic cytoplasm (see Figure 5). This

morphology is characteristic of lymphomas which arise in patients with autoimmune disorders, such as Hashimoto's thyroiditis. Pleomorphic diffuse large B cell lymphoma is a term reserved for lymphomas that contain a mixture of centroblasts and immunoblasts (see Figure 4). In anaplastic diffuse large B-cell lymphoma (see Figure 5) the large pleomorphic nuclei may resemble Reed-Sternberg cells of Hodgkin lymphoma; they may occur in cohesive sheets resembling carcinoma, and they may exhibit sinusoidal growth, resembling anaplastic large-cell lymphoma of T/NK origin. However, the cells of this neoplasm express evidence of B-cell differentiation, CD19+, CD20+, surface or cytoplasmic immunoglobulin +, and are negative for both ALK and CD15.

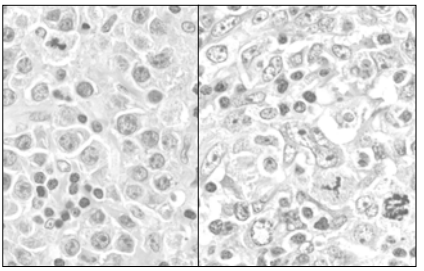

Figure 4. Diffuse large B-cell lymphoma. Left: Centroblastic variant. Right: Pleomorphic variant. (H&E)

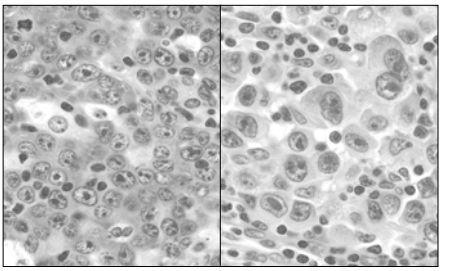

Figure 5. Diffuse large B-cell lymphoma. Left: Immunoblastic variant. Right: Anaplastic variant. (H&E)

From the definition accepted by the WHO panel, T-cell/histiocyte-rich diffuse large B-cell lymphoma includes less than 10% large neoplastic B-cells among variable proportions of benign histiocytes and small T-lymphocytes.[4,5] T-cell/histiocyte-rich diffuse large B-cell lymphoma in itself presents a rich spectrum of morphologic possibilities and potential pitfalls in diagnosis.[9,10] (see Figures 6 and 7) When the histiocytes predominate in the background, the differential diagnosis may include toxoplasmosis, Hodgkin's lymphoma, and the lymphoepithelioid cell variant of peripheral T-cell lymphoma, unspecified (see Figure 6). When the small T-lymphocytes

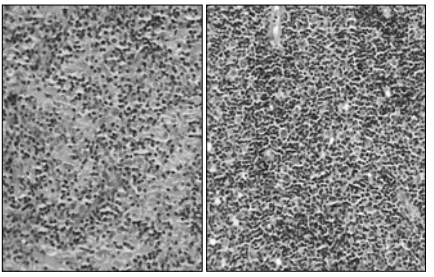

Figure 6. T-cell/histiocyte-rich diffuse large B-cell lymphoma. Left: Predominantly histiocytic background resembling granulomatous disease, Hodgkin lymphoma, and peripheral T-cell lymphoma. Right: Predominantly small T-cell background gives the lymphoma a resemblance to low grade lymphomas, particularly T-cell type. (H&E)

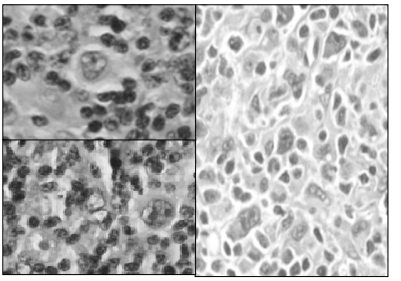

Figure 7. T-cell/histiocyte-rich diffuse large B-cell lymphoma. Upper left: Centroblast-like cells. Lower left: L&H–like cells. Right: Reed-Sternberg-like cells. (H&E)

predominate, the infiltrate may resemble an immune reaction or a low-grade lymphoma (see Figure 6).

Furthermore, in addition to the variable proportions of benign histiocytes and T-lymphocytes in the background of T-cell/histiocyte-rich large B-cell lymphoma, the large malignant B-cells themselves have a broad range of appearances.[9,10] In some cases they resemble L&H cells of nodular lymphocyte-predominant Hodgkin lymphoma; in some they resemble centroblasts; and in others they resemble Reed-Sternberg cells of classical Hodgkin lymphoma (see Figure 7). The cells with these different appearances even tend to express different immunophenotypes.[10] T-cell/histiocyte-rich diffuse large B-cell lymphoma may have a close relationship with lymphocyte predominant Hodgkin lymphoma.[11] In some series, T-cell/histiocyte-rich diffuse large B-cell lymphoma was found to present in a higher clinical stage than is usual for diffuse large B cell lymphomas.[5,11,12] Others have found it to be a more heterogeneous entity without significant differences from diffuse large B-cell lymphoma.[5]

Clearly, while the distinctions among the above morphologic variants of diffuse large B-cell lymphomas are of as yet uncertain clinical value, pathologists' awareness of this morphologic spectrum of B-cell lymphomas is important, both to avoid the missed diagnosis of malignancy and to avoid the mistaken classification as a low-grade lymphoma, Hodgkin lymphoma, or T/NK cell lymphoma.

4.1 Plasmablastic Lymphoma

Plasmablastic lymphoma, described by Delecluse, is a rare but distinctive clinicopathologic entity which typically presents as a mass in the oral cavity of an HIV positive patient, but may arise in the setting of multicentric Castleman's disease.[4,5,13] The neoplasm is highly aggressive. The histopathology (see Figure 8) may be identical to that of immunoblastic lymphoma; however, the neoplastic cells exhibit evidence of plasma cell differentiation rather than mature B-cell differentiation. They express plasma cell markers CD138+ and CD38+, and, unlike the immunoblastic variant of diffuse large B-cell lymphoma, they are negative for CD20 and CD45. Recently these neoplasms have been shown to be highly associated with both EBV and HHV-8 infections.[14]

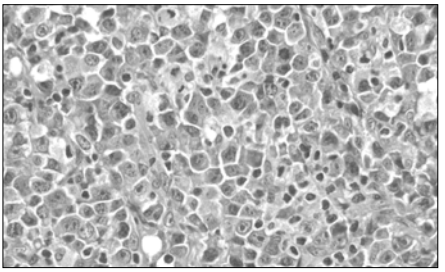

Figure 8. An example of plasmablastic lymphoma. (H&

Plasmablastic lymphoma overlaps with anaplastic multiple myeloma in both morphologic and immunophenotypic features. However, the clinical setting is quite different, and the cells of plasmablastic lymphoma exhibit a higher growth fraction than myeloma, and also lack an admixture of mature plasma cells which is typically present in myeloma.[4,5,13]

4.2 Diffuse Large B-Cell Lymphoma with Expression of Full-Length ALK

Diffuse large B-cell lymphoma with expression of full-length ALK is a distinctive immunophenotypic variant described by Delsol.[15] The cells of this neoplasm resemble monomorphic immunoblasts or plasmablasts, sometimes with occasional Reed-Sternberg-like cells. While the cells of this neoplasm are ALK positive (granular cytoplasmic and Golgi positivity by standard immunohisto-chemistry), these B cell neoplasms lack the t(2;5) seen in ALK positive anaplastic large-cell lymphomas of T/NK cell origin. They overexpress the *full-length* (native) ALK protein, and they do not exhibit "anaplastic" morphology. Furthermore, the immunophenotype of this lymphoma is unusual, with the cells expressing cytoplasmic IgA and light chain restriction, but lacking most of the usual B- and T-cell markers except CD34 and CD57.[4, 5, 15]

5. MEDIASTINAL (THYMIC) LARGE B-CELL LYMPHOMA

Primary mediastinal (thymic) large B-cell lymphoma presents as a large anterior mediastinal mass, in women more commonly than in men, in the 30- to 60-year-old age group.[4,5,16] This lymphoma is thought to be derived from a type of B-cell that is native to the thymus, and it always involves the thymus. Mediastinal large B-cell lymphomas of *nodal* origin are *excluded* from this category.

The cells usually express leukocyte common antigen CD45 and mature B cell antigens CD20 and CD19, but they do not express immunoglobulins and are weak or negative for HLA class I and II antigens. The cells characteristically overexpress the MAL gene,[17] and recent studies show a gene expression profile that is similar to that of classical Hodgkin lymphoma,[18] and distinctly different from most diffuse large B-cell lymphomas. The cells are negative for bcl-2, bcl-6, and Myc rearrangements, and are dimly positive for CD30.[4, 5, 19]

Morphologically, this lymphoma is frequently composed of sheets of large-cells with clear cytoplasm, and often there is prominent fibrosis in the stroma (hence the previous designations "mediastinal clear cell lymphoma," and "sclerosing mediastinal lymphoma"). Figure 9 illustrates an example of this entity. The differential diagnosis includes sclerosing carcinoma, malignant melanoma, and nodular sclerosing Hodgkin lymphoma.

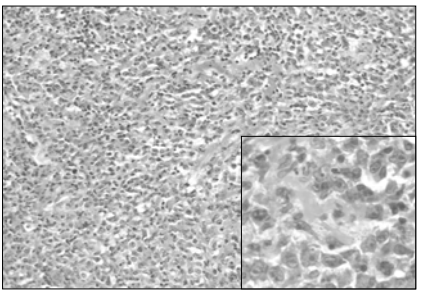

Figure 9. Mediastinal (thymic) large B-cell lymphoma. Insert: higher magnification. (H&E)

6. INTRAVASCULAR LARGE B-CELL LYMPHOMA

Intravascular large B-cell lymphoma presents in adults, with symptoms of vascular occlusion.[4,5] Multiorgan disease is typical, with frequent involvement of brain (dementia, focal symptoms), the skin (plaque formation), and multiple parenchymal organs. The

malignant cellls are hypothesized to have a defect in their expression of homing receptors (66 cases studied lacked adhesion molecules CD29 and CD54).[20]

The neoplastic cells are frequently large and vesicular with some resemblance to vascular endothelial cells (see Figure 10), and the disease was therefore formerly called "malignant angioendotheliomatosis."

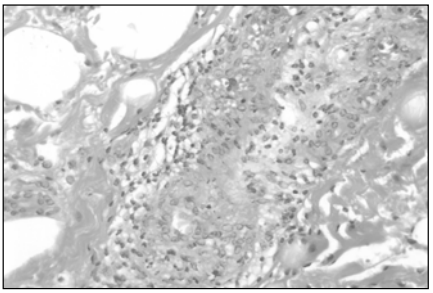

Figure 10. Intravascular large B-cell lymphoma The large vesicular nuclei of the lymphoma may resemble the reactive vascular endothelium. (H&E)

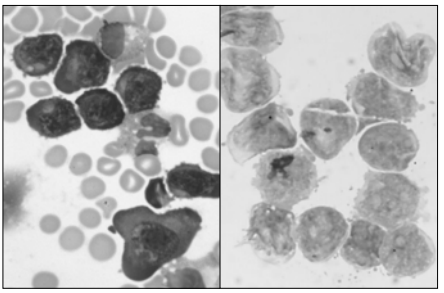

Figure 11. Primary effusion lymphoma in pleural fluid. The large and pleomorphic cells may mimic carcinoma and do not react with B-and T-cell surface markers. (Wright-Giemsa stain)

7. PRIMARY EFFUSION LYMPHOMA

Primary effusion lymphoma consists of large, bizarre, pleomorphic cells in serous effusions (see Figure 11). The malignant cells contain human herpes virus 8 antigens, and also usually show evidence of Epstein–Barr virus.[2, 4, 21] This neoplasm typically occurs in the setting of HIV infection, but has been described in postrenal transplant, and in elderly males. Recently, primary effusion lymphomas have been shown to exhibit a plasma cell gene expression profile, so that these malignant cells appear very similar to the cells of plasmablastic lymphoma.[22]

The diagnosis of primary effusion lymphoma can be problematic, because these large-cells may resemble non-hematopoietic neoplasms, and because they lack expression of most T-cell, B-cell, and plasma cell antigens (including a lack of CD19, CD38, and CD138, but occasional positivity for early T-cell antigen cytoplasmic CD3). The cells are usually positive for leukocyte common antigen CD45.

8. BURKITT LYMPHOMA

The WHO classification recognizes three distinctive clinical variants of Burkitt lymphoma, and these have been well-described in the literature.[2,4,5] Endemic Burkitt lymphoma is the classical EBV-associated jaw tumor of 4- to 7-year-old children in the malaria belt. Sporadic Burkitt lymphoma presents as abdominal masses in children and adults, and is less consistently associated with EBV. Immunodeficiency-associated Burkitt lymphoma has a 25–40% association with EBV infection. The cells of Burkitt lymphoma express mature B-cell markers CD19+, CD20+, CD22+, and express surface IgM and light chain restriction. In addition, they express germinal center markers CD10 and bcl 6.

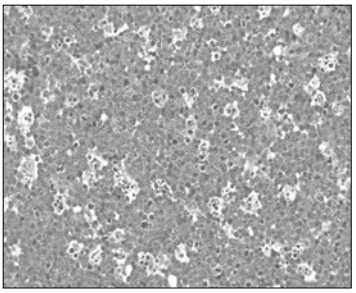

Figure 12. Burkitt lymphoma. Low power showing the starry sky appearance. (H&E)

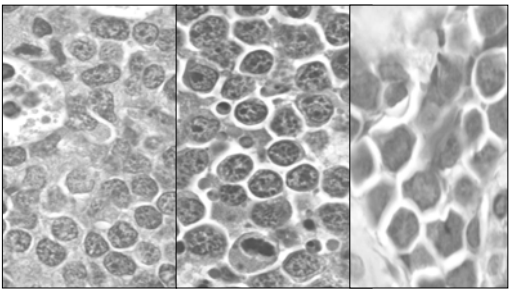

Figure 13. Burkitt lymphoma. Left: typical variant with uniform round nuclei, fine chromatin, and indistinct nucleoli. Center: Atypical variant with less uniformity and prominent nucleoli. Right: Artifactual changes. Nuclear shrinkage and chromatin smearing may mimic a low grade lymphoma. (H&E)

The classical morphology of Burkitt lymphoma (see Figures 12 and 13)—the "starry sky" seen in tissue sections, and the vacuolated cytoplasm seen on touch preparations and smears—is widely known and supposedly pathognomonic of the diagnosis. However, it is now agreed that diagnosis of Burkitt lymphoma requires evidence of an isolated Myc translocation. The result of this definition is that there are some cases that qualify as Burkitt lymphoma on the molecular basis, but that are too pleomorphic to fit the classical morphological description (see Figure 13). These are termed "atypical Burkitt lymphoma," and are expected to behave as classical Burkitt lymphoma.[2, 4, 5]

Conversely, there are lymphomas that morphologically resemble Burkitt lymphoma and have the c-myc translocation, but that also exhibit additional chromosomal abnormalities. Figure 14 illustrates a follicular lymphoma that has transformed into a tumor with Burkitt morphology and with a probable c-Myc translocation, in addition to the original t(14;18). Lymphomas such as these are known as "two-hit" lymphomas, are extremely aggressive, and do not respond to therapy in the way that a Burkitt lymphoma would respond.[2, 23, 24] While the case illustrated is a transformation from a patient with a known follicular lymphoma, such cases can present as de novo malignant lymphomas and must be distinguished from true Burkitt lymphoma which will have an isolated c-myc translocation. The WHO panel recommends that these "two-hit" cases be termed "unclassifiable aggressive B-cell lymphoma." The term "Burkitt-like lymphoma" is discouraged, because these histological lookalikes, (with unrelated pathogenesis) should not be confused with the distinctive entity of Burkitt lymphoma.[2]

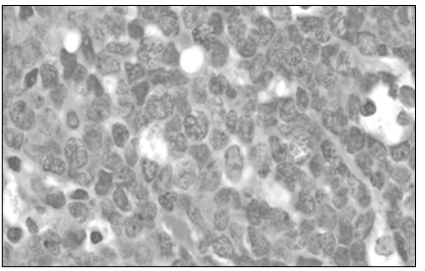

Figure 14. A transformed follicular lymphoma resembling a Burkitt lymphoma. (H&E)

9. CONCLUSIONS

Our goal in this presentation has been to familiarize practicing pathologists with the WHO terminology for the aggressive B-cell lymphomas, and to provide a number of examples to illustrate these entities. We have addressed some of the difficulties in the classification and diagnosis of these aggressive neoplasms. It will be noted, with dismay perhaps, that some of the most distinctive and best-defined entities among these disorders are the rarest of all. There remain large groups of common, heterogeneous lymphomas that have less-defined pathogenesis, and among these there are clearly subsets of tumors that will not respond to conventional therapy. So far, the unresponsive tumors cannot be separated from the others prior to therapy. Some of the most exciting current work in lymphomas is occurring on the molecular level. As molecular mechanisms of lymphomagenesis are revealed, the possibility of developing targeted therapy for these neoplasms comes closer to reality. It may be anticipated that, with time, further distinctive lymphoma entities will be separated and defined by molecular means, and these will be added to the classification scheme as they are established.

10. ACKNOWLEDGEMENT

The authors would like to express thanks to both Dr. Howard Meyerson and Dr. Vishnu Reddy for the use of their photomicrographs of confirmed cases of primary effusion lymphoma. We would also like to thank the contributors to the XI Workshop of the European Association for Hematopathology, for providing excellent case examples of aggressive B-cell lymphomas. Some of the illustrations herein were photographed from the glass slides that were contributed to the workshop (Figures 1, 5, 6, 8, 9, and 12).

11. REFERENCES

1. Pittaluga S: Diffuse large B-cell lymphoma: morphological and immunohistochemical correlations *Society for Hematopathology Symposium at the Annual Meeting of United States and Canadian Academy of Pathology* 2003.
2. Jaffe ES: Classical Burkitt lymphoma and variants: strategies for accurate diagnosis *Society for Hematopathology Symposium at the Annual Meeting of United States and Canadian Academy of Pathology* 2003.
3. Said J: Transformation to aggressive B-cell lymphoma *Society for Hematopathology Symposium at the Annual Meeting of United States and Canadian Academy of Pathology* 2003.
4. Jaffe ES, Harris NL, Stein H, Vardiman JM. *Pathology and Genetics of Tumors of Hematopoietic and Lymphoid Tissues*:*World Health Organization Classification of Tumors*. Lyons, Fr: IARC Press, 2001.
5. Chan J. Tumors of the lymphoreticular system. In: Fletcher C, ed. *Diagnostic Histopathology of Tumors*, vol. II. London, UK: Church Livingstone, 2000; 1099-315.
6. Maitra A, McKenna RW, Weinberg AG, Schneider NR, Kroft SH, Precursor B-cell lymphoblastic lymphoma: a study of nine cases lacking blood and bone marrow involvement and review of the literature. *American Journal of Clinical Pathology*, 115(6), 868-75 (2001).
7. Swerdlow SH, Williams ME, From centrocytic to mantle cell lymphoma: a clinicopathologic and molecular review of 3 decades. *Human Pathology*, 33(1), 7-20 (2002).
8. Salar A, Fernandez de Sevilla A, Romagosa V, et al., Diffuse large B-cell lymphoma: is morphologic subdivision useful in clinical management? *European Journal of Hematology*, 60(3), 202-8 (1998).
9. Camilleri-Broet S, Molina T, Audouin J, Tourneau AL, Diebold J, Morphological variability of tumour cells in T-cell-rich B-cell lymphoma: a histopathological study of 14 cases. *Virchows Archiv*, 429(4-5), 243-8 (1996).

10. Lim MS, Beaty M, Sorbara L, et al., T-cell/histiocyte-rich large B-cell lymphoma: a heterogeneous entity with derivation from germinal center B-cells. *American Journal of Surgical Pathology*, 26(11), 1458-66 (2002).
11. Delabie J, Vandenberghe E, Kennes C, et al., Histiocyte-rich B-cell lymphoma: a distinct clinicopathologic entity possibly related to lymphocyte predominant Hodgkin's disease, paragranuloma subtype. *American Journal of Surgical Pathology*, 16(1), 37-48 (1992).
12. Achten R, Verhoef G, Vanuytsel L, De Wolf-Peeters C, T-cell/histiocyte-rich large B-cell lymphoma: a distinct clinicopathologic entity. *Journal of Clinical Oncology*, 20(5), 1269-77 (2002).
13. Delecluse HJ, Anagnostopoulos I, Dallenbach F, et al., Plasmablastic lymphomas of the oral cavity: a new entity associated with the human immunodeficiency virus infection. *Blood*, 89(4), 1413-20 (1997).
14. Cioc AM, Allen C, Kalmar JR, Suster S, Baiocchi R, Nuovo GJ, Oral plasmablastic lymphomas in AIDS patients are associated with human herpesvirus 8. *American Journal of Surgical Pathology*, 28(1), 41-6 (2004).
15. Delsol G, Lamant L, Mariame B, et al., A new subtype of large B-cell lymphoma expressing the ALK kinase and lacking the 2; 5 translocation. *Blood*, 89(5), 1483-90 (1997).
16. Moller P, Lammler B, Eberlein-Gonska M, et al., Primary mediastinal clear cell lymphoma of B-cell type. *Virchows Archiv - A, Pathological Anatomy and Histopathology*, 409(1), 79-92 (1986).
17. Copie-Bergman C, Gaulard P, Maouche-Chretien L, et al., The MAL gene is expressed in primary mediastinal large B-cell lymphoma. *Blood*, 94(10), 3567-75 (1999).
18. Rosenwald A, Wright G, Leroy K, et al., Molecular diagnosis of primary mediastinal B-cell lymphoma identifies a clinically favorable subgroup of diffuse large B-cell lymphoma related to Hodgkin lymphoma. *Journal of Experimental Medicine*, 198(6), 851-62 (2003).
19. Higgins JP, Warnke RA, CD30 expression is common in mediastinal large B-cell lymphoma. *American Journal of Clinical Pathology*, 112(2), 241-7 (1999).
20. Ponzoni M, Arrigoni G, Gould VE, et al., Lack of CD 29 (beta1 integrin) and CD 54 (ICAM-1) adhesion molecules in intravascular lymphomatosis. *Human Pathology*, 31(2), 220-6 (2000).
21. Nador RG, Cesarman E, Chadburn A, et al., Primary effusion lymphoma: a distinct clinicopathologic entity associated with the Kaposi's sarcoma-associated herpes virus. *Blood*, 88(2), 645-56 (1996).
22. Jenner RG, Maillard K, Cattini N, et al., Kaposi's sarcoma-associated herpesvirus-infected primary effusion lymphoma has a plasma cell gene expression profile. *Proceedings of the National Academy of Sciences of the United States of America*, 100(18), 10399-404 (2003).
23. Macpherson N, Lesack D, Klasa R, et al., Small noncleaved, non-Burkitt's (Burkitt-like) lymphoma: cytogenetics predict outcome and reflect clinical presentation. *Journal of Clinical Oncology*, 17(5), 1558-67 (1999).
24. Voorhees PM, Carder KA, Smith SV, Ayscue LH, Rao KW, Dunphy CH, Follicular lymphoma with a Burkitt translocation--predictor of an aggressive clinical course: a case report and review of the literature. *Archives of Pathology and Laboratory Medicine*, 128(2), 210-3 (2004).

CHAPTER 13
DEMYSTIFYING THE DIAGNOSIS OF GLIOMAS

Cheryl Ann Palmer, M.D.*

1. INTRODUCTION

Grading of gliomas of the central nervous system remains a controversial subject among neuropathologists. Different grading systems have proliferated, likely due to the inability of one system to completely classify all tumors. Most of the systems used today are based on the 1929 system of Bailey and Cushing. As expected, all of the systems have their advantages and proponents, as well as their drawbacks. Dissension among various institutions regarding grading systems and the propagation of different grading systems via publications in medical journals also serve to confuse the clinicians responsible for the care of patients with brain tumors, largely neurologists, neuro-oncologists, and neurosurgeons.

One of the first astrocytic tumor grading systems, the Kernohan system, is not generally in use today. This system employed four grades of astrocytoma. Epidemiological studies of this system, however, demonstrated no difference in survival between astrocytoma grades III and IV: in essence, both grades were glioblastomas.

Another modification of grading systems involved the St. Anne/Mayo Clinic grading classification, a four-tiered categorization based on the presence of predetermined histologic criteria. As we shall see later in this lecture, by definition, nearly all astrocytomas exhibit some degree of nuclear pleomorphism. One of the histologic criteria employed in the St. Anne/Mayo Clinic grading classification, however, was nuclear atypia. For this reason, the classification became more of a three-tiered system, rather than a four-tiered system, as originally intended.

A grading system based on criteria proposed by Ringertz and modified by Burger also served as a focal point in the definition of astrocytic tumors. The three tiers of this system were designated as astrocytoma, anaplastic astrocytoma, and glioblastoma multiforme. Astrocytoma describes a neoplasm with mild hypercellularity and nuclear atypia as compared with normal brain astrocytes. Anaplastic astrocytomas display moderate hypercellularity and contain mitotic figures, and may display vascular

* Associate Professor, Departments of Pathology and Neurology, Division of Neuropathology, University of Alabama, Birmingham, AL.

proliferation, but lacks necrosis. Glioblastoma multiforme demonstrates hyper-cellularity, pleomorphism, mitotic activity, vascular proliferation, and necrosis.

The newest World Health Organization (WHO) system has attempted to combine facets of many older systems by using both numeric grades (grades I–IV) as well as verbal designations (see Table 1). This is the system currently in use by most neuropathologists worldwide. One useful update in this system, which was not addressed in the prior version, is the introduction of a separate grade for pilocytic astrocytomas and subependymal giant-cell astrocytomas. As the prognosis and survival curves of pilocytic astrocytomas and subependymal giant cell astrocytomas have long been known to be different from all infiltrating astrocytomas, future compilations of clinical studies will enable the elimination of these two tumor types from therapeutic protocols.

Table 1. WHO classification of astrocytic neoplasms

WHO Grading System, 2000
Grade I : Pilocytic astrocytomas and subependymal giant-cell astrocytomas
Grade II : Fibrillary infiltrating astrocytoma
Grade III : Anaplastic astrocytoma
Grade IV : Glioblastoma multiforme

The most vital point concerning the various grading systems is the need for pathologists and clinicians to understand the system to be used between them and recognize its strengths and liabilities. This important step will aid in proper treatment for patients harboring central nervous system neoplasms.

2. ASTROCYTIC NEOPLASMS

2.1 Pilocytic Astrocytomas

More common in children and young adults, these tumors have regions of the brain they like to frequent. Formerly known by such terms as cerebellar astrocytoma, optic nerve glioma, pontine glioma, and hypothalamic glioma, the majority of these tumors are classified histologically today as pilocytic astrocytomas, WHO Grade I.

Radiographic images of pilocytic astrocytomas commonly demonstrate a cystic lesion surrounding some amount of central enhancement (see Figure 1). This enhancement pattern can aid in the differentiation between pilocytic astrocytomas and infiltrating low-grade fibrillary astrocytomas, which is usually the most common alternative histologic pattern. Fibrillary astrocytomas generally do not enhance with the administration of contrast material.

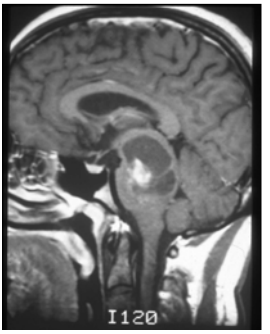

Figure 1. Sagittal T1-weighted MRI scan demonstrating a cystic, enhancing lesion in the pons and midbrain.

Grossly, pilocytic astrocytomas are frequently cystic structures containing a mural nodule (see Figure 2). They are usually well-circumscribed and may compress the surrounding brain parenchyma rather than infiltrate it.

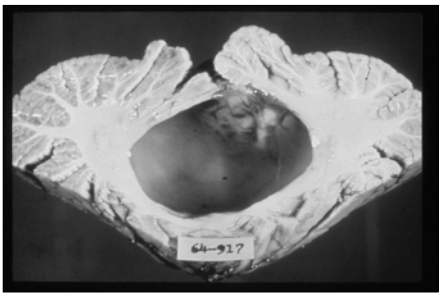

Figure 2. Pilocytic astrocytoma associated with a cyst in the cerebellum.

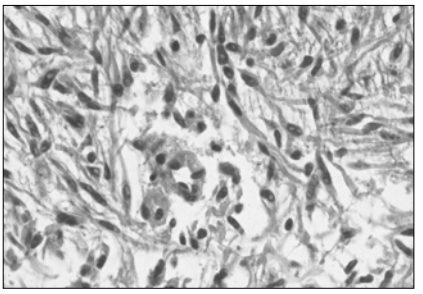

Figure 3. H&E-stained section of typical "piloid" cytoplasmic processes of the pilocytic astrocytoma.

Under the microscope, the origin of the tumor's name is apparent, ("pilus": Latin = hair,) as the tumor cells contain elongated, hairlike processes generally arranged in a loosely woven background (see Figure 3). Rosenthal fibers, which are bright pink eosinophilic structures located in the processes of astrocytes, may be seen, as well as eosinophilic granular bodies (EGBs). Although commonly seen in pilocytic astrocytomas, Rosenthal fibers and EGBs are not specific for this diagnosis.

Some pilocytic astrocytomas contain areas with histology identical to oligodendrogliomas. This should not dissuade the pathologist from making the diagnosis of pilocytic astrocytoma. The background of the tumor may contain numerous microcysts, and mucin deposition can be present. The tumor nuclei may be rather pleo-morphic, but mitoses are rare. Marked endothelial proliferation is not uncommonly seen. This is the most likely reason for the enhancing appearance on radiographic images. This vascular proliferation may erroneously prompt consi-deration of a more malignant neoplasm. Necrosis is not an expected finding in pilocytic astrocytomas, though, and when observed, should engender caution in making this diagnosis.

Well-circumscribed, pilocytic astrocytomas differ greatly in prognosis from the otherwise "infiltrating" astrocytomas, and surgical removal of pilocytic astro-cytomas can effect a cure, if they are located in a surgically accessible region. There is also evidence that pilocytic astrocytomas are somewhat chemosensitive, and this therapy is customarily employed in younger patients whose rapidly myelinating brains would suffer serious sequelae from cranial irradiation.

2.2 Subependymal Giant-Cell Astrocytomas

Nearly always seen in conjunction with tuberous sclerosis, this well-demarcated tumor is generally located within the lateral ventricular system.

Subependymal giant-cell astrocytomas (SEGCAs) are thought to evolve from the hamartomatous collections of astrocytes, "candle gutterings," located under the ventricular lining. They are frequently asymptomatic until they attain a size where

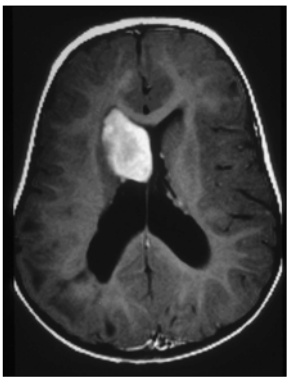

Figure 4. Contrast-enhanced axial MRI scan demonstrating a well-circumscribed tumor in the lateral ventricle.

obstruction of the foramen of Monro occurs. As seen in the accompanying MRI scan, SEGCAs are well-circumscribed and enhance homogeneously with contrast material. Calcification may be present (see Figure 4).

Grossly, SEGCAs are fleshy, and do not demonstrate central cavitation (see Figure 5). They appear to have an attachment to the ventricular wall. If lateral ventricular outflow is blocked, obstructive hydrocephalus will be seen.

Microscopically, the initial impression of SEGCAs is one of malignancy, given the large-cells with abundant glassy eosinophilic cytoplasm and large nuclei. The cells frequently abut one another, and intervening background neuropil may not be present. Minimal infiltration into the surrounding brain parenchyma is seen, however, unlike the typical infiltrating astrocytoma. Other histologic characteristics of anaplasia are generally missing: mitoses are infrequent and necrosis and vascular proliferation are absent. Imm-unocytochemically, the cells are often only weakly positive or nonreactive for GFAP, a surprising finding compared with their H&E similarities to large astrocytes. This, combined with the occasional immuno-reactivity for neurofilament stains, alludes to the tumor's hamartomatous lineage.

Although SEGCAs do enlarge, they do so quite slowly, and surgical debulking generally eliminates symptoms. The prognosis regarding the tumors is quite good, although patients with tuberous sclerosis (TS) have different functional outcomes than the rare SEGCA patient without TS.

2.3 Pleomorphic Xanthoastrocytoma

Recognized as a separate entity, the pleomorphic xanthoastrocytoma (PXA) is more frequent in adolescents and young adults. It is most commonly located in the superficial cortex of the temporal lobe and is often responsible for a long-standing seizure disorder. Frequently cystic, the tumor is nonetheless adherent to the nearby cortex.

The appearance of the PXA under the microscope often prompts the diagnosis of a more malignant, aggressive tumor. The nuclei are quite large and multicontoured, with densely compacted chromatin. Despite the frightening appearance of the nuclei, accompanying mitotic activity is sparse or absent and necrosis is not seen. Other helpful histologic characteristics include fascicular patterning, lipidization of cells (hence the "xantho" prefix), and numerous areas of lymphocyte collections.

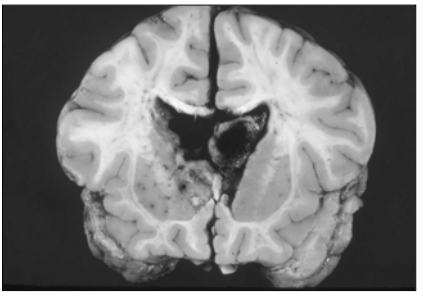

Figure 5. Coronal section of tuberous sclerosis brain with ventricular “candle gutterings” and SEGCA.

Although formerly considered as a curable astrocytic neoplasm, more recent

epidemiological studies have shown frequent recurrence and, sporadically, malignant degeneration. Nonetheless, most of the patients with PXA live for many years after the diagnosis is made.

2.4 Desmoplastic Cerebral Astrocytoma of Infancy (DCAI)

Very rare tumors of the first two years of life, few cases of DCAI have been reported to date. The tumor appears large and well-circumscribed, with a predilection for the superficial frontoparietal region. Histologically and perhaps histogenetically, the DCAI shares similarities with another desmoplastic neoplasm occurring in infancy, the desmoplastic infantile ganglioglioma (DIG). Some neuropathologists feel that the DCAI and the DIG may be variations of one type of neoplastic process.

The histologic hallmark of the DCAI is a dense desmoplasia, which can lend a mesenchymal appearance to the tumor. Its superficial location frequently leads to the mistaken diagnosis of meningioma, even though meningothelial tumors are quite uncommon in children. The DCAI may be quite hypercellular in some areas, suggesting a more anaplastic lesion than is actually the case. Striking positivity for glial fibrillary acidic protein confirms the glial nature of the lesion. The tumor shares an electron microscopic feature with normal subpial astrocytes: the presence of a basal lamina, which may provide clues to the tumor's histiogenesis.

Although follow-up data is limited, successful surgical resection may effect a fairly good prognosis.

2.5 Infiltrating Fibrillary Astrocytoma

The prognosis regarding infiltrating astrocytic tumors (WHO grade II) is vastly different from the pilocytic (WHO grade I) variety. Complete surgical resection is not possible, and there is currently no cure available for these tumors. They also commonly progress to more malignant lesions as time passes, via mechanisms that involve chromosomal modulation and signal in-duction, as well as chromosomal aberra-tions. Genetic studies of WHO grade II astrocytomas have revealed frequent loss of heterozygosity (LOH) of chromosome 17p, which contains the p53 tumor suppressor gene.

It is presumed that the majority of the low-grade astrocytomas are composed of fibrillary astrocytes. Protoplasmic astro-cytomas, presumably arising from proto-plasmic astrocytes, are quite rare and the biologic behavior of such tumors is unknown due to their paucity.

Fibrillary astrocytomas are most commonly located in the cerebral hemispheres of younger adults, and occasionally the brainstem and spinal cords of children. They lack many of the gross and histologic features of pilocytic astrocytomas, from which they must be distinguished. Imaging qualities of these tumors are also different from pilocytic astrocytomas, in that fibrillary astrocytomas are poorly defined, infiltrative, and generally do not enhance with intravenous contrast materials. Grossly, the neoplasms may be microcystic and appear well-circumscribed, but this sharp demarcation is misleading.

Most grading systems define fibrillary astrocytomas as mildly hypercellular astrocytic neoplasms with some pleomorphism, but lacking cellular features of anaplasia such as mitoses, endothelial proliferation, and necrosis (see Figure 6). Many of the cells lack obvious cytoplasm, giving the appearance of “bare nuclei.” This can sometimes

assist the neuropathologist in differentiating neoplastic astrocytes from reactive astrocytes, that is, "gliosis." Microcysts, containing proteinaceous fluid, may also be seen.

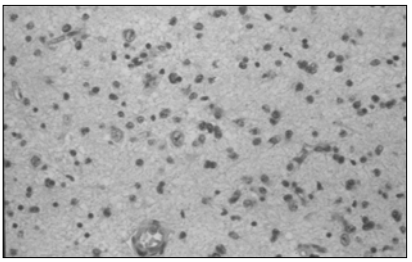

Figure 6. H&E appearance of WHO grade II astrocytoma.

The prognosis regarding fibrillary astrocytomas is not certain, as many past studies have included other astrocytic tumors without stratification, such as pilocytic astrocytomas, leading to inflated survival times. These tumors are not benign biologically, however, despite the histologic appearance of indolence. Several epidemiological surveys have determined median survival to be roughly 7 to 8 years, and rebiopsy of recurrent fibrillary astrocytomas frequently reveals anaplastic degeneration. Treatment of fibrillary astrocytomas is highly individualized, based on tumor location and the extent of surgical resection possible. Recent recognition that radiation therapy has a deleterious effect on cognitive function many years after the therapy is complete has caused many clinicians to withhold irradiation of fibrillary astrocytomas when possible, until such a time as malignant degeneration occurs.

2.6 Anaplastic Astrocytomas, WHO Grade III

It is generally accepted that anaplastic astrocytomas (AAs) may evolve from malignant transformation of fibrillary astrocytomas or arise de novo. Similar to the rest of the infiltrating astro-cytic tumors, AAs most frequently occur in the cerebral hemispheres, but unlike low-grade astro-cytomas, are more common in adults (see Figure 7). Radiographi-cally, the majority of AAs enhance with the adminis-tration of intra-venous contrast material.

Most grading systems delineate AAs as having hypercellularity, pleomo-rphism and hyperchroma-sia of the nuclei, mitotic figures, and frequent endothelial prolixferation (see Figure 8).

The newest WHO system states that the presence of endothelial proliferation, as well as the presence of necrosis obviates the diagnosis of AA, instead upgrading the tumor diagnosis to glioblastoma multiforme.

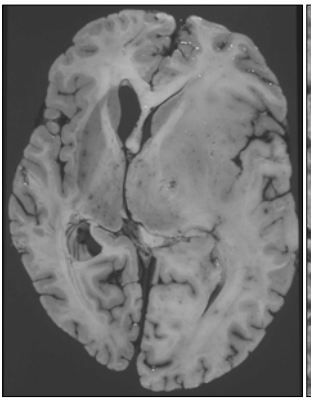

Figure 7. Gross appearance of anaplastic astrocytoma, WHO grade III.

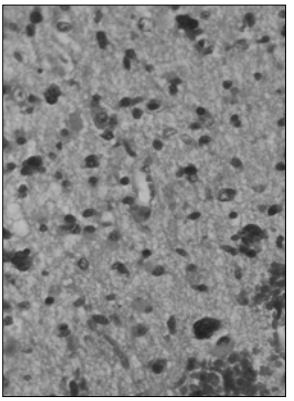

Figure 8. H&E appearance of a WHO grade III anaplastic astrocytoma.

AAs eventually all transform into glioblastomas, the most malignant glial tumor, likely because of the accumulation of acquired chromosomal defects. In addition to the 17p LOH frequently seen in grade II astrocytomas, many AAs also display mutations of chromosomes 22, 13 (retinoblastoma gene), 16p, 9q, and 19q.

Treatment of AAs generally involves radiation therapy, commonly with the addition of a chemotherapeutic agent. Despite treatment, average survival with AA is only roughly 2 to 3 years.

2.7 Gemistocytic Astrocytomas

Mention should be made here of a variant of astrocytoma commonly known as the gemistocytic astrocytoma. Most modern grading systems do not recognize this entity as a separate type of tumor, but rather assign it by histologic features into a specific grade of astrocytoma.

The majority of cells in the gemistocytic astrocytomas are, of course, gemistocytic ("gemistos": Greek = laden, full) astrocytes that contain abundant, glassy eosinophilic cytoplasm and hyperchromatic nuclei (see Figure 9). Most (but not all) of these tumors also show an elevated mitotic index, engendering a grade of anaplastic astrocytoma. In addition, epidemiological studies have revealed that gemistocytic astrocytomas have a very high incidence of transformation into glioblastomas, with estimates ranging around 80%.

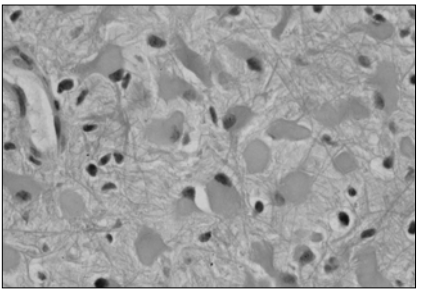

Figure 9. H&E appearance of gemistocytic astrocytoma.

2.8 Gliomatosis Cerebri

This fairly uncommon entity is a diffuse, infiltrative astrocytic neoplasm that generally encompasses one entire hemisphere or both hemispheres. Prior to the advent of MRI scanning, gliomatosis cerebri was rarely diagnosed, but the sensitivity of the scans of today show abnormal intensities, especially on T2-weighted images.

Despite the extensive infiltration of the neoplasm, the histology of the tumor cells is fairly benign, although scattered pleomorphic nuclei can be seen, and hyperchromasia is not uncommon (see Figure 10). Mitotic activity is negligible, though, and endothelial proliferation and necrosis are not present.

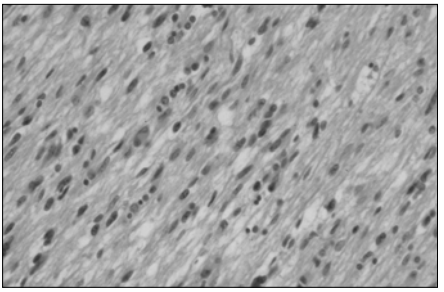

Figure 10. H&E appearance of gliomatosis cerebri.

2.9 Glioblastoma Multiforme

The glioblastoma multiforme (GBM) is the most malignant grade of astrocytic neoplasm. This is unfortunate, as it is also the most common malignant primary brain tumor in adults, though GBM does occasionally occur in children. Chiefly supratentorial, they may also be the result of transformation of a prior fibrillary astrocytoma or AA. It is also presumed that GBM may arise de novo, mostly from anecdotal observations.

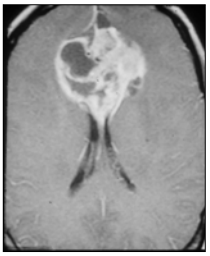

Figure 11. Enhanced MRI image of a glioblastoma ultiforme.

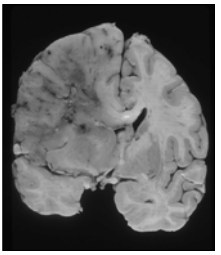

Figure 12. Gross appearance of a GBM. Note poorlydefined border and variegated appearance.

Radiographic images demonstrate an enhancing lesion surrounded by edema (see Figure 11). Frequently, the tumors cross the corpus callosum and spread into the opposite hemisphere, consequently earning the nickname of "butterfly glioma." Another common appearance on images is a ring-enhancing lesion, indistinguishable from a bacterial abscess. When the diagnosis of a presumed GBM is to be made by stereotactic biopsy, care must be directed to avoid the central portion inside the ring of enhancement: this is generally confluent necrosis, the lack of viability of which may result in nondiagnostic tissue.

Grossly, the GBM has a variegated appearance, thus the origin of the "multiforme" surname (see Figure 12). Red, tan, yellow, orange, and grey hues comprise various regions of the tumor, and necrosis is generally obvious. Multifocal regions of hemorrhage are commonly present. Although occasional GBMs appear to be grossly well-circumscribed, most are infiltrative when viewed through a microscope. Edema, imparting a yellowish softening to the nearby white matter, is often distributed throughout the affected hemisphere.

Histologically also, glioblastomas take on many different forms. Although most are diffusely infiltrative, occasional tumors have quite well-defined leading edges. The central regions of the tumor usually appear histologically more malignant than the periphery, drawing attention to the fact that biopsies far from the epicenter may not demonstrate all of the features of the central regions, and may result in a diagnosis of low-grade astrocytoma or AA. GBMs have all of the recognized correlates of central nervous system anaplasia: hypercellularity, nuclear pleomorphism and hyperchromasia, endothelial and vascular proliferation (see Figure 13), elevated mitotic index, and generally, multifocal necrosis. Multiple multinucleated, bizarre tumor giant cells can be seen in some of the neoplasms (see Figure 14).

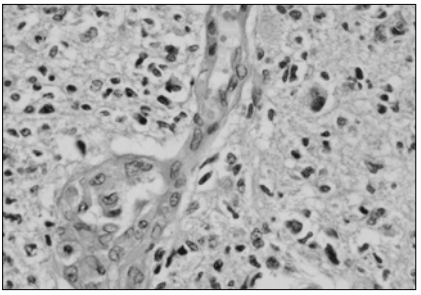

Figure 13. Vascular endothelial proliferation in a GBM (H&E).

Myxoid degeneration is not uncommon in some regions. Another

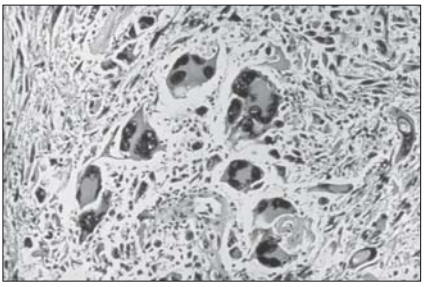

Figure 14. Tumor giant cells in a GBM (H&E).

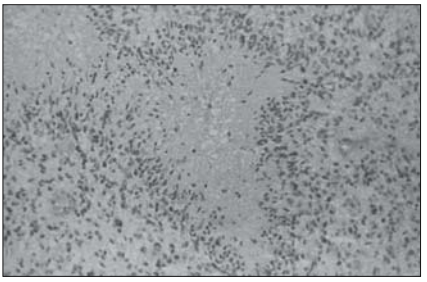

Figure 15. Pseudopalisading in GBM (H&E).

feature classically seen in, although not specific for GBMs, is pseudopalisading (see Figure 15). This involves clustering of cells around a central portion of necrosis and gives a serpiginous appearance at low-power.

Chromosomal abnormalities often accompany transition of AAs to GBMs. In addition to the aberrations in AAs, GBMs also frequently demonstrate LOH of chromosome 10 as well as amplification of the epidermal growth factor receptor (EGFR).

Treatment results are dismal, and despite radiation therapy and chemotherapy, mean survival with GBM is only about 12 months. Well-recognized poor prognostic risk factors include increased age at presentation, tumor biopsy as opposed to surgical resection, and a low preoperative Karnofsky rating (a scale designed to measure functional neurologic impairment).

2.10 Gliosarcoma

Although the treatment and prognosis of the gliosarcoma is no different than that of GBM, the histologic findings are somewhat different. The gliosarcoma shares a malignant glial component identical with GBM, but a separate neoplastic process (a "collision tumor," as it has been called) involves malignant transformation of mesenchymal elements.

Theories concerning the origin of this mesenchyme include erosion of the underlying GBM into the dura, causing a neoplastic alteration of dural tissue, or exuberance of endothelial proliferation such that it, too, becomes neoplastic.

Microscopically, the sarcomatous portion generally involves a spindle-cell proliferation in a herringbone pattern, but in other examples, greater disorganization is seen (see Figure 16). The diagnosis can be confirmed with stains more specific for the mesenchymal element, such as reticulin or trichrome.

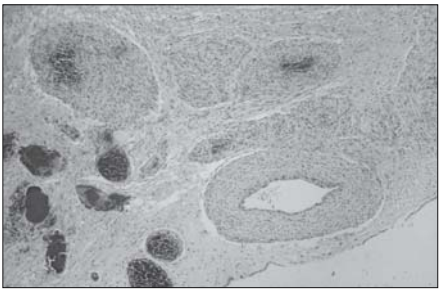

Figure 16. H&E appearance of a gliosarcoma.

3. OLIGODENDROGLIAL NEOPLASMS

Although far less common than astrocytic neoplasms, oligodendroglial neoplasms have attracted much attention recently due to the fairly new discovery that a significant proportion of these tumors are chemosensitive. Recent improvements in neuropathologic techniques, as well as recognition of the importance of shared experience, have improved the efficacy of the diagnosis of oligodendroglial tumors. The consequent result is an appearance that oligodendroglial neoplasms are becoming more prevalent, rather than that their recognition is occurring with greater frequency.

The WHO grading system assigns two grades to oligodendroglial tumors: II and III. WHO grade II tumors are oligodendrogliomas, while WHO grade III are anaplastic oligodendrogliomas.

3.1 Oligodendroglioma

More common in adults, oligodendrogliomas are found primarily in the cerebral hemispheres. They often impart a diffuse, wispy appearance to the white matter on MRI scans, and calcification is a common finding (see Figure 17).

Grossly, they can involve both white and grey matter, effacing the grey-white junction by their cortical infiltration (see Figure 18). They may appear fairly well-circumscribed or diffusely infiltrate normal structures.

The microscopic appearance of oligodendrogliomas is well-known for the “fried egg” appearance, which is an artifact (but fortunately a reproducible one) of tissue processing. Increased recent recognition of oligodendrogliomas without this classic appearance is contributing to their diagnostic efficacy (see Figure 19).

In oligodendrogliomas, the nuclei are small, round, and contain a stippled chromatin pattern. Also noteworthy is the delicate background capillary pattern, referred to as a “chicken-wire” pattern. The tumor's infiltration of the grey matter can give a striking pattern of “perineuronal satellitosis,” and, though not specific for oligodendrogliomas, is a helpful finding. Multifocal calcifications, often occurring in a “rind” around the tumor, are also useful. Columnar patterning is not uncommon and should cause the pathologist to at least favor an oligodendroglial rather than astrocytic lineage. Nonanaplastic

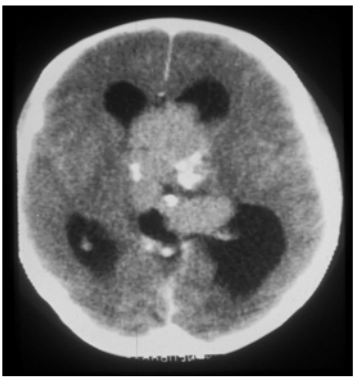

Figure 17. Enhanced CT appearance of an oligodendroglioma arising in the fornix. Calcification is prominent.

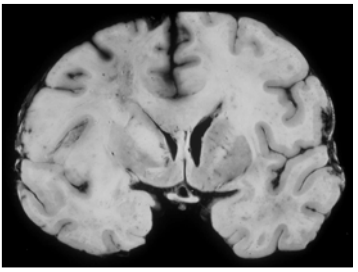

Figure 18. This oligodendroglioma has effaced the grey-white junction, enlarging the corpus callosum and internal capsule.

oligodendroglial tumor cells are usually GFAP negative with immunohistochemical staining.

Genetic abnormalities are quite different in oligodendrogliomas from gliomas of astrocytic lineage. A majority of grade II oligodendrogliomas display LOH of chromosomes 1p and 19q.

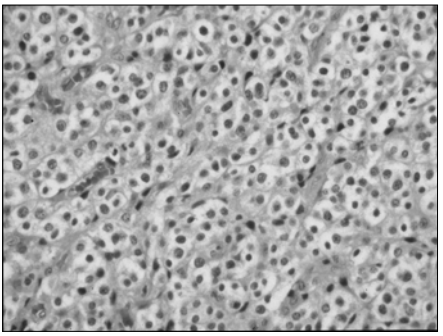

Figure 19. "Fried egg" appearance of an oligodendroglioma (H&E).

3.2 Anaplastic Oligodendroglioma

The majority of studies delineating chemosensitivity (and in some instances, radiosensitivity) in oligodendroglial tumors center around the treatment of WHO grade III malignant or anaplastic oligodendrogliomas (AO). These clinical trials have also involved research into the role of bone marrow transplantation in treatment of AO.

Grossly, anaplastic oligodendro-gliomas may appear indistinguishable from glioblastomas (see Figure 20).

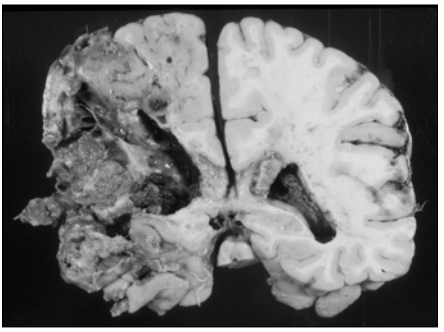

Figure 20. Gross appearance of an anaplastic oligodendroglioma.

It would seem that the sequential development of histologic alterations in oligodendroglial neoplasms mirrors their anaplastic progression: nuclear pleomorphism, hyperchromasia, increased mitoses, and the appearance of endothelial proliferation and necrosis (see Figure 21). As oligodendroglial neoplasms develop increasing anaplasia, the histologic features blend with astrocytic tumors. Although lower-grade oligodendrogliomas do not produce glial filaments (explaining their negative immunohistochemistry for glial fibrillary acidic protein), cells known as "minigemistocytes" begin to appear as these tumors develop more malignant characteristics (see Figure 22). Differentiated from gemistocytic astrocytes, minigemistocytes have rounded contours and few cellular processes. The nuclei are eccentric and the cytoplasm is generally more granular and may have a whorled appearance.

Eventually, loss of perinuclear haloes, and the development of pseudopalisading, make distinction from GBM quite difficult (and possibly theoretical). In instances such as this, most neuropathologists render a diagnosis of GBM, although frequently commenting on the tumor's possible origin from oligodendroglioma.

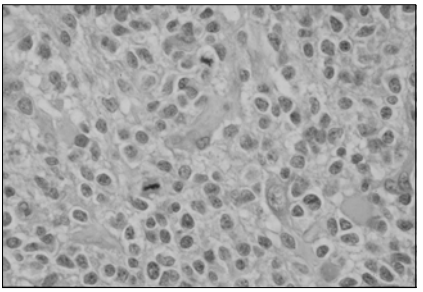

Figure 21. H&E appearance of an anaplastic oligodendroglioma: increased nuclear hyperchromasia, mitoses and vascular proliferation. Note that suggestions of perinuclear halos are still present.

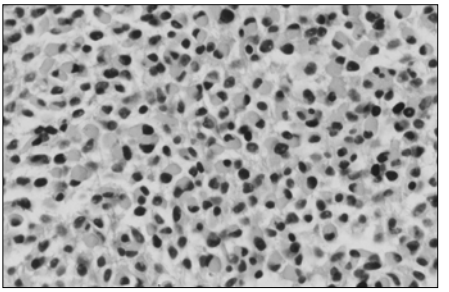

Figure 22. "Minigemistocytes" in an anaplastic oligodendroglioma. (H&E)

Although not curable by surgical resection, oligodendroglial tumors generally do respond well to radiation therapy, although, as mentioned with low-grade astrocytomas, fewer clinicians are willing to subject patients who may live another decade to tumor-treatment doses of cranial irradiation. A fairly recent discovery vital to the evolving treatment of anaplastic oligodendrogliomas involve their molecular genetics. As with grade II oligodendrogliomas, grade III AOs also often display LOH of 1p and 19q. Comparison of these genetic alterations with tumor response has revealed that AOs with 1p and 19q LOH are typically more sensitive to PCV chemotherapy (procarbazine, CCNU, and vincristine). Although still considered investigational findings, genetic analysis of oligodendroglial tumors will likely become routine in the future. With this increasing body of evidence that these tumors are chemotherapy-sensitive, chemotherapy may become the front line treatment, even in lower-grade oligodendroglial tumors.

3.3 Mixed Oligoastrocytomas

Although there is an abundance of controversy surrounding the very existence of mixed gliomas, most neuropathologists recognize these tumors as a separate diagnostic entity. To justify this diagnosis, tumors must have two clearly different cellular populations, one oligodendroglial and the other astrocytic. There is no consensus about the percentage the two cellular lineages comprise, but significant volumes of both should be present. Immunohistochemistry with GFAP may better enable evaluation of cellular components. The terms "mixed glioma" and "mixed oligoastrocytoma" and that both populations are histologically bland (WHO grade II), whereas "anaplastic mixed glioma" implies that one or both components appear malignant (WHO Grade III).

4. REFERENCES

1. Bigner DD, McLendon RE, Bruner JM, *Russell & Rubinstein's Pathology of Tumors of the Nervous System*, 6th ed., Oxford University Press, New York, 1998.
2. Burger PC, Scheithauer BW, *Tumors of the Central Nervous System,* Armed Forces of Institutes of Pathology, Washington DC, 1994.

3. Burger PC, Scheithauer BW, Vogel FS, *Surgical Pathology of the Nervous System and Its Coverings,* 4th ed., Churchill Livingston, New York, 2002.
4. Carbone DP, Oncogenes and tumor suppressor genes. *Hospital Practice (Office Edition)*, **28**(6), 145-8, 53-6, 61 (1993).
5. Harris CC, Hollstein M, Clinical implications of the p53 tumor-suppressor gene. *New England Journal of Medicine*, **329**(18), 1318-27 (1993).
6. Kleihues P, Cavenee WK. *Tumors of the Nervous System: World Health Organization Classification of Tumors: Pathology and Genetics*. Lyons, France: IARC Press, 2000.

CHAPTER 14
ODONTOGENIC TUMORS FOR GENERAL PATHOLOGISTS

Nasser Said-Al-Naief, D.D.S., M.S.*

1. INTRODUCTION

The process of tooth formation (odontogenesis) encompasses complex processes, which combine two principal phenomenons: cellular morphodifferentiation and histodifferentiation. Epithelial odontogenic tumors, in essence, recapitulate odontogenesis at various stages of development and are histologically related to remnants of odontogenic epithelium, left behind near the crown and root portions, following the cessation of this complex and detailed process. Theoretically, odontogenic tumors may develop from these rests or any of the cells that contributed to the process of odontogenesis.

Based on structural components and histomorphological features, odontogenic tumors will be separated into three categories: purely epithelial without mesenchymal component as well as mixed epithelial and mesenchymal tissue with or without hard tissue formation, and those that are derived from odontogenic mesenchyme with or without epithelium (see Table 1).[1] A summary of the clinicopathological and radiographical features of the various entities in each group are listed in tables 2-4.

2. ODONTOGENIC EPITHELIAL TUMORS WITHOUT ODONTOGENIC MESENCHYME

Table 2 summarizes the clinciopathologic features of odontogenic epithelium without odontogenic mesenchyme.

2.1 Ameloblastoma, Infiltrating (Solid)

Various histological subtypes of ameloblastoma have been described; almost 80% of those are of the infiltrating or the solid type.[2] The rest occur as unicystic or peripheral.[3] The solid ameloblastoma is typically a slow growing, usually asymptomatic tumor which may possibly attain large sizes. The two predominant histologic patterns seen are the follicular and plexiform patterns with well-defined nests or follicles seen in the first,

* Assistant Professor, Department of Pathology, University of Alabama, Birmingham, AL.

Table 1. WHO Classification of Benign Odontogenic Tumors (Modified from Ref. 1)

Odontogenic epithelium without odontogenic mesenchyme	Odontogenic epithelium with odontogenic mesenchyme ± hard tissue
Ameloblastoma	Ameloblastic fibroma
Squamous odontogenic tumor (SOT)	Ameloblastic fibroodontoma
Calcifying epithelial odontogenic tumor (CEOT)	Odontoameloblastoma
	Adenomatoid odontogenic tumor
Odontogenic mesenchyme ± odontogenic epithelium	Calcifying odontogenic cyst/odontogenic ghost cell tumor
Odontogenic fibroma	Odontoma
Odontogenic myxoma/fibromyxoma	
Benign cementoblastoma	

while interconnecting sheets, strips or islands of cells are seen in the second (see Figure 1). Both patterns show the same basic cytology, namely palisaded peripheral columnar cells that exhibit reverse nuclear polarization with subnuclear vacuolization and central loose, stellate reticulum-like cells, simulating these seen in the developing enamel organ. Nuclei are uniform and lack pleomorphism or atypia (see Figure 2). Mitoses are not a common feature, and should be a worrisome sign if encountered.[2] Cysts may also be encountered within the follicles. The term "acanthomatous ameloblastoma" is used when squamous metaplasia and or keratinization occurs within the islands of either type (see Figure 3). Other patterns may also be seen include granular cell, basaloid, and keratoameloblastoma[2] and the latter is a very rare variant with only few cases reported.[4-8] In the granular cell pattern, large-cells with granular pink cytoplasm are identified within the stellate reticulum[9-11] and these cells are characterized by numerous lysosomes when examined by electron microscopy.[12,13] The basaloid pattern of ameloblastoma shows small epithelial islands and do not tend to display well-developed stellate-reticulum-type cells as seen in other variations. Additionally, cells in the periphery of the follicle are cuboidal rather than columnar and may be slightly hyperchromatic.[14] It is generally agreed upon that various patterns have no prognostic indications and the importance of

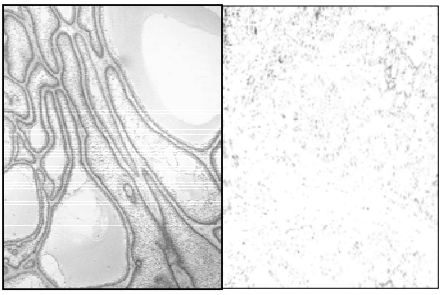

Figure 1. Left: Ameloblastoma, follicular pattern. Islands and nests of ameloblastic epithelium. Note the columnar, palisaded peripheral layer with peripheral vacuolization and the loose, stellate reticulum-like center. Right: Ameloblastoma, plexiform pattern. Interconnected cords of ameloblastic epithelium with identical cytological features to the follicular variant. (H&E)

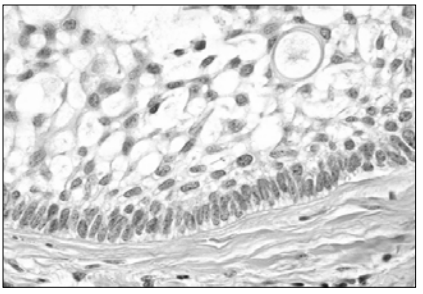

Figure 2. Ameloblastoma: High magnification showing a portion of follicle, rimmed by palisaded, columnar cells exhibiting reverse nuclear polarity, and vacuolization. Loose spindle- to stellate-shaped cells (stellate reticulum-like cells) are present in the center of the follicle. (H&E)

Table 2. Summary of clinicoradiographical features of odontogenic epithelial tumors without odontogenic mesenchyme

Entities	Age and Gender	Location	Radiographic features	Treatment / prognosis
Ameloblastoma, solid	2nd–4th decades / M = F	Posterior mandible >>> maxilla > other	MLRL* > ULRL†, root resorption is uncommon but possible	Depending on extent of disease, marginal resection or hemi-mandibulectomy/hemimanxillexctomy with prolonged follow-up due to high recurrence rate
Ameloblastoma, unicystic	≤ 2nd decade / M > F?	Pericoronal RL‡ in posterior mandible >>> other	ULRL in pericoronal location > well-defined ULRL	Depending on histology: Enucleation or local resection with follow-up-recurrence rate is much lesser than the solid type
Squamous odontogenic tumor (SOT)	Wide age range, young to old / M = F	Anterior maxilla and posterior mandible	Ill-defined or well-defined RL in lateral or interradicular position.	Conservative local excision or curettage; maxillary lesions may be more aggressive > mandibular lesions.
Calcifying epithelial odontogenic tumor (CEOT)	Wide age range (3rd to 5th decade ± M = F	Posterior mandible >>>> maxilla	MLRL > ULRL ± RO§, may also occur in pericoronal location	Conservative local resection reduces recurrence when compared to curettage; maxillary lesions may be more aggressive.

* MLRL: Multilocular radiolucency.
† ULRL: Unilocular radiolucency.
‡ RL: Radiolucency.
§ RO: Radioopacity.

recognizing various patters primarily focuses on the recognition of the tumor and proper treatment and follow up.

One histological variant, the desmoplastic ameloblastoma, deserves special attention and recognition [2,6,15-19] primarily because (1) it has different clinopathological features from the other subtypes with the tendency to involve Asian females (especially those who are Malaysian and Chinese); (2) radiographically, this subtype appears as ill-defined, unilocular or multilocular, radiolucent/ radioopaque lesions which can be easily mistaken for benign fibro-osseous lesions, rather than an ameloblastoma; and (3) curettage of the infiltrating type may result in a high recurrence rate. Therefore, these tumors are best removed with adequate margins of 1 cm of surrounding normal marginal bone to minimize recurrence, and en bloc resection is the usual treatment of choice. Additionally, patients with ameloblastoma have to be followed for many years because recurrence may be seen years after initial surgery.

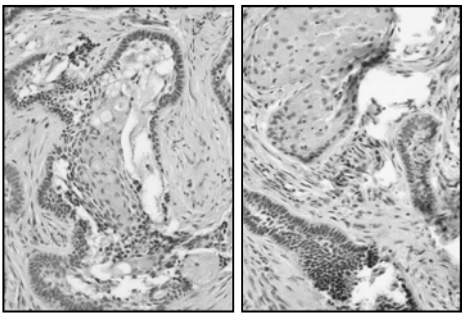

Figure 3. Left: Acanthomatous variant of ameloblastoma. Squamous metaplasia with keratinization is observed within the ameloblastic island. Also note the cystic change at one side of the follicle, which is a frequent finding in ameloblastoma. Right: Granular cell change may also be seen in ameloblastoma, and this corresponds to abundance of lysosomes. (H&E)

Desmoplastic ameloblastoma involves both jaws with equal frequency. Histologically, the lesion is characterized by mature, dense, fibrous tissue stroma with scattered compressed ameloblastic islands, giving an impression of compressed epithelial cords. Hyalinization surrounding the compressed ameloblastic islands, and occasional osteoid production, may also be seen.[2,6,17-19]

2.2 Unicystic Ameloblastoma

Unicystic ameloblastoma is an important clinicopathological form of ameloblastoma that should be recognized and separated from conventional, solid infiltrating ameloblastoma.[20-24] It occurs on an average of one decade earlier than the solid counterpart. Radiographically, it presents as a unilocular radiolucency, more frequently encountered in pericoronal location (associated with an impacted tooth).

Histologically, a cyst lined with a ameloblastic epithelium is seen, with a palisaded, columnar basal layer that exhibits reverse nuclear polarity and vacuolization (see Figure 4). An important histologic feature was described in this lesion in 1970 by Vickers and Gorlin; was the presence of ameloblastic features, limited to cystic lining, with hyperchromatic nuclei, widened parabasalar intercellular spaces and a discrete zone of subepithelial hyalinization in the presence of a thickened or reduplicated basal lamina.[24] The latter is referred to as “inductive effect” while, in reality, this phenomenon may not reflect such effect, because, as with the conventional type, hard tissue formation including tooth structure is not a feature of ameloblastoma.[3] When ameloblastomatous changes are confined in the lining (cystic) epithelium, it is referred to as unicystic ameloblastoma. Occasionally the epithelium may proliferate and protrude into the cystic

lumen as a mass or infiltrate into the cystic wall and then will be referred to as "luminal ameloblastoma" and "mural ameloblastoma," respectively. Recognition of the latter subtype (which can assume a follicular, plexiform, or mixed pattern) is especially important because the neoplasm will be managed similarly to the conventional ameloblastoma by thorough curettage or local resection, while the unicystic luminal or intraluminal forms may be treated by simple enucleation with careful follow-up, similar to dentigerous cyst (an odontogenic cyst seen in a pericoronal position to an impacted tooth).[3] The overall recurrence rate of unicystic ameloblastoma is estimated to be 10–25%.[21, 22, 25-27]

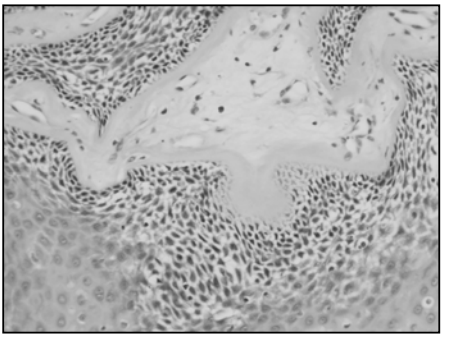

Figure 4. Unicystic ameloblastoma. Developed in the lining of a dentigerous cyst (surrounds the crown of an impacted tooth). Note the subepithelial hyalinization present, which should alert the pathologist to the possibility of the presence a developing unicystic ameloblastoma.. (H&E)

2.3 Peripheral Ameloblastoma

The peripheral or soft tissue counterpart of the central tumor is a rare entity, usually presenting as a swelling or a soft surface mass involving the gingiva, or less commonly elsewhere in the oral cavity.[28-33] The variation in locations of peripheral ameloblastoma confirms its potential derivation from remnants of the dental lamina in a supraperiosteal location or the surface epithelial basal layer as a possible site of origin as well. Histological documentation of surface epithelial origin with extension toward the connective tissue is necessary to render the diagnosis of an otherwise histologically typical ameloblastoma. The lesion does not exhibit aggressive behavior and usually does not invade underlying bone. Recurrence is infrequent after local excision.[33] Malignant examples have been also reported but considered rare.[31, 32]

2.4 Malignant Ameloblastoma

Controversy exists regarding the classification of malignant ameloblastoma. In the 1992 WHO classification,[1] malignant ameloblastoma is defined as a neoplasm where the pattern of an otherwise typical ameloblastoma is seen in both the primary tumor and the metastatic disease, with the majority of these tumors metastasizing to the lungs, cervical lymph nodes, and spine,[3] while ameloblastic carcinoma indicates cytologically malignant tumors in both primary and metastatic disease including an increased nuclear-to-cytoplasm ratio, hyperchromasia, abundant mitosis, and necrosis.[3,34] Ameloblastic carcinoma may also be grouped in the broad category of malignant odontogenic lesions: "odontogenic carcinoma" which encompasses primary intraosseous carcinoma, malignant variants of other odontogenic epithelial tumors, and malignant transformation in preexisting odontogenic cysts. Treatment includes conservative and aggressive methods depending on size, location, and extent of disease.[3]

2.5 Squamous Odontogenic Tumor (SOT)

SOT is a benign neoplasm or hamartoma, derived from the epithelial rests of Malassez of the periodontal membrane. Clinically, the lesions causes localized loosening of teeth, mimicking periodontal disease. Maxillary lesions tend to be more aggressive than their mandibular counterparts.[35] Radiographically, the lesion shows well-defined radiolucency within the alveolar bone; margins tend to be well-corticated. Microscopically, bland squamous epithelial islands or anastomosing strands surrounded by mature fibrous connective tissue with moderate vascularity is seen. The islands lack the central stellate reticulum pattern, the peripheral columnar cell palisading, and any other features reminiscent of ameloblastoma. Islands are not atypical and have well-defined intercellular bridges.[36-38] Spherical, PAS (periodic acid Schiff) positive eosinophilic masses may be observed. Odontogenic cysts of inflammatory or developmental origin may also contain proliferations of cells which have been referred to as SOT-like proliferation.[39]

2.6 Calcifying Epithelial Odontogenic Tumor (CEOT)

CEOT is a benign epithelial odontogenic tumor that shares several clinical features with ameloblastoma, including site, radiographic appearance, and possibly age distribution.[40,41] It may be seen in a wide age distribution ranging from 8 to 80. More tumors are found in the posterior mandible than in the maxilla.[2] Generally, a poorly defined multilocular radiolucency with variably sized radio-opaque flecks is seen on radiographic examination. CEOT may or may not be associated with an impacted tooth, and smaller tumors may appear unilocular on radiographs, mimicking simple inflammatory cysts. Histologically, sheets of polyhedral epithelial cells displaying intercellular bridges with abundant eosinophilic cytoplasm are seen. Nuclei vary in size and multiple nuclei are not unusual (see Figure 5). Additionally, cells may exhibit pleomorphism which may be significant enough to cause concern for pathologists. However, the absence of mitoses and necrosis without inflammation can help establish the correct diagnosis. Additionally, the presence of so-called Liesegang ring-type calcifications (well-demarcated, concentric-appearing calcifications) within the tumor cells and amyloid-like material within the tumor cells are considered helpful diagnostic clues to establish the diagnosis.[41, 42] (see Figure 6). CEOT may show a clear-cell-predominant pattern where the clear cells stain positive for glycogen and negative for mucin, and this pattern has been associated with a high rate of recurrence and has been also described in the presence of histologic perineural invasion.[41,43] CEOT is generally managed surgically, preferably with conservative resection with about 1 cm of microscopically clear margins. Although clinically, they are considered less aggressive than ameloblastoma, an

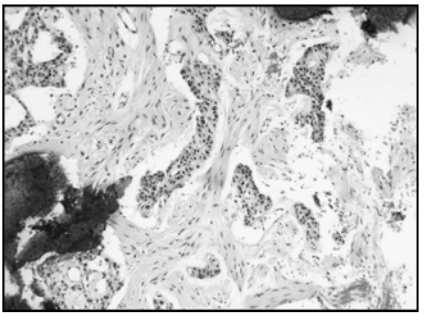

Figure 5. CEOT. Islands and strands of polyhedral epithelial cells are noted and often exhibit cytologic atypia. A hint of cribriform pattern may also be seen. (H&E)

Table 3. Summary of clinicoradiographical features of odontogenic epithelial tumors with odontogenic mesenchyme

Name	Age and Gender	Location	Radiographic features	Treatment and prognosis
Ameloblastic fibroma	2nd decade/ M > F	Posterior mandible > other	UL* or ML†	Enucleation / curettage, recurrence is unusual (important to follow-up)
Ameloblastic fibro-odontoma	1stdecade ± / M = F	Posterior mandible >> other	UL (RL‡ + RO§) > ML, overlying an unerupted molar	Enucleation / curettage , recurrence is unusual (important to follow-up)
Adenomatoid odontogenic tumor	1st-2nd decades / F > M	Maxilla >> mandible	UL pericoronal RL (+ RO) > other	Enucleation with rare or no recurrence
Calcifying epithelial odontogenic tumor.	Wide age arrange, Ave = 4th decades / M = F?	Posterior mandible >> maxilla	ML (RL + RO) >> UL RL	Conservative excision will minimize recurrence potential when compared to simple curettage
Odontoma	1st and 2nd decades	Maxilla > mandible	RO + RL	Simple, conservative excision with no recurrence

* UL: Unilocular.
† ML: Multilocular.
‡ RL: Radiolucency.
§ RO: Radioopacity.

overall recurrence rate of 14% after as long as 10 years of follow-up was noted by Franklin and Pindborg. [41] Patients should be closely monitored for recurrence.

3. ODONTOGENIC EPITHELIAL TUMORS WITH ODONTOGENIC MESENCHYME ± HARD TISSUE

This group comprises interesting and diverse lesions that range from true neoplasms to hamartomatous growths in biologic behavior (see Table 3). It is referred to as "mixed" reflecting the epithelial and mesenchymal derivation of these tumors.[44-46] The mixed odontogenic tumors have been studied as a group for many years.[45] Earlier investigations implied that ameloblastic fibroma eventually matures into ameloblastic fibro-odontoma which in tern fully matures to an odontoma, an idea that was soon after rejected based on histological and clinicopathological features and demographics that did not back-up such concept.[44, 46]

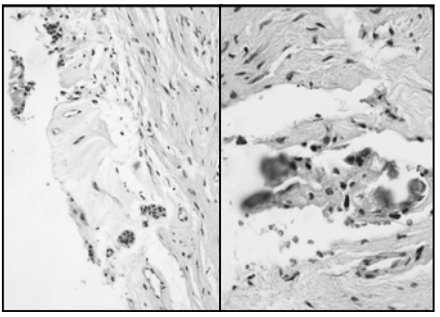

Figure 6. CEOT. Left: Amyloid-like eosinophilic material is present, surrounding the epithelial nests. Right: Amyloid-like eosinophilic material and calcification are identified. (H&E)

3.1 Ameloblastic Fibroma

This true odontogenic neoplasm (derived from odontogenic epithelial and mesenchymal tissues) is more frequently seen in the mandible than in the maxilla, has slight male predilection, and quite frequently is discovered following the investigation of a lesion preventing the eruption of, or displacing, the mandibular first molar. It occurs primarily in the mandibular second primary molar-permanent first molar or the second premolar-first molar areas. Histologically, this neoplasm is characterized by cords, strands, or nests of odontogenic epithelium with very scanty cytoplasm and basophilic nuclei, supported by a mass of dental papilla-like tissue that contains epithelium resembling the dental lamina during odontogenesis. The papilla-like tissue is composed of spindle- or stellate-shaped cells with a loose, myxomatous background (see Figure 7).[3] Mitoses are rare to nonexistent and—if increased mitotic figures a detected in the spindle cell components (mesenchymal element), along with nuclear atypia, anaplasia, and necrosis, especially when present in the setting of a recurrent lesion—should make the pathologist suspicious for a sarcomatous transformation of the mesenchymal components, and the development of ameloblastic fibrosarcoma.[47,48] Curettage is the treatment of choice, and is considered curative. Recurrence is uncommon, although it has been reported.[49]

3.2 Ameloblastic Fibro-Odontoma (AFO)

Similar to ameloblastic fibroma, this lesion is also composed of odontogenic epithelium and mesenchyme, with the addition of dental hard tissue formation (dentin

and enamel matrix).[50] As previously mentioned, this should not be considered a lesion that starts as an ameloblastic fibroma that would ultimately differentiate into, mature to, or even arise in an odontoma, but should be rather considered as a separate, but related, tumor that shows lesser or greater degrees of differentiation relative to the stage of tooth formation. They do though exhibit similarity to ameloblastic fibroma by presenting as a painless mass that may or may not cause swelling, displacement of teeth, or prevention of eruption of a permanent tooth. It tends to show prevelance for males.[51] Radiographically, AFO presents as a radiolucent lesion with radio-opaque flecks representing hard tissue formation. Histologically, it shows cords, strands, and nests of odontogenic epithelium, present in a delicate, noncollagenized, myxomatous matrix (resembling ameloblastic fibroma but with the addition of dentin or dentinoid or enamel material). This neoplasm is best treated with thorough curettage if possible, or by surgical excision and it does not have a great tendency for recurrence if inadequately removed. Large, grossly disfiguring tumors have been sporadically reported.[50]

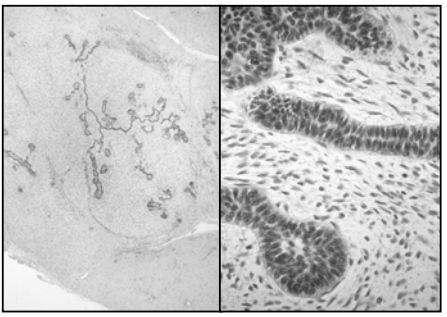

Figure 7. Ameloblastic fibroma: Low-(left) and power high-(right) photomicrographs showing strands and islands of odontogenic ameloblastic epithelium with a stellate reticulum-like area, surrounded by cellular dental papilla-like tissue. (H&E)

3.3 Odontoma

Odontoma represents the most highly differentiated of the mixed odontogenic tumors group, to a degree that is considered as hamartoma by most authorities. It is considered by far the most common odontogenic tumor.[49,52] Two variants have been recognized, the complex and the compound.[49,53] The complex type occurs most often in the posterior segments of the jaws, primarily in association with impacted third molar teeth. The mean age at diagnosis is in the early third decade.[53,54] The compound odontoma is composed of many, miniature teeth surrounded by a dental follicle, the same tissue that surrounds the normal developing tooth. It shows the highest degree of histo- and morphodifferentiation among all odontogenic tumors. Although the teeth may be morphologically abnormal, histologically normal enamel and dentin tissue is seen, as compared to complex odontoma where an admixture of mature dental hard tissue is seen, less recognizable as teeth, thus representing ultimate histo- but not morphodifferentiation (see Figure 8). Complex odontoma shows a predilection for posterior mandibular occurrence while the compound subtype is more often found in the anterior segments of the jaws (see Figure 9).[49] Regardless of type, surgical excision is the treatment of choice with excellent prognosis. Odontomas may occasionally exist in association with various, other odontogenic tumors and cysts including the coexistence with ameloblastoma or the so-called odonto-ameloblastoma.

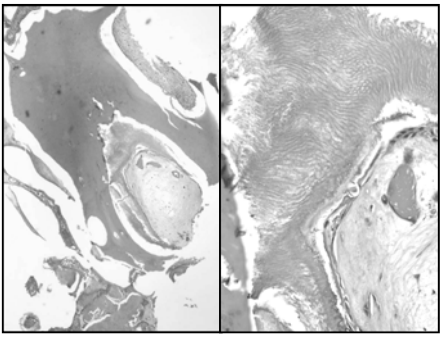

Figure 8. Odontoma. Left: Histologically resembles a fully developed tooth. The term "compound odontoma" is used when tissue layers are organized to resemble a fully formed tooth. Right: Decalcified enamel layer appearing as empty rods. A small portion of dentin is identified in the top left-hand corner. (H&E)

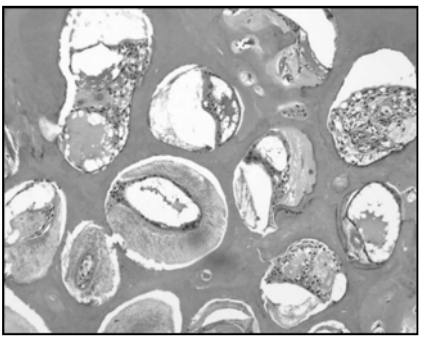

Figure 9. Complex odontoma. Tumor is composed of haphazardly arranged mass of tooth structures. (H&E)

3.4 Odonto-Ameloblastoma

This is a very rare odontogenic tumor with a predominantly mandibular occurrence and involving young individuals.[55] Radiographically, it is characterized by a large, expansile radiolucency with radioopaque masses that represent odontomas of either histological subtype (see odontoma above). Microscopically, odonto-ameloblastoma is characterized by typical areas of ameloblastoma in addition to dentin, enamel matrix, dental papilla, or dental pulp. Root formation may be also present, depending on the extent of differentiation of the dental structures. This tumor is best managed as an ameloblastoma curettage may lead to multiple recurrences.[3,56]

3.5 Adenomatoid Odontogenic Tumor (AOT)

AOT is an uncommon benign odontogenic tumor of epithelial origin that exhibits an inductive effect on adjacent mesenchymal tissue which results in the formation of amyloid-like material.[1] Although this lesion has been labeled as true neoplasm of the jaw in the past, more recently, some authors have reportedly classified it as a hamartoma.[2] Intraosseous and much less common peripheral variants have been recognized. The origin of AOT remains controversial. The central lesion may originate from the postsecretory ameloblasts subsequent to amelogenesis, or the stratum intermedium, or the inner enamel epithelium of the developing enamel organ, at the preameloblastic stage.[3,57] Additionally, the basal cell layer of the overlying surface epithelium may also be the source of this lesion.[58] AOT is predominantly found in teenagers, with a known female predilection. Additionally, there may be a racial predilection favoring Asians and blacks.[59] AOT also has prevalence for the anterior maxilla.[2] In most cases, the lesions appear as unilocular radiolucency pericoronal to an impacted canine with possible radio-opaque flecks detected within the lesions.[60] Microscopically, AOT is a well-encapsulated tumor that shows tapered, needle-like, spindle cells and polyhedral cells arranged in aggregates with an overall swirling or nodular pattern (see Figure 10). These cells are juxtaposed to

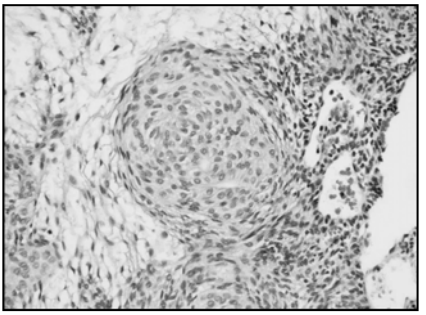

Figure 10. AOT. Tumor cells are arranged into nesting and whorled patterns. (H&E)

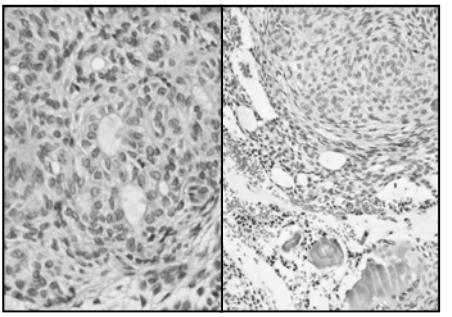

Figure 11. AOT. Duct-like structures and small cystic spaces and calcification are also characteristic of AOT. (H&E)

cystic or glandular (duct-like) spaces lined by cuboidal and columnar cells. Both features combined are characteristic of AOT (see Figure 11).[61] Homogenous, amphophilic staining PAS-positive, diastase resistant material, with calcifications, may be seen and thought to represent amyloid-like or enamel proteins,[1,62,63] which have been found to exhibit histochemical qualities of enamel matrix material.[60] AOT is best managed by enucleation or conservative excision with extremely low recurrence potential.[64]

3.6 Calcifying Odontogenic Cyst and Odontogenic Ghost Cell Tumor

Calcifying odontogenic cyst (COC) is an uncommon developmental odontogenic cyst which can occur as an intraosseous or extraosseous lesion, with the first definitely predominant. This lesion display features of a cyst and solid neoplasms.[65,66] Histologically, COC resembles, to a large extent, ameloblastoma, having similar proliferative epithelial histology, however, with the addition of ghost cells and intraepithelial calcifications, resembling "Pilomatrixoma" of the skin.[67] Odontogenic ghost cell tumor is a rare, locally aggressive odontogenic neoplasm arising from preexisting calcifying odontogenic cysts or in a de novo relationship. Clinically, this lesion is seen over a wide age range and usually presents in an intraosseous location. It may also present as a nonhealing extraction site,[68] an expansile jaw lesion,[69] an ulcerative mass, and as a painful or asymptomatic swelling.[70] Radiographically, it displays an irregular and destructive variably mixed radiolucent/radio-opaque lesion that may cross the midline and may possibly infiltrate surrounding tissues like the maxillary and ethmoid sinuses.[68,69] Microscopically, an odontogenic ghost cell tumor contains an epithelial component that resembles ameloblastoma occurring in association with a calcifying odontogenic cyst, with the addition of pale-staining ghost cells. Some of the latter contain dystrophic mineralization. Focal or diffuse cytological atypia may also be noted. Additionally, the epithelial component is characterized by the presence of large, pleomorphic, polygonal cells with central vesicular to hyperchromatic nuclei. Dentinoid material may also be present. It is best managed by resection with wide margins. Partial maxillectomy or mandibulectomy with evaluation for metastatic disease is advised, because metastases have been documented.[69]

4. MESENCHYMAL TUMORS

Table 4 summarizes the clinical and radiographic features of two commonly encountered mesenchymal tumors of odontogenic origin, namely, odontogenic myxoma and cementoblastoma.

Table 4. Summary of clinicoradiographic features of mesenchymal tumors

Name	Age and gender	Location	Radiographic features	Treatment and prognosis
Odontogenic myxoma	2nd-3rd decades/M = F	Mandible>maxilla	UL* or ML† with possible tooth resorption	Curettage or resection
Cementoblastoma	2nd decade or younger/ M = F?	Posterior mandible >> other	RO‡ mass fused to roots, surrounded by RL§ rim.	Surgical extraction of tooth and mass, no recurrence

* UL: Unilocular.
† ML: Multilocular
‡ RO: Radioopacity.
§ RL: Radiolucency.

4.1 Odontogenic Myxoma

This is a relatively uncommon odontogenic tumor of mesenchymal/ ectomesenchymal origin,[49] which is derived from undifferentiated odontogenic mesenchyme of the dental papilla of the developing tooth.[3] Investigations have demonstrated that this tumor originates from fibroblasts, histiocytes, or myofibroblasts.[71] Odontogenic myxomas are known for a high rate of recurrence and tend to involve younger individuals in the second or third decade of life. They most frequently involve tooth-bearing areas of the mandible and maxilla, usually asymptomatic and typically considered to be slow-growing neoplasms. Radiographically, they present as unilocular or multilocular radiolucencies with an ill-defined or well-defined sclerotic margins.[72,73] Microscopically, they are similar to soft tissue myxomas, showing uniformly distributed, loosely arranged bipolar and stellate cells, supported by a myxoid to slightly fibrous stroma (see Figure 12).[71,74] Most cells are slender and elongated with branching cytoplasmic processes extending away from centrally placed nuclei. Nests of odontogenic epithelium may or may not be

Figure 12. Odontogenic myxoma. Low-power image showing stellate and spindle cells, embedded in myxoid stroma. Insert: High-power showing stellate and spindle cells, embedded in myxoid stroma. (H&E)

present in varying amounts but are not characteristic of this lesion. Nuclei tend to be round when cut in cross-sections or spindled and fusiform if cut in longitudinal sections.[71,73-76] The stroma is rich in acid mucopolysaccharides, particularly chondroitin sulfate and hyaluronic acid.[71] Kim and Ellis have emphasized the importance of differentiating a true myxoma from a dental follicle with myxoid changes with further important implications on management modalities.[77] The myxomatous dental follicle is generally more highly collagenized than the myxoma and has lining odontogenic epithelium, odontogenic epithelial rests, and, often, foci of calcification. A myxoid component within follicular tissue is present in about 75% of cases; however, the myxoid changes are focally observed, rather than uniform and diffuse as seen in the myxoma.[77] Odontogenic myxomas are nonencapsulated and gelatinous in nature, which influences treatment and prognosis. Smaller lesions may be curetted, while larger lesions, especially those with ill-defined radiographic margins, may require local resection. Large, multilocular, and expansile lesions should be treated with en bloc resection.[78]

4.2 Cementoblastoma

Cementoblastoma is a rare benign neoplasm of cementoblastic origin occurring in juxtaposition to the roots of the teeth. Most lesions are found within the mandible, usually within the posterior segment of the alveolus. A slight female predilection has been noted.[79] In most cases, pain is the presenting feature. Lesions may be seen in relationship to erupted permanent teeth, although involvement of unerupted teeth has been also reported.[3] The lesion shows characteristic radiographic features, namely, a large radio-opaque mass, fused to the root(s) of the tooth, with a radiolucent halo identified encircling the mass. The halo is in continuation with the periodontal ligament of the tooth. Pathologic findings characteristically show dense masses of cementum-like tissue with prominent basophilic lines, irregular lacunae, and cellular fibrovascular stroma (see Figure 13). Attenuated, cellular fibrous connective tissue margins are present, corresponding to the radiolucent rim seen radiographically (see Figure 14). Plump

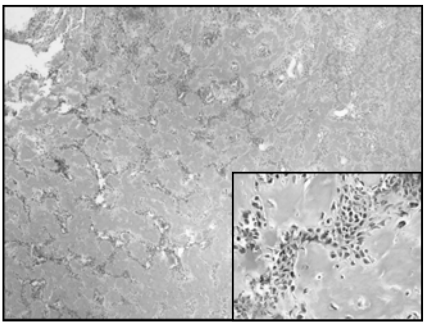

Figure 13. Cementoblastoma. Low-power image showing dense mass of cementum tissue. This mass fuses to the root of teeth. Insert: High-power magnification revealing the presence of prominent cementoblastic rimming, characteristic of this lesion Note the high resemblance to osteoblastoma of bone. (H&E)

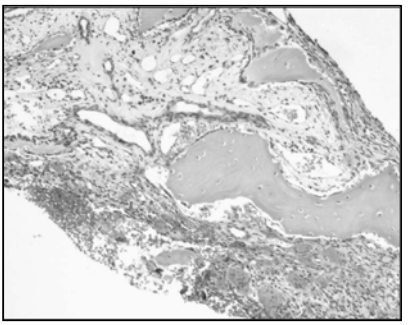

Figure 14. Cementoblastoma. At the periphery of the lesion, an increase in vascularity is seen. Additionally, an increase in the number of giant cells is also noted where the mass fuses with the roots of teeth. (H&E0

cementoblasts, often with plasmacytoid features, surround the calcified tissue in a linear pattern. Cementocytes within the lacunae are also large, but smaller than the marginally located cementoblasts.[80] Histologically, there is a close relationship between cementoblastoma, osteoblastoma, and osteoid osteomas.[81,82] Radiographic examinations are necessary because fusion with the root may differentiate one from the other.

5. ACKNOWLEDGEMENT

The author would like to express thanks to both Mrs. Vanessa Pickens and Mrs. Noelle Le Lievre for their secretarial support.

6. REFERENCES

1. Kramer IR, Pindborg JJ, Shear M, *Histologic Typing of Odontogenic Tumors* (Springer-Verlag, Berlin, 1992).
2. Melrose RJ, Benign epithelial odontogenic tumors. *Seminars in Diagnostic Pathology*, **16**(4), 271-87 (1999).
3. Sciubba JJ, Fantasia JE, Kahn LB, *Tumors and Cysts of the Jaws* (Armed Forces Institute of Pathology, Washington, DC, 2001).
4. Takeda Y, Satoh M, Nakamura S, Ohya T, Keratoameloblastoma with unique histological architecture: an undescribed variation of ameloblastoma. *Virchows Archiv*, **439**(4), 593-6 (2001).
5. Said-al-Naief NA, Lumerman H, Ramer M, et al., Keratoameloblastoma of the maxilla: a case report and review of the literature. *Oral Surgery, Oral Medicine, Oral Pathology, Oral Radiology, and Endodontics*, **84**(5), 535-9 (1997).
6. Raubenheimer EJ, van Heerden WF, Noffke CE, Infrequent clinicopathological findings in 108 ameloblastomas. *Journal of Oral Pathology and Medicine*, **24**(5), 227-32 (1995).
7. Norval EJ, Thompson IO, van Wyk CW, An unusual variant of keratoameloblastoma. *Journal of Oral Pathology and Medicine*, **23**(10), 465-7 (1994).
8. Altini M, Lurie R, Shear M, A case report of keratoameloblastoma. *International Journal of Oral Surgery*, **5**(5), 245-9 (1976).
9. Nasu M, Takagi M, Yamamoto H, Ultrastructural and histochemical studies of granular-cell ameloblastoma. *Journal of Oral Pathology*, **13**(4), 448-56 (1984).
10. Ide F, Shimoyama T, Horie N, Basaloid squamous cell carcinoma versus basal cell ameloblastoma.[comment]. *Oral Oncology*, **34**(2), 154-5 (1998).
11. Hartman KS, Granular-cell ameloblastoma. *Oral Surgery, Oral Medicine, Oral Pathology*, **38**(2), 241-53 (1974).
12. Brocheriou C, Hauw JJ, Auriol M, Guilbert F, Cernea P, Chomette G, [Ultrastructural study of 6 cases of ameloblastoma]. *Annales d Anatomie Pathologique*, **20**(3), 231-44 (1975).
13. Navarrette AR, Smith M, Ultrastructure of granular cell ameloblastoma. *Cancer*, **27**(4), 948-55 (1971).
14. Wu PC, Chan KW, A survey of tumours of the jawbones in Hong Kong Chinese: 1963-1982. *British Journal of Oral and Maxillofacial Surgery*, **23**(2), 92-102 (1985).
15. Eversole LR, Leider AS, Hansen LS, Ameloblastomas with pronounced desmoplasia. *Journal of Oral and Maxillofacial Surgery*, **42**(11), 735-40 (1984).
16. Waldron CA, el-Mofty SK, A histopathologic study of 116 ameloblastomas with special reference to the desmoplastic variant. *Oral Surgery, Oral Medicine, Oral Pathology*, **63**(4), 441-51 (1987).
17. Keszler A, Paparella ML, Dominguez FV, Desmoplastic and nondesmoplastic ameloblastoma: a comparative clinicopathological analysis. *Oral Diseases*, **2**(3), 228-31 (1996).
18. Philipsen HP, Reichart PA, Takata T, Desmoplastic ameloblastoma (including "hybrid" lesion of ameloblastoma): biological profile based on 100 cases from the literature and own files. *Oral Oncology*, **37**(5), 455-60 (2001).
19. Takata T, Miyauchi M, Ito H, et al., Clinical and histopathological analyses of desmoplastic ameloblastoma. *Pathology, Research and Practice*, **195**(10), 669-75 (1999).
20. Gardner DG, Corio RL, Plexiform unicystic ameloblastoma: a variant of ameloblastoma with a low-recurrence rate after enucleation. *Cancer*, **53**(8), 1730-5 (1984).
21. Philipsen HP, Reichart PA, Unicystic ameloblastoma: a review of 193 cases from the literature. *Oral Oncology*, **34**(5), 317-25 (1998).

22. Robinson L, Martinez MG, Unicystic ameloblastoma: a prognostically distinct entity. *Cancer*, **40**(5), 2278-85 (1977).
23. Reichart PA, Philipsen HP, Sonner S, Ameloblastoma: biological profile of 3677 cases. *European Journal of Cancer. Part B, Oral Oncology*, **31B**(2), 86-99 (1995).
24. Vickers RA, Gorlin RJ, Ameloblastoma: delineation of early histopathologic features of neoplasia. *Cancer*, **26**(3), 699-710 (1970).
25. Gardner DG, Plexiform unicystic ameloblastoma: a diagnostic problem in dentigerous cysts. *Cancer*, **47**(6), 1358-63 (1981).
26. Gardner DG, Corio RL, The relationship of plexiform unicystic ameloblastoma to conventional ameloblastoma. *Oral Surgery, Oral Medicine, Oral Pathology*, **56**(1), 54-60 (1983).
27. Leider AS, Eversole LR, Barkin ME, Cystic ameloblastoma: a clinicopathologic analysis. *Oral Surgery, Oral Medicine, Oral Pathology*, **60**(6), 624-30 (1985).
28. Woo SB, Smith-Williams JE, Sciubba JJ, Lipper S, Peripheral ameloblastoma of the buccal mucosa: case report and review of the English literature. *Oral Surgery, Oral Medicine, Oral Pathology*, **63**(1), 78-84 (1987).
29. Gardner DG, Peripheral ameloblastoma: a study of 21 cases, including 5 reported as basal cell carcinoma of the gingiva. *Cancer*, **39**(4), 1625-33 (1977).
30. Stanley HRJ, Krogh HW, Peripheral ameloblastoma; report of a case. *Journal of Oral Surgery*, **12**(6), 760-5 (1959).
31. Califano L, Maremonti P, Boscaino A, De Rosa G, Giardino C, Peripheral ameloblastoma: report of a case with malignant aspect. *British Journal of Oral and Maxillofacial Surgery*, **34**(3), 240-2 (1996).
32. Baden E, Doyle JL, Petriella V, Malignant transformation of peripheral ameloblastoma. *Oral Surgery, Oral Medicine, Oral Pathology*, **75**(2), 214-9 (1993).
33. Buchner A, Sciubba JJ, Peripheral epithelial odontogenic tumors: a review. *Oral Surgery, Oral Medicine, Oral Pathology*, **63**(6), 688-97 (1987).
34. Neville BN, Allen CM, Damm DD, Bouquot JE. Odontogenic cysts and tumors. In: Neville BW, Damm DD, Allen CM, Bouquot JE, Neville BW, eds. *Oral and Maxillofacial Pathology*, 2nd ed. New York, NY: W.B. Saunders, 2001; 610-33.
35. Goldblatt LI, Brannon RB, Ellis GL, Squamous odontogenic tumor: report of five cases and review of the literature. *Oral Surgery, Oral Medicine, Oral Pathology*, **54**(2), 187-96 (1982).
36. Leider AS, Jonker LA, Cook HE, Multicentric familial squamous odontogenic tumor. *Oral Surgery, Oral Medicine, Oral Pathology*, **68**(2), 175-81 (1989).
37. Mills WP, Davila MA, Beuttenmuller EA, Koudelka BM, Squamous odontogenic tumor: report of a case with lesions in three quadrants. *Oral Surgery, Oral Medicine, Oral Pathology*, **61**(6), 557-63 (1986).
38. Pullon PA, Shafer WG, Elzay RP, Kerr DA, Corio RL, Squamous odontogenic tumor: report of six cases of a previously undescribed lesion. *Oral Surgery, Oral Medicine, Oral Pathology*, **40**(5), 616-30 (1975).
39. Wright JM, Jr., Squamous odontogenic tumorlike proliferations in odontogenic cysts. *Oral Surgery, Oral Medicine, Oral Pathology*, **47**(4), 354-8 (1979).
40. Pflaumer SM, Newll JO, Greer ROJ, Calcifying epithelial odontogenic tumor: a rare maxillary presentation with clinicopathologic correlations. *Pathology Case Reviews*, **4**(16-20 (1999).
41. Franklin CD, Pindborg JJ, The calcifying epithelial odontogenic tumor: a review and analysis of 113 cases. *Oral Surgery, Oral Medicine, Oral Pathology*, **42**(6), 753-65 (1976).
42. Pindborg JJ, Calcifying epithelial odontogenic tumor. *Acta Pathologica et Microbiologica Scandinavica*,**111**(Supplementary), 71 (1955).
43. Hicks MJ, Flaitz CM, Wong ME, McDaniel RK, Cagle PT, Clear cell variant of calcifying epithelial odontogenic tumor: case report and review of the literature. *Head and Neck*, **16**(3), 272-7 (1994).
44. Eversole LR, Tomich CE, Cherrick HM, Histogenesis of odontogenic tumors. *Oral Surgery, Oral Medicine, Oral Pathology*, **32**(4), 569-81 (1971).
45. Gardner DG, The mixed odontogenic tumors. *Oral Surgery, Oral Medicine, Oral Pathology*, **58**(2), 166-8 (1984).
46. Slootweg PJ, An analysis of the interrelationship of the mixed odontogenic tumors--ameloblastic fibroma, ameloblastic fibro-odontoma, and the odontomas. *Oral Surgery, Oral Medicine, Oral Pathology*, **51**(3), 266-76 (1981).
47. Leider AS, Nelson JF, Trodahl JN, Ameloblastic fibrosarcoma of the jaws. *Oral Surgery, Oral Medicine, Oral Pathology*, **33**(4), 559-69 (1972).
48. Altini M, Thompson SH, Lownie JF, Berezowski BB, Ameloblastic sarcoma of the mandible. *Journal of Oral and Maxillofacial Surgery*, **43**(10), 789-94 (1985).
49. Regezi JA, Kerr DA, Courtney RM, Odontogenic tumors: analysis of 706 cases. *Journal of Oral Surgery*, **36**(10), 771-8 (1978).

50. Miller AS, Lopez CF, Pullon PA, Elzay RP, Ameloblastic fibro-odontoma: report of seven cases. *Oral Surgery, Oral Medicine, Oral Pathology*, **41**(3), 354-65 (1976).
51. Tomich CE, Benign mixed odontogenic tumors. *Seminars in Diagnostic Pathology*, **16**(4), 308-16 (1999).
52. Gunhan O, Erseven G, Ruacan S, et al., Odontogenic tumours: a series of 409 cases. *Australian Dental Journal*, **35**(6), 518-22 (1990).
53. Budnick SD, Compound and complex odontomas. *Oral Surgery, Oral Medicine, Oral Pathology*, **42**(4), 501-6 (1976).
54. Kaugars GE, Miller ME, Abbey LM, Odontomas. *Oral Surgery, Oral Medicine, Oral Pathology*, **67**(2), 172-6 (1989).
55. Kaugars GE, Zussmann HW, Ameloblastic odontoma (odonto-ameloblastoma). *Oral Surgery, Oral Medicine, Oral Pathology*, **71**(3), 371-3 (1991).
56. Frissell CT, Shafer WG, Ameloblastic odontoma; report of a case. *Journal of Oral Surgery*, **6**(9), 1129-33 (1953).
57. Poulson TC, Greer RO, Jr., Adenomatoid odontogenic tumor: clinicopathologic and ultrastructural concepts. *Journal of Oral and Maxillofacial Surgery*, **41**(12), 818-24 (1983).
58. Yazdi I, Nowparast B, Extraosseous adenomatoid odontogenic tumor with special reference to the probability of the basal-cell layer of oral epithelium as a potential source of origin: report of a case. *Oral Surgery, Oral Medicine, Oral Pathology*, **37**(2), 249-56 (1974).
59. Aldred MJ, Gray AR, A pigmented adenomatoid odontogenic tumor. *Oral Surgery, Oral Medicine, Oral Pathology*, **70**(1), 86-9 (1990).
60. Mori M, Makino M, Imai K, The histochemical nature of homogeneous amorphous materials in odontogenic epithelial tumors. *Journal of Oral Surgery*, **38**(2), 96-102 (1980).
61. Courtney RM, Kerr DA, The odontogenic adenomatoid tumor: a comprehensive study of twenty new cases. *Oral Surgery, Oral Medicine, Oral Pathology*, **39**(3), 424-35 (1975).
62. el-Labban NG, The nature of the eosinophilic and laminated masses in the adenomatoid odontogenic tumor: a histochemical and ultrastructural study. *Journal of Oral Pathology and Medicine*, **21**(2), 75-81 (1992).
63. Saku T, Okabe H, Shimokawa H, Immunohistochemical demonstration of enamel proteins in odontogenic tumors. *Journal of Oral Pathology and Medicine*, **21**(3), 113-9 (1992).
64. Philipsen HP, Reichart PA, Zhang KH, Nikai H, Yu QX, Adenomatoid odontogenic tumor: biologic profile based on 499 cases. *Journal of Oral Pathology and Medicine*, **20**(4), 149-58 (1991).
65. Hong SP, Ellis GL, Hartman KS, Calcifying odontogenic cyst: a review of ninety-two cases with reevaluation of their nature as cysts or neoplasms, the nature of ghost cells, and subclassification. *Oral Surgery, Oral Medicine, Oral Pathology*, **72**(1), 56-64 (1991).
66. Toida M, So-called calcifying odontogenic cyst: review and discussion on the terminology and classification. *Journal of Oral Pathology and Medicine*, **27**(2), 49-52 (1998).
67. Gorlin RJ, Pindborg JJ, Clausen F, P,, Vickers RA, The calcifying odontogenic cyst—a possible analogue of the cutaneous calcifying epithelioma of Malherbe: an analysis of fifteen cases. *Oral surgery, Oral Medicine, Oral Pathology*, **15**(1235-43 (1962).
68. McCoy BP, MK OC, Hall JM, Carcinoma arising in a dentinogenic ghost cell tumor. *Oral Surgery, Oral Medicine, Oral Pathology*, **74**(3), 371-8 (1992).
69. Grodjesk JE, Dolinsky HB, Schneider LC, Dolinsky EH, Doyle JL, Odontogenic ghost cell carcinoma. *Oral Surgery, Oral Medicine, Oral Pathology*, **63**(5), 576-81 (1987).
70. Ellis GL, Shmookler BM, Aggressive (malignant?) epithelial odontogenic ghost cell tumor. *Oral Surgery, Oral Medicine, Oral Pathology*, **61**(5), 471-8 (1986).
71. Slootweg PJ, Wittkampf AR, Myxoma of the jaws: an analysis of 15 cases. *Journal of Maxillofacial Surgery*, **14**(1), 46-52 (1986).
72. Peltola J, Magnusson B, Happonen RP, Borrman H, Odontogenic myxoma: a radiographic study of 21 tumours. *British Journal of Oral and Maxillofacial Surgery*, **32**(5), 298-302 (1994).
73. Barros RE, Dominguez FV, Cabrini RL, Myxoma of the jaws. *Oral Surgery, Oral Medicine, Oral Pathology*, **27**(2), 225-36 (1969).
74. White DK, Chen S, Mohnac AM, Miller AS, Odontogenic myxoma: a clinical and ultrastructural study. *Oral Surgery, Oral Medicine, Oral Pathology*, **39**(6), 901-17 (1975).
75. Hendler BH, Abaza NA, Quinn P, Odontogenic myxoma: surgical management and an ultrastructural study. *Oral Surgery, Oral Medicine, Oral Pathology*, **47**(3), 203-17 (1979).
76. Keszler A, Dominguez FV, Giannunzio G, Myxoma in childhood: an analysis of 10 cases. *Journal of Oral and Maxillofacial Surgery*, **53**(5), 518-21 (1995).
77. Kim J, Ellis GL, Dental follicular tissue: misinterpretation as odontogenic tumors. *Journal of Oral and Maxillofacial Surgery*, **51**(7), 762-7; discussion 7-8 (1993).

78. Richter M, Chausse JM, [Resection and reconstruction of mandible for treatment of two rare benign tumors]. *Swiss Dent*, **11**(3), 39-45 (1990).
79. Ulmansky M, Hjorting-Hansen E, Praetorius F, Haque MF, Benign cementoblastoma: a review and five new cases. *Oral Surgery, Oral Medicine, Oral Pathology*, **77**(1), 48-55 (1994).
80. Ackermann GL, Altini M, The cementomas: a clinicopathological re-appraisal. *Journal of the Dental Association of South Africa*, **47**(5), 187-94 (1992).
81. Slootweg PJ, Maxillofacial fibro-osseous lesions: classification and differential diagnosis. *Seminars in Diagnostic Pathology*, **13**(2), 104-12 (1996).
82. van der Waal I, Greebe RB, Elias EA, Benign osteoblastoma or osteoid osteoma of the maxilla: report of a case. *International Journal of Oral Surgery*, **12**(5), 355-8 (1983).

CHAPTER 15
EFFECTIVE COMMUNICATION OF ANTIMICROBIAL SUSCEPTIBILITY DATA BY PATHOLOGISTS TO CLINICIANS

Ken B. Waites, M.D., F(AAM)*

1. INTRODUCTION

Despite predictions in the mid-twentieth century that bacterial and viral diseases would be wiped out by the year 2000, microbial infections in the early years of twenty-first century have remained major causes of morbidity and mortality. The emergence and spread of antimicrobial-resistant bacteria in the hospital environment, and more recently in community settings, augmented by frequent reports in the lay press, has heightened the awareness of primary care physicians as well as specialists in the importance of surveillance for antimicrobial-resistant bacteria, and that the administration of antimicrobial chemotherapy should be guided by in vitro susceptibility data whenever possible. The increased attention focused on microbiology data by clinicians has a secondary effect in that it mandates involvement of the clinical pathologist as a leader in how laboratory information is obtained and communicated to physicians in the most accurate, timely, and effective manner. Keeping abreast of the epidemiologic trends in antimicrobial resistance locally and nationally, maintaining awareness of current guidelines and recommendations for susceptibility testing, communication of data in an understandable format, and regular interactions with clinicians require considerable time allotment by the pathologist in order to ensure optimum patient management and fiscal responsibility to the hospital or laboratory that generates the data.

The objectives of this article are (1) to discuss the importance of effective communication of microbiology data to clinicians; (2) to provide selected examples of contemporary issues where up-to-date laboratory testing and reporting are important; and (3) to identify the role of the clinical pathologist in these matters.

* Professor and Director of Clinical Microbiology, Department of Pathology, University of Alabama, Birmingham, AL; Microbiology Consultant, Veterans Affairs Medical Center, Birmingham, AL.

2. REPORTING LABORATORY RESULTS

The potential influence of the clinical pathologist in how antimicrobial agents are utilized in the health care setting cannot be overstated because the content and design of laboratory reports normally falls under the purview of the diagnostic laboratory in most health care institutions, and the manner in which information is presented and interpreted may affect how physicians prescribe drugs. The likelihood of bacteriological cure is greatest when patients receive a drug to which the infecting organism is susceptible, even though a bacteriological cure may also occur in some cases where the organism is resistant, indicating the importance of the host immune system in combatting disease. Thus, accuracy and completeness in reporting susceptibility data for the most appropriate drugs are very important.

In the simplest terms, a laboratory susceptibility report for a particular bacterial organism provides descriptive data for antimicrobial agents potentially suitable for use in treatment of the infection. At the University of Alabama at Birmingham (UAB) Medical Center, reports are limited to a categorical interpretation, that is, susceptible, intermediate, or resistant, rather than reporting individual minimal inhibitory concentrations (MICs). The term "susceptible" indicates that the infection may be appropriately treated with a dosage of the agents recommended for that type of infection, unless contraindicated. The term "resistant" means that the microorganism is not inhibited by the usual achievable systemic concentration of the agents given in normal dosage and/or clinical efficacy has not been reliable. Intermediate resistance means that the MIC of the drug approaches obtainable blood and tissue concentrations, but the drug may be used to treat infections in body sites where the drug is concentrated, or when higher than normal doses of the drug are used. Examples of the latter are the use of fluoroquinolones to treat urinary tract infections and macrolides to treat respiratory infections in which the antimicrobials or their metabolites may be concentrated in the urine or lung, respectively. Laboratory reports can be further enhanced by application of a variety of rules regarding how information is presented, and in some cases, comments regarding proper interpretation of the results. Automated microbiology systems and hospital computer systems have varied capabilities with respect to customizing reports after the microbiology laboratory personnel verify them.

Antibiotic costs are a major portion of hospital pharmacy expenditures. The UAB pharmacy budget exceeds $20 million per year for the top 100 drugs used. Antimicrobial agents account for approximately 20% of this budget. There are many alternative antimicrobial agents available for use in treatment of hospital infections, several of which may have overlapping spectra of activities and widely differing costs. Because clinical laboratory personnel cannot know detailed circumstances concerning each patient with a bacterial infection that can influence choices of antimicrobial agents, it is common practice for microbiology laboratories to determine in vitro susceptibilities for 20 or more antimicrobial agents for each microorganism tested using commercial microdilution panels that are read manually or by using an automated instrument such as the MicroScan WalkAway® (Dade MicroScan, West Sacramento, CA). Physicians have a wide array of options in selecting the most appropriate treatment regimens, but it also places important responsibilities in the hands of the pathologist to designate how the susceptibility data are communicated in the laboratory report for most efficient and cost-effective drug utilization. The value of laboratory reports can be enhanced by customization according to the needs of the individual health care system based on microorganism type, patient

type, body site of infection, pharmacy formulary content, resistance profile, toxicity, and cost. Acquisition costs for a 10-day treatment of an infection caused by gram-negative bacilli using gentamicin is approximately $10, whereas the cost for imipenem is almost $900. Use of less costly agents should be encouraged whenever suitable and laboratory reports should be designed to encourage physicians to do so.

The Director of the Microbiology Laboratory should work very closely with pharmacy and clinical services to customize susceptibility reports with the goals of limiting unnecessary and sometimes misleading descriptions of antimicrobial susceptibilities. The MicroScan WalkAway® instrument tests antimicrobial susceptibilities on the same microtiter panel in which bacterial identification is performed. There is one generic panel with drugs for gram-negative bacteria and another for the gram-positives. It is rarely necessary or appropriate to report results for every drug that is tested. Cefotaxime and ceftriaxone are third-generation cephalosporins with very similar spectra of activities against most gram-negative bacilli. Although there are some differences in their pharmacological behaviors and required dosage intervals, they are sufficiently similar to one another that a hospital should contract with its suppliers to achieve the least-expensive agent of the two and make it the formulary representative. Because cefotaxime is currently available in generic form, while ceftriaxone remains a patented proprietary agent, the former drug is much less expensive and its use is strongly encouraged by our pharmacy service. Therefore, the laboratory reports list only cefotaxime, even though both agents are tested, so that physicians will be encouraged to use it as opposed to a more expensive alternative.

Figure 1 shows a computerized cascade system in which antimicrobial agents are reported according to resistance patterns and acquisition costs in order to save money and limit the use of more costly and sometimes more toxic broad-spectrum agents that should be reserved for serious infections that are not likely to respond to other drugs. First-generation cephalosporins are less expensive than third-generation cephalosporins, which are less-expensive than beta-lactam-beta-lactamase inhibitor combinations and carbapenems. Restricting reporting of carbapenems such as imipenem to bacteria that are resistant to all other beta-lactams encourages the use of less-expensive agents and preserves the activity of the carbapenems.

Figure 2 shows the susceptibility profile for imipenem against the 9 most commonly isolated gram-negative bacterial species at UAB in 1990 and again in 2003. Its in vitro activity has been maintained consistently for more than 90% of nonduplicate clinical isolates during this 13-year period with very little variability for all organisms except *Pseudomonas aeruginosa*, presumably because it is restricted both in laboratory reporting and in usage in the medical center.

Whether usage of expensive broad-spectrum agents such as imipenem or newer drugs such as linezolid and the various antifungals should require permission from specific clinical services such as Infectious Disease is a matter that is best handled on an institutional basis. However, as the costs for antimicrobials continue to increase along with drug resistance in both gram-negative and gram-positive pathogens, many hospitals are taking the approach that administration of costly drugs should require documentation with appropriate microbiological testing and approvals by designated medical specialists before they are released by the pharmacy. Usage of less-expensive agents is also encouraged by listing drugs in order of increasing cost on the laboratory report and listing the daily acquisition costs and recommended dosage when possible so physicians will have to view this information with every patient report.

Report cefotaxime (3rd generation) only if resistant to cefazolin or cephalothin (1st generation)

Report cefepime (non-formulary) only if resistant to cefotaxime

Report imipenem only if resistant to cephalothin, cefazolin, cefotaxime, ceftazidime, cefepime, and piperacillin/tazobactam

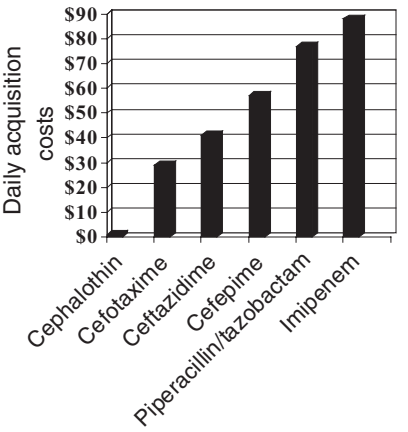

Figure 1. Cascade system for reporting narrow-spectrum less costly beta lactam antimicrobials unless resistance necessitates reporting of more broad-spectrum expensive agents for *Enterobacteriaceae*. Approximate acquisition costs for the hospital are based on 2003 data for the maximum daily dosages.

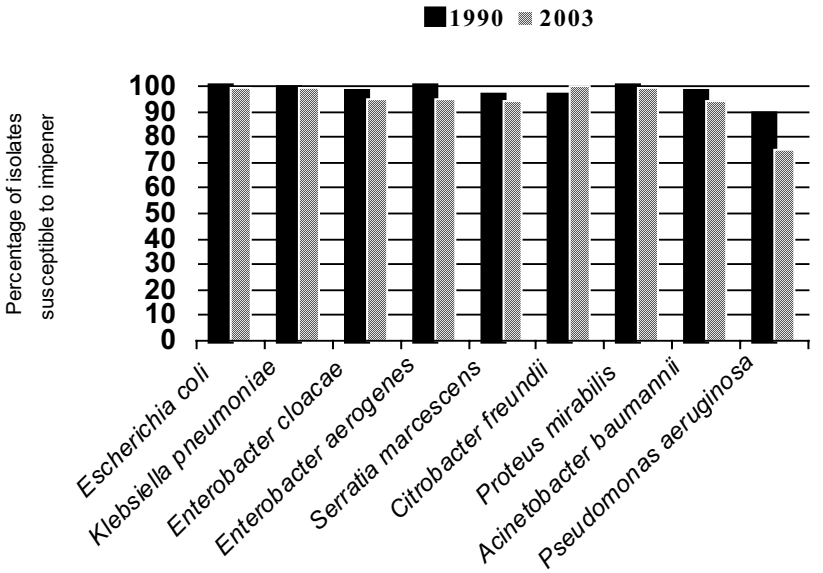

Figure 2. Percentages of nine gram-negative bacterial species susceptible to imipenem at UAB in 1990 versus 2003 demonstrating that greater than 90% of clinical isolates for eight of the nine species were consistently susceptible with very little difference between the time periods studied.

The microbiology laboratory should also set up its reporting system to be selective according to body site and avoid misleading organism–antimicrobial agent combinations. This includes not reporting oral antimicrobial agents on bacteria isolated from blood or cerebrospinal fluid specimens because they would not be appropriate for use in treatment of bacteremia or meningitis. Trimethoprim-sulfamethoxazole should not be reported on *Enterococcus* species because it is inappropriate for treatment of infections due to these organisms and the organisms may appear falsely susceptible in vitro. Other examples of potentially misleading organism–drug reports that should be avoided are included in publications of the National Committee for Clinical Laboratory Standards.[1]

Antimicrobial susceptibility summaries in the form of printed antibiograms that are limited to nonduplicate isolates and are unit specific, as well as comprehensive summaries for all hospitalized patients, should be distributed to the medical staff and pharmacy on at least an annual basis. We also make these available through a website that is accessible from any hospital computer.

The decisions on which antimicrobials are tested and reported in the laboratory are based on active discussions undertaken at regular meetings of the health system Pharmacy and Therapeutics Committee. Such committees are normally comprised of clinicians, representatives from nursing services, administration, and pharmacy. It is critical for a pathologist to be involved in order to make certain that the microbiology laboratory is effectively communicating with these other entities within the medical center to make certain that laboratory data accurately reflect what the committee intends regarding antimicrobial reporting and usage. Whether this means that the pathologist should be a regular member of the committee or a member of a specific antimicrobial subcommittee is a matter of individual institutional preference, but active laboratory representation in this decision-making process is the prerequisite for successful utilization of antimicrobials in the hospital setting.

The major automated microbiology systems including the MicroScan WalkAway® and Vitek 2® (bioMérieux, Hazelwood, MO) instruments have software programs that allow organism identification and susceptibility data to be accessible to pharmacy directly from the laboratory through electronic means. These systems also have programs that can be customized to prevent inadvertent reporting of incorrect or potentially misleading results that may have occurred due to technical or personnel errors. They can also be customized to flag unexpected susceptibility or resistance profiles such as reports of *Staphylococcus aureus* that is nonsusceptible to vancomycin so that the test can be repeated and/or verified by an alternative method before reporting on a patient's medical record to ensure the results are indeed correct. Implementing such computer programs and associated rules can potentially prevent the pathologist from having to provide explanations to clinicians regarding reports that included unexpected susceptibility data or errors that were in fact due to a technical problem with the instrument or laboratory processing. Utilization of antimicrobial susceptibility data transferred electronically from the microbiology laboratory proactively by pharmacists to guide antimicrobial usage was shown to reduce the costs of antimicrobials within a pharmacy budget by 10%, even when the total drug budget increased over a three-year period in a large urban hospital, thus emphasizing the importance of such communication from the laboratory in cost-control.[2]

A recent innovation at UAB involves interim communication of negative blood culture results after 24 hours and again after 72 hours in an attempt to raise the awareness of physicians and hospital pharmacists as to whether or not empiric antimicrobials

initiated because of possible bacteremia are still required. This is a reasonable practice because more than 96% of all true bacteremias may detected within 72 hours using the BacT/ALERT ® automated blood culture instrument (bioMérieux, Hazelwood, MO) and only 8–10% of all blood cultures collected will ever be positive.[3,4] Although we have not been doing this for a sufficient time to determine the extent to which this practice will result in cost savings by reducing the number of unnecessary antimicrobial doses given, the potential for such savings and improvement in patient care does exist.

3. NEW CHALLENGES FOR CLINICAL LABORATORIES IN DETECTION OF ANTIMICROBIAL RESISTANCE

3.1 Detection of Resistant Staphylococcus Aureus

One of the most significant problems in the emergence of antimicrobial resistance over the past decade has been the increasing rate of methicillin resistance in *S. aureus* (MRSA) that now exceeds 50% in many large medical centers. Figure 3 illustrates our experience at UAB as an example of what has occurred locally since the mid-1990s. Microbiology laboratories use oxacillin rather than methicillin to identify methicillin resistance because of its superiority and greater consistency in laboratory assays, hence the terms oxacillin resistance and methicillin resistance can be used synonymously.

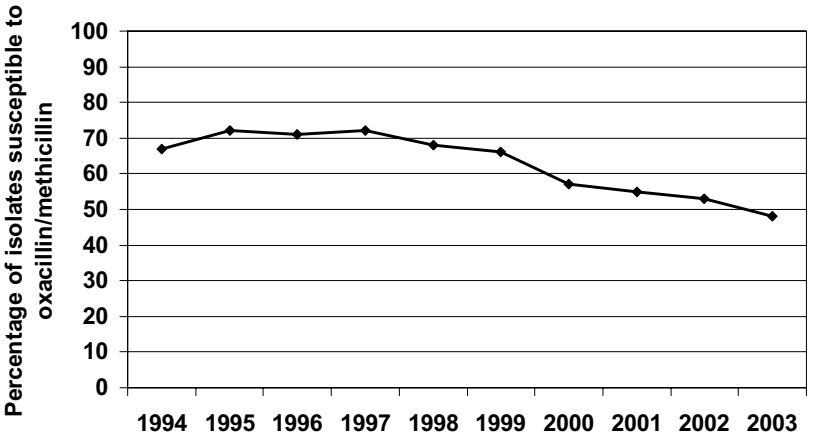

Figure 3. Rates of oxacillin susceptibilities for *S. aureus* at UAB between 1994 and 2003 showing a gradual decline with the majority of clinical isolates now resistant.

Within the past few years, rapid methods for detection of MRSA have become commercially available and can be easily implemented in clinical microbiology laboratories.[5] One method, the Velogene Rapid MRSA Identification Assay® (Alexon-Trend Inc., Ramsey, MN), is a 90-min genotypic test using a chimeric probe for the cycling-mediated recognition of the *mecA* gene that mediates methicillin resistance in staphylococci. A phenotypic test, the Oxoid Rapid PBP2' Test for MRSA, distributed by

Remel Laboratories (Lenexa, KS) and other suppliers is a much simpler assay that requires less than 15 minutes to perform and involves a latex agglutination procedure to detect the presence of penicillin binding protein PBP 2', the gene product of *mecA.* Since we implemented the PBP2' test at UAB in early 2003 we have tested 5 to 10 *S. aureus* isolates obtained from hospitalized persons on a daily basis and observed 100% concordance for the rapid results for PBP2' with oxacillin resistance determined by standard overnight MIC assay using the MicroScan WalkAway®. Infection control and pharmacy services are notified of the results on a daily basis. This allows confirmation of MRSA a day sooner than would be possible by standard susceptibility tests. Pharmacists can then proactively verify whether or not vancomycin is needed based on the laboratory report and discuss therapeutic alternatives, if appropriate, with physicians. Patients shown to have MRSA can be placed into isolation a day sooner by infection control and potentially lessen the likelihood of nosocomial transmission. The current acquisition cost for materials to perform the PBP2' test for one year at UAB is approximately $15,000. Hospital costs for caring for a patient with MRSA infection may exceed $60,000,[6] thus use of this rapid test would be very cost effective if it prevents a single MRSA infection each year as a result of more rapid isolation of infected or colonized persons.

Higher rates of methicillin resistance in community-acquired staphylococcal infections, particularly in children, are also quite worrisome because this affects therapeutic choices for empiric management of infections while awaiting microbiology data with the potential for poor patient outcomes.[7,8] Moreover, physicians often do not even order microbiological cultures and susceptibility tests before initiating treatment. These changing patterns in antimicrobial resistance in *S. aureus* and the numerous coagulase-negative *Staphylococcus* species (CNS) has led to renewed interest in the use of drugs such as clindamycin to treat these infections because it is available orally, is generally well-tolerated, and is sometimes active against MRSA isolates, particularly those acquired in the community as opposed to the hospital.[7] Clinical isolates of *S. aureus* and CNS that are susceptible in vitro to clindamycin but are resistant to erythromycin may have inducible macrolide-lincosamide-streptogramin B (MLS_B) resistance due to the presence of erythromycin ribosomal methylase *(erm)* genes. For these strains, there is a high rate of mutation to constitutive resistance, which would then be selected during clindamycin therapy. In other strains, the same erythromycin/clindamycin susceptibility pattern may be produced by strains that harbor *msrA,* which encodes an ATP-dependent efflux pump that confers resistance only to 14- and 15-membered ring macrolides and type B streptogramins but not to lincosamides, such as clindamycin.[7] For infections due to these *msrA* strains, clindamycin may be an important therapeutic option. However, treatment failures may ensue for infections caused by strains possessing e*rm* genes when clindamycin is used because of its induction effect.[7]

New procedures have been published by the NCCLS regarding confirmatory testing to detect inducible clindamycin resistance in staphylococci.[1] The double-disk diffusion "D test" (see Figure 4) has been implemented in our laboratory and is performed when requested by physicians. We continue to use the MicroScan WalkAway® system to determine MICs for *S. aureus* by microbroth dilution. Susceptibility tests for CNS, when necessary, are performed using the Kirby–Bauer agar-disk diffusion method because biochemical identification to species level is not necessary for patient care purposes, and the agar disk diffusion method is considerably less expensive than using MicroScan® panels. The D test can be performed directly on the Mueller–Hinton agar plates used for agar disk diffusion tests for CNS if erythromycin and clindamycin disks are placed

adjacent to each other at the prescribed distances. Performing the D test for *S. aureus* isolates would require an additional manual test unless it is set up on the blood agar plate used for the inoculum purity check that is performed for each MicroScan® panel. In our laboratory, the technologists review the susceptibility profiles of each *S. aureus* isolate. Clindamycin results are suppressed on reports for any isolate that has erythromycin resistance and clindamycin susceptibility. A comment on the laboratory report instructs physicians to contact the laboratory if clindamycin is to be considered for treatment of the infection so that the D test can be performed. All positive D tests necessitate reporting clindamycin as resistant. Performing the D test on S. *aureus* isolates only by request from physicians eliminates the need for the laboratory to expend personnel time and supplies unless clindamycin will actually be used for treatment purposes. Very little is known about the epidemiology of staphylococci with inducible clindamycin resistance. The incidence can vary according to type of institution, patient population, geographic location, whether or not an isolate is resistant to oxacillin, and whether it is *S. aureus* versus CNS.[7] Thus, it is important for microbiology laboratories to determine the frequency with which such strains occur in the patient population served in order to determine when and how laboratory testing to detect inducible clindamycin resistance should be implemented. There are many other examples of how customizing susceptibility reports with instructive comments can aid physicians in proper utilization of antibiotics that will also allow the microbiology to conserve materials and personnel time. These types of comments should be developed by the pathologist in consultation with the technical staff of the laboratory, pharmacy, and clinical services.

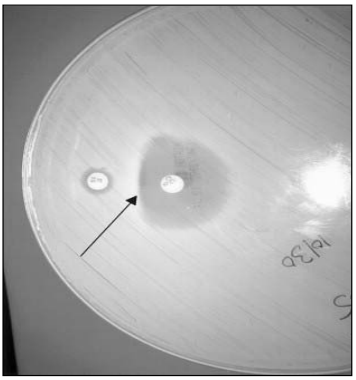

Figure 4. Double-disk diffusion "D" test to detect inducible clindamycin resistance in staphylococci based on induction of resistance by a 15 μg erythromycin disk placed 15-26 mm from a 2 μg clindamycin disk. Blunting of the inhibitory zone around the clindamycin disk forming a D shape denotes a positive test as indicated by the arrow. Isolates are reported as resistant to clindamycin irrespective of MICs determined prior to induction. Figure is reproduced by permission from reference 8.

Vancomycin-resistant *Enterooccus faecium* (VRE) was first reported in the late 1980s and made its first appearance at UAB in 1994. By 2003, 77% of *E. faecium* were resistant to vancomycin at our hospital. Like MRSA, VRE tends to spread clonally as a nosocomial pathogen. Figure 5 demonstrates the persistence of a single VRE clone over a three-year period, infecting 14 patients between 1997 and 1999, thereby emphasizing the importance of timely and accurate laboratory detection. A rapid test to detect VRE harboring the *vanA* gene similar to the Velogene® assay for MRSA is currently under investigation for future clinical application.[9] Availability of this technology to facilitate early recognition of VRE will undoubtedly be a very important advance for clinical laboratories if it proves to be accurate and amenable for incorporation into a laboratory workflow.

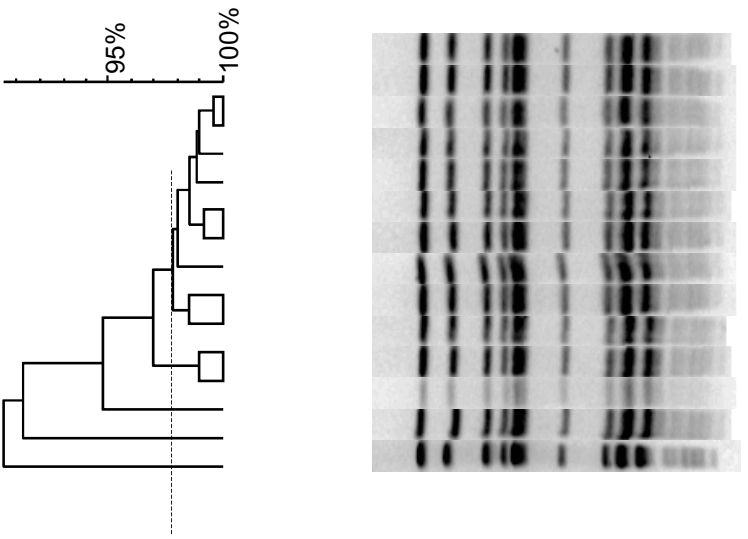

Figure 5. Pulsed field gel electrophoresis (PFGE) patterns and dendrogram of a single clone of vancomycin-resistant *Enterococcus faecium* isolated from 14 patients at UAB. Five isolates were from 1997; 8 isolates were from 1998; and 1 isolate was from 1999 indicating persistence of infecting organisms in the nosocomial environment for many months. This figure is reproduced with permission from Ref. 11.

Intermediate vancomycin resistance (VISA) was first documented in *S. aureus* in the United States in 1997.[10] This resistance in which vancomycin MICs range from 8 to 16 μg/ml is believed to have arisen from widespread use of vancomycin to treat MRSA infections with an additional by-product being the development and spread of VRE throughout the 1990s.[11] Perhaps the most disturbing events are recent reports of high-level vancomycin resistance in *S. aureus* (VRSA) isolates in Pennsylvania and Michigan with vancomycin MICs = 32 –1024 μg/ml in which the organisms were proven to contain both the *mecA* gene and the *van*A gene that mediates high-level vancomycin resistance.[12,13] Conjugation between these species is the presumed route of development of these cases of VRSA. A schematic diagram illustrating the time course and perceived relationships between MRSA, VRE, VISA, and VRSA is shown in Figure 6.

The significance for the pathologist in the understanding and appreciation of newly described antimicrobial resistance profiles such as VISA and VRSA lies in the fact that it is the responsibility of the diagnostic laboratory to assist in guidance of proper utilization of antimicrobial agents by clinicians for optimum patient care as well as to minimize selective pressure, and ensure prompt isolation of infected persons as necessary to prevent transmission of nosocomial infection. To achieve these goals, in vitro susceptibility data should be reported as rapidly as possible, hence the value of rapid assays for organisms such as MRSA as described above. It is also essential that clinical

laboratories utilize testing protocols that will accurately identify such resistance as soon as it is encountered, even when very rare. Accurate detection of antimicrobial resistance is not difficult in most instances if proper well-validated laboratory protocols are followed and adequate quality control practices are maintained. However, accurate detection of resistant organisms can sometimes be complex and difficult, particularly for emerging resistance profiles with which laboratory personnel are unfamiliar and for which existing susceptibility testing methods have not been challenged.

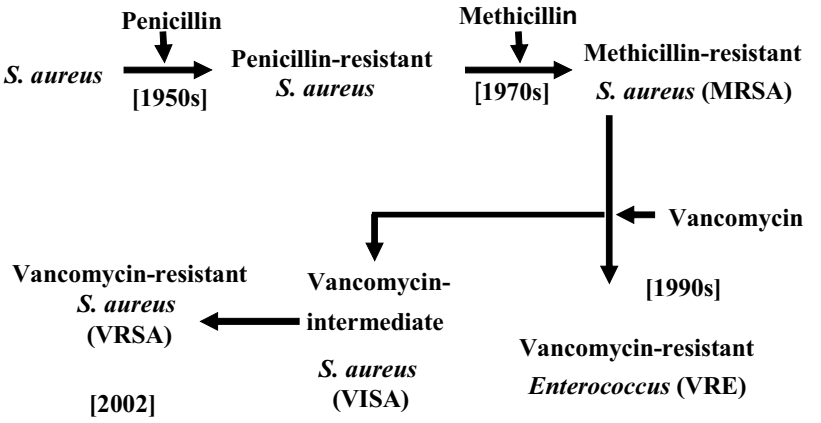

Figure 6. Schematic model and timeline demonstrating relationships and emergence of antimicrobial resistance in *S. aureus*.

In the early to mid-1990s, when VRE began to occur commonly in many hospitals, there was concern when it became apparent that some of the widely used commercial automated microbiology systems could not adequately detect it, necessitating modification and revision of their MIC systems and software.[14] Thus, it was no great surprise when subsequent studies demonstrated that VRSA isolates may not be adequately characterized by agar disk diffusion or even the MicroScan WalkAway® and Vitek 2® instruments using current drug formulations and versions of their software.[1,15] Even though the number of reported VISA and VRSA clinical isolates has been very small thus far and the extent to which automated microbiology systems will be able to detect them has not been studied in depth, our laboratory recently began a supplemental test for screening all *S. aureus* isolates for vancomycin resistance. The procedure includes inoculation onto a brain–heart infusion agar medium containing 6 μg/ml of vancomycin (Remel Laboratories) in addition to the standardized testing using the MicroScan WalkAway® instrument. Any detectable growth will be subjected to endpoint MIC determination using a method such as the agar gradient (Etest) technique (AB BIODISK, Solna, Sweden) and referred to the Centers for Disease Control and Prevention. Accurate detection of VISA and VRSA is extremely important both for individual patient management and prevention of nosocomial spread. Dissemination of VISA and VRSA

could have considerably greater impact than VRE because of the greater virulence of *S. aureus* than *E. faecium.*

3.2 Detection of Extended Spectrum Beta Lactamases in Gram-negative Bacilli

Although emerging resistance in gram-positive bacteria is extremely important, significant resistance profiles in gram-negative bacteria that can be equally challenging for clinicians to manage and for laboratories to detect and characterize must not be overlooked. Laboratories must be properly equipped to detect extended-spectrum beta-lactamase (ESBL) production in *Escherichia coli* and *Klebsiella* species. ESBLs are enzymes derived from mutations of older TEM and SHV plasmid-mediated beta lactamases. This type of resistance was first identified in Europe in the early 1980s and has since spread to North America where it is typically associated with nosocomial infections that often occur in patients in intensive care units who have had extensive exposure to various antimicrobials, who have undergone surgery and/or require ventilatory assistance.[16,17] Outbreaks of ESBL-producing bacteria resulting in numerous fatalities have been described throughout the United States and although they are still uncommon in many hospitals, their occurrence appears to be increasing worldwide.[17] Estimated North America ESBL rate in *Klebsiella* spp. is 4.2–44% and 3.3–4.7% for E. *coli* according to recent surveys.[17] The presence of an ESBL typically confers resistance to extended-spectrum penicillins, cephalosporins, and aztreonam, but usually not to cephamycins or carbapenems. Organsims with ESBLs are often concomitantly resistant to drugs in other classes such as aminoglycosides and fluoroquinolones, so accurate detection and susceptibility testing is very important. As ESBL-producing *Enterobacteriaceae* have the propensity to spread resistance by clonal strain transmission or conjugative plasmid transfer, they also pose challenging infection control issues.[17] Our MicroScan WalkAway® instrument has software that will flag possible ESBL-producing bacteria based on specific susceptibility profiles for targeted drugs such as cefpodoxime, cefotaxime, ceftriaxone, ceftazidime, and aztreonam. A combined disk diffusion method described by the NCCLS[1] and shown in Figure 7 is then be used to confirm the presence of ESBL production. This supplemental testing to confirm ESBLs is important because conventional testing using automated systems may not always detect this resistance when MICs are determined and interpreted according to NCCLS guidelines.[1,18] If the presence of an ESBL-producing microorganism is confirmed, all cephalosporins and penicillins, except beta lactam-beta lactamase inhibitor combinations are reported as resistant, irrespective of the actual MIC and a descriptive

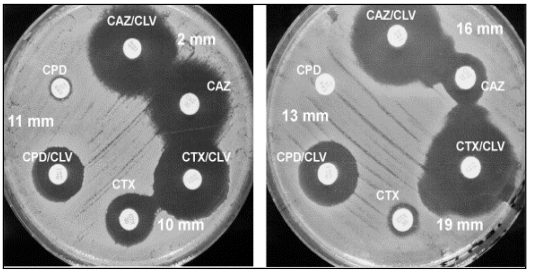

Figure 7. Detection of ESBL production using the combined disk test in *Klebsiella oxytoca* (left) and *E. coli* (right). Note the increased zone diameters around cefotaxime (CTX), ceftazidime (CAZ), and cefpodoxime (CPD) disks when tested in the presence of clavulanic acid (CLV) versus the zone diameters for the agents tested alone. A ≥ 5 mm increase in zone diameter for at least one combination indicates ESBL production. [Anonymous, 2004 #4] This figure is reproduced with permission from Ref 17.

comment advising physicians of the significance of ESBLs appears on the report along with the susceptibility results. The main limitation at present is that the methods endorsed by the NCCLS for detection of ESBLs are limited to *E. coli* and *Klebsiella* spp., even though ESBL production is likely to occur in many other gram-negative bacilli.

4. SUMMARY AND CONCLUSIONS

As antimicrobial-resistant gram-positive and gram-negative bacterial infections continue to emerge over time, influenced by selective pressure, and the costs of treating these infections increase, the ability of microbiology laboratories to accurately detect drug-resistant bacteria and communicate susceptibility test results effectively to clinicians in a timely manner is more important than ever. Ongoing cooperation and coordination of activities among clinical pathologists, technical personnel, pharmacy, clinical services, and infection control using up-to-date laboratory methodologies and interpretive criteria to develop laboratory reports that are transmitted efficiently through computerized communication systems customized for use within each particular institution are essential to provide optimum patient care, control resistance, and conserve resources.

5. REFERENCES

1. Anonymous. Performance *Standards for Antimicrobial Susceptibility Testing;* Fourteenth Informational Supplement, NCCLS Document M100-S-14, vol. 23. Wayne, PA: National Committee for Clinical Laboratory Standards, 2004.
2. Schentag JJ, Ballow CH, Fritz AL, et al., Changes in antimicrobial agent usage resulting from interactions among clinical pharmacy, the infectious disease division, and the microbiology laboratory. *Diagn Microbiol Infect Dis*, 16(3), 255-64 (1993).
3. Hardy DJ, Hulbert BB, Migneault PC, Time to detection of positive BacT/Alert blood cultures and lack of need for routine subculture of 5- to 7-day negative cultures. *J Clin Microbiol*, 30(10), 2743-5 (1992).
4. Wilson ML, Introduction. *Clinics in Laboratory Medicine*, 14(1-7 (1994).
5. Arbique J, Forward K, Haldane D, Davidson R, Comparison of the Velogene Rapid MRSA Identification Assay, Denka MRSA-Screen Assay, and BBL Crystal MRSA ID System for rapid identification of methicillin-resistant *Staphylococcus aureus*. *Diagn Microbiol Infect Dis*, 40(1-2), 5-10 (2001).
6. Carbon C, Costs of treating infections caused by methicillin-resistant staphylococci and vancomycin-resistant enterococci. *J Antimicrob Chemother*, 44 Suppl A(31-6 (1999).
7. Siberry GK, Tekle T, Carroll K, Dick J, Failure of clindamycin treatment of methicillin-resistant *Staphylococcus aureus* expressing inducible clindamycin resistance in vitro. *Clin Infect Dis*, 37(9), 1257-60 (2003).
8. Naimi TS, LeDell KH, Como-Sabetti K, et al., Comparison of community- and health care-associated methicillin-resistant *Staphylococcus aureus* infection. *Jama*, 290(22), 2976-84 (2003).
9. Appleman MD, Citron DM, Kwok R, Evaluation of the Velogene genomic assay for detection of vanA and vanB genes in vancomycin-resistant *Enterococcus* species. *J Clin Microbiol*, 42(4), 1751-2 (2004).
10. Anonymous, *Staphylococcus aureus* with reduced susceptibility to vancomycin—United States, 1997. *MMWR Morb Mortal Wkly Rep*, 46(33), 765-6 (1997).
11. Chavers LS, Moser SA, Benjamin WH, et al., Vancomycin-resistant enterococci: 15 years and counting. *J Hosp Infect*, 53(3), 159-71 (2003).
12. Anonymous, From the Centers for Disease Control and Prevention. Vancomycin-resistant *Staphylococcus aureus*--Pennsylvania, 2002. *Jama*, 288(17), 2116 (2002).
13. Anonymous, From the Centers for Disease Control. *Staphylococcus aureus* resistant to vancomycin—United States, 2002. *Jama*, 288(7), 824-5 (2002).
14. Tenover FC, Swenson JM, O'Hara CM, Stocker SA, Ability of commercial and reference antimicrobial susceptibility testing methods to detect vancomycin resistance in enterococci. *J Clin Microbiol*, 33(6), 1524-7 (1995).
15. Tenover FC, Weigel LM, Appelbaum PC, et al., Vancomycin-resistant *Staphylococcus aureus* isolate from a patient in Pennsylvania. *Antimicrob Agents Chemother*, 48(1), 275-80 (2004).

16. Jacoby GA, Epidemiology of extended-spectrum beta-lactamases. *Clin Infect Dis*, 27(1), 81-3 (1998).
17. Sturenburg E, Mack D, Extended-spectrum beta-lactamases: implications for the clinical microbiology laboratory, therapy, and infection control. *J Infect*, 47(4), 273-95 (2003).
18. Jacoby GA, Extended-spectrum beta-lactamases and other enzymes providing resistance to oxyimino-beta-lactams. *Infect Dis Clin North Am*, 11(4), 875-87 (1997).

CHAPTER 16
ACQUISITION AND USE OF DIGITAL IMAGES FOR PATHOLOGY EDUCATION AND PRACTICE

Kristina T. C. Panizzi, M.A.E.,[*] Kristopher N. Jones, M.D., M.P.H.,[†] and Peter G. Anderson, D.V.M., PhD[‡]

1. INTRODUCTION

Digital imaging systems are rapidly becoming a valued asset in the field of pathology education and practice as more emphasis is being placed upon digital technology and improved efficiency in medicine. Pathology is an image-intensive discipline which relies upon the diagnostic clarity and accuracy of pathological specimens, and technological advances in image acquisition and delivery have spurred the emergence of pathology as an increasingly "digital" discipline. Well-implemented digital imaging systems can maximize efficiency, reduce costs, and allow for the rapid repurposing of resources in addition to facilitating collaborations among educators and practitioners. Pathology collections that previously were underutilized or lie dormant in storage may now be resurrected from the notorious "image graveyard" through digitization efforts. However, acquisition of digital images can easily lead to the development of "digital image graveyards" if appropriate measures are not taken to ensure that these images are easily retrievable and accessible for use in teaching or in practice. As such, an understanding of image acquisition in addition to editing, processing, storage, management, and delivery of digital images is crucial in revitalizing pathology collections and reaping the benefits that digital imagery provides in terms of efficiency, collaboration, and repurposing.

[*] University of Alabama, Birmingham AL
[†] University of Alabama, Birmingham AL
[‡] University of Alabama, Birmingham AL

2. QUALITY OF DIGITAL IMAGES FOR DIAGNOSTIC AND EDUCATIONAL USE

A common issue that arises in regard to digitization of pathology images is the question of whether the digital images have sufficient diagnostic quality to be useful—particularly in pathology practice. Because pathologists rely upon the quality of clinical samples to make a diagnosis, the quality of digital images used for diagnosis or peer review of diagnostic accuracy is a significant concern as any variations in diagnosis may substantially influence clinical approaches to patients and understandings of clinical disease[1, 2]

Cruz et al.[1] reported diagnostic accuracy using digital images in routine practice to be 97.6% versus reports of diagnostic accuracy using digital images in teleconsultation services as 88.1% by Weinberg et al. (1996)[3] and 88.2% by Halliday et al.[4] Cruz et al attributed the difference in diagnostic accuracy from these studies to be mainly due to the fact that teleconsultation services often involve images representing rare or hard-to-diagnose cases versus the specimens typically encountered in routine practice.[1] In addition, this study demonstrated agreement between the original diagnosis and the peer review using digital images in 88.1% of the cases, with peer reviewers acknowledging that the diagnosis could be determined with fewer images in 30.2% of these cases. Concordance between original diagnosis and peer review was not achieved in the remaining 11.8% of cases due either to a lack of images considered diagnostically "essential" or to poor image quality. Reasons for poor image quality included problems with brightness and contrast, substantial color differences between the digital images and the original samples, or inadequate definition or detail in the digital images. Cruz et al. found that an insufficient number of digital images was more relevant to diagnostic assessment in routine practice than the quality of the digital images.[1] These authors also noted that color adjustments following image acquisition are typically time-consuming but may be necessary because in 14.7% of the digital images from their study the color varied substantially from the original samples. Though color adjustment was not necessary in all cases for diagnostic purposes, these authors caution that small variations in color may conceal details essential for diagnosis.

It is also important to consider that image quality not only depends upon the capture system, image and monitor resolution, color palette, and compression ratio but also upon the quality of the specimens (resection, process, staining) and the expertise of the individual capturing the image (e.g., ensuring that the equipment is focused). Other criteria to consider in the diagnostic use of digital images is whether or not the appropriate areas of interest are selected for capture and whether or not the image is captured at an appropriate magnification to make a diagnosis.

Given continuing advances in digital technology and image capture systems and additional studies involving the diagnostic quality of digital images, it is likely that digital imaging will become an even more significant component of pathology practice. When deciding whether or not to use digital images for diagnostic purposes, an emphasis needs to be placed upon ensuring that sufficient numbers of diagnostic images are captured, that areas of diagnostic interest are captured, and that specimens are quality processed, properly illuminated, and captured at higher powers of magnification and high resolution. Subtle adjustments may then be made in brightness and contrast and color balance as needed. Quality of digital images resides not only in the acquisition and processing of images digitally but also in the quality and preparation of specimens for capture.

3. DIGITAL IMAGE ACQUISITION

Acquisition of digital images for pathology education and practice is perhaps the easiest, least time-consuming, and most straightforward component in the process of "going digital." It is pertinent in acquiring digital images that consideration is given foremost to how a digital image will be used and to what type of resolution is required for this use. Although capturing a digital image may only require a few seconds or minutes, much greater expenditures in time and effort lie in the processing and archiving of the digital image. If an image is captured that does not suit the needs of the pathologist for practice or for teaching purposes, then problems may arise later in terms of diagnostic applicability, usefulness, and delivery and the time expended from capture to archiving will have been wasted. In general, most issues with image acquisition may be solved by first asking "what's the most demanding need I will ever have of this image?" and "how big of an image do I really need?" and then acquiring the image in a way that meets that need. When this is known, specifications for hardware, software, and storage may become obvious.

Decisions as to how to acquire digital images may depend upon the particular subject matter being captured (e.g., whether the specimen is gross or microscopic) and the type of media being employed (e.g., de novo capture, film, print, glass slide). In addition, output requirements should be considered, such as whether the image will be displayed on a monitor or projection screen, printed on paper, or printed to film. File size limitations are a third consideration in terms of the method of delivery (e.g., local or network access), storage options (e.g., CD, DVD, hard drive, tapes), and available storage volume. In addition, one must consider existing hardware and software capabilities as well as limitations and costs of upgrading and maintaining this hardware and software.

In general, images that are used for printing purposes usually require the greatest resolution, and this can be used as a rule of thumb when determining what resolution is needed to capture images. Typically, 300 ppi (~dpi) is a sufficient resolution for most print applications. A simple formula can be used to determine the recommended resolution for a given print image:

(Print width inches x 300 ppi) x (Print height inches x 300 ppi)

Using this formula, a digital image to be printed at 8in. x 12in. needs to be acquired using a resolution of at least 2400 ppi to produce a 2400 x 3600 pixel image; the resulting file size would be approximately 25 MB as an uncompressed (lossless) TIFF (Tagged Image File Format). However, typically, a print image of 3.33in. x 5in. is sufficient for most pathology reports and journal publications, in which case a scanner capable of at least 1000-ppi resolution can be used to acquire an image of 1000 x 1500 pixels with a corresponding file size of approximately 4.5 MB (TIFF). Capture resolution is still sufficiently high to produce a quality digital image and quality print output, but the file size is significantly reduced—which aids in memory and storage requirements, especially when capturing and managing several hundred images.

4. IMAGE CAPTURE SYSTEMS

4.1 Analog Video Camera with Analog Capture Card

Images may be acquired digitally by using an analog video camera and connecting this device to a computer equipped with an analog capture card. The analog capture card converts the analog signal from the video data into a compressed digitized format.[5] This method is fairly cost-effective in terms of equipment and the images are captured in "real-time." The disadvantage is that the image data is compressed in the conversion from analog to digital, so there is some loss of data in the transfer. In addition, low resolution and low quality of the analog video signal may be reflected in the digital image output, thereby reducing the quality of the digital image obtained.

4.2 Digital Video Camera with Firewire Capture Card

Images may be acquired using a digital video camera with an IEE1394 on-camera Firewire interface; the camera can then be connected to a computer system equipped with an IEE1394 Firewire card. In addition to capturing images in "real-time," the digital video camera captures images in an already compressed and digitized format, so the information is transferred to the computer system without requiring further compression.[5] Digital video cameras have a higher resolution and signal quality compared to analog video cameras, and because the signal is already digitized and compressed, there is no loss of image data in transfer. The drawback of using digital video is mainly a cost issue as digital video cameras may be costly depending upon the specifications, and Firewire capture cards are more costly than analog capture cards.

4.3 Digital Camera

Digital cameras are rapidly flooding the market and vary in price and quality depending upon technology, resolution, connection interfaces, and "real-time" capabilities. Digital cameras may be used freehand or attached to a photostand to capture images or may be mounted on microscopes in order to capture digital photomicrographs. Digital cameras vary in megapixel resolution, and determining the resolution needed depends upon how the image will be used and cost considerations—typically, the higher the megapixel resolution, the greater the cost of the camera. Digital cameras are currently available as high as 7–8 megapixel resolution at significant cost, but quality digital images may be obtained with a less-pricey 3-megapixel camera, which will easily print a 5in. x 7in. image at 300 dpi.

4.4 Scanners

Scanners are beneficial in the conversion of slides, electron micrographs, glass slides, radiographs, film negatives, photographs, and print to a digital format. Again, in considering the type of scanner to purchase, one must consider what materials need to be scanned and how these materials will be used. Various scanners are available and have different resolutions, capabilities, software interfaces, and costs. Scanners may be limited to one use (e.g., scanning Kodachromes) or may be multifunctional (e.g., can scan both slides and glass slides).

The two most common types of scanners employed in pathology education and practice are film scanners and flatbed scanners. In general, film scanners transmit light through an image (such as a slide), whereas flatbed scanners reflect the light off the image (such as a photograph). Film scanners are often the most versatile; many have multi-format capabilities that allow scanning of film negatives, slides, glass slides, and radiographs.

5. DIGITAL IMAGE PROCESSING

Perhaps the greatest time expenditure in digital image capture is the actual processing and editing of the digital images after they have been acquired. Various image processing software is available to allow for image manipulation such as adjustments in brightness or contrast and resizing of images. Fortunately, such image adjustments can be made relatively easily by incorporating batch processing procedures that significantly reduce the time involved in processing digital images, especially when processing large numbers of images.

When an image is acquired digitally, certain image adjustments are sometimes necessary to ensure that the image projects an appropriate brightness and contrast and so as to rectify any slight variations in image color that may have occurred due to the illumination of the specimen or factors related to the image capture system.

6. IMAGE EDITING CONSIDERATIONS

6.1 Adjustments in Brightness and Contrast

Adjustments in brightness and contrast may be necessary to account for variations in the specimen thickness and/or surface features, lighting, and capabilities or limitations of the image capture system. During the image acquisition process, it is helpful to ensure the image receives appropriate planar lighting so as to reduce the level of brightness and contrast needed post-acquisition.

Many photo processing software packages include an autolevel feature which automatically balances the overall brightness of a digital image by locating the lightest and darkest areas of the image and adjusting the overall image brightness based upon that information. As such, it is typically necessary for an image to contain both black and white extremes so that these can be used as balance points in the autolevel process. In the same vein, many programs also possess an autocontrast feature that allows for the contrast to be automatically adjusted by also locating the brightest and darkest areas of the image and balances the contrast between these two extremes. However, autocontrasting is not always necessary in image processing as autoleveling typically provides adequate image correction.

Autoleveling is typically used for adjusting the uniform brightness of gross specimens and does not typically yield problematic results because lighting, shadows, and autopsy labels are usually sufficient to provide the two extremes for autoleveling to work correctly. With microscopic specimens, however, typically a black border (if not already present) has to be digitally added before autoleveling can be performed; this addition of a dark border is necessary for appropriate autoleveling because the darkest area of a microscopic specimen may be light as well.

A black border may be added to a microscopic image by canvas sizing the image to a larger dimension on a black background; the actual image size remains unchanged as only a border is added in the process. The darkest color in the image becomes the artificially-added black border, and the lightest color is the light background of the image excluding the border (e.g., whitish in the case of a glass slide). Applying autolevel then corrects the overall brightness of the microscopic image, and the image can subsequently be cropped to eliminate the black border.

It also may be necessary with both gross and microscopic images to make further adjustments in brightness and contrast manually or in cases where autoleveling and/or autocontrasting do not produce desirable results. However, one should exert caution in adjusting image brightness to the extent that the specimens appear "washed out" or adjusting the image contrast such that details are lost as areas become highly contrasted, colors are significantly adjusted, or the white areas within the image become "glaring" (usually the mark of an overly contrasted image). If an image is not well-featured following adjustments in brightness and contrast, the image may need to be reprocessed or, worse case, recaptured.

6.2 Adjustments in Color

A digital image may require slight adjustments in color depending upon the type of illumination, film or filters used, and the color capabilities, calibrations, and limitations of the image capture system. Thus, it may be necessary to adjust color balance in a gross or microscopic image to compensate for these variations.

Color bias (or casts) in an image may be removed using color balancing techniques so that the digital image may more accurately reflect the color balance of the original specimen; for example, an image with a yellow cast may be color balanced such that the yellow cast is removed and the image appears more like the original. Similarly, color may be added to an image to offset variations. Color balancing in Adobe Photoshop 7.0, for example, allows for the shadows, midtones, and highlights within an image to be adjusted on scales from cyan to red, magenta to green, and yellow to blue; for example, adjusting a scale toward red adds more red to the image, while adjusting a scale toward blue adds more blue to the image. Although Photoshop offers several other color-adjusting features, this simple color balance feature usually is sufficient to compensate for any color variation.

It is also worthwhile to note that color adjustment may not be necessary in the majority of cases because any variation in color between the original specimen and the digital scan may be minimal due to appropriate calibration (white balance) of the image capture system or may be rectified by the initial adjustments in brightness and contrast.

6.3 Adjustments in Image Size: Cropping and Resizing Images

After an image has been acquired digitally, it is often necessary to adjust the image size, either by "cropping" excess background or unwanted borders from the image, or "resizing" the image to prepare the image for delivery, such as to print or to post on the Web. Before cropping or resizing an image or making other adjustments, it is highly advisable that the original raw image be saved and archived; in this way, the original raw image may be accessed if modifications to the copy prove unsatisfactory. Typically, the

larger the image, the greater the uncompressed file size because there is more data that the image contains; thus, more storage space is needed to archive the image.

When resizing images, images should be resized proportionally (e.g., using the "constrain proportions" feature, if available) so as to avoid introducing any distortion into the images. It is also important to keep in mind that it is always better to resize an image to a smaller dimension than to resize an image to a larger dimension. When an image is resized to a larger dimension than the captured size, then the resolution is reduced as the pixels in the image become more "spaced out." As such, it is wise to capture images at the greatest image size that one may potentially need and to resize to smaller dimensions during image processing.

6.4 Adjustments in Image Sharpness

Typically, problems with sharpness of a digital image are usually the result of a problem with how the image was captured (e.g., whether the image capture system was calibrated or if autofocus was engaged), a problem with the image capture system itself (e.g., if autofocus failed because of equipment malfunction), or whether the original image used for acquisition (as in the case of a slide or video) was in focus. When acquiring digital images, it is highly recommended that a focused image be captured as focus is critical in the overall quality of the image. Although photo processing software can make some focal adjustments (such as by sharpening), an unfocused image at the outset will result in loss of details and definition in the acquired digital image. This consideration is especially important if the digital images will be used in routine practice for diagnostic purposes or for diagnostic assessment.

Sharpening may or may not be necessary with digital images and may be performed manually as needed or automatically applied to all of the images in a specified folder using a batch processing procedure. "Unsharp masking" is one sharpening tool that may be used to designate the degree of sharpening that one wishes to apply to the images. One of the dangers with sharpening images is that they may appear much more pixellated following sharpening, depending upon the image quality and the magnification of the image (e.g., some low-power microscopic images). The decision to sharpen images rests upon the pathologist's satisfaction with the results obtained. Depending upon the specifications of the image capture system and the quality of the digital output, one may decide that sharpening is necessary or that sharpening only needs to be applied to particular images.

6.5 Adjustments in Image Rotation

It may be necessary in some instances to rotate digital images post-acquisition, particularly if the digital images were captured at a 90- or 180-degree rotation. This is typically the case with slides, for example, and the rotation is due to the way the slides were loaded in the film scanner and/or the orientation of the slide holder on the image capture system. Image processing programs may allow for 90- for 180- degree image correction, and this may be performed manually (image-by-image as necessary) or through a batch processing procedure. Adobe Photoshop, for example, allows for 90- or 180- degree image correction, arbitrary image correction either clockwise or counterclockwise (in cases where images require less than 90-degree correction), and horizontal or vertical "flipping" of an image. In Photoshop, any of these rotations may be

dconducted manually image by image or applied automatically to all of the images processed in a particular batch.

7. DIGITAL IMAGE FORMATS

Various digital image formats exist and are classified as compressed or uncompressed. Uncompressed image formats are used to save the image data "as is" (i.e., no data is compressed during the "save" process). Uncompressed formats are typically the preferred format in saving captured images in terms of quality and versatility, as an uncompressed image may be modified multiple ways and multiple times without a detrimental effect on image quality. In contrast, compressed image formats actually involve a compression of the image data so detrimental effects on image quality may occur if an image is modified and saved multiple times; as such, compressed image formats usually represent the "final product" after all modifications have been made to the image and the image has been resized as needed. Compressed images are advantageous over their uncompressed counterparts in that compressed images have a much smaller file size. For this reason, compressed image formats are preferable for use in Web delivery or for inclusion in PowerPoint presentations as the smaller file size significantly reduces loading and download times.

7.1 Uncompressed Image Formats

Uncompressed image formats do not discard image data, so file sizes tend to be large and the images tend to be high quality (provided they have been captured at a sufficient resolution in line with a pathologist's imaging needs). Several uncompressed image formats exist, with BMP, TIFF, and PSD being the most common. BMP (Bitmaps) is a Windows uncompressed format that supports 256 colors whereas TIFF supports approximately 16.7 million colors; PSD is the native Adobe Photoshop file format which preserves layering effects when an image is edited in Photoshop. TIFF is the preferred uncompressed format for saving captured images because of its high color depth and universality.

7.2 Compressed Image Formats

Compressed image formats may be lossy or lossless. "Lossless" compression means that all of the data contained in an image is retained irrespective of the compression, whereas "lossy" compression means that redundant image data is lost during the compression.[6] Although lossy compression may not result in noticeable differences in image quality, problems with image quality can occur when a lossy image is altered or resaved multiple times; because data is irreversibly lost each time the file is compressed, the image quality may be significantly reduced.

In general, it is advisable that any modifications to digitized images be made in the uncompressed image format and the "final version" of the images be saved to a compressed image format to reduce file size and facilitate image loading for display purposes (e.g., Web browsers, PowerPoint). If any future modifications to the image are necessary, it is highly recommended that the uncompressed image file is used to make the

changes rather than the compressed file; the modified version may then be saved in a compressed format which is used to replace the pre-existing compressed image.

7.3 Examples of Lossless Compression Image Formats

GIF (Graphics Interchange Format) is a lossless compression image format that supports up to 8 bits of color per pixel, or 256 pixels of color. The compression algorithm takes advantage of line-by-line pattern repetition within the image, encoding this information in data attached to the image; thus, there is no loss of data in the compression—the information is encoded to compress the file and then decoded to display the image.[6-8] As such, sharp-edged or flat-color images compress well quality-wise to GIF format.[8] However, because GIF only supports 256 pixels of color, GIF is not the preferred compressed format for images that have high color depth or exhibit subtle differences or random patterns of color.[7]

PNG (Portable Network Graphic) is a lossless compression image format that supports up to 16 bits per pixel (grayscale) or 48 bits per pixel (true color).[8] PNG is more advantageous than GIF in that PNG can support 16.7 million colors in comparison to the 256 colors supported by GIF; in addition, PNG is touted to have better compression and to load faster than GIF.[8] PNG also allows for the transparency of individual pixels without altering the entire image; thus, a PNG image may be displayed as fading along a gradient from transparent to opaque.[7] Because PNG is a recent edition to the compressed file family, PNG is not supported by all browsers in comparison to GIF and may require a browser plug-in for the images to be displayed.[6]

7.4 Examples of Lossy Compression Image formats

JPEG (Joint Photographic Experts Group Format) is a lossy compression format that supports up to 24 bits of color per pixel (16.7 million colors) and is popular for compression of digitized images due to its availability across a variety of platforms and image capture devices.[6,9] Because JPEG is a lossy format, image data is lost with compression of the image. The compression algorithm first divides the images into blocks of information and then transforms these blocks of information into a series of curves based upon the colors represented within a particular block; the smallest curves are discarded depending upon the amount of image compression that is specified.[7, 8] Therefore, the JPEG format provides a “best fit” compression becuase not all of the pixels that were represented in the uncompressed image are contained within the compressed image—only a “best representation” of those pixels.[7] These differences are typically not observable unless there is a large degree of compression which distorts image quality (i.e., produces evident pixellation) or the compressed image is modified and/or saved multiple times. Also, it should be noted that the greater is the compression of a JPEG image, the smaller is the file size, but the larger the reduction in image quality because this means that more information is lost (as compared to the same image at a lower compression).

JPEG is typically used in pathology to compress gross or microscopic images because there is no change in color depth in the image compression (16.7 million color retention). The compression algorithm for JPEG is specific for images and based upon how color is perceived by the human eye; therefore, JPEG should not be used for compression of black-and-white drawings, line art, text, or other images which have

sharp-edges—otherwise, image quality may be distorted as the image may appear blocky or pixellated.[6-8]

p-JPEG (Progressive JPEG) is an up-and-coming lossy compression format that loads on the screen by fading in, in contrast to JPEG images which load from the top down.[6]

7.5 Compression or No Compression?

The decision to compress or not to compress an image depends upon ultimately how that image will be used in pathology practice or teaching. Typically, the digitized image should be acquired in an uncompressed file format and saved. TIFF is generally the preferred uncompressed format as compared to BMP simply on the basis that TIFF has a greater color depth (16.7 million colors). The uncompressed file format should be used for printing or archive purposes or in instances when the image will be altered or modified in the future. A copy of the acquired digitized image in its uncompressed and unmodified state should always be kept and archived for future use as this will prevent having to recapture the image (which may not be possible because the specimen may no longer be available for imaging).

Any modifications to the captured image should be conducted in the uncompressed state. After a satisfactory result is obtained following adjustments in brightness and contrast, cropping, color balance, and sharpening, the modified image should be resaved in an uncompressed format and archived. This modified image can then be used in the future for further modifications of the image or for printing purposes or converted to a compressed file format for Web or presentation purposes. For PowerPoint presentations, in particular, resizing the images to ~ 800 x 600 is adequate for keeping the presentation file size low (as compared to the same number of images that have not been resized or compressed).

Because problems with image quality emerge when compressed files are modified and/or saved multiple times, compressed images should always be the final output in order to preserve image quality. Also, no matter how an image is acquired or whether it will be used in a compressed or uncompressed format, it is important to keep in mind that appropriate lighting and magnification as well as a quality image capture system are critical in digital image acquisition for the best results; for microscopic images, medium, high, or oil-immersion magnification is recommended over low magnification to improve digital image quality and eliminate fuzziness.[10]

8. BATCH IMAGE PROCESSING SIMPLIFIED

The time involved in digital image processing can be significantly reduced in many cases by employing batch image processing strategies. In batch image processing, several editing tasks may be automated and applied to a group of images, leaving only minor customizations to be performed where necessary on select images following the batch process. Adobe Photoshop 7.0, for example, has a two-step batch processing function which may be employed: the first step creates the batch (i.e., defines the order of the image editing procedures), and the second step automates the batch (i.e., defines the source images and where the images will be saved).

8.1 Important Considerations Before Batch Processing

Before performing a batch, it is necessary to determine whether or not the acquired images have a border. If the image does not have a border, then cropping may not be necessary in the batch process. If the images have a border (e.g., Kodachrome scans), then cropping of this border may be included as part of the batch processing. It is crucial, however, to view the uncropped images first using an image viewer program (e.g., ACDSee Image Viewer, ACD Systems, Ltd., Victoria British Columbia, Canada) to determine roughly whether or not there is significant variation in border thickness and to determine which image "best represents" the collection in terms of border thickness. This is necessary because the border is considered part of the digital image and automated cropping crops all of the images to the same size regardless of their border. Typically, most image borders should be relatively uniform or absent if an image is directly captured (e.g., digital camera); in the case of slide scans, however, less uniform borders may arise depending upon how the film is positioned in the mount and the content of the slides—borders may differ in thickness or may be slightly rotated.

If not all images have a similar border thickness (e.g., some have thick borders and some have thin) and too much cropping is applied, then significant or relevant portions of the image may be eliminated. For this reason, choosing an image with a minimal amount of border and determining its image size with the border cropped is usually a good estimation for automated cropping. Typically, one needs to ask the question, "How much border can I remove from the greatest number of images without losing diagnostic or essential details?" The more uniform the image border among the images is, the more likely that the estimated crop size will minimize the need for further cropping. If necessary, further cropping may be carried out automatically (by using a second batch) or manually (in the instance of a few images which cannot be cropped easily by automation). Automatically cropping images using a batch versus manually cropping images dramatically reduces the time expenditures in image processing.

To determine the crop size for an image that has a border, open the selected image in a photo processing program, such as Adobe Photoshop, and crop the border. When the border has been cropped, determine the image dimensions (width and height)—these will be inputted in the batch so that all of the images will be cropped to this dimension.

With respect to microscopic images captured digitally, these images may not have a border that needs to be cropped. In this case, as previously discussed, it will be necessary to artificially create a black border prior to autoleveling to ensure that the microscopic images display appropriate brightness and contrast; this step is seldom necessary for gross pathology images. Insertion and removal of this black border may be achieved automatically as part of the batch process wherein the black border is inserted prior to the autolevel function and removed following the autolevel.

A black border on an image can be applied in Adobe Photoshop by using the "canvas size" function and by choosing a black background, and the border may be applied to the height and/or width of the image. Note that canvas sizing the image does not "resize" the image itself but rather only adds additional pixels of a specified color to the image to create a border effect. For example, a 1500 (w) x 1000 (h) pixel image that is canvas sized on a black background to 1510 (w) x 1000 (h) pixels will have a 5-pixel width black margin on the left, a 1500-pixel width image in the center, and a 5-pixel width black margin on the right. The image is then autoleveled and the ten additional border

pixels are removed by canvas sizing the image back to its original dimensions, in this case 1500 (w) x 1000 (h) pixels.

The thickness of this artificial border is up to the discretion of the individual who is processing the images; the main point is that the number of border pixels applied upon the initial canvas sizing is equal to the number of border pixels removed during the second canvas sizing. Also, it is important to note that Adobe Photoshop provides options wherein pixels may be added to one side of the image only during canvas sizing; thus, in removing the border, it is important to remember to remove the additional pixels from the same side to which they were applied.

9. DIGITAL IMAGE STORAGE

9.1 Image Storage Devices and Archival Quality/Life Expectancy

When acquiring and processing digital images, storage considerations become important, especially when capturing and processing large numbers of images. For pathology education and practice, it is much more useful to consider storage in terms of actual file storage for archiving and processing rather than simply temporary storage specific to the image capture device (e.g., Compact Flash, microdrives, portable drives). Image capture devices used for pathology are typically fixed on a system, so there is less need for temporary devices to aid in transport of the images—though temporary devices are beneficial in the clinic for portability purposes, such as with the use of digital cameras and PDAs. Storage demands depend ultimately on how many images are being captured and how they are being used and archived. Having sufficient hard drive space on the image capture system and removable storage options available (such as removable hard drives, CDs, and DVDs) typically is the best investment storagewise.

Removable (portable) hard drives or large internal hard drives can provide tremendous storage capacity for images. Hard drives may be purchased at low cost and can provide gigabytes of storage, with an estimated average hard drive cost of $1–3 per gigabyte of storage. The advantage of removable hard drives for digital imaging purposes is that they increase storage capacity of a given system and can be moved from system to system as needed, provided a removable hard drive bay has been installed. The disadvantages to consider are that they are prone to failure over time (much more than CDs or DVDs as storage devices) and information on a failed drive may be unrecoverable or retrieval costs may be considerable. In addition, some large hard drives encounter incompatibilities with certain systems such that the system will not “read” the hard drive, so use of the removable drive is restricted in those cases to only those systems that are compatible with the drive.

CDs and DVDs are also a tremendous benefit in archiving digital images. CDs provide approximately +/– 700 MB of storage versus DVDs which may provide +/– 4.5 GB of storage. CDs are relatively inexpensive compared to DVDs, and CD burners are available with write speeds up to 48x, thus allowing for speedy transfer of data. DVD burners currently have slower write speeds but the impact on efficiency may be minimal as more images can be stored on a DVD than on a CD.

9.2 Storage Workflow

Image acquisition, processing, and storage may be performed on one system with sufficient memory and storage or on multiple systems. Given the magnitude of image capture devices available and the sharing of imaging facilities in both pathology education and practice, it is more likely that more than one system will be used.

A general scheme for increasing efficiency and productivity is to have at least three separate work stations each equipped with removable hard drives—a "capture" system, a "burner" system, and an "imaging" system. The capture system is equipped with an image capture device and any accompanying image capture software interfaces. Digital images are captured on the "capture" system and saved to the removable hard drive; this hard drive is then removed and another hard drive is substituted so that additional captures can be made. The removable hard drive from the "capture" system is then inserted into the open bay of the "burner" system and the original files are archived to CD and/or DVD. More than one copy of the original files should be made, particularly in cases where the images will be removed from the hard drive. After the images have been archived using the "burner" system, the hard drive is removed and inserted into the open bay of the "imaging" system. The "imaging" system is equipped with photo processing software, and the images are automatically batch processed and manually tweaked as needed. The modified images can then be saved to the removable hard drive, which may then be relocated to the "burner" system for archiving of the modified images on CD and/or DVD. For online or network usage, the images may be batch resized on the "imaging" station, archived on the "burner" station, and then uploaded to the server/network for online usage.

10. DIGITAL IMAGE MANAGEMENT

Digital image management is a crucial component of preventing the "image graveyard" effect in both pathology education and practice. Basically, image management involves knowing what images have been acquired, categorizing and organizing them for easy retrieval, and displaying the images readily when needed. Without image management strategies in place, digital images may lie dormant on a hard drive just as photo and glass slides may lie dormant on a storage shelf. When only a few digital images have been captured (less than 100, for example), it is relatively easy to remember which images are available and decide how they will be used. As more and more images are captured and processed (e.g., hundreds or thousands), the more important it becomes to be able to manage the images so that they can be used for some purpose (other than only taking up space on a hard drive).

One of the first considerations in image management is scalability—how many images one expects to process and archive and how these images will be used. Will the images be accessed on a sole workstation, thus requiring only local management solutions, or will the images be accessible on a broad scale via a network or the Web by one or more users? Different image management software systems may need to be employed depending upon the needs of the pathologist.

Both proprietary and open standard formats are available for image management and are equipped with viewing features that allow for viewing the images and/or thumbnails of the images in addition to various other features (e.g., browsing, editing, renaming,

batching, organizing). Whether to use a proprietary or open standard format depends upon what the program offers and how this best fits one's needs and cost considerations. Open standard formats are usually freely available (such as on the Web), may be application- and platform-independent, and are typically free (no purchase or license required or additional fees). Proprietary formats are usually "owned" applications (via a company or group) that may be freely available but usually require purchase of the software and/or licenses. Technical support may vary with both open standard formats and proprietary formats—either it will be nonexistent, provided as a courtesy service or via a discussion forum among users of the software, or require a fee (often with proprietary software, either through the software purchasing or licensing or as an additional service fee).

Additional considerations in choosing image management systems include the metadata and search/browse capabilities the management system provides. Being able to view images in the management system is essential, but being able to view the size of the image, the dimensions of the image, and other information about the image (e.g., resolution, colorspace) is also beneficial (e.g., ACDSee image browser). Also, being able to search and browse for images can dramatically increase the efficiency of image retrieval—both when processing images and for usage.

For network management of images or Web-based delivery, the images must be accessible either by a shared network drive or via a Web server. WWW-photo sharing services and static or dynamic content solutions are available for Web delivery of images. WWW-photo sharing services allow for images to be uploaded to a remote site for low or no cost and vary in the features offered (e.g., editing, organizing, annotation, password protection). Static content solutions often involve locally installed software that allows for images and text to be combined in a Graphical User Interface and produces a static HTML output that may be loaded on a Web server. Static content solutions tend to be relatively cheap, usually involve local management software with no remote authoring access, and may require extensive manual updating depending upon what changes are necessary and what modifications in the program need to be made. In contrast, dynamic content solutions are usually database-driven and allow for images and text to be displayed and updated "on-the-fly." Dynamic database-driven solutions tend to be robust, readily updatable, may have remote Web authoring access, allow for multiple authors to engage in image management, and feature updates as the programs continue to be developed. However, dynamic solutions may also be costly, and proprietary solutions may not allow for easy transfer of data to another solution as pathologists' needs change.

11. DIGITAL IMAGE REPOSITORIES

As pathology images have become digitized and readily accessible via the Web, digital repositories have emerged which allow for the usage and repurposing of materials.[11] and the implications of these digital repositories are important for both pathology education and practice. Digital repositories, such as online pathology image databases, provide access to materials that have previously been inaccessible or not available in a digital format; such access to these digital materials facilitates collaboration among pathology educators and practitioners in allowing them to share cases, diagnostic findings, image collections, and curriculum. Digital repositories allow for the archiving, cataloging, sharing, storage, and easy search and retrieval of materials that may

efficiently accessed and reused and repurposed for various tasks, thereby expanding the global knowledge base and facilitating e-curricula.[11-13]

11.1 Pathology Education Instructional Resource (PEIR)

The Pathology Education Instructional Resource (PEIR) (http://peir.net) at the University of Alabama at Birmingham Department of Pathology is an educational resource that can be used by health science educators of all disciplines.[12] The cornerstone of the PEIR resource is a digital image repository that is an example of how digital images can be used for pathology education and practice.

The PEIR Digital Library (PDL) (http://peir.path.uab.edu/pdl) is a public access digital image repository of over 50,000 pathology images which are searchable by collection, image type, and keyword and is available free for nonprofit educational purposes. The PDL search engine incorporates the use of the National Library of Medicine's Medical Meta-thesaurus, thereby maximizing the number of results per database query based upon synonymous terms.[14] The PDL also contains numerous features to facilitate easy search and retrieval of images, including thumbnail display, image shopping cart, multiple image size download capabilities, and an online "on-the-fly" image editor. The PDL is powered by ACD System's ImageShark Web Image Server which is an ISAPI extension DLL designed to handle CGI requests on a Microsoft IIS Web server; ImageShark generates images of varying size and resolution from one unmodified source file, thereby reducing storage space and enabling dynamic generation of images.[15] Total Web site hits for the PDL have exceeded 2.7 million over the past eight months, with an average of 11,500 Web pages viewed daily. The PEIR Web site and this digital image repository has become a valuable resource that is used by health professions educators from all over the world.

12. CONCLUSION

As technologic advances continue at a breathtaking pace, digital imaging has become easier and more affordable for everyday use in both clinical and educational pathology applications. Because pathology is an image-intensive discipline, the use of high-quality digital imaging systems has improved the efficiency and accuracy of pathology practice and education. The collection, processing, and management of the large number of images that accumulate in a busy clinical practice present a challenge. However, with careful planning and a vigilant eye to the final outcome; effective and efficient systems for managing digital images can provide a useful tool for use by busy pathologists in a variety of professional endeavors.

13. REFERENCES

1. Cruz D, Valenti C, Dias A, Seixas M, Schmitt F, Digital image documentation for quality assessment. *Archives of Pathology and Laboratory Medicine*, 125(11), 1430-5 (2001).
2. Foucar E, Error identification: a surgical pathology dilemma. *American Journal of Surgical Pathology*, 22(1), 1-5 (1998).
3. Weinberg DS, Allaert FA, Dusserre P, et al., Telepathology diagnosis by means of digital still images: an international validation study*,* 1996 Sep; 27(9):1001]. *Human Pathology*, 27(2), 111-8 (1996).

4. Halliday BE, Bhattacharyya AK, Graham AR, et al., Diagnostic accuracy of an international static-imaging telepathology consultation service. *Human Pathology*, 28(1), 17-21 (1997).
5. Renaud D, Desktop video: a starter's guide to video editing. Available at http://www.hardwarecentral.com/hardwarecentral/tutorials/923/1 Accessed May 26th 2004
6. Anonymous Compression: optimizing web graphics Available at http://www.webreference.com/dev/graphics/compress.html Accessed June 2nd 2004
7. Eisenberg JD, Why good images go bad: a guide to effective use of images on your Available at http://catcode.com/imgguide/index.html Accessed June 2nd 2004
8. Wide area communication. Creating graphics for the web: compression basics. Available at http://www.widearea.co.uk/designer/compress.html Accessed June 2nd 2004
9. Alvira N, Digital imaging theory *American Society of Clinical Pathology National Meeting* 2000.
10. Shireman PK: Digitizing and digitizers *American Society of Clinical Pathology National Meeting* 2000.
11. Fleiszer DM, Posel NH, Steacy SP, New directions in medical e-curricula and the use of digital repositories. *Academic Medicine*, 79(3), 229-35 (2004).
12. Jones KN, Anderson PG, Development of an online pathology education instructional resource to facilitate pathology education. *Archives of Pathololgy and Laboratroy Medicine*, 124(812 (2000).
13. Jones KN, Kreisle R, Geiss RW, Holliman JH, Lill PH, Anderson PG, Group for research in pathology education online resources to facilitate pathology instruction. *Archives of Pathology and Laboratory Medicine*, 126(3), 346-50 (2002).
14. Woode DE, Jones KN, Anderson PG, A reusable software plug-in enabling expansion of biomedical database queries using the UMLS. *Archives of Pathology and Laboratroy Medicine*, 2001(125), 107 (2001).
15. Jones KN, Woode DE, Panizzi KT, Anderson PG, Managing digital image libraries with ImageShark™ image server. *Archives of Pathololgy and Laboratroy Medicine*, 125(108 (2001).

INDEX